Year : 2013

Regulation of Nav1.7 and Nav1.8 voltage-gated sodium channels by Nedd4-2 and ß-subunits and its implication in neuropathic pain

LAEDERMANN Cédric J.

LAEDERMANN Cédric J., 2013, Regulation of Nav1.7 and Nav1.8 voltage-gated sodium channels by Nedd4-2 and ß-subunits and its implication in neuropathic pain

Originally published at : Thesis, University of Lausanne

Posted at the University of Lausanne Open Archive.
http://serval.unil.ch

Centre l'Antalgie, Service d'Anesthésiologie (Lausanne)
Département des Neurosciences Fondamentales (Lausanne)
Département de Recherche Clinique (Berne)

Regulation of $Na_v1.7$ and $Na_v1.8$ voltage-gated sodium channels by Nedd4-2 and β-subunits and its implication in neuropathic pain

Thèse de doctorat en Neuroscience (PhD)

Présentée à la
Faculté de Biologie et de Médecine de l'Université de Lausanne
par

Cédric J. LAEDERMANN
Diplomé en Biologie à l'Université de Lausanne

Jury

Prof. Isabelle Décosterd, Directrice de thèse
Prof. Hugues Abriel, Directeur de thèse
Prof. Olivier Staub, Président du Jury
Prof. Brigitte Kieffer, Experte
Prof. Anita Lüthi, Experte

Lausanne 2013

UNIL | Université de Lausanne
Faculté de biologie et de médecine

LEMANIC NEURO SCIENCE DOCTORAL SCHOOL

Programme doctoral interuniversitaire en Neurosciences des Universités de Lausanne et Genève

Imprimatur

Vu le rapport présenté par le jury d'examen, composé de

Président	Monsieur Prof. Olivier **Staub**
Directeur de thèse	Madame Prof. Isabelle **Decosterd**
Co-directeur de thèse	Monsieur Prof. Hugues **Abriel**
Experts	Madame Prof. Anita **Luethi**
	Madame Prof. Brigitte **Kieffer**

le Conseil de Faculté autorise l'impression de la thèse de

Monsieur Cédric Laedermann

Master of Science de l' Université de Lausanne

intitulée

Regulation of $Na_v1.7$ and $Na_v1.8$ voltage-gated sodium channels by Nedd4-2 and β subunits and its implication in neuropathic pain

Lausanne, le 4 juillet 2013

pour Le Doyen
de la Faculté de Biologie et de Médecine

Prof. Olivier Staub

Summary

In mammals, the presence of excitable cells in muscles, heart and nervous system is crucial and allows fast conduction of numerous biological information over long distances through the generation of action potentials (AP). Voltage-gated sodium channels (Na_vs) are key players in the generation and propagation of AP as they are responsible for the rising phase of the AP. Na_vs are heteromeric proteins composed of a large pore-forming α-subunit (Na_v) and smaller β-auxiliary subunits. There are ten genes encoding for $Na_v1.1$ to $Na_v1.9$ and NaX channels, each possessing its own specific biophysical properties. The excitable cells express differential combinations of Na_vs isoforms, generating a distinct electrophysiological signature.

Noteworthy, only when anchored at the membrane are Na_vs functional and are participating in sodium conductance. In addition to the intrinsic properties of Na_vs, numerous regulatory proteins influence the sodium current. Some proteins will enhance stabilization of membrane Na_vs while others will favour internalization. Maintaining equilibrium between the two is of crucial importance for controlling cellular excitability. The E3 ubiquitin ligase Nedd4-2 is a well-characterized enzyme that negatively regulates the turnover of many membrane proteins including Na_vs. On the other hand, β-subunits are known since long to stabilize Na_vs membrane anchoring.

Peripheral neuropathic pain is a disabling condition resulting from nerve injury. It is characterized by the dysregulation of Na_vs expressed in dorsal root ganglion (DRG) sensory neurons as highlighted in different animal models of neuropathic pain. Among Na_vs, $Na_v1.7$ and $Na_v1.8$ are abundantly and specifically expressed in DRG sensory neurons and have been recurrently incriminated in nociception and neuropathic pain development.

Using the spared nerve injury (SNI) experimental model of neuropathic pain in mice, I observed a specific reduction of Nedd4-2 in DRG sensory neurons. This decrease subsequently led to an upregulation of $Na_v1.7$ and $Na_v1.8$ protein and current, in the axon and the DRG neurons, respectively, and was sufficient to generate neuropathic pain-associated hyperexcitability. Knocking out Nedd4-2 specifically in nociceptive neurons led to the same increase of $Na_v1.7$ and $Na_v1.8$ concomitantly with an increased thermal sensitivity in mice. Conversely, rescuing Nedd4-2 downregulation using viral vector transfer attenuated neuropathic pain mechanical hypersensitivity. This study demonstrates the significant role of Nedd4-2 in regulating cellular excitability *in vivo* and its involvement in neuropathic pain development.

The role of β-subunits in neuropathic pain was already demonstrated in our research group. Because of their stabilization role, the increase of β1, β2 and β3 subunits in DRGs after SNI led to increased Na_vs anchored at the membrane. Here, I report a novel mechanism of regulation of α-subunits by β-subunits *in vitro*; β1 and β3-subunits modulate the glycosylation pattern of $Na_v1.7$, which might

account for stabilization of its membrane expression. This opens new perspectives for investigation Na_vs state of glycosylation in β-subunits dependent diseases, such as in neuropathic pain.

Résumé

Chez les mammifères, la présence de cellules excitables dans les muscles, le cœur et le système nerveux est cruciale; elle permet la conduction rapide de nombreuses informations sur de longues distances grâce à la génération de potentiels d'action (PA). Les canaux sodiques voltage-dépendants (Na_vs) sont des participants importants dans la génération et la propagation des PA car ils sont responsables de la phase initiale de dépolarisation du PA. Les Na_vs sont des protéines hétéromériques composées d'une grande sous-unité α (formant le pore du canal) et de petites sous-unités β accompagnatrices. Il existe dix gènes qui codent pour les canaux sodiques, du $Na_v1.1$ au $Na_v1.9$ ainsi que NaX, chacun possédant des propriétés biophysiques spécifiques. Les cellules excitables expriment différentes combinaisons des différents isoformes de Na_vs, qui engendrent une signature électrophysiologique distincte.

Les Na_vs ne sont fonctionnels et ne participent à la conductibilité du Na+, que s'ils sont ancrés à la membrane plasmique. En plus des propriétés intrinsèques des Na_vs, de nombreuses protéines régulatrices influencent également le courant sodique. Certaines protéines vont favoriser l'ancrage et la stabilisation des Na_vs exprimés à la membrane, alors que d'autres vont plutôt favoriser leur internalisation. Maintenir l'équilibre des deux processus est crucial pour contrôler l'excitabilité cellulaire. Dans ce contexte, Nedd4-2, de la famille des E3 ubiquitin ligase, est une enzyme bien caractérisée qui régule l'internalisation de nombreuses protéines, notamment celle des Na_vs. Inversement, les sous-unités β sont connues depuis longtemps pour stabiliser l'ancrage des Na_vs à la membrane.

La douleur neuropathique périphérique est une condition débilitante résultant d'une atteinte à un nerf. Elle est caractérisée par la dérégulation des Na_vs exprimés dans les neurones sensoriels du ganglion spinal (DRG). Ceci a été démontré à de multiples occasions dans divers modèles animaux de douleur neuropathique. Parmi les Na_vs, $Na_v1.7$ et $Na_v1.8$ sont abondamment et spécifiquement exprimés dans les neurones sensoriels des DRG et ont été impliqués de façon récurrente dans le développement de la douleur neuropathique.

En utilisant le modèle animal de douleur neuropathique d'épargne du nerf sural (spared nerve injury, SNI) chez la souris, j'ai observé une réduction spécifique des Nedd4-2 dans les neurones sensoriels du DRG. Cette diminution avait pour conséquence l'augmentation de l'expression des protéines et des courants de $Na_v1.7$ et $Na_v1.8$, respectivement dans l'axone et les neurones du DRG, et était donc suffisante pour créer l'hyperexcitabilité associée à la douleur neuropathique. L'invalidation pour le gène codant pour Nedd4-2 dans une lignée de souris génétiquement modifiées a conduit à de similaires augmentations de $Na_v1.7$ et $Na_v1.8$, parallèlement à une augmentation à la sensibilité thermique. A l'opposé, rétablir une expression

normale de Nedd4-2 en utilisant un vecteur viral a eu pour effet de contrecarrer le développement de l'hypersensibilité mécanique lié à ce modèle de douleur neuropathique. Cette étude démontre le rôle important de Nedd4-2 dans la régulation de l'excitabilité cellulaire *in vivo* et son implication dans le développement des douleurs neuropathiques.

Le rôle des sous-unités β dans les douleurs neuropathiques a déjà été démontré dans notre groupe de recherche. A cause de leur rôle stabilisateur, l'augmentation des sous-unités β1, β2 et β3 dans les DRG après SNI, conduit à une augmentation des Na_vs ancrés à la membrane. Dans mon travail de thèse, j'ai observé un nouveau mécanisme de régulation des sous-unités α par les sous-unités β *in vitro*. Les sous-unités β1 et β3 régulent l'état de glycosylation du canal $Na_v1.7$, et stabilisent son expression membranaire. Ceci ouvre de nouvelles perspectives dans l'investigation de l'état de glycosylation des Na_vs dans des maladies impliquant les sous-unités β, notamment les douleurs neuropathiques.

Résumé destiné à un large publique

Les canaux sodiques (Na_vs) sont impliqués dans la transmission de l'influx nerveux dans les neurones ; ils sont à la base de la génération des potentiels d'action, vecteurs de l'information électrique. Les Na_vs ne sont fonctionnels qu'une fois exprimés à la membrane ; plus leur nombre est grand, plus l'information se transmet efficacement.

Les Na_vs forment une famille composée de dix différents isoformes, chacun ayant des propriétés spécifiques. $Na_v1.7$ et $Na_v1.8$, hautement exprimés dans le système sensoriel périphérique, sont considérés comme les plus importants dans le contexte de la douleur. La régulation de l'expression membranaire de $Na_v1.7$ et $Na_v1.8$ va modifier la conductance sodique et par conséquent l'excitabilité cellulaire des neurones sensoriels, ce qui va directement influencer l'intensité de la douleur. Il a déjà été démontré que dans les douleurs chroniques, ces canaux s'accumulent dans le système sensoriel périphérique, résultant dans l'hyperexcitabilité du système. Les mécanismes pouvant mener à cette accumulation des Na_vs n'ont été que peu investigués dans le cadre des douleurs chroniques. Cependant, plusieurs mécanismes de régulation membranaire des Na_vs ont déjà été identifiés. Nedd4-2, membre de la famille des ubiquitin ligases, participe à l'internalisation des canaux sodiques et diminue donc leur expression à la membrane. A l'opposé, les sous-unités β vont plutôt participer à la stabilisation des Na_vs à la membrane.

Dans notre groupe de recherche, nous utilisons un modèle animal de douleur neuropathique, le modèle d'épargne du nerf sural (spared nerve injury, SNI) qui nous permet d'étudier les mécanismes à la base de la douleur neuropathique chez la souris. Il implique le sectionnement d'une partie du nerf sciatique, ce qui génère une hyperexcitabilité du système sensoriel périphérique. Dans ce modèle, j'ai pu montrer que la diminution de l'expression de Nedd4-2 dans les neurones sensoriels est à l'origine de l'augmentation de l'expression de $Na_v1.7$ et $Na_v1.8$. Pour démontrer le lien de causalité entre la diminution de Nedd4-2 et l'augmentation de $Na_v1.7$ et $Na_v1.8$, j'ai généré une lignée de souris génétiquement modifiée et invalidée pour le gène codant pour Nedd4-2. J'ai observé les mêmes augmentations de $Na_v1.7$ et $Na_v1.8$, confirmant que la diminution de Nedd4-2 est suffisante pour générer de l'hyperexcitabilité cellulaire. De plus, ces souris ont aussi un phénotype d'hypersensibilité à la chaleur, démontrant le lien entre hyperexcitabilité cellulaire et augmentation de l'intensité de la douleur. Finalement, en utilisant une approche de thérapie génique, j'ai pu montrer que restaurer l'expression de Nedd4-2 dans les neurones sensoriels après le SNI est suffisant pour diminuer le développement de l'hypersensibilité mécanique. Ceci indique que Nedd4-2 a un rôle important de régulation de $Na_v1.7$ et $Na_v1.8$ et est donc impliqué dans les processus de modulation de la douleur.

Notre groupe de recherche a montré que l'expression des sous-unités β était augmentée dans les neurones sensoriels suite au SNI. De par leur rôle stabilisateur des Na_vs, cette augmentation des sous-unités β induit l'accumulation des Na_vs exprimés à la membrane. J'ai pu montrer que les sous-unités β régulent l'état de glycosylation de $Na_v1.7$ de façon différentielle, ce qui peut contribuer à sa stabilisation à la membrane. Cette découverte d'un nouveau mécanisme de régulation ouvre de nouvelles perspectives quant à la glycosylation des Na_vs dans des pathologies impliquant les sous-unités β, notamment les douleurs neuropathiques.

Acknowledgements

I would like to thank all the people that have stood by me, accompanied me and supported me through my thesis.

First of all, I want to thank my two thesis co-directors, Prof. Isabelle Decosterd and Prof. Hugues Abriel. I received tremendous benefit from having two directors, with their own different way of perceiving and performing science, and their expertises in different fields. Together, they guided me whenever necessary, but also let me have my own experiences throughout my thesis. Pro-activity, rigour and enthusiasm were their leitmotiv.

I would like to thank the president and the members of the jury for the time they spent reading the manuscript and evaluating my work.

I want to thank the whole Decosterd's Lab that spent many years with me and helped me with several aspects of my work. Thanks to Marie for her support during hard moments, and for her help with PCRs, western blotting, surgery, and particularly for all the administrative tasks she reminded me to do. Thanks to Romain-Daniel for all his precious advice, the "café-philo" and the great tennis games during these 4 years we spent side by side in the office. Thanks to Dr. Suter, for opening me up to a clinical view of the pain field and coaching me during congresses. Thanks to Guylène for all the behavioural pain tests she performed for me. Thanks to Isabelle Chang for performing western blots on very difficult tissue and proteins for months, but also for her refreshing sense of humour. Thanks to Christine, Verdad, Xavier and Ahmed for the countless discussions we had together around the labmeeting table, a coffee or a Holy Cow Burger. Thanks to Maria and Francine for the "macarons", and their unwavering kindness.

I would like to thank the people working in the DPT, and particularly in Abriel's Laboratory. Thanks to Séverine for introducing me to patch clamp and biophysical properties of sodium channels and Liliana for spending full days next to me in front of our respective setups. Thank to Maxime and Anne-flore for teaching me basics in biochemistry (and more rarely for the beers in "Les Fontaines"). A thank you to Jean-Sébastien, Ninda, Diana, Valentin, Yassine, Ludovic, Maria, and the rest of Abriel Lab, for the nice and fulfilling conversations we had when I had to chance to come and visit the lab in Bern.

I want to thank Stephan Kellenberger and Maxime Blanchard from the DPT for helping me with *ex vivo* patch clamp experiments. Thanks to Monique for always providing me with HEK cells whenever needed and to Isabelle Rivier for her availability and kindness.

Thanks to Camille, Nicolas and Daniel, who also performed their thesis at the same time as I did. We had many discussions and mutual complaints about the difficulty of performing a Ph.D.

Thanks to my family. Thanks to my mother for having always been so enthusiastic and proud of my work. Thanks to my father for always trusting in me and giving me encouragements. Thanks to my sister for all the profound discussions we had; science, religion, family, and so on. Thanks to my brother for his unalterable good mood and the laughs we had together. Thanks to my brother-in-law, Alex, for motivating me to do sport challenges; the typical example of a healthy competition.

Thanks to my “non-scientific” friends. Adrian, who brought me so often to work in his car and listened about my work, particularly on Monday morning when it’s a little harder. Thanks to Marc, Jonathan, Pascal and Rafael for the mental support in stressful periods but also for the good moments of relaxation.

I have an affectionate thought for Laetitia, Vincent and Gaby. May they rest in peace.

A very special thank to Céline, who always supported me and for her daily encouragements. She has shared to good and the bad moments in these past 5 years.

Last but not least, a special thank to Erin, who is about to enter my life. I cannot wait to get to know her and already love her very deeply. Welcome to this world Erin.

List of abbreviations

AMPA: α-amino-3-hydroxy-5-méthylisoazol-4-propionate

AP: Action potential

ASIC: Acid sensing ion channel

β: Na_vs β-subunit

BDNF: Brain-derived neurotrophic factor

C2: Calcium-dependent lipid binding domain 2

CaCC: Calcium-activated chloride channel

CaMK: Calcium/calmodulin-dependent protein kinase

Ca_vs: Voltage-gated calcium channel

CCI: Chronic constriction injury

ClC: chloride channel

CFA: complete Freund's adjuvant

CGRP: Calcitonin gene-related peptide

COX: Cyclooxygenase

CNS: Central nervous system

CREB: C-AMP Response Element-binding protein

DEG/ENaC: Degenerins/ Epithelium amiloride-sensitive sodium channel

DH: Dorsal horn

DRG: Dorsal root ganglia

DUB: Deubiquitylating enzyme

E1: Ubiquitin-activating enzyme

E2: Ubiquitin-conjugating enzyme

E3: Ubiquitin-protein ligase

ENaC: Epithelium amiloride-sensitive sodium channel

ERK: MAPK family member, extracellular signal-regulated kinase

EEA: Excitatory amino acid

ER: Endoplasmic reticulum

FBF: Fibroblast growth factor

GABA: Gamma-aminobutyric acid

GAPDH: Glyceraldehyde-3-phosphate dehydrognease

GDNF: Glial cell line-derived neurotrophic factor

GFAP: Glial fibrillary acidic protein

GPI: glycosyl-phosphatidylinositol

HCN: Hyperpolarization-activated cyclic nucleotide-gated

Hect: Homologous to E6-AP COOH terminal

HEK cells: Human Embryonic Kidney cells

IB4: Isolectin binding protein 4

IGE: Photosensitive generalized epilepsy

IκB: Inhibitor of NF- κB

IKK: Inhibitor of NF- κB kinase

IL: Interleukins

I_{Na}: Sodium current

K: Lysine

KCC: Potassium chloride co-transporter

KCNQ: Voltage-gated potassium channe, subfamily Q

KCNKx: Voltage-gated potassium channel, subfamily K, member x

K_v: Voltage-gated potassium channel

LTD: Long term depression

LTP: Long term potentiation

MAPK: Mitogen-activated protein kinase

Na_v: Voltage-gated sodium channel

Nedd4/Nedd4-2: Neuronal precursor cell-expressed developmentally downregulated gene 4/4-2

Nedd4-2CS: inactive catalytic site Nedd4-2 mutant

NF-κB: Nuclear Factor κB

NGF: Nerve growth factor

MGS: Mouse Grimace Scale

NMDA: N-methyl-D-aspartate

NO: Nitric oxide

NOS: Nitric oxide synthase

NP: Neuropathic pain

NSAIDS: Non-steroidal anti-inflammatory analgesics

P: Proline

P2X: Purinergic receptor

PAG: Periaqueductal gray

PG: Prostaglandin

PKA: Protein kinase A

PKC: Protein kinase C

Pl3K: Phosphoinositide 3-kinase

PNS: Peripheral nervous system

qPCR: Quantitative real-time RT-PCR

rAAC: Rostral anterior cingulated cortex

RING: Really interesting new gene

RVM: Rostral ventromedial medulla (RVM)

SC: Spinal cord

SCNxA: gene coding for sodium channel, voltage-gated, type x, alpha subunit

SCNxB: gene coding for sodium channel, voltage-gated, type x, beta subunit

SGK: Serum glucocorticoid-induced kinase

SNI: Spared nerve injury

SNL: Spinal nerve ligation

SP: Substance P

SSNRIs: selective serotonin and norepinephrine reuptake inhibitors

TNF-α: Tumor necrosis factor alpha

TCA: Tricyclic antidepressant

TrkA: Tyrosine kinase receptor A

TRP: Transient receptor potential

TRPA1: Transient receptor potential cation channel 1

TRPM8: Transient receptor potential melastatin-type 8

TRPV1: Transient receptor potential vanilloid-type 1

TTX: Tetrodotoxin

Usp2: Ubiquitin carboxyl-terminal hydrolase 2

WHO: World Health Organization

Y: Tyrosine

Table of content

1. Introduction

Pain is a continuum of disagreeable sensory and emotional experience. On one extreme, pain carries a beneficial defensive function, whose system of detecting and coding noxious and dangerous stimuli is referred to as nociception. On the other extreme is the pathological aspect of pain, and particularly neuropathic pain, which serves no apparent advantageous function. Between the two, mechanisms of gain-of-sensitivity amplify the pain signal, aiming at avoiding further damage, but in pathological cases this amplification may outlive resolution of injury, and as a result chronic pain sets in.

In this thesis, I will start by discussing general aspects of pain such as its anatomy and function. I will then go on to the other extreme of the spectrum and discuss current knowledge about neuropathic pain. This disorder is often associated with nervous system hyperexcitability. In this regard, I will discuss the role of voltage-gated sodium channel (Na_vs) in normal and pathological pain. Finally, I will discuss mechanisms of regulations of Na_vs, putting in perspective their involvement in neuropathic pain-associated hyperexcitability. This will introduce the two main research articles that came out of this thesis and that are presented in chapter 2.

In Appendix, I added a third article where I am co-first author, which should be soon submitted to *Molecular Pain*, and two articles to which I also contributed, one in *Anesthesiology* and one in *Neuroscience*.

1.1. Pain:

1.1.1. Definition:

Humans and other animals experience countless episodes of pain during a lifetime. Pain allows living organisms to escape from damaging situation, to protect a damaged body the time required for its healing and to avoid similar situations in the future. Doubtlessly, the acquirement of a system able to remember danger is one of the major evolutionary drives necessary for surviving in a hostile environment. When this body alarm does not work properly, for instance by not switching off when necessary or by being perpetually activated, individuals experience a chronic pain state, having no apparent useful function. As a result, patients endure debilitating conditions of living, potentially leading to several psychiatric comorbidities such as depression and anxiety (Bair Mj 2003). Conversely, in some genetic pathologies such as congenital insensitivity to pain, the signal is permanently shut off, which results in an inappropriate behavioural response and reduced life expectancy (Nagasako, Oaklander et al. 2003). Pain is the main complaint when visiting emergency departments and represents more than 50% of clinical cases (Cordell, Keene et al. 2002).

Because of its multidimensional aspects, no single definition can easily integrate the diverse features of pain. Hence, definitions already underwent several refinements by The International Association for the Study of Pain (IASP). The last one was proposed in 2008 and described pain as follow: "***An unpleasant sensory and emotional experience associated with actual or potential tissue damage or described in terms of such damage*** ". Thus, pain intensity (sensory) and unpleasantness (emotional) can influence one another and do not only depend on the strength of the damaging stimulus but are also shaped by higher cognitive processes.

1.1.2. History:

Pain is one of the most important individual sensations and was very differently perceived across epochs and as a consequence, many divergent theories to explain it emerged. In the Ancient Greek Civilization, Aristotle believed that pain was a curse originating outside the body and was the result of a divine punishment. The injury was thought to be the entry point of the evil spirit through the body. Hippocrates believed that pain was due to an imbalance in the vital fluids of a human. At that time, it was widely believed that the heart was the central organ for this process.

Figure 1 Descartes pain pathway. The scheme representing a man's foot getting burnt by fire. A hollow tube beginning at the end of the foot and finally reaching the brain was represented as the connection between the noxious stimuli and the place where the alarm rings.

It was not until 1664 and René Descartes that the idea of pain travelling along nerves to eventually reach the brain was accepted. Descartes theorized that the body may be compared to a machine with complex wiring, and that alleviating pain was not necessarily dependent upon the willpower of a god. He rather suggested that pain could be treated by locating and then cutting pain fibers within the body to prevent painful signals to reach the brain. The idea of pain switched from a mystical to a physical experience. In the nineteenth century, a new theory emerged, ***the specific theory***, which stated that pain is an independent sensory pathway, different from touch or other senses. To drive these different modalities, researchers postulated that there exist different kinds of sensory receptors, of nerves and of spinal cord pathways, which are recruited depending on the nature of the stimulus. Another theory was competing with this concept, ***the intensive theory***, which defenders argued that a given nerve fiber could carry distinct sensations such as tick, touch and pain. This theory relied on additive mechanisms; non-noxious stimuli could accumulate, reach a certain threshold and eventually elicit pain signals. Finally, in 1965, ***the gate control theory*** by Ronald Melzack and Patrick Wall emerged, that somehow integrated both the specific and the intensive theories. The novelty of this concept was the postulate that the spinal cord contains a neurological gate that either

blocks pain signals or allows them to continue on to the brain. Non-painful transmission could deplete pain signals by activating an inhibitory interneuron in the spinal cord (Melzack and Wall 1965) (see chapter 1.1.5.1.). Soon after came the discovery of the ***endogenous opioid system***. Reynolds demonstrated that electrical stimulation of the periaqueductal gray matter (PAG) (Reynolds 1969) or the dorsal raphe nucleus (Akil, Mayer et al. 1972) elicits analgesia, an effect that is reversed by administration of the opioid antagonist naloxone (Akil, Mayer et al. 1976). Placebo analgesia is also based on the endogenous opioid system (Levine, Gordon et al. 1978). The next important step was the discovery of pain memory by Clifford Woolf (Woolf 1983) referred to as ***central sensitization***. In his work, Clifford Woolf showed that a peripheral injury led to a maladaptive plasticity in the dorsal horn neurons (decreased threshold, increase of receptive fields, increase of response and spontaneous activity of the central neuron); a mechanism that could explain the transition from acute to chronic pain condition (see chapter 1.3.5). Last but not least, because of the explosion of neurobiological tools, the identification of ***transducers*** became widespread. It started with the identification of Transient receptor potential vanilloid-type 1 (TRPV1) by David Julius (Caterina, Schumacher et al. 1997), a membrane protein responsible for heat sensing. Since then, the discovery of increasing receptors and ion channels has greatly developed.

1.1.3. Role of the peripheral nervous system:

Since Melzack and Wall's theory, many detailed mechanisms have been added to the model, but the general framework remains intact. Pain is initiated by a specific subpopulation of peripheral sensory neurons, called ***nociceptive neurons***, which constitute the primary afferent. Nociceptive neurons get activated when stimulus intensities reach the noxious range. These nerve fibers project on the dorsal horn of the spinal cord, allowing the pain signal to reach the central nervous system. They further follow different spinal cord pathways to reach the brain where they will be processed in the purely sensitive cortex and also in the emotional nuclei of the limbic system. Eventually, the brain can modulate the entrance of pain signals into the central nervous system via descending inhibitory of facilitatory pathways. I will now discuss in more detail the nociceptive pathway. For an extensive review see Almeida *et al*. (Almeida, Roizenblatt et al. 2004).

1.1.3.1 Anatomy and function of nociceptive neurons:

By their capacity to sense potential damaging stimuli, nociceptive neurons represent the first line of defence of the body. They can be found in any area of the body capable of sensing pain, either externally or internally, such as the skin, muscles, internal organs, arterial vessels and so on.

The cell bodies of these neurons are located in the ***dorsal root ganglia*** (***DRG***, Figure 2) or the trigeminal ganglion for the innervations of the face, and have both a peripheral and central axonal branch that project to their target organ and to the spinal cord, respectively. Nociceptive neurons possess four functionally distinct features: (*1*) the free ending, that transduces the external stimuli into an electrical component, (*2*) the axon, that conducts this electrical information, (*3*) the cell body, which is necessary for the machinery to function properly and (*4*) the presynpatic termination that transmits the pain information into the central nervous system.

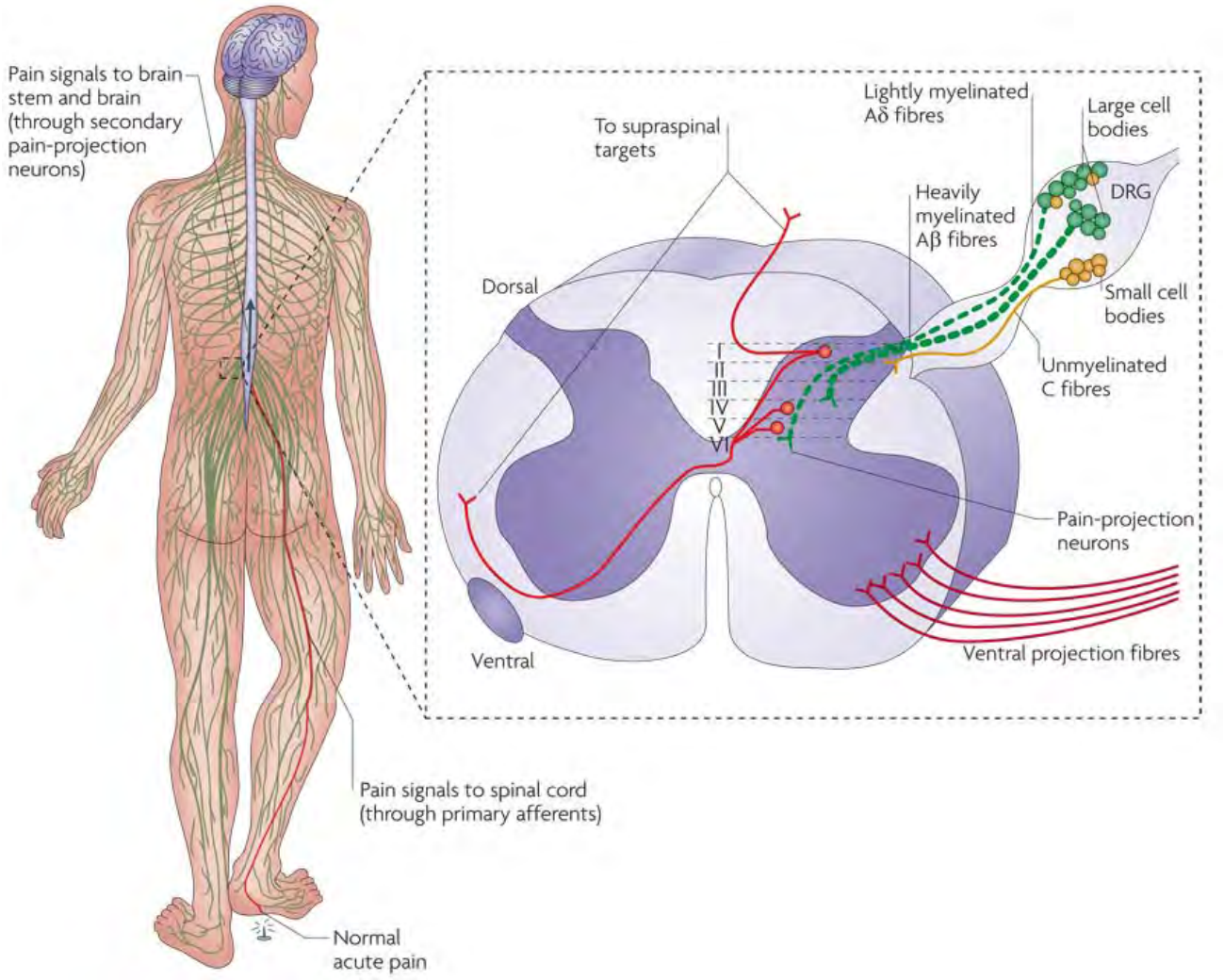

Figure 2. Anatomy of nociceptive neurons. Somatosensory neurons cell bodies are located in dorsal root ganglia (DRGs) located next to the spinal cord. Most nociceptive neurons are unmyelinated and have small diameter axons (C-fibers, yellow) and project to superficial lamina I and II of the dorsal horn. A-fiber nociceptors (Aδ, green) are myelinated with faster conduction velocities and in addition to projecting to superficial lamina I, they also project into deeper lamina V. Modified from (Milligan and Watkins 2009)

1.1.3.2. Fibers:

Nociceptive neurons can be classified into two major classes. The first includes Aδ medium diameter myelinated fibers and convey what is called “fast” pain (the initial component of acute

pain). The other includes small diameter unmyelinated C-fibers, that mediate “slow” pain (Julius and Basbaum 2001). As represented in Figure 2, they project to different layers of the spinal cord.

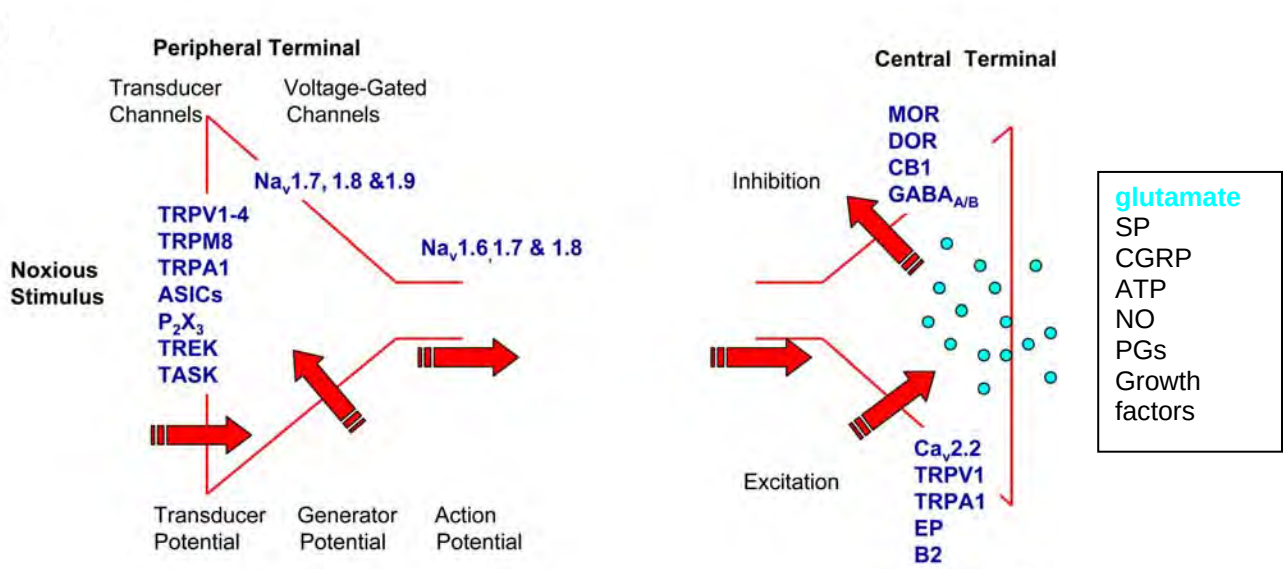

Figure 3. Function of nociceptive neurons. Several high threshold transducers depolarize the cell in response to stimuli until Na_vs generate AP. The axon conducts the AP from the peripheral terminal to the central terminal. The depolarization activates Ca_vs that will lead to calcium influx and ultimately to synaptic transmission. The central terminal also releases multiple regulating molecules. Nociceptive release glutamate as well as multiple synaptic modulators. Modified from (Woolf and Ma 2007).

1.1.3.3. Transducers:

Most of nociceptive neurons are capable of detecting a wide range of stimulus modalities such as heat and mechanical stimulus, and are thus defined as ***polymodal*** (Dubin and Patapoutian 2010). To integrate such variable stimuli, nociceptive neurons express a large variety of ***transducer*** proteins such as receptors and ion channels, each possessing their own specific properties (Figure 3). Nociceptive neurons can thus be classified according to their differential expression of membrane proteins. Transient receptor potential (TRP) vanilloid-type 1 (TRPV1) is responsible for conferring neurons with heat sensitivity. This channel only activates when temperatures are higher than 43 degrees or upon capsaicin (pungent ingredient in chilli peppers) binding whereas TRP melastatin-type 8 (TRPM8) senses cold temperature or menthol (Wang and Woolf 2005). Acid sensing ion channels (ASICs) sense an acidic environment whereas chemical irritants are activating TRP cation channel 1 (TRPA1) receptors (Julius and Basbaum 2001; Fukuoka, Yamanaka et al. 2012). Transducers implicated in mechanical sensation are still under debate and remain to be identified (Wood and Eijkelkamp 2012). For instance, DEG/ENaC channels are important in mechano-transmission in C. elegans, and because they are largely expressed in high- and low-threshold mechanosensitive neurons, the mammalian orthologs acid sensing ion channels (ASICs) were proposed to carry the same function. Knockout animals for these genes have aberrant responses to mechanical stimuli (Price, Lewin et al. 2000; Price, McIlwrath et al. 2001). However, mechanically

evoked currents of cultured DRG neurons in these animals did not show a difference with wild-type mice (Drew, Rohrer et al. 2004).

Nociceptive neuron classification can also be divided into two classes depending on the expression of ***peptidergic genes*** (Nagy and Hunt 1982). Peptidergic neurons are releasing calcitoning gene related peptide (CGRP), substance P (SP) and express tyrosine kinase receptor A (TrkA) while ***non-peptidergic*** neurons express isolecting-binding protein 4 (IB4) (Marmigere and Ernfors 2007). The fact that these two populations project to distinct layers in the dorsal horn, respond to different neurotrophic factors and have different electrophysiological properties suggest different physiological functions (Snider and McMahon 1998; Stucky and Lewin 1999; Braz, Nassar et al. 2005) that remain to be determined.

1.3.3.4. Voltage-gated ion channels:

After being activated at their free endings upon transducers opening, nociceptive neurons further transmit the pain signal by voltage-gated ion channels, which allow the transmission of action potentials (AP) along the axon. Voltage-gated sodium and potassium channels (Na_vs and KCNQ or K_vs) are key players in the generation of AP in neurons, and voltage-gated calcium channels (Ca_vs) play a significant role in synaptic transmission to the spinal cord.

1.3.3.5. Voltage-gated sodium channels:

Voltage-gated sodium channels (***Na_vs***) are responsible for the rising phase of the AP and also regulate neurons resting membrane potential. Sodium currents were first recorded by Hodgkin and Huxley who demonstrated the three principal features of Na_vs: (*1*) voltage-dependent activation, (*2*) rapid inactivation and (*3*) selective ion conductance (Hodgkin and Huxley 1952) which are the indispensable characteristics needed to generate and propagate APs. Upon minor depolarization Na_vs will activate following the “all or nothing” paradigm, generating a fast inward Na+ current. They remain open only for a short time, in the range of a millisecond, and then close thanks to the fast inactivation process. The membrane potential needs to be repolarised for a sufficiently long period for the recovery from inactivation process to occur, which is required to allow generation of a second AP. The previous highlight the three main conformations that Na_vs can undergo: closed, open and inactivated.

Not before 1980 and the emergence of new biochemical methods, were the researchers able to characterize in more details Na_v protein (Beneski and Catterall 1980) and the crystallography structure was only revealed in 2011 (Payandeh, Scheuer et al. 2011). The α-subunit is encoded by a single gene, which is structurally divided into four homologous domains (I-IV) connected by an intra and/or extracellular loop (Figure 4). Each domain is composed of six α-helical transmembrane

segments: S5 and S6 are composing the pore of the channel where as S1 to S4 are identified as being the voltage-sensors.

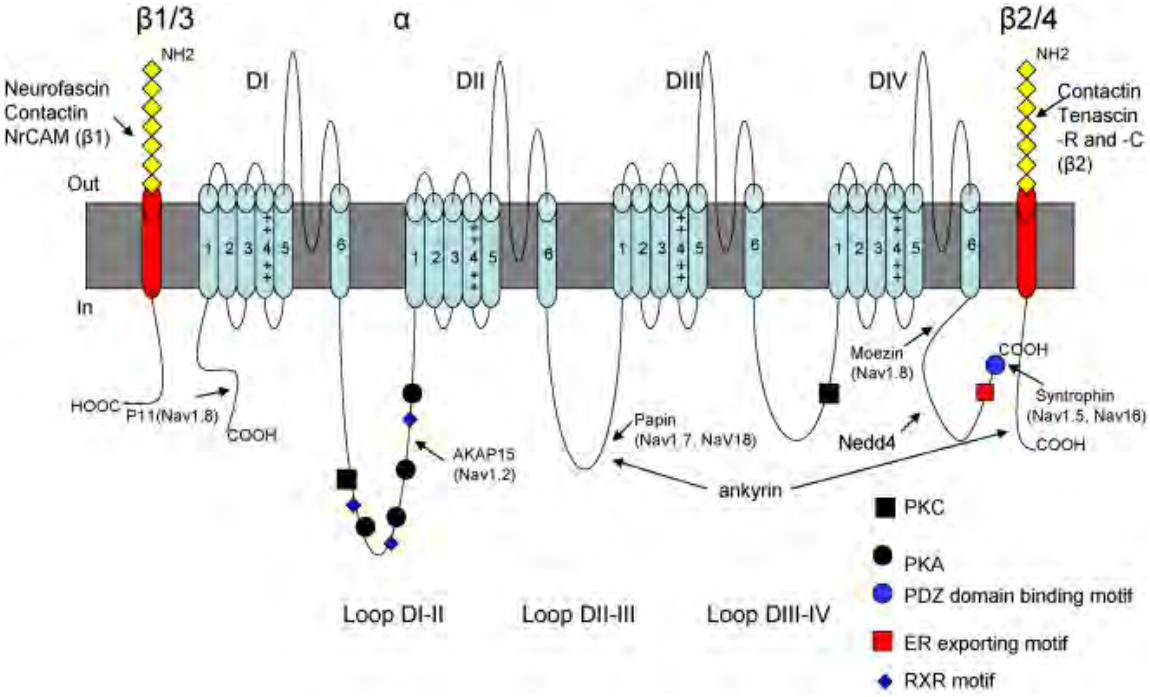

Figure 4. Scheme of the primary structure of Na_v. The α-subunit consists of four homologous domains each containing six trans-membrane domains. β-subunits, and binding site of several other regulatory proteins (see chapter 1.3.4.3 to 1.3.4.8) are also represented. Modified from (Shao, Okuse et al. 2009).

There are nine discrete genes (*SCNxA*) encoding for the α-subunits $Na_v1.1$ to $Na_v1.9$ isoforms (plus another atypical tenth isoform, NaX (Akopian, Souslova et al. 1997)), which are differentially expressed in the sensory system (Figure 5) and present different biophysical properties.

Table 1. Summary of DRG sodium channels

Na^+ channel Isoform	Type (Pharmacology/ kinetics)	Distribution	Unique biophysical characteristics in DRG	Role in AP generation
$Na_v1.1$	TTX-S, fast	Widespread	Unknown	Unknown
$Na_v1.2$	TTX-S, fast	Embryonic	Depolarized activation/inactivation for a TTX-S channel; can produce resurgent current	May maintain firing when misexpressed in MS damaged neurons
$Na_v1.3$	TTX-S, fast	Embryonic	Rapid repriming, ramp current, persistent current	Ectopic firing when misexpressed in axotomy/SCI.
$Na_v1.4$	TTX-S, fast	Not present	N/A	N/A
$Na_v1.5$	TTX-R, fast	Embryonic	Not fully characterized	Unknown
$Na_v1.6$	TTX-S, fast	Widespread	Rapid repriming; persistent current; can produce resurgent current	Maintains high frequency firing when present
$Na_v1.7$	TTX-S, fast	Widespread	Slow onset of inactivation leading to ramp current, slow repriming	Ramp current amplifies small inputs
$Na_v1.8$	TTX-R, slow	Widespread	Very depolarized activation/ inactivation, rapid repriming	Major contributor to action potential upstroke and repetitive firing in small neurons
$Na_v1.9$	TTX-R, persistent	Most small cells (esp. IB4+)	Hyperpolarized activation, overlapping activation/inactivation curves, ultra-slow inactivation	May be involved in setting RMP, amplification of inputs and/or maintaining activation of $Na_v1.8$.

Figure 5. Summary of DRG sodium channels. From (Rush, Cummins et al. 2007)

The different isoforms tightly collaborate to generate electrogenesis in cells. Thus, in addition to myelination, the variable combinations of isoforms, with their own electrical properties, give rise to different conduction velocity in DRG neurons (Rush, Cummins et al. 2007). All isoforms, except $Na_v1.2$, $Na_v1.4$ and $Na_v1.5$, are expressed in DRG nociceptive neurons (Fukuoka and Noguchi 2011; Ho and O'Leary 2011). The slow sodium-dependent activity that can be recorded from nociceptive neurons is due to the presence of slow TTX resistant isoforms ***$Na_v1.8$*** and $Na_v1.9$ (Gaumann, Brunet et al. 1992; Akopian, Sivilotti et al. 1996; Cummins, Dib-Hajj et al. 1999). These neurons also expressed TTX sensitive isoforms $Na_v1.1$, $Na_v1.6$, and ***$Na_v1.7$***, the latter being the most importantly expressed in DRGs (Ho and O'Leary 2011).

Human mutations for the genes coding for $Na_v1.7$ and $Na_v1.8$ are often linked with pathological pain states (Dib-Hajj, Binshtok et al. 2009; Liu and Wood 2011) highlighting their important role in pain transmission. For instance, a loss of function for $Na_v1.7$ leads to congenital insensitivity to pain (Cox, Reimann et al. 2006) and conversely, gain of function for this gene lead to inherited painful channelopathies (Yang, Wang et al. 2004; Fertleman, Baker et al. 2006) such as erythromelalgia and paroxysmal extreme pain disorder.

$Na_v1.7$ produces a fast-activating and -inactivating current as well as a slow-repriming current (Klugbauer, Lacinova et al. 1995) making it not best designed for generating repetitive firing. Furthermore, thanks to its slow closed-state inactivation, it is able to generate ramp current in response to small depolarization (Cummins, Howe et al. 1998). This ability of $Na_v1.7$ to amplify subthreshold stimuli increases the likelihood of a neuron to reach its threshold for firing AP. For this reason, $Na_v1.7$ is considered as a threshold channel. Another characteristic of $Na_v1.7$ is its ability to produce resurgent currents (Jarecki, Piekarz et al. 2010). This current is triggered by repolarization after a strong depolarization and can contribute to the formation of conglomerate APs (burst firing) (Raman and Bean 1997).

$Na_v1.8$, thought to be mostly a sensory specific isoform (Akopian, Sivilotti et al. 1996), presents distinct biophysical properties as compared to $Na_v1.7$. It has slower-inactivating kinetics but a faster repriming rate, which allows it to generate repetitive firing (Renganathan, Cummins et al. 2001). Voltage-dependence of both activation and inactivation is set at depolarized membrane potentials, making $Na_v1.8$ available even at low voltage. Consequently, $Na_v1.8$ is thought to be an important contributor to AP upstroke.

The other TTX resistant isoform, $Na_v1.9$, is preferentially expressed in small diameter DRG neurons (Dib-Hajj, Tyrrell et al. 1998; Tate, Benn et al. 1998) and is presumably associated with nociception (Fang, Djouhri et al. 2006). Because it activates at around -70 mV, it produces a

persistent current that has been proposed to participate in setting resting membrane potential (Herzog, Cummins et al. 2001).

The TTX sensitive isoform $Na_v1.3$ is able to generate relatively large ramp currents in response to slow ramp current depolarisations (Cummins, Aglieco et al. 2001). Because it is not significantly expressed in adult DRG neurons it is unlikely to participate in excitability. However, $Na_v1.3$ was demonstrated to be upregulated in diverse pain states (Waxman, Kocsis et al. 1994; Black, Cummins et al. 1999) and, hence could contribute to reduce the threshold for AP generation. Noteworthy, recovery from inactivation can be up to three times faster than $Na_v1.7$, supporting a role in repetitive firing.

$Na_v1.1$ and $Na_v1.6$ are the two other TTX sensitive isoforms expressed in DRGs, but their role in pain are yet unclear. The regulatory mechanisms of Na_vs will be discussed in chapter 1.3.4.3. to 1.3.4.8., so that they can be put in perspective of neuropathic pain development.

1.3.3.6. Voltage-gated potassium channels:

Voltage-gated potassium channels (***K_vs***) are responsible for the falling phase of AP leading to cell membrane repolarization and hyperpolarization, which results in decrease of cell excitability. Because they do not inactivate at membrane potential, they generate a steady voltage-dependent outward current that is responsible for the stabilization of the membrane potential in the presence of small depolarizing currents. Recent studies in various pain models identified the *Kv7* channels (*KCNQ*) as important players in pain pathways (Lawson 2006). *Kv7* genes encode for homotetrameric proteins and are composed of five different members, $K_v7.1$ to $K_v7.5$; and out of these five only one is excluded from the nervous system ($K_v7.1$) (Jentsch 2000). It has been found that the anticonvulsant drug retigabin increases potassium current and reduces the transmission of Aδ and C-fibres into the spinal cord (Passmore, Selyanko et al. 2003), concomitantly with the hyperpolarization of the primary afferent (Rivera-Arconada and Lopez-Garcia 2006). More recently, retigabin has been found to attenuate C-fiber activity triggered by heat stimulation in humans (Lang, Fleckenstein et al. 2008) suggesting that enhancement of K_vs activity might be of therapeutic potential. However, the role of K_vs has only been sparsely investigated in pain so far.

1.3.3.7. Voltage-gated calcium channels:

Voltage-gated calcium channels (***Ca_vs***) (Catterall, Perez-Reyes et al. 2005) play several crucial physiological roles by modulating synaptic plasticity, neurotransmitter release and gene transcription to cite a few. When arriving at the central terminals of the primary afferent, AP cause a membrane depolarization that will activate Ca_vs allowing calcium influx, which in turns triggers synaptic vesicle exocytose. Glutamate and other multiple neurotransmitters will thus be secreted

and participate in transmission and modulation of spinal sensory signals (Figure 3). Ca_vs can be divided into two classes based on their voltage activation characteristic: low voltage-activated, known as T-type and high voltage-activated, represented by L, N, P/Q and R-type channels. Ten different $Ca_v\alpha$ subunits have been identified in mammals and are further associated with modulatory $\alpha_2\delta$, β and γ subunits accounting for remarkably large possible combinations.

Because these different classes exhibit different biophysical properties, they are specialized in distinct aspects in the processing of pain. For instance N-type channels such as $Ca_v2.2$ are largely found in superficial lamina of the spinal cord and blocking this channel gives rise to analgesic effects (Cao 2006). T-type channels are also found in DRGs, where $Ca_v3.2$ is the most predominantly expressed and presumably enhance sensory neurons excitability, possibly contributing to amplify pain transmission (Messinger, Naik et al. 2009). Drugs targeting these channels are of increasing interest even though finding specific blockers might represent an immense challenge for the drug developers. For a review on Ca_vs see (Park and Luo 2010) (see also chapter 1.3.7.).

1.1.4. Role of ion channels and Channelopathies:

In the previous chapter I discussed properties and function of several ion channels that are selectively expressed in nociceptive neurons, and some of them are also expressed in higher structures of the pain pathways. These players (Figure 6) have been demonstrated to have a role in pain generation or maintenance by using both genetically-modified animals and screening for human mutations. In some cases, theses mutations can lead to different pathological pain symptoms. Mutations can occur in transduction, transmission (axonal or synaptic) or modulatory mechanisms. An extensive review of these mutations and their consequences can be found in (Cregg, Momin et al. 2010).

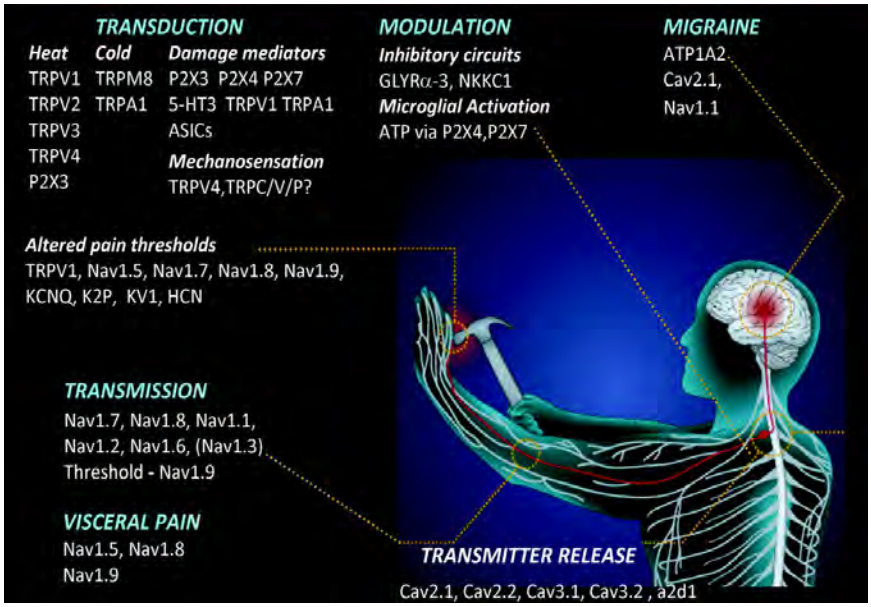

Figure 6. Ion channels associated with pain syndromes. The ion channels were identified using genetically-modified mice and monogenic human diseases. Ion channels are classified by the principal deficits they produce in pain pathways. These deficits can occur at different stages. Ion channels responsible for migraines and visceral pain are also shown. From (Cregg, Momin et al. 2010)

1.1.5. Role of the central nervous system:

1.1.5.1 Central terminal of nociceptive neurons and the spinal cord:

Central afferents of primary sensory neurons project in the dorsal horn of the spinal cord. The grey matter of the spinal cord can be divided into 10 laminas defined by distinct electrophysiological and cytoarchitectural properties. Nociceptive neurons from Aδ fibres project mainly to lamina I, and to a lesser extent on lamina V, whereas C-fibers project specifically to ***lamina I and II***, accounting for a notable specific somatotopic projections (Figure 2 and (Almeida, Roizenblatt et al. 2004)). The specificity of this stratification is further highlighted by projections of peptidergic and non-peptidergic afferents; the first category exclusively projects to layer I and dorsal part of layer II where as the second project exclusively to the mid-region of layer II (Snider and McMahon 1998). Nociceptive neurons synthesize a diversity of substances that are involved in the central transmission of pain signal (Figure 3). Glutamate and other excitatory amino acids (EAAs) are of critical importance at the synapse, but other regulatory substances such as substance P, calcitonin gene-related peptide (CGRP), adenosine triphosphate (ATP), nitric oxide (NO), phospholipid metabolites such as prostaglandins (PGs) and several neurotrophins (growth factors) are involved in the fine tuning of synaptic transmission. Inhibitory (glycinergic and GABAergic) and excitatory interneurons further participate in the modulatory input of primary afferents into the central nervous system. Last but not least, two players found in the dorsal horn are the glial (astrocytes) and microglial cells (immune cells) that can also modulate synaptic transmission, mostly via the release of small molecules and by scavenging synaptic cleft neurotransmitters (Basbaum, Bautista et al. 2009).

1.1.5.2. Ascending pathways:

Neurons within laminae I and V constitute the major output projecting to the brain (Basbaum and Jessell, 2000). These second-order neurons are at the origin of multiple ascending pathways, with two important tracts: the ***spinothalamic tract***, which carries pain messages to the thalamus and brainstem and accounts for the sensory-discriminative aspects of pain, and the ***spinoreticulothalamic tract*** implicated in both the emotional and the sensory component of pain by its projection to the parabrachial nuclei, which further connect to nuclei of the limbic system (Figure 7). Many other spinal pathways exist such as spinomesencephalic, spinohypothalamic or spinocervical (Almeida, Roizenblatt et al. 2004).

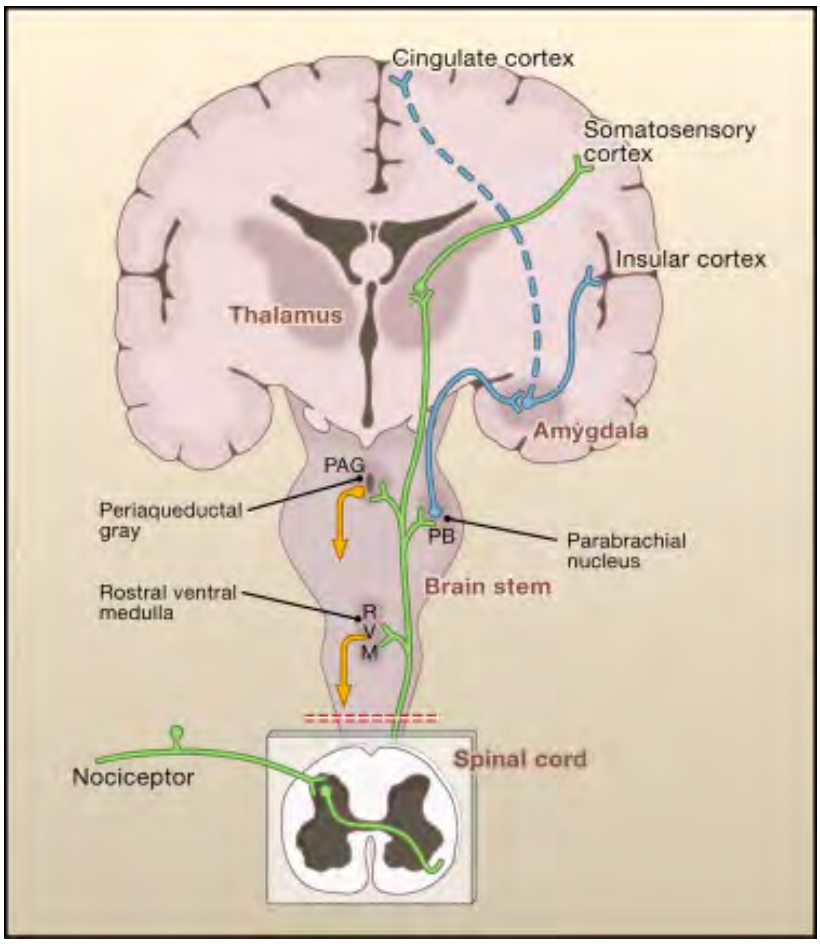

Figure 7. Spinothalamic and spinoreticulothalamic tract. Two main pathways convey the information from the second-order neuron to the brain. A first subset of these projection neurons transmits information to the somatosensory cortex via the thalamus (in green), providing information about the location and intensity of the painful stimulus. The other subset of neurons project to the cingulate and insular cortices via connections in the brainstem (parabrachial nucleus) and amygdala, contributing to the affective component of the pain experience. This ascending information also accesses neurons of the rostral ventral medulla and midbrain periaqueductal gray, which can further engage descending feedback pathways that regulate the input into the second order neuron. From (Basbaum, Bautista et al. 2009)

1.1.5.3. Brain:

First and second-order neurons will ultimately project to subcortical and cortical structures. There is no single brain area implicated in pain (Apkarian, Bushnell et al. 2005) but rather an activation of largely distributed structures and nuclei in the brain, the so-called ***pain matrix***. Some of these structures are typically specialized in sensory-discriminative modality such as the somatosensory cortex, and others are implicated in the emotional aspect of pain such as the amygdala, the hippocampus or the cingulate cortex. Even structures implicated in more cognitive functions such as the prefrontal cortex, are activated upon pain stimulation and might also be implicated in regulating pain signal processing in the brain (Tracey and Bushnell 2009).

The brain is also involved in descending pain modulation (Figure 7). The structures responsible for this modulation are multiple, including the hypothalamus, the amygdala or the rostral anterior cingulate cortex (rAAC). They project on the periaqueductal gray region and then to the rostra ventromedial medulla (RVM), making these two areas the main relays before these projections reach dorsal horn neurons. These descending circuits are mostly noradrenergic and serotoninergic and are opioid-sensitive (Ossipov, Dussor et al. 2010). These “Top-down” modulatory pathways have been shown to underlie the clinically important phenomenon of placebo effect.

1.1.6. Nociception pharmacology:

Many drugs have been developed to treat pain across ages. Opium as probably been used for more than 5000 years to alleviate pain. Acetylsalicylic acid - ***aspirin*** - was patented in 1897 by Bayer, but the use of plant extracts, including willow bark and spiraea, containing salicylic acid was probably used since way longer to treat pain and fever. More recently, ***paracetamol*** was developed and is nowadays the most widely used medication to alleviate pain. However, its mechanism of action is still largely unknown and probably targets several different pronociceptive molecules. Prostanoids, metabolites of arachidonic acid through the ***cyclooxygenase*** (COX) pathway, are the best known lipid mediators that contribute to pain. The COX enzymes are described to be present in at least three versions, the best studied ones being COX1 and COX2. COX1 is constitutively expressed and has several physiological functions such as regulating blood fluidity (palettes aggregations) and blood pressure (vasodilatation, vasoconstriction). COX2 is induced in inflamed tissue and leads to prostalglandin E2 (PGE2) production. PGE2 is significantly involved in pain pathways, but also in inflammation and fever. Thus, many analgesics, including paracetamol, target the arachidonic acid pathway, often via COX inhibition. The non-steroidal anti-inflammatory analgesics (***NSAIDS***) are widely used medications. They are divided into two subclasses, the non-selective NSAIDS, which inhibit both COX2, leading to analgesic effect but also COX1, making it also responsible for multiple side effects. A more recent class specifically inhibits COX2, the selective NSAIDS and as a consequence mediates fewer side effects. Aspirin and ibuprofen are typical members of the NSAIDS.

Opioids bind to specific opioid receptors, disseminated throughout the nervous system and other tissues. There are three principal classes of opioid receptors, μ, κ, δ (Massotte and Kieffer 1999). They are all inhibitory G-protein coupled receptors (GPCRs) and thus elicit inhibitory responses upon ligand binding. Noteworthy, each receptor elicits specific intracellular pathway and different neuronal responses. As a consequence, and because of their ubiquitous expression in the nervous system, opioids influence on numerous physiological functions such as reward, stress, mood, respiration and gastrointestinal motility. For these reasons, opioids are known to have many side effects. There exist a multitude of endogenous ligands synthesized by the body. All these agonists also elicit different signalling and trafficking pathways leading to alternative internalization and desensitization mechanisms, highlighting the complexity of the opioidergic system. Extensive review on the current knowledge of opioids agonists and their receptors can be found in (Pradhan, Smith et al. 2012).

Local anaesthetics drugs act by blocking Na_vs, preventing the pain signal to reach to central nervous system. Local anaesthetics bind more readily to Na_vs that are in the inactivated state and are thus more effectively blocking neurons that fire, a process referred to as state dependent

blockade. The site of binding is thought to be located in an intracellular portion of the sodium channel (Ragsdale, McPhee et al. 1994).

The WHO (World Health Organization) classifies the use of analgesics by levels; the pain ladder. The first level is composed of non-opioid analgesics. The second step is the use of weak opioids (codein and tramadol) and finally strong opioids (morphine and derivatives) are recommended for the third step. Other molecules acting as Na_vs blockers (e.g. tricyclic antidepressants and anticonvulsants) or Ca_vs modulators (e.g. gabapentinoids) are also available but are rather used to treat chronic pain. These so called ***adjuvant pharmacological agents*** will thus be discussed in chapter 1.3.7.

1.2. Types of Pain:

Nociceptive pain is an essential physiological warning against damages which is mediated by high threshold primary sensory neurons. If the damage occurred anyway, the injury and the subsequent inflammation will lead to the sensitization of the nociceptive system (Woolf and Salter 2000), resulting in ***inflammatory pain***. The expression of inflammatory pain is therefore linked to the persistence of inflammation, but should fade away when tissue is healed. ***Neuropathic pain*** results from damage to the nervous system and becomes persistent after the apparent resolution of initial insult. A fourth type of pain, ***dysfunctional pain***, that includes fibromyalgia and tension type headache, is present even when no injury is detected and is thought to be due to a central abnormal process of pain inputs, but the exact mechanisms remain unknown. In the upcoming chapters, I will discuss neuropathic pain in more details.

1.3. Neuropathic pain:

1.3.1. Definition:

Neuropathic pain (NP) as defined by the IASP is a "***Pain caused by a lesion or disease of the somatosensory nervous system***" (Loeser and Treede 2008). It may appear in the context of many different diseases such as multiple sclerosis, diabetic neuropathy, stroke, cancer or nerve injury. This highlights the several distinct etiologies that neuropathic pain presents (Ducreux, Attal et al. 2006) and suggests that more than one mechanism may be responsible for generating multifaceted neuropathic pain symptoms (Woolf 2004; Scholz, Mannion et al. 2009). Conversely, among different neuropathic pain etiologies, some mechanisms might be common (Woolf and Decosterd 1999). Among neuropathic pain conditions, mononeuropathy has the highest incidence rate (Dieleman, Kerklaan et al. 2008), highlighting the clinical importance of nerve injury. Compression of roots by disk hernia is a common feature of neuropathic pain, and diabetic peripheral neuropathy

and post-herpetic neuropathy are also important contributors to the development of neuropathic pain. Nevertheless, a rule of this pathology is that it must directly involves the nociceptive pathways (Boivie, Leijon et al. 1989) and is the manifestation of maladaptive plasticity in the nervous system.

Figure 8. « La Columna Rota » (the Broken Spine). A self-portrait of Frida Kahlo (a Mexican painter) who suffered from chronic pain all her life after being injured in a serious car accident when she was 18 years old.

1.3.2. Epidemiology:

Neuropathic pain is estimated to affect more than 75 million people worldwide with poor success in alleviating pain (Brower 2000). Epidemiological studies from different countries and on different numbers of patients report varying prevalence rates for neuropathic pain. A large study performed in more than 30'000 individuals of the French population reported that around 20% of patients suffered from moderate to severe chronic pain and that one third of these patients, i.e. 7% of the population presented neuropathic characteristics (Bouhassira, Lanteri-Minet et al. 2008). The prevalence of chronic pain increased with age, and was significantly higher for females (Perquin, Hazebroek-Kampschreur et al. 2000) and depends on genetic background (LaCroix-Fralish and Mogil 2009). ***Comorbidities*** such as depression, anxiety and poor sleep are often observed in patients suffering from neuropathic pain (Turk, Audette et al. 2010) as well as work incapacity.

1.3.3. Mechanisms:

Neuropathic pain is associated with a ***hyperexcitability*** of the central and the peripheral nervous systems, resulting in ***ongoing pain***, ***allodynia*** (innocuous stimuli that become painful), ***hyperalgesia*** (exaggerated and prolonged pain response in response to noxious stimuli) and negative symptoms such as ***hypoalgesia***. Increased neuronal activity can explain both spontaneous and exaggerated stimulus-evoked pain. First, a process of peripheral sensitization generates an hyperexcitability of peripheral sensory neurons evoking a primary neuropathic pain. The second step is the central sensitization mediated by increased synaptic strength between first and second order neurons, presumably triggered by increased electrical input among other molecular mechanisms. Central sensitization also involves glial reaction and loss of interneuron inhibition (see chapter 1.3.5.).

1.3.4. Peripheral sensitization:

Peripheral sensitization occurs during and after peripheral inflammation and is due to the modification of the chemical environment and the accumulation of factors secreted by nociceptive neurons or by recruited cells such as mast cells, inflammatory cells and keratinocytes. These factors are of diverse origins but include protons (H+), nerve growth factors (NGF), cytokines (such as IL-1β, IL-6), tumor necrosis factor alpha (TNFα), prostaglandins (PGE2), several neurotransmitters (serotonin, ATP), peptides (SP, CGRP). This mixture is commonly referred to as "***the inflammatory soup***" (Basbaum, Bautista et al. 2009). When binding their targets, these molecules will activate multiple intracellular pathways including Protein Kinase C (PKC) (Hucho, Dina et al. 2005), Protein Kinase A (PKA) (Varga, Bolcskei et al. 2006), phosphoinositide 3-kinase (Pl3K) (Malik-Hall, Dina et al. 2005), and the Mitogen-activated protein (MAP) kinase ERK (Jin and Gereau 2006), among others. Two of the concrete effect of these cascades are the phosphorylation of TRPs (Mantyh, Koltzenburg et al. 2011) and Na_vs (Dib-Hajj, Cummins et al. 2010). This leads to increased neuronal excitability (Woolf and Ma 2007) by reducing its threshold and increasing its responsiveness. As a result, low-intensity stimuli may activate the nociceptive pathway. Once the inflammation fades away, these mechanisms should also disappear. However, in some cases, pronociceptive molecules are found long-lastingly in the site of injury, such as NGF and cytokines (Leung and Cahill 2010; Dogrul, Gul et al. 2011; Gaudet, Popovich et al. 2011) that can produce long-term changes. The case of TRPV1, illustrates these mechanisms. After nerve injury and diabetic neuropathy, TRPV1 is long-lastingly upregulated in sensory fibers (Hudson, Bevan et al. 2001; Pabbidi, Yu et al. 2008) and was demonstrated to be associated with pain hypersensitivity. In addition, this receptor begins to be expressed in large myelinated A-fibers (Hong, Agresta et al. 2008) a process referred to as ***phenotypic switch*** (Ueda 2006). By inducing profound changes in gene expression (Costigan, Befort et al. 2002), peripheral sensitization can confer to neurons a new molecular identity. For instance, substance P (SP) or brain-derived neurotrophic factor (BDNF), normally only expressed in nociceptive neurons, start to also be synthesized by Aβ-fibers (Malcangio, Ramer et al. 2000; Fukuoka, Tokunaga et al. 2002).

1.3.4.1. Spontaneous discharge:

A common aspect of neuropathic pain is the presence of pain in the absence of any identified stimulus. Spontaneous pain arises as a result of ectopic activity in the peripheral nervous system, driven by C-fibres (Djouhri, Koutsikou et al. 2006) and A-fibers (Liu, Wall et al. 2000). This spontaneous electric activity can originate from the site of injury (England, Gamboni et al. 1993; England, Happel et al. 1996), from both injured and non-injured DRG neurons (Wall and Devor 1983; Liu, Wall et al. 2000; Wu, Ringkamp et al. 2001; Ma, Shu et al. 2003; Zhang, Zhou et al.

2004; Amir, Kocsis et al. 2005; Djouhri, Koutsikou et al. 2006) or from along the axons (Devor, Govrin-Lippmann et al. 1993). Because local anesthetics suppress ectopic discharges and attenuate allodynia and hyperalgesia (Mao and Chen 2000; Suter, Papaloïzos et al. 2003; Scholz, Broom et al. 2005), sodium channels are thought to play an important role in the generation of ectopic activity. Other channels such as potassium channels KCNQ18 and KCNK10 (Tulleuda, Cokic et al. 2011) or K_vs (Kim, Choi et al. 2002), cation-nonselective, cyclic nucleotide-modulated channels (HCNs) (Lee, Chang et al. 2005) and Ca-activated chloride channels (CaCCs) (Hilaire, Campo et al. 2005) were demonstrated to be modulated after neuropathic pain and proposed to play a role in spontaneous discharges.

1.3.4.2. Implication of Na_vs in neuropathic pain:

It has long been known that Na_vs, by modifying the intrinsic electrical properties of neuronal membranes, are largely accountable for the neuropathic pain-associated hyperexcitability (Matzner and Devor 1994; Zhang, Donnelly et al. 1997). It is thought that a modification of the kinetics or the biophysical properties of the Na_vs after nerve injury is probably due to a change of expression of the different isoforms (Dib-Hajj, Cummins et al. 2010). This modification of expression can also account for the spontaneous membrane potential oscillation leading to a reduction in the firing threshold, which in turns is involved in the spontaneous activity of sensory neurons (Amir, Michaelis et al. 1999).

Altogether, these observations point out the importance of Na_vs in the development of neuropathic pain, yet which isoforms take part and how they are implicated, remains largely unknown.

$Na_v1.7$:

Despite its evident role in human pathological pain, $Na_v1.7$'s role in neuropathic pain is still equivocal. For instance, $Na_v1.7$ mRNA was reported to be reduced after SNI in rats (Berta, Poirot et al. 2008). However, transcriptional levels do not necessarily reflect the expression of functional proteins. Reduced levels of $Na_v1.7$ were also reported in human studies after nerve injury (Coward, Aitken et al. 2001). Contrasting with these observations, protein level of $Na_v1.7$ is increased in a model of diabetic neuropathy (Hong, Morrow et al. 2004) as well as in human painful dental pulp (Luo, Perry et al. 2008). The nociceptor-specific knockout of $Na_v1.7$ does not prevent mice from developing neuropathic pain-mediated mechanical allodynia (Nassar, Stirling et al. 2004) but rather appears to be important for inflammatory and acute pain. Gain-of-function mutations of $Na_v1.7$ were recently reported to be associated with painful peripheral neuropathy syndromes (Faber, Hoeijmakers et al. 2012). Further evidence of its role in inflammatory pain, rather than neuropathic pain, was demonstrated by knocking-down $Na_v1.7$ with a viral vector in primary afferents leading

to an attenuated development of hyperalgesia (Yeomans, Levinson et al. 2005). Other studies have reported an increase of $Na_v1.7$ expression after injection of pro-inflammatory mediators (Gould, Gould et al. 2000; Black, Liu et al. 2004). Rather than being implicated in neuropathic pain by virtue of expression in the sensory system, $Na_v1.7$ was recently reported to play an important role in neuropathic pain in lumbar sympathetic ganglion neurons (Minett, Nassar et al. 2012).

$Na_v1.8$:

$Na_v1.8$ was reported to be downregulated in terms of mRNA (Berta, Poirot et al. 2008), protein (Decosterd, Ji et al. 2002) and currents (Cummins and Waxman 1997; Berta, Poirot et al. 2008) in rat neuropathic pain models. Several explanations have been proposed to explain how a decrease of $Na_v1.8$ could contribute to hyperexcitability. It was proposed that a high induction of translation in order increase *de novo* protein synthesis or the translocation of the Na_vs mRNA in the sciatic nerve could account for the reduction of $Na_v1.8$ mRNA. In terms of protein, the decrease of $Na_v1.8$ could be due to redistribution of the Na_vs proteins into uninjured neurons or along the sciatic nerve (Gold, Weinreich et al. 2003). In apparent contradiction with the above mentioned studies, another group reported an increase of $Na_v1.8$ mediated current (Abdulla and Smith 2002). The nociceptor-specific knockout of $Na_v1.8$ (Akopian, Souslova et al. 1999) demonstrated the importance of this isoform for sensing thermal, mechanical and inflammatory pain, but again authors reported no evidence for an implication in neuropathic pain (Kerr, Souslova et al. 2001). This was also confirmed by using diphtheria toxin to kill sensory neurons expressing $Na_v1.8$ where animals exhibited normal development of neuropathic like symptoms (Abrahamsen, Zhao et al. 2008). However another study also using knockout mice line showed little implication of $Na_v1.8$ in neuropathic pain (Leo, D'Hooge et al. 2010). In line with this, knocking down $Na_v1.8$ using small interfering RNA (Dong, Goregoaker et al. 2007) or specific antisense oligodesoxynucleotides (Lai, Gold et al. 2002) reversed mechanical allodynia in neuropathic rats. It is likely that $Na_v1.8$ involvement depends on the type of lesion and the model of chronic pain (Joshi, Mikusa et al. 2006).

$Na_v1.3$:

Many studies reported an increase of mRNA for $Na_v1.3$ in DRG using different experimental pain model (Waxman, Kocsis et al. 1994; Berta, Poirot et al. 2008), concomitant with an increase of the repriming rate of TTX sensitive currents, typical of $Na_v1.3$ biophysical properties (Cummins and Waxman 1997). The implication of $Na_v1.3$ was confirmed in a study using antisense nucleotides to silence this isoform, which attenuated neuropathic like symptoms as well as ectopic discharges. However, the $Na_v1.3$ knockout mice developed normal neuropathic pain-like sysmptoms (Nassar, Baker et al. 2006).

$Na_v1.9$:

$Na_v1.9$ role is also subject to discussion, but it is thought to play a role in inflammatory pain rather than neuropathic pain as observed with the knockout mice line (Amaya, Wang et al. 2006).

$Na_v1.1$ and $Na_v1.6$:

The function of $Na_v1.1$ or $Na_v1.6$ is poorly understood and their implication in pathological pain conditions has never been investigated in detail. A study of Black *et al.* (Black, Liu et al. 2004) showed that neither $Na_v1.6$ nor $Na_v1.1$ were altered after carrageenan injection.

1.3.4.3. Regulation and trafficking of Na_vs:

Controlling Na_v channel expression will impact on cellular excitability and involves the participation of multiple players (Figure 4). Mechanisms of transcriptional and translational regulation to control Na_v channel expression have already been described (Diss, Fraser et al. 2004). Na_vs are designated to sense membrane potential oscillations, which lead to their opening and depolarizing Na+ influx. Consequently, only when anchored at the membrane are Na_vs functional. However, not solely membrane anchored channels are present in a cell, there is also large pool of intracellular Na_vs in a cell that can be rapidly recruited to the membrane when necessary (Schmidt, Rossie et al. 1985; Ritchie, Black et al. 1990). This pool may serve as a reserve and permits a neuron to respond rapidly to any kind of stimuli, allowing the increasing of channel surface expression faster than *de novo* synthesis would otherwise allow.

Thus, tight balance between membrane anchored and intracellular pool, a process referred to as trafficking, is crucial for controlling cellular excitability. Maintaining this equilibrium is mediated by multiple enzymes, auxiliary subunit and partner proteins (Cusdin, Clare et al. 2008) that will be specialized in internalization or in stabilization of Na_vs at the membrane. I will discuss some of these regulatory mechanisms in the upcoming chapters.

1.3.4.4. Regulation by partner proteins:

Contactin (Ranscht 1988), which is a glycosyl-phosphatidylinositol (GPI)-anchored glycoprotein acting as an adhesion protein, is known to interact with sodium channels *in vitro* (Kazarinova-Noyes, Malhotra et al. 2001) and *ex vivo* (Rush, Craner et al. 2005), leading to a modification of Na^+ current densities. Many other proteins such as ankyrin (Malhotra, Kazen-Gillespie et al. 2000), spectrin (Bennett and Baines 2001), dystrophin and syntrophin (Gee, Madhavan et al. 1998; Abriel and Kass 2005) also modulate cell surface expression of Na_v isoforms. Ankyrin was already investigated following peripheral nerve injury (Kretschmer, Nguyen et al. 2002). The authors

proposed that this altered expression of ankyrin lead to the recruitment and clustering of $Na_v1.7$ and $Na_v1.8$ in neuromas, and might be responsible for neuropathic pain-associated hyperexcitability. Obviously, these interactions are often more complex and involve multiple players. Highlighting this, contactin interaction with ankyrin and β-subunits was shown to be necessary for $Na_v1.2$ to be expressed at high density at the plasma membrane (McEwen, Meadows et al. 2004). It is also known that syntrophin and dystrophin are acting as a complex to regulate $Na_v1.5$ membrane expression (Gavillet, Rougier et al. 2006). However, these proteins, and others (Shao, Okuse et al. 2009), have only been sparsely investigated in terms of neuropathic pain.

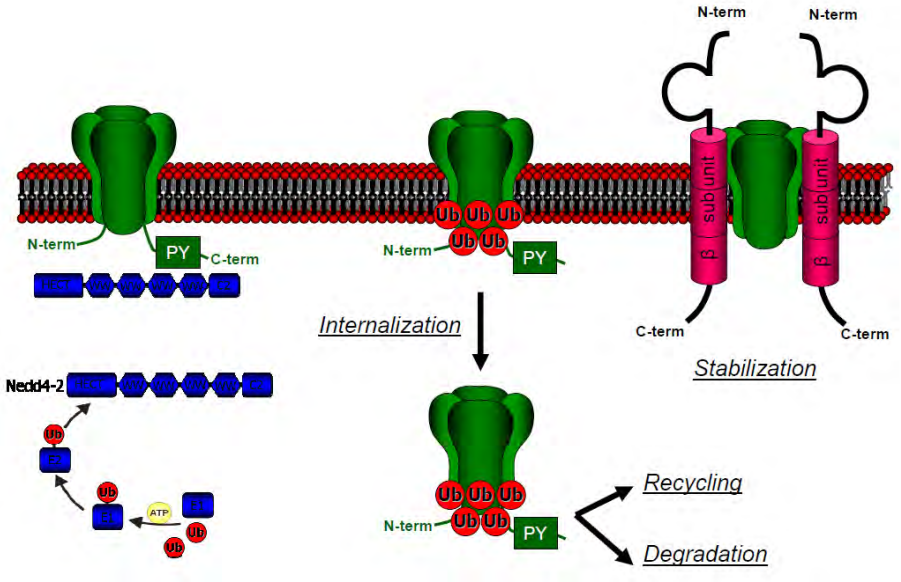

Figure 9. Two mechanisms involved in Na_v turnover are shown in this scheme; the Nedd4-2 internalizing pathway and the β-subunit stabilizating pathway. The specific interaction takes place between one of Nedd4-2 WW domain and Na_vs PY-motif, which leads to the channel internalization. Once internalized, the channels may be directed toward a degradation pathway or recycled back to the plasma membrane.
β-subunits stabilize the channel at the membrane and modify Na_v gating properties via direct physical interference with the voltage-sensors.

1.3.4.5. Na_vs β-subunits:

The β-subunits are multifunctional as they participate in cell-cell adhesion and cell migration, they interact with extracellular matrix and cytoskeleton molecules (Isom 2001). There are currently four different identified genes coding for the different β-subunits; *SCN1B* that codes for β1 (Isom, De Jongh et al. 1992) and its associated splice variant β1A (Kazen-Gillespie, Ragsdale et al. 2000) which is known to be secreted, *SCN2B* that codes for the β2 (Isom, Ragsdale et al. 1995), *SCN3B* for β3 (Morgan, Stevens et al. 2000) and *SCN4B* for β4 subunit (Yu, Westenbroek et al. 2003). These subunits are composed of an extracellular immunoglobulin-like in the N-terminal region, a single transmembrane segment and an intracellular carboxyl terminus tail (Isom, De Jongh et al. 1992). β1 and β3-subunit interaction with the α-subunit occurs via a non-covalent link (Hartshorne, Messner et al. 1982). This interaction occurs via the extracellular loop of the β-subunit and involves multiple interaction sites (Qu, Rogers et al. 1999), identified as charged residues (McCormick, Isom et al. 1998) but also involves the C-terminal cytoplasmic tail of β1 for the interaction to occur

(Meadows, Malhotra et al. 2001; Yu, Ko et al. 2005). β2 and β4-subunits are associated with the α-subunits via disulfide bonds (Hartshorne, Messner et al. 1982; Messner and Catterall 1985; Yu, Westenbroek et al. 2003) through their extracellular immunoglobulin-like structure, and the residues responsible for these interactions were recently identified (Chen, Calhoun et al. 2012). The assumed stoichiometry for α-β association is 1:1 (Catterall 1992).

The pore-forming α-subunit is by itself functional and thus sufficient to allow Na+ conductance, but β–subunits can modulate the biophysical properties and the cell membrane stabilization of Na_vs (Figure 9) (Isom, Scheuer et al. 1995). The mechanism by which β-subunits regulates α-subunit gating properties is driven by direct interaction that interferes with the voltage-sensor (Zimmer and Benndorf 2002). The effects of the different β-subunits on biophysical properties put in light conflicting results depending on the cell type used (i.e. *Xenopus* oocytes and mammalian cell lines, (Nuss, Chiamvimonvat et al. 1995; Sangameswaran, Fish et al. 1997; Smith and Goldin 1998; Morgan, Stevens et al. 2000; Fahmi, Patel et al. 2001; Vijayaragavan, O'Leary et al. 2001; Zimmer and Benndorf 2002; Vijayaragavan, Powell et al. 2004)) and are presumably due to differential endogenous β-subunits expression as well as other partners (Meadows and Isom 2005) endogenously present.

β-subunits can also affect current in *ex vivo* cell culture as highlighted by I_{Na} current recorded from *SCNB* knockout animals (Lopez-Santiago, Pertin et al. 2006; Lopez-Santiago, Brackenbury et al. 2011). Our laboratory previously reported an increase of β2 subunit following nerve injury-induced neuropathic pain (Pertin, Ji et al. 2005). Moreover, β1 and β3-subunits were also reported to be increased in pathological pain (Shah, Stevens et al. 2000; Coward, Jowett et al. 2001) and could thus be implicated in modulating cellular excitability. Confirming this hypothesis, sensory neuron knockout of β2 subunit led to an attenuation of mechanical allodynia development after neuropathic pain (Pertin, Ji et al. 2005).

1.3.4.6. Post-translational regulation:

Several post-translational mechanisms were reported to regulate Na_v surface expression (Figure 4). The protein kinase (PK) pathways is a well documented regulatory mechanisms of membrane Na_vs regulation (Shao, Okuse et al. 2009) principally mediated by PKAs (Zhou, Shin et al. 2002; Carr, Day et al. 2003; Vijayaragavan, Boutjdir et al. 2004; Chen, Yu et al. 2006), PKCs (Cantrell, Tibbs et al. 2002; Tateyama, Kurokawa et al. 2003; Vijayaragavan, Boutjdir et al. 2004), Ca2+, calmodulin (CaM) and Ca2+-dependent CaM kinase II (CaMKII)(Biswas, Deschênes et al. 2008). The effects on peak current or on biophysical properties of PKAs and PKCs, the sites of phosphorylations and the sodium channels isoforms have been extensively studied (Chahine, Ziane

et al. 2005). The role of these PKs was already demonstrated to be implicated in the development of chronic pain as discussed in chapter 1.3.4.

1.3.4.7. Glycosylation:

Another important post-translational modification affecting sodium channel function is glycosylation. In the ER and the Golgi, Na_v α-subunits undergo extensive sequential glycosylation (Waechter, Schmidt et al. 1983; Schmidt and Catterall 1987), a process involving the addition of *N*-acetylglucosamine which are capped by sialic acid residues and sequential addition of oligosaccharide chains. Glycosylation can represent up to 30% of the α-subunit molecular weight (Messner and Catterall 1985) with an estimated stoichiometry of up to 100 sialic acid molecules per channel (James and Agnew 1987). Glycosylation serves various functions such as protein folding, cell signalling, cell-cell adhesion and regulation, as well as being implicated in development and immunity (Moremen, Tiemeyer et al. 2012). Glycosylation is known since long to influence on the Na_v α-subunit by modifying the voltage dependence of gating properties (Recio-Pinto, Thornhill et al. 1990; Bennett, Urcan et al. 1997; Zhang, Hartmann et al. 1999; Tyrrell, Renganathan et al. 2001), probably by interfering with the electric field near gating sensors (Bennett, Urcan et al. 1997; Cronin, O'Reilly et al. 2004). It was proposed that the extracellular sialic acid residues, which are negatively charged at physiological pH, influence on how much the voltage sensor domains sense the transmembrane electrical potential difference (Ednie and Bennett 2011). Similar to α-subunits, β-subunits are also known to undergo extensive glycosylation, up to 36% of the total mass of the subunits, probably in its extracellular domain containing potential N-glycosylation sites (Isom, De Jongh et al. 1992; Johnson, Montpetit et al. 2004).

1.3.4.8. Ubiquitylation:

Mechanisms:

Ubiquitylation is another well recognized post-translational process that negatively regulates the cell surface expression of many different plasma membrane proteins (Staub and Rotin 2006). Ubiquitylated proteins undergo internalization followed by degradation or recycling mechanisms (Abriel and Staub 2005). Ubiquitin is a small and highly conserved polypeptide of 76 amino acids that serves as a tag that becomes covalently attached to the lysine residues of the targeted protein. For a protein to be ubiquitylated, it needs three enzymatic successive steps (Pickart 2001): Ubiquitin is first activated by an ubiquitin-activating enzyme (E1) in an ATP-dependent manner. Ubiquitin is then transferred to an ubiquitin-conjugating enzyme (E2) via a thioester bond. This complex further interacts with an ubiquitin-protein ligase (E3) that will eventually ubiquitylate the substrate protein. E3 enzyme provides the specificity of the cascade as they promote the

conjugation of ubiquitin on the target protein by binding to a recognition motif in the target protein, usually on a lysine residue (Ciechanover 2005). There are at least 1000 different E3 enzymes in the human genome (Hicke, Schubert et al. 2005) further highlighting the specificity role of E3. As to compare, only ~10 different genes encode for E1 and ~100 for E2. The ubiquitin molecule possesses seven lysine residues that can serve for the formation of ubiquitin chains molecules called polyubiquitin chains. The fate of ubiquitylated proteins depends on the pattern of ubiquitylation; polyubiquitylated proteins (generally lysine K48) are generally degraded by the proteasome while monoubiquitylated (or diubiquitylated, generally on lysine K63) occurs to membrane proteins pending for internalization, which can further lead to lysosomal degradation or to recycling (Shih, Sloper-Mould et al. 2000; Ciechanover 2005).

There are two major classes of E3 ubiquitin ligases: the RING finger (really interesting new gene) E3s, dependent on Zn2+ binding, and the Hect (homologous to E6-AP COOH terminal) E3s. The latter contain a HECT domain, which is the catalytic site responsible for the ubiquitylating the substrate protein (Huibregtse, Scheffner et al. 1995). The Nedd4/Nedd4-like (neuronal precursor cell-expressed developmentally downregulated gene 4) ubiquitin ligase family, composed of at least 9 members (Ingham, Gish et al. 2004), is an important member of the Hect E3 ligases and is the best described family involved in the ubiquitylation of membrane proteins. In addition to the catalytic HECT domain, these members are composed of a NH2-terminal C2 (calcium-dependent lipid binding domain)(Rizo and Sudhof 1998) responsible for substrate localisation and variable number, from two to four, of WW domains (Staub and Rotin 1996) responsible for substrate recognition. The WW motifs binds to a short, proline-rich and conserved motif (Sudol and Hunter 2000) called PY motif, consisting of PPxY sequence (Lu, Zhou et al. 1999; Kanelis, Rotin et al. 2001). The Nedd4 family contains nine members in human; *NEDD4*, *NEDD4-2*, *SMURF1*, *SMURF2*, *WWP1*, *WWP2*, *NEDL1*, *NEDL2* and *ITCH* (Harvey and Kumar 1999; Ingham, Gish et al. 2004) (Figure 10). Nedd4 is presumably the ancestral member of the family, whereas Nedd4-2 emerged later in the evolution process (Yang and Kumar 2009). Nedd4 was first identified as part of a set of genes strongly downregulated in developing mouse brain (Sazuka, Tomooka et al. 1992). Nedd4 and Nedd4-2 are most closely related to each other and are widely expressed in different tissues in the body such as heart, kidney or the nervous system.

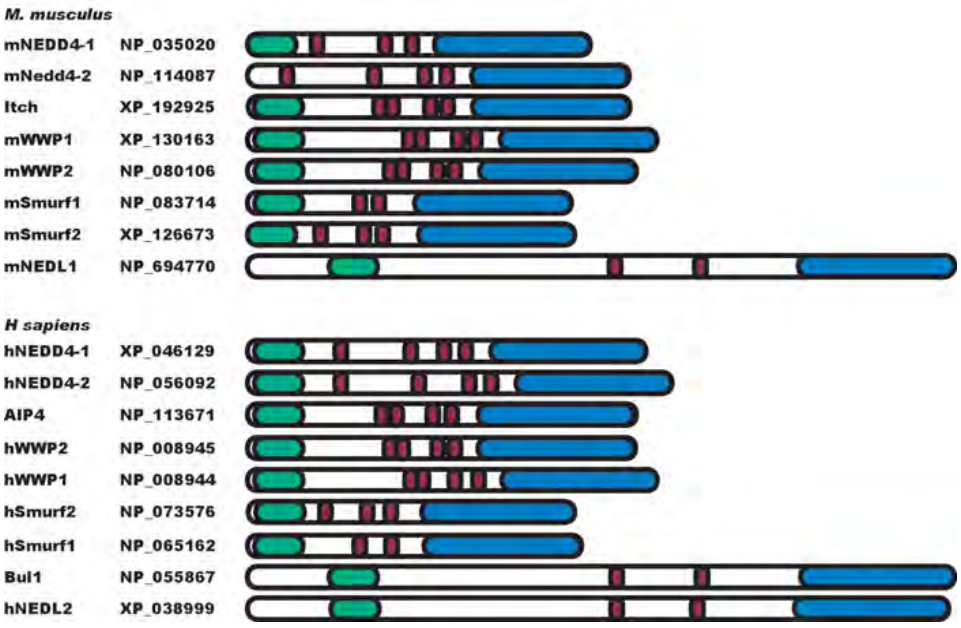

Figure 10. The Nedd4 Family of E3 ubiquitin ligase in mice and humans. The accension number of each isoform is shown. In green is the C2 lipid binding domain, in red/purple are WW protein-protein interaction domain and in blue in the HECT catalytic site. Modified from (Ingham, Gish et al. 2004)

The case of epithelial sodium channel ENaC:

The amiloride-sensitive epithelial sodium channel (ENaC), a channel important for controlling the electrolyte homeostasis was the first, and is probably the best described ion channel that undergoes the ubiquitin-mediated trafficking pathways. Mutations leading to a truncated ENaC were identified in Liddle's syndrome, an hereditary hypertensive disease (Shimkets et al., 1994). ENaC subunits all possess a PY motif, and mutating this motif was sufficient to generate a hypertensive phenotype (Schild, Lu et al. 1996), which is traduced by an increased ENaC function (Firsov, Schild et al. 1996). Other groups highlighted the importance of the PY motif (Harvey, Dinudom et al. 1999; Fotia, Dinudom et al. 2003; Henry, Kanelis et al. 2003), which suggested a role for the Nedd4 family in this regulation. This was confirmed *in vitro* where Nedd4-2 (Abriel, Loffing et al. 1999; Kamynina, Debonneville et al. 2001), and to a lesser extent Nedd4-1 (Henry, Kanelis et al. 2003), were shown to downregulate ENaC cell surface expression. Knocking out Nedd4-2 made the demonstration of a functional effect of Nedd4-2 *in vivo*. These knockout mice showed salt-sensitive hypertension, presumably mediated by an increased ENaC activity (Shi et al., 2008) and the subsequent increase Na+ reabsorption.

Nedd4-2 regulates Na_vs:

Interestingly, except for $Na_v1.4$ and $Na_v1.9$, every Na_vs isoform also possesses a conserved PY motif at their α-subunit C-terminal, making them potential targets of the Nedd4 ubiquitin ligase family (Figure 9). Nedd4-2 regulation of $Na_v1.5$ was extensively investigated in HEK cells by our group, and we reported (*1*) a decrease in current density, (*2*) which was dependent on the PY motif, (*3*) concomitant with the ubiquitylation of the sodium channel, (*4*) relied on an intact catalytic site of Nedd4-2 and (*5*) interaction between the two protein (van Bemmelen, Rougier et al. 2004). These

results were further transposed to other neuronal isoform $Na_v1.2$ and $Na_v1.3$ in the same cell expression system (Rougier, van Bemmelen et al. 2005). Notably, the first proline of PPxY motif can be substituted for a leucin without notable loss of affinity (Kasanov, Pirozzi et al. 2001), a motif found in $Na_v1.6$ (Rougier, van Bemmelen et al. 2005). This is in line with the fact that Nedd4-2 was also reported to decrease $Na_v1.6$ *in vitro* (Gasser, Cheng et al. 2010).

1.3.5. Central Sensitization:

We discussed the importance of peripheral hyperexcitability and its involvement in neuropathic pain. Upon repetitive stimulation, such as the one driven by peripheral hyperexcitability, the synaptic strength between primary and secondary order neuron increases. This leads to hyperexcitability of the dorsal horn neurons and is referred to as central sensitization, a mechanisms first described by Clifford Woolf (Woolf 1983). In his initial work, Clifford Woolf showed that after injury, dorsal horn neurons have a decrease in the cutaneous mechanical threshold, expansion in the size of receptive fields, increase of neuronal response as well as spontaneous discharges, which were not abolished when blocking sensory input directly at the site of injury. Central sensitization is considered as an activity-dependent form of plasticity that shares similarities with LTP (Ji, Kohno et al. 2003; Scholz, Broom et al. 2005). Post-synaptic EPSPs in the spinal cord are mediated by NMDA glutamate receptors leading to the subsequent activation of calcium-induced intracellular kinases. This leads to the phosphorylation of AMPA and NMDA receptors and subsequently to their recruitment at the synapse, thus enhancing glutamatergic responses. All the intracellular pathways and receptors involved in the early phase of central sensitization mechanism are extensively described in the review from Latremoliere (Latremoliere and Woolf 2009). A second late phase of central sensitization involves the mitogen-activated protein kinase (MAPK) cascade, leading to activation of CREB phosophorylation and triggers transcription of pronociceptive genes.

Another important mechanism significantly contributes the persistent enhancement of synaptic transmission; disinhibition. This occurs in two different ways, the loss of GABAergic inhibitory interneurons (Moore, Kohno et al. 2002) and the subsequent reduction of inhibitory currents, and the downregulation of potassium chloride co-transporter KCC2 in dorsal horn neurons (Coull, Boudreau et al. 2003). This exchanger is responsible for maintaining a low level of chloride intracellularly and its disruption leads to accumulation of this anion in the cell. As a result GABAergic and glycinergic inhibitory interneurons have depolarizing effect on dorsal horn neurons, increasing cellular excitability.

The last established important mechanism responsible for central sensitization is the microglial activation (Watkins, Milligan et al. 2001; Beggs and Salter 2007). In short, activation of MAPKs

pathways will leads to the subsequent release of pronociceptive cytokins and neurtrophines that will impact on microglial neurotransmitter-scavenging capacity (Gosselin, Suter et al. 2010).

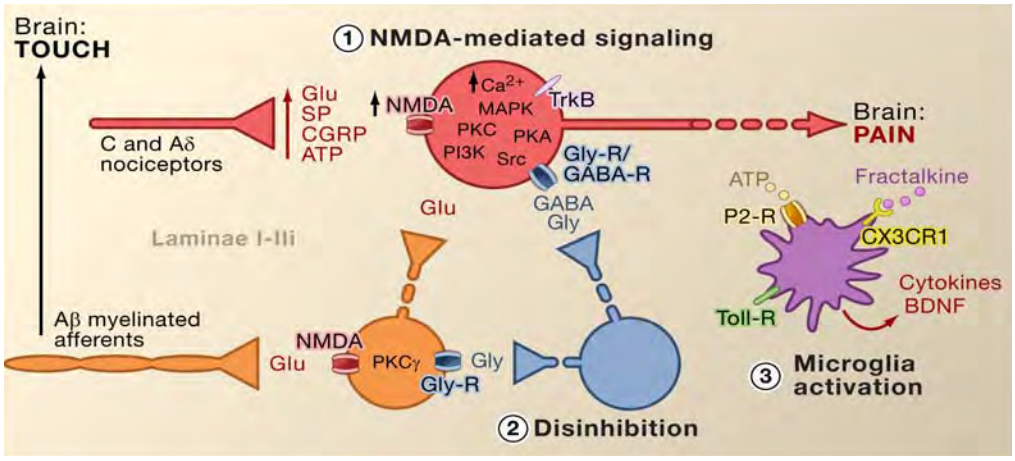

Figure 11. Central Sensitization. The three major mechanisms leading to sensitization are highlighted on this scheme: NMDA-mediated increase of synaptic strength, the loss of inhibition and the microglial activation. Modified from (Basbaum, Bautista et al. 2009)

1.3.6. Alteration in descending pathways:

The role of the rostra ventromedial medulla (RVM) has been shown to be critical in the maintenance of hyperalgesic states following peripheral nerve injury. The mechanisms are largely unknown, but neurons within the RVM undergo changes in excitability, which contribute to the maintenance of overrated spinal nociceptive inputs (Gebhart 2004).

1.3.7. Neuropathic pain Pharmacology:

Treatments to alleviate acute and inflammatory pain are largely ineffective in neuropathic pain patients. Pharmacological treatment for neuropathic pain is limited, with only about 50% of patients obtaining partial pain relief, the other half being pharmaco-resistant. The fact that treatments are often inadequate could be due to the multiple mechanisms beyond the disease. Conventional analgesics were showed to be ineffective in relieving neuropathic pain symptoms while opioids are effective in alleviating pain in some patients.

Gabapentin, an anticonvulsant initially developed to interact with GABA receptors, is effective for alleviating neuropathic pain symptoms, but is thought to act through α_2-δ of Ca_vs (Taylor, Gee et al. 1998). Calcium channels are becoming an increasingly attractive target for development of novel analgesic drugs (Perret and Luo 2009). Opioids are also effective in specific form of neuropathic pain treatment (Foley 2003), but are sometimes discouraged because of development of tolerance, risk of addiction and side effects.

One of the first drug used in clinical trials was the tricyclic antidepressants (TCA) amitriptyline (Watson 1983) but produced many side effects. Nowadays, new classes of antidepressant, such as specific serotonin and norepinephrine reuptake inhibitors (SSNRIs) are better tolerated.

Noteworthy, there are some evidences that the analgesic effect of noradrenaline reuptake inhibition is necessary, while serotonine reuptake inhibition alone with the selective serotonin reuptake inhibitors (SSRI) is not sufficient for alleviating neuropathic pain (Lee and Chen 2010). The clinical rationale for using antidepressant is that in addition to controlling supraspinal availability of serotonine and norepinephrine in the descending inhibitory control pathway, they also activate μ and δ-opioid receptors and inhibit NMDA receptors (Micó, Ardid et al. 2006). Interestingly, they have also been reported to block Na_vs (Dick, Brochu et al. 2007). Anticonvulsant, such as carbamazepin and lamatrogin and which are also commonly used to treat neuropathic pain, have also been reported to negatively modulate Na_vs function (Dickenson, Matthews et al. 2002) but have sever side effect such as agranulocytosis (de Leon, Santoro et al. 2012). Other sodium channel blockers, such as lidocaine topical application (McQuay *et al*., 1995), lidocaine systemic injection (Kalso, Tramer et al. 1998) and transdermal formulation of lidocaine (Gammaitoni, Alvarez et al. 2003) have already proven effective in treating some forms of neuropathic discomfort. Finally, mexiletine - an antiarrhythmic - is also a sodium channel blockers used to treat neuropathic pain (Priest and Kaczorowski 2007). The previous demonstrates the importance of Na_vs in neuropathic pain.

Because none of the previously mentioned medications operate efficiently and satisfactorily individually, they are used in combination. First-line medications include TCAs, SSNRIs and α_2-δ Ca_vs antagonist (Dworkin, O'Connor et al. 2007). Opioids are usually used in second-line medication, but remain inefficient in many cases.

New promising perspectives for developing treatment to treat neuropathic pain are also carried by new therapeutical approaches such as cell based and gene therapy. For instance expressing preproenkephalin genes using viral vectors is currently on clinical trial phase I.

1.3.8. Animal Models of Neuropathic pain:

In vitro cellular biochemistry had helped identifying the important molecules potentially implicated in neuropathic pain, but a better understanding of the pathology requires for an entire organism to integrate every components of the pain experience.

As already discussed, multiple diseases of the nervous system are associated with neuropathic pain and the clinical manifestations vary depending on the type. For instance, diabetic peripheral neuropathy and post-herpetic neuropathy are important contributors to the development of neuropathic pain (Dieleman, Kerklaan et al. 2008). However, streptozotocin and other chemically-induced models of neuropathic pain have slow onsets and result in variable development of hypersensitivity and many other adverse effects (Courteix, Eschalier et al. 1993; Fox, Eastwood et al. 1999) making them not so reproducible when experimenting pain hypersensivity. Among

neuropathic pain conditions, mononeuropathy has the highest incidence rate (Dieleman, Kerklaan et al. 2008). The development of animal models for nerve injury–induced neuropathic pain has significantly contributed to the discovery of mechanisms that contribute to neuropathic pain syndromes. The animals in these models have been shown to develop abnormal pain sensations similar to those reported in neuropathic pain patients.

The first behavioral model used complete transection of nerve and aimed at studying *anesthesia dolorosa* (Wall, Devor et al. 1979), which is pain in the absence of any sensory input in the rat and where autotomy (self mutilation of the paw as an indirect sign of spontaneous pain) was observed after a total denervation of the limb by the transection of femoral and sciatic nerves. However this model does not allow the measurement of allodynia and hyperalgesia and does not best reflects the partial nerve injury observed in most neuropathic pain patients. To overcome this problem, partial transection (ligation or constriction) of nerves were developed and among them, spinal nerve ligation (SNL, (Kim and Chung 1992)), chronic constriction injury (CCI, (Bennett and Xie 1988)) and the spared nerve injury model (SNI, (Decosterd and Woolf 2000)). The latter involves a lesion of two of the three terminal branches of the sciatic nerve, the common peroneal and tibial nerves, whereas the sural nerve is spared. The SNI results in increased mechanical and thermal sensitivity in the territory of the sural nerve, thus mimicking some of the clinical features of neuropathic pain (Woolf and Mannion 1999). This model enables the neurons being severed and the ones that are intact to be intermingled in the same dorsal root ganglion (DRG) allowing chemical cross-talk between cells, but the proper role of injured versus non-injured neurons in the development of pain hypersensibility remains equivocal. Hyperalgesia and allodynia are relatively easy to investigate in animal models, but the measurement of ongoing pain is more problematic. It is thought that autotomy or spontaneous foot lifting behavior reflects ongoing pain, but this is still debated. Much hope is coming from the development of the Mouse Grimace Scale (MGS) (Langford, Bailey et al. 2010), a facial-expression-based pain coding system which is thought to reliably reflect sponteanous pain in animals.

1.4. Aim of my thesis:

In this introduction, I extensively discussed the peripheral component of neuropathic pain-associated hyperexcitability. I highlighted the significant role of Na_vs in normal and pathological pain. Notably, $Na_v1.7$ and $Na_v1.8$ have been shown to be crucial in the transmission of pain signals as illustrated by the increasing identified mutations of these isoforms, leading to increased sodium conductance. However, mechanisms that regulate the membrane pool of Na_vs, also important for modulating sodium conductance, are poorly understood. During my thesis research work, I investigated two antagonist mechanisms of Na_vs regulation; the ***"internalizing Nedd4-2 pathway"***

and the ***"stabilizing β-subunit pathway"***. I will first address the question of the *in vivo* implication of Nedd4-2 in the generation of neuropathic pain by dysregulating $Na_v1.7$ and $Na_v1.8$ expression. This part of my work has been accepted for publication in the *Journal of Clinical Investigation*. The second part of highlights a novel role for β-subunit in glycosylating Na_v α-subunit *in vitro* which opens perspectives for investigating the potential physiological role of Na_v glycosylation in pain pathways. This research is summarized in a manuscript that is published in *Frontiers in Cellular Neuroscience*.

2. Results

2.1. Dysregulation of voltage-gated sodium channels by ubiquitin-ligase NEDD4-2 in neuropathic pain

This article is published in *the Journal of Clinical Investigation* (Laedermann, Cachemaille et al. 2013).

The core findings in this study are that the Nedd4-2 protein is an essential regulator of Na_vs *in vivo*, and that it is responsible for the genesis of neuropathic pain.

In this manuscript, we explored the role of Nedd4-2 expressed in dorsal root ganglion (DRG) cells in the regulation of $Na_v1.7$ and $Na_v1.8$, and its potential involvement in the pathogenesis of neuropathic pain. We used a multi-facetted approach involving (1) the use of a mouse neuropathic pain model (spared nerve injury, SNI), (2) the generation of a mouse model with DRG-specific genetic ablation of Nedd4-2, (3) Nedd4-2 gene transfer experiments in DRG cells using viral vectors and (4) the utilization of a specific $Na_v1.7$ selective blocker (ProTxII) to isolate $Na_v1.7$-mediated current for the first time.

The main findings in this study are that in DRG cells of the SNI mouse model, there is a specific reduction of Nedd4-2 expression with concomitant increased expression and function of $Na_v1.7$ and $Na_v1.8$-mediated current. Similar alterations were observed in mice with knocked out expression of Nedd4-2 in DRG cells, demonstrating a causal link between Nedd4-2 downregulation and $Na_v1.7$ and $Na_v1.8$ upregulation. These mice also showed an altered pain phenotype. Finally, we demonstrated that upon Nedd4-2 gene transfer in DRG cells of SNI animals, the SNI-mediated hypersensitivity phenotype could be partially rescued.

Since Nedd4-2 can also regulate other sodium channel isoforms and membrane proteins (i.e. glutamate receptors), a better understanding of Nedd4-2 in sodium channel dysfunction may have far-reaching implications not only to pain, but also to epilepsy, migraines or cognitive impairment.

In this article, I performed electrophysiological recordings in both cell expression system and dissociated DRG neurons. I performed all the biochemical experiments inherent to Figure 2 and generated the constructs (GST-fusion proteins, $Na_v1.7$ and Nedd4-2 mutants). I also performed biochemistry on native DRG tissues. I performed qRT-PCR. I started the breeding of SNS-Nedd4-$2^{fl/fl}$ mouse line and genotyped them. I participated in the design, production and quantification of the rAAV2/6 viral vectors. I wrote the first draft and corrected versions of the manuscript.

Dysregulation of voltage-gated sodium channels by ubiquitin ligase NEDD4-2 in neuropathic pain

Cédric J. Laedermann,[1,2] Matthieu Cachemaille,[1] Guylène Kirschmann,[1] Marie Pertin,[1] Romain-Daniel Gosselin,[1] Isabelle Chang,[1] Maxime Albesa,[2] Chris Towne,[3] Bernard L. Schneider,[3] Stephan Kellenberger,[4] Hugues Abriel,[2] and Isabelle Decosterd[1,5]

[1]Pain Center, Department of Anesthesiology, University Hospital Center (CHUV) and University of Lausanne, Lausanne, Switzerland. [2]Department of Clinical Research, University of Bern, Bern, Switzerland. [3]Brain Mind Institute, Ecole Polytechnique Fédérale de Lausanne (EPFL), Lausanne, Switzerland. [4]Department of Pharmacology and Toxicology and [5]Department of Fundamental Neurosciences, University of Lausanne, Lausanne, Switzerland.

Peripheral neuropathic pain is a disabling condition resulting from nerve injury. It is characterized by the dysregulation of voltage-gated sodium channels (Na_vs) expressed in dorsal root ganglion (DRG) sensory neurons. The mechanisms underlying the altered expression of Na_vs remain unknown. This study investigated the role of the E3 ubiquitin ligase NEDD4-2, which is known to ubiquitylate Na_vs, in the pathogenesis of neuropathic pain in mice. The spared nerve injury (SNI) model of traumatic nerve injury–induced neuropathic pain was used, and an $Na_v1.7$-specific inhibitor, ProTxII, allowed the isolation of $Na_v1.7$-mediated currents. SNI decreased NEDD4-2 expression in DRG cells and increased the amplitude of $Na_v1.7$ and $Na_v1.8$ currents. The redistribution of $Na_v1.7$ channels toward peripheral axons was also observed. Similar changes were observed in the nociceptive DRG neurons of *Nedd4L* knockout mice (*SNS-Nedd4L*$^{-/-}$). *SNS-Nedd4L*$^{-/-}$ mice exhibited thermal hypersensitivity and an enhanced second pain phase after formalin injection. Restoration of NEDD4-2 expression in DRG neurons using recombinant adenoassociated virus (rAAV2/6) not only reduced $Na_v1.7$ and $Na_v1.8$ current amplitudes, but also alleviated SNI-induced mechanical allodynia. These findings demonstrate that NEDD4-2 is a potent posttranslational regulator of Na_vs and that downregulation of NEDD4-2 leads to the hyperexcitability of DRG neurons and contributes to the genesis of pathological pain.

Introduction

Neuropathic pain is a direct consequence of alterations in the somatosensory system. It affects approximately 7% of the general population and is insufficiently treated with currently available drugs (1). Following nerve injury, there is ectopic spontaneous activity of afferent neurons due to the increased expression of voltage-gated sodium channels (Na_vs) (2, 3). This hyperexcitability mediates enduring changes in the nervous system, contributing to both peripheral and central sensitization (4). Na_vs are heteromeric glycosylated protein complexes composed of a large pore-forming α subunit and auxiliary β subunits (5, 6). Nine genes encode for distinct channel isoforms ($Na_v1.1$ to $Na_v1.9$), each displaying specific properties. They are classified according to their sensitivity to tetrodotoxin (TTX). All isoforms, except $Na_v1.4$ and $Na_v1.5$, are expressed in the dorsal root ganglia (DRG) and trigeminal ganglia (TG) nociceptive neurons, with $Na_v1.8$ and $Na_v1.9$ being expressed almost exclusively in DRG/TG neurons and $Na_v1.7$ in DRG/TG and sympathetic ganglion neurons (7). $Na_v1.7$ is expressed at higher levels in DRG/TG than are other TTX-sensitive isoforms (7, 8) and plays an essential role in the modulation of human pain perception. Naturally occurring mutations in *SCN9A*, the gene encoding $Na_v1.7$, lead to either congenital insensitivity or severe episodic hypersensitivity to pain (9–11). In addition, $Na_v1.7$ and $Na_v1.8$ gain-of-function mutations in painful peripheral neuropathy syndromes were recently described (12, 13). Not only are $Na_v1.7$ and $Na_v1.8$ important in inherited pain disorders, but also in acquired pain disorders, where their increased expression has already been linked to diverse chronic pain symptoms (14–16). Studies using knockout mice have implicated $Na_v1.7$ and $Na_v1.8$ in acute and inflammatory pain (17–20), but their involvement in hyperexcitability and neuropathic pain remains to be determined.

The control of Na_v density at the cell membrane is crucial to ensuring normal neuronal excitability. Despite extensive research on the subject, the regulation of Na_vs in neuropathic pain remains poorly understood. Na_vs are subject to posttranslational modifications that may influence their cell membrane availability. Ubiquitylation is a key process that orchestrates the internalization and subsequent degradation or recycling of Na_vs (21). The final and limiting step is the covalent attachment of ubiquitin moieties to lysine residues of the target protein. This is accomplished by ubiquitin protein ligases, such as NEDD4-2 (neuronal precursor cell expressed developmentally downregulated-4 type 2). NEDD4-2 is a member of the NEDD4/NEDD4-like E3 subfamily of ubiquitin ligases, whose type I WW domains interact with the PY motifs (PPxY) of target proteins. All Na_v isoforms, except $Na_v1.4$ and $Na_v1.9$, possess a PY motif and are potential targets of NEDD4-2. In vitro experiments have indicated that NEDD4-2 can negatively regulate the epithelial sodium channel ENaC (22) and Na_vs (23, 24). The functional relevance of NEDD4-2 in sensory neurons, as well as its possible involvement in pain sensitivity, have yet to be investigated.

Authorship note: Hugues Abriel and Isabelle Decosterd contributed equally to this work.

Conflict of interest: The authors have declared that no conflict of interest exists.

Citation for this article: *J Clin Invest.* 2013;123(7):3002–3013. doi:10.1172/JCI68996.

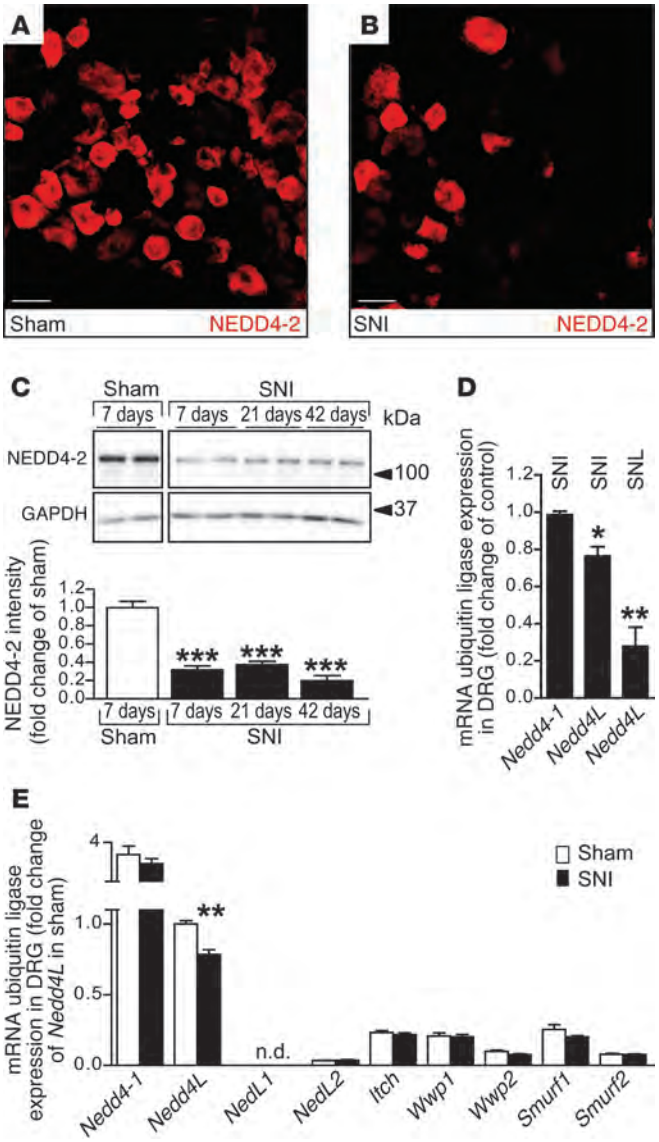

Figure 1

Peripheral nerve injury reduces NEDD4-2 expression in DRG. (**A** and **B**) Immunofluorescence of NEDD4-2 in coronal sections of L4 DRG from sham-operated and SNI mice. Scale bars: 30 μm. (**C**) Representative Western blot analysis showing the decrease in NEDD4-2 at days 7, 21, and 42 after SNI in L4/5 DRG and its associated quantification. Data are expressed as the means ± SEM; $n = 4$ samples for each time point per group. $^{***}P < 0.001$ by 1-way ANOVA with Bonferroni's post-hoc test. GAPDH was used as a loading control. Lanes were run on the same gel but were noncontiguous. (**D**) Effect of SNI and SNL on *Nedd4-1* and *Nedd4L* transcripts in L4/5 DRG 7 days after SNI or SNL (injury of L5 spinal nerve). Bar graph showing transcriptional levels of *Nedd4-1* and *Nedd4L* normalized to *GAPDH* in SNI and SNL groups over the control group (sham for SNI and L4 DRG for SNL). Data represent the mean ± SEM; $n = 4$ samples per group. Isolated L4/5, L5, or L4 DRG from 2 mice were pooled for each sample and run in triplicate. $^{*}P = 0.011$, $^{**}P = 0.004$, Student's *t* test. (**E**) Constitutive transcript levels of *Nedd4*/*Nedd4*-like E3 subfamily members in L4/5 DRG 7 days after sham and SNI surgery. Transcript levels were normalized using *HPRT* as a reference gene and further normalized to *Nedd4L* levels in sham-operated mice. Data are expressed as the means ± SEM; $n = 3$–4 samples per group, which were run in triplicate. $^{**}P = 0.005$, Student's *t* test. We detected no amplification of *NedL1* in the DRG samples.

NEDD4-2 was recently shown to be decreased in rat DRG in the spared nerve injury (SNI) model of traumatic nerve injury–induced neuropathic pain (25). The present study postulated that reduced levels of NEDD4-2 jeopardize the correct addressing or anchoring of Na_vs in DRG nociceptive neurons. NEDD4-2 expression was controlled in cellular expression systems and in mice with DRG-specific gene deletions or rAAV-mediated gene transfers. This enabled the selective investigation of the effect of NEDD4-2 on $Na_v1.7$ and $Na_v1.8$ currents, as well its impacts on pain sensitivity. The results provide what we believe to be the first in vivo mechanistic evidence that NEDD4-2 enables the fine-tuning of neuronal excitability in DRG cells. Furthermore, these results may demonstrate that the pathological reduction of NEDD4-2 underlies traumatic nerve injury–induced neuropathic pain.

Results

Peripheral nerve injury reduces NEDD4-2 expression in DRG. The protein and mRNA levels of *Nedd4L* were measured to explore whether *Nedd4L* is regulated after nerve injury in mice and whether it contributes to phenotypic changes in DRG neurons. A substantial decrease of NEDD4-2 expression was observed by immunofluorescence in lumbar L4/L5 DRG 7 days after SNI (Figure 1, A and B). This decrease was further quantified using Western blot analysis. SNI decreased NEDD4-2 protein levels by greater tha 60% in DRG, an effect that lasted for at least 6 weeks (Figure 1C). Both SNI and spinal nerve ligation (SNL) reduced *Nedd4L* transcript levels (Figure 1D). *Nedd4L* mRNA was abundantly expressed in lumbar L4/5 DRG and was the only member of the *Nedd4*/*Nedd4*-like E3 subfamily to be downregulated after SNI (Figure 1E).

NEDD4-2 interacts with, ubiquitylates, and downregulates $Na_v1.7$ in HEK293 cells. Since $Na_v1.7$ is essential for pain sensation, NEDD4-2 downregulation of $Na_v1.7$ in mammalian cells was investigated, as previously reported in *Xenopus* oocytes (24). Whole-cell Na^+ currents (I_{Na}) were recorded in HEK293 cells cotransfected with $Na_v1.7$ and NEDD4-2. NEDD4-2 decreased $Na_v1.7$ current density by approximately 80% (Figure 2, A and B). The biophysical properties of $Na_v1.7$ were unaffected by NEDD4-2 (Supplemental Table 1 and Supplemental Figure 1A; supplemental material

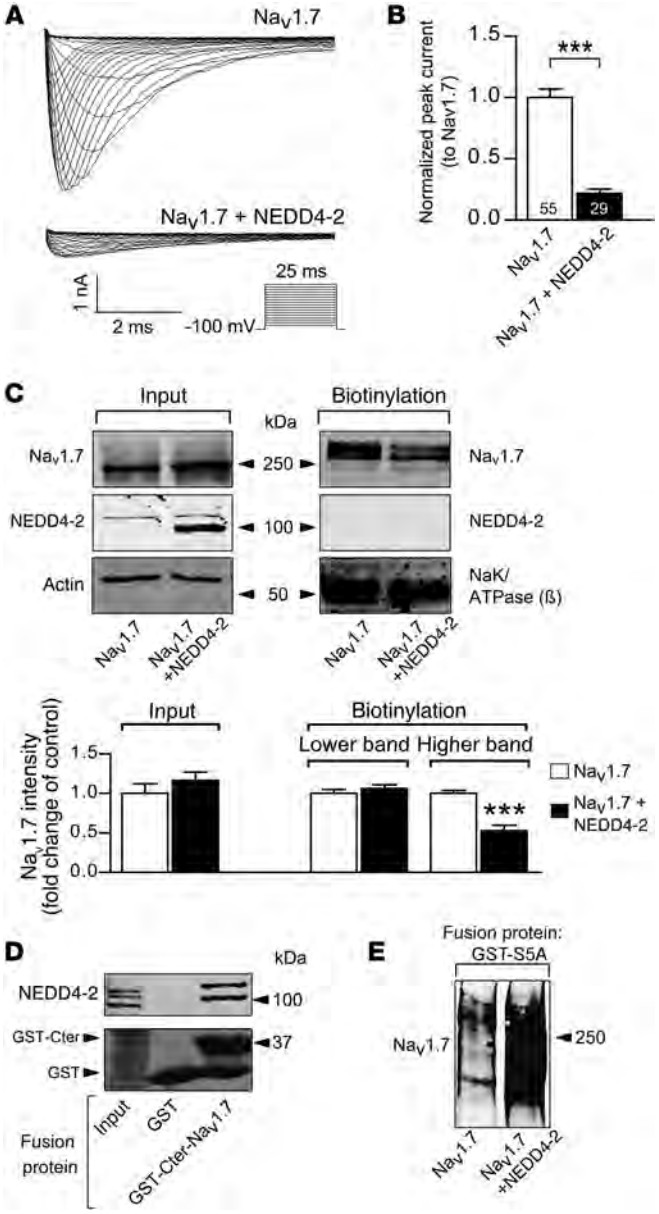

Figure 2

NEDD4-2 downregulates membrane Na$_v$1.7. (**A**) Representative current traces obtained with a V-I protocol (see Methods) on HEK293 cells after Na$_v$1.7 transfection or cotransfection with NEDD4-2. (**B**) Quantification of current densities from **A**. NEDD4-2 reduced Na$_v$1.7 current density (***P < 0.001). See Supplemental Figure 1A and Supplemental Table 1 for values and biophysical properties. (**C**) Surface biotinylation of HEK293 cells and their associated quantification. In membrane fractions, NEDD4-2 reduced the fully glycosylated form of Na$_v$1.7 (***P < 0.001), whereas the core glycosylated form remained unchanged (P = 0.416). Na$_v$1.7 total expression was unchanged (P = 0.337; Input). The β1 subunit of the NaK/ATPase and actin were used as loading controls in input and biotinylation fractions, respectively. Deglycosylation experiments are presented in Supplemental Figure 1B. NEDD4-2 antibody recognizes both endogenous (120 kDa) and transfected (100 kDa) proteins. (**D**) GST pull-down experiment showing Na$_v$1.7 PY motif interaction with NEDD4-2. HEK293 cells were transfected with NEDD4-2, and soluble fractions were mixed GST proteins or GST-Cter-Na$_v$1.7 fusion proteins. Bound NEDD4-2 was analyzed by Western blot. The entire Western blot with PY motif mutants can be seen in Supplemental Figure 2E. (**E**) NEDD4-2–mediated ubiquitylation. HEK293 cells were transfected with Na$_v$1.7 or cotransfected with NEDD4-2, and soluble fractions were mixed with GST-S5A proteins to pull down ubiquitylated proteins. Bound Na$_v$1.7 was analyzed by Western blotting. The entire Western blot with PY motif mutants can be seen in Supplemental Figure 2F.

available online with this article; doi:10.1172/JCI68996DS1), suggesting that NEDD4-2 mainly reduces the number of channels at the cell surface. Cell-surface proteins were then biotinylated and precipitated. Upon NEDD4-2 cotransfection, expression of the fully glycosylated form of Na$_v$1.7 (Supplemental Figure 1B) was decreased by approximately 50% in the plasma membrane fraction, but remained unchanged in the total lysate (Figure 2C, see also Supplemental Figure 1, C and D, for additional in vitro experiments). The interaction between Na$_v$1.7 and NEDD4-2 was examined by pull-down experiments using GST fused to the furthest 66 C-terminal amino acid residues of Na$_v$1.7, which include the PY motif (GST-Cter-Na$_v$1.7). Na$_v$1.7 GST fusion proteins interacted with endogenous and transfected NEDD4-2, whereas GST alone did not (Figure 2D). Finally, whether Na$_v$1.7 could be a substrate of NEDD4-2 ubiquitylating activity was tested by pulling down ubiquitylated proteins using GST fused to the ubiquitin-binding proteasomal subunit S5A (GST-S5A). Overexpression of NEDD4-2 substantially increased GST-S5A–bound Na$_v$1.7 (Figure 2E). Taken together, these results support a model in which NEDD4-2 interacts with and ubiquitylates Na$_v$1.7 and thus controls the level of the functional channel at the cellular membrane in mammalian cells. Additional in vitro experiments demonstrating the importance of the PY motif in the NEDD4-2 downregulatory effect on Nav1.7 are presented in Supplemental Figure 2, A–F and in the Supplemental Results.

SNI changes the expression of Na$_v$s. In freshly dissociated L4/5 mouse DRG neurons, the different Na$_v$ components were functionally dissected out 1 week after SNI by performing whole-cell patch-clamp recordings. From total I_{Na} (Na$_v$total), the specific Na$_v$1.7 channel blocker ProTxII (26) and TTX were used to isolate the following 3 currents: the Na$_v$1.7-mediated current (ProTxII-sensitive current, referred to as Na$_v$1.7 for simplicity), the remain-

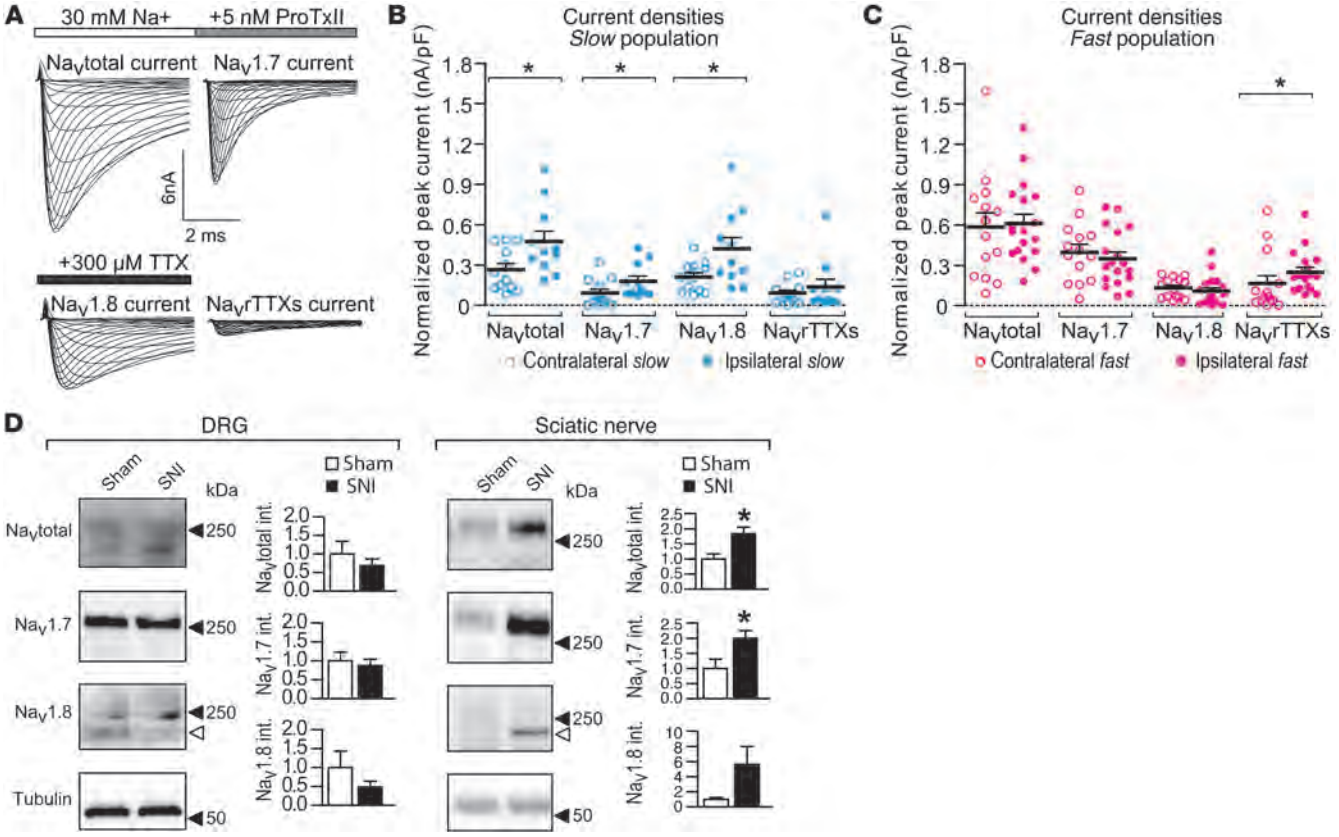

Figure 3

Increase in $Na_v1.7$ and $Na_v1.8$ currents in DRG neurons and increased expression of $Na_v1.7$ along the sciatic nerve after SNI. (**A**) Typical recordings of I_{Na} in DRG neurons using the V-I protocol and pharmacological isolation of Na_vtotal, $Na_v1.7$, $Na_v1.8$, and Na_vrTTXs currents with ProTxII and TTX (see Methods). (**B** and **C**) Scatter dot plot representing Na_vtotal, $Na_v1.7$, $Na_v1.8$, and Na_vrTTXs current densities in contralateral and ipsilateral sides recorded in L4/5 DRG neurons 1 week after SNI. *Slow* (**B**, in cyan) and *fast* (**C**, in magenta) neurons are shown. Mann-Whitney *U* test. See Supplemental Figure 3A for the total population and see Supplemental Table 2 for values and biophysical properties. (**D**) Left panel: representative Western blot analysis and quantification of Na_v α subunits: Na_vtotal, $Na_v1.7$, and $Na_v1.8$ in DRG 7 days after SNI. No modifications in Na_vtotal ($P = 0.496$), $Na_v1.7$ ($P = 0.690$), or $Na_v1.8$ ($P = 0.311$) were observed in sham- and SNI-operated mice. Right panel: same as above, but for sciatic nerve preparation. $Na_v1.7$ (*$P = 0.045$) and Na_vtotal (*$P = 0.021$) were significantly increased in SNI compared with the sham samples. The $Na_v1.8$ signal in the SNI sample did not reach significance compared with the background signal in the sham-operated group ($P = 0.105$) (see Supplemental Figure 3B). The 2 open arrowheads correspond to a distinct band of $Na_v1.8$, with lower molecular weight than the band observed at 250 kDa. Data are expressed as the means ± SEM; $n = 4$ samples for each group. Student's *t* test. Tubulin was used as a loading control. Int., intensity.

ing TTX-sensitive currents ($Na_v1.1$, $Na_v1.2$, $Na_v1.3$, and $Na_v1.6$ currents collectively referred to as Na_vrTTXs), and the TTX-resistant currents (referred to as $Na_v1.8$, since $Na_v1.9$ was inactivated by an ad-hoc electrophysiological protocol; see Methods) (Figure 3A). Recorded cells were small neurons (<30 pF), considered to be nociceptive neurons (27). Despite the fact that the distinction between intact or severed neurons was not made, a significant increase in the Na_vtotal ($P = 0.013$) and Na_vrTTXs ($P = 0.021$) current densities after SNI were measured (ipsilateral compared with the contralateral side, Supplemental Figure 3A). Since the expression of Na_vs in DRG is heterogeneous, the analysis was refined by segregating cells into *fast* and *slow* neurons, as previously reported (27). A neuron was characterized as *slow* when the I_{Na} density ratio of the $Na_v1.8/Na_v$total was greater than 0.5, with $Na_v1.8$ displaying slower inactivation kinetics. Conversely, when this ratio was less than 0.5, the neuron was defined as *fast* (27). This selection revealed that SNI significantly increased $Na_v1.7$ and $Na_v1.8$ current densities in the *slow* subpopulation only (Figure 3B). The *fast* subpopulation showed a small but significant increase in Na_vrTTXs alone (Figure 3C; $P = 0.014$).

SNI had only a minor impact on the biophysical properties (voltage dependence of steady-state activation and inactivation) of some of the Na_v components (Supplemental Table 2). In line with previous studies (28, 29), nerve injury induced an acceleration of the recovery from inactivation (repriming) for every component of I_{Na} of the *fast* subpopulation (Supplemental Table 2).

Western blots of pooled L4/5 DRG revealed no detectable modification of the expression levels of Na_vtotal, nor that of $Na_v1.7$ ($P = 0.039$) or $Na_v1.8$ ($P = 0.024$) 1 week after SNI (Figure 3D). However, $Na_v1.7$ and Na_vtotal levels were significantly increased in the sciatic nerve. $Na_v1.8$ was undetectable in the nerves of sham-operated animals. The signal intensity was not significantly modified after SNI, but a distinct band at the expected molecular weight (230–240 kDa) was visible in all 4 SNI samples (see Supplemental Figure 3B).

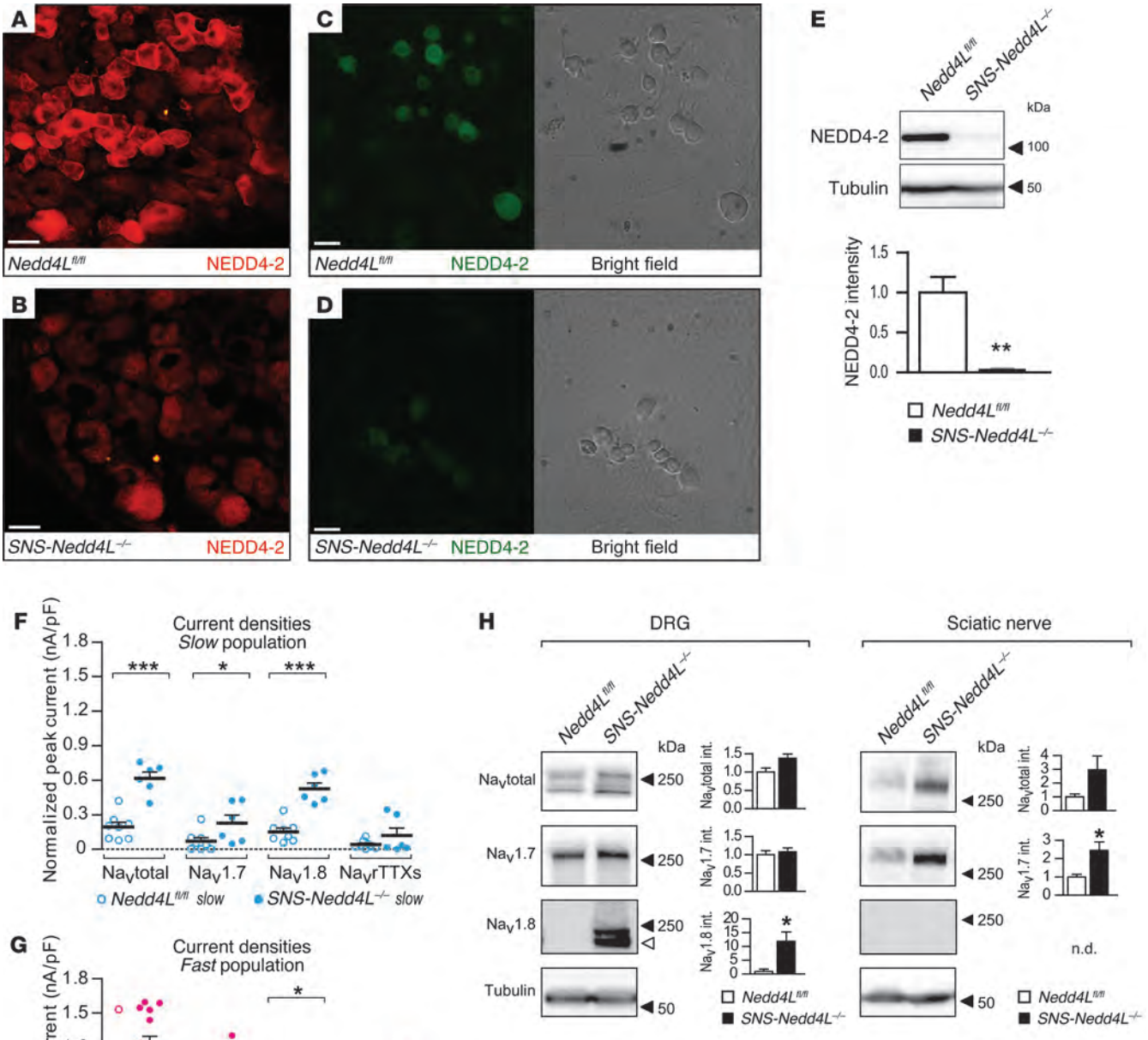

Figure 4

SNS-Nedd4L$^{-/-}$ mice show increased $Na_v1.7$ and $Na_v1.8$ currents in DRG neurons and increased expression of $Na_v1.7$ along the sciatic nerve. (**A** and **B**) Immunofluorescence of NEDD4-2 in coronal sections of L4 DRG from *Nedd4L*$^{fl/fl}$ and *SNS-Nedd4L*$^{-/-}$ mice. Scale bars: 30 μm. (**C** and **D**) Immunofluorescence and corresponding bright-field images of NEDD4-2 in DRG neurons from *Nedd4L*$^{fl/fl}$ and *SNS-Nedd4L*$^{-/-}$ mice after whole-cell patch-clamp recordings (36 hours after dissociation). Scale bars: 30 μm. (**E**) Western blot and quantification showing NEDD4-2 decrease in the DRG (**P = 0.003) of *SNS-Nedd4L*$^{-/-}$ mice compared with control *Nedd4L*$^{fl/fl}$ mice. (**F** and **G**) Scatter dot plots representing Na_vtotal, $Na_v1.7$, $Na_v1.8$, and Na_vrTTXs current densities in L4/5 DRG neurons from *SNS-Nedd4L*$^{-/-}$ and *Nedd4L*$^{fl/fl}$ mice. *Slow* (**F**, in cyan) and *fast* (**G**, in magenta) neurons are shown. Mann-Whitney *U* test. See Supplemental Figure 4A for total population and Supplemental Table 3 for values and biophysical properties. (**H**) Left panel: Western blot analysis and quantification of Na_v α subunits in the DRG of *SNS-Nedd4L*$^{-/-}$ and *Nedd4L*$^{fl/fl}$ mice. No significant modifications in Na_vtotal (P = 0.054) or $Na_v1.7$ (P = 0.646) were observed, whereas the $Na_v1.8$ signal was increased in the *SNS-Nedd4L*$^{-/-}$ mice (*P = 0.020). Right panel: same as above, but for sciatic nerves. $Na_v1.7$ was significantly increased (*P = 0.022), whereas the increase in Na_vtotal was not significant (P = 0.089). Data are expressed as the means ± SEM; n = 4 samples for each group. Student's *t* test. Tubulin was used as a loading control in **E** and **H**.

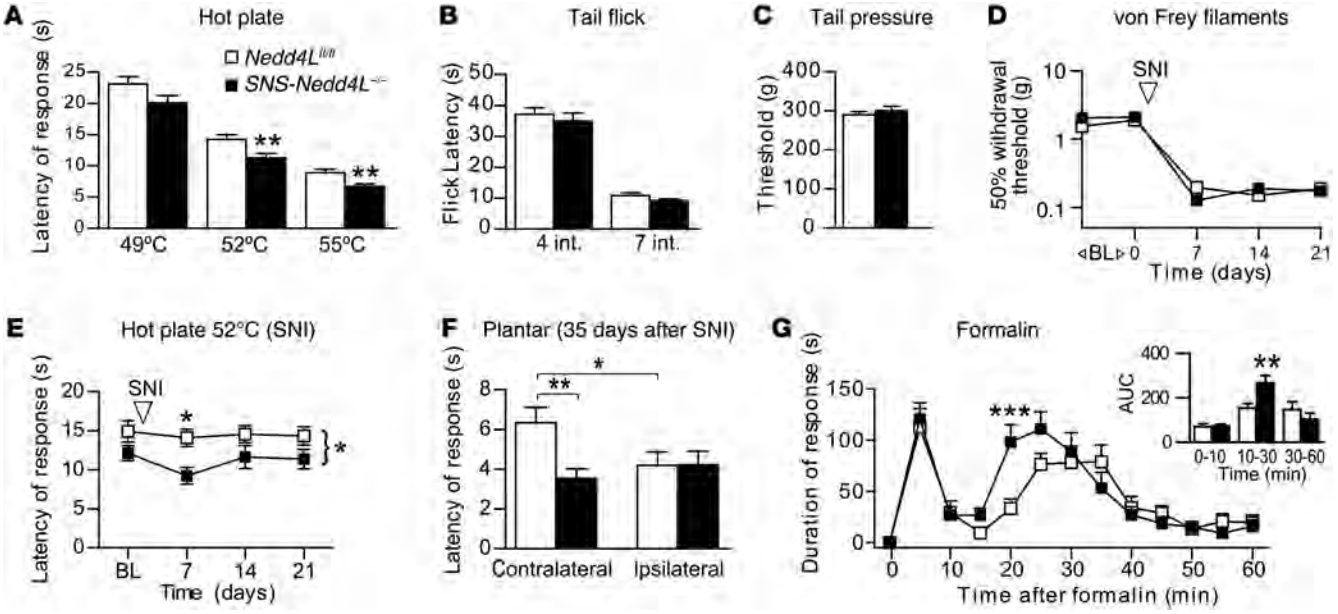

Figure 5

SNS-Nedd4L$^{-/-}$ mice show increased thermal sensitivity and an increased second pain phase after formalin injection. (**A**) Significantly higher thermal sensitivity was detected in the hot-plate test at 52°C and 54°C in *SNS-Nedd4L*$^{-/-}$ mice. $P = 0.112$ at 49°C, $^{**}P = 0.009$ at 52°C, and $^{**}P = 0.008$ at 55°C; Mann-Whitney *U* test. (**B**) No differences were observed in the tail-flick test. $P = 0.414$ at intensity 4 and $P = 0.830$ at intensity 7 (AU); Mann-Whitney *U* test. (**C**) Responses to the tail pressure test were unchanged. $P = 0.452$, Student's *t* test. (**D**) Basal responses to mechanical stimulation and development of SNI-related mechanical allodynia-like behavior were not different. $P > 0.05$, 2-way ANOVA on log values with post-hoc Bonferroni's tests. (**E**) Higher thermal sensitivity was detected at 52°C in *SNS-Nedd4L*$^{-/-}$ mice, but this effect was not further increased after SNI. $^{*}P < 0.05$ between groups using 2-way ANOVA with repeated measures. $^{*}P < 0.05$ on day 7 with post-hoc Bonferroni's tests. (**F**) Plantar test 35 days after SNI. Higher thermal sensitivity was detected in *SNS-Nedd4L*$^{-/-}$ mice as compared with the noninjured paws of *Nedd4L*$^{fl/fl}$ mice (contralateral). SNI induced thermal hyperalgesia in the injured paws of *Nedd4L*$^{fl/fl}$ mice compared with noninjured paws. $^{*}P = 0.013$ and $^{**}P = 0.006$ at intensity 3 (AU), Student's *t* test. (**G**) Time course of the nocifensive response to formalin injection revealed an increased response in *SNS-Nedd4L*$^{-/-}$ mice during the second phase of the test. $^{***}P < 0.001$, 2-way ANOVA with repeated measures with post-hoc Bonferroni's tests. Insert shows the bar graph of this effect through AUC quantification. $^{**}P = 0.009$, Mann-Whitney *U* test. Data are expressed as the means ± SEM and n = 7– 28 animals per group for all panels.

Na_v expression in SNS-Nedd4L$^{-/-}$ knockout mice. To investigate the contribution of NEDD4-2 to the expression of Na_vs in DRG in vivo and its impact on pain, a DRG neuron–specific *Nedd4L*-deficient mouse line was generated (*SNS-Nedd4L*$^{-/-}$; see Supplemental Methods). Mice carrying a homozygous *Nedd4L* flox allele (*Nedd4L*$^{fl/fl}$) (30) were crossed with mice heterozygously expressing Cre recombinase under the control of the *$Na_v1.8$* promoter (referred to as *SNS-Cre*), which is predominantly active in DRG nociceptive neurons (31). Cre expression in this mouse line has been extensively characterized (32) and differs from another *$Na_v1.8$-Cre* mouse line generated by the Wood laboratory (33). NEDD4-2 expression was greatly reduced in the DRG neurons of *SNS-Nedd4L*$^{-/-}$ mice (Figure 4, A–E). A slight signal was still detectable in the *SNS-Nedd4L*$^{-/-}$ mice, most likely due to a residual expression of NEDD4-2 in neurons not expressing $Na_v1.8$ (Figure 4E). Whole-cell patch-clamp recordings showed a 2-fold upregulation of Na_v-total, $Na_v1.7$ ($P = 0.027$), and $Na_v1.8$ ($P < 0.001$) current densities in neurons from *SNS-Nedd4L*$^{-/-}$ mice (Supplemental Figure 4A and Supplemental Table 3) compared with neurons from *Nedd4L*$^{fl/fl}$ control littermates. The Na_vrTTXs component was not significantly altered. Subsequent analyses of *slow* and *fast* neuronal subpopulations revealed that, similar to the SNI condition, the changes were predominant in *slow* neurons (a 2-fold increase for Na_vtotal [$P = 0.001$], $Na_v1.7$ [$P = 0.042$], and $Na_v1.8$ [$P < 0.001$] current densities) (Figure 4, F and G). The biophysical properties were largely unaltered in the knockout mice (Supplemental Table 3), consistent with a major role of NEDD4-2 in the regulation of $Na_v1.7$ and $Na_v1.8$ membrane density.

We then evaluated whether the expression of Na_vs was modified in DRG and the sciatic nerves of *SNS-Nedd4L*$^{-/-}$ mice (Figure 4H). We observed a markedly increased Western blot signal for $Na_v1.8$ in the DRG of knockout mice, while the signal was undetectable in *Nedd4L*$^{fl/fl}$ DRG neurons. These observations were confirmed by immunofluorescence measurements (Supplemental Figure 4B). Although the $Na_v1.7$ signal from DRG was not changed between the groups, a stronger signal was observed in the sciatic nerves of the *SNS-Nedd4L*$^{-/-}$ mice, similar to that observed after SNI. $Na_v1.8$ immunoreactivity was not detected in the sciatic nerves of the knockout mice or in those of the control mice, suggesting that the mechanisms underlying $Na_v1.8$ redistribution in nerves after SNI are independent of NEDD4-2 downregulation.

Pain-related responses in SNS-Nedd4L$^{-/-}$ knockout mice. We then investigated whether peripheral deficiency of NEDD4-2 could modify pain behavior. While response latencies to radiant heat (tail-flick test) (Figure 5B) and acute mechanical nociception (tail pressure test) (Figure 5C) were unchanged, acute thermal hypersensitivity in *SNS-Nedd4L*$^{-/-}$ mice was observed with the hot-plate test at 52°C and 55°C (Figure 5A). We also performed the hot-

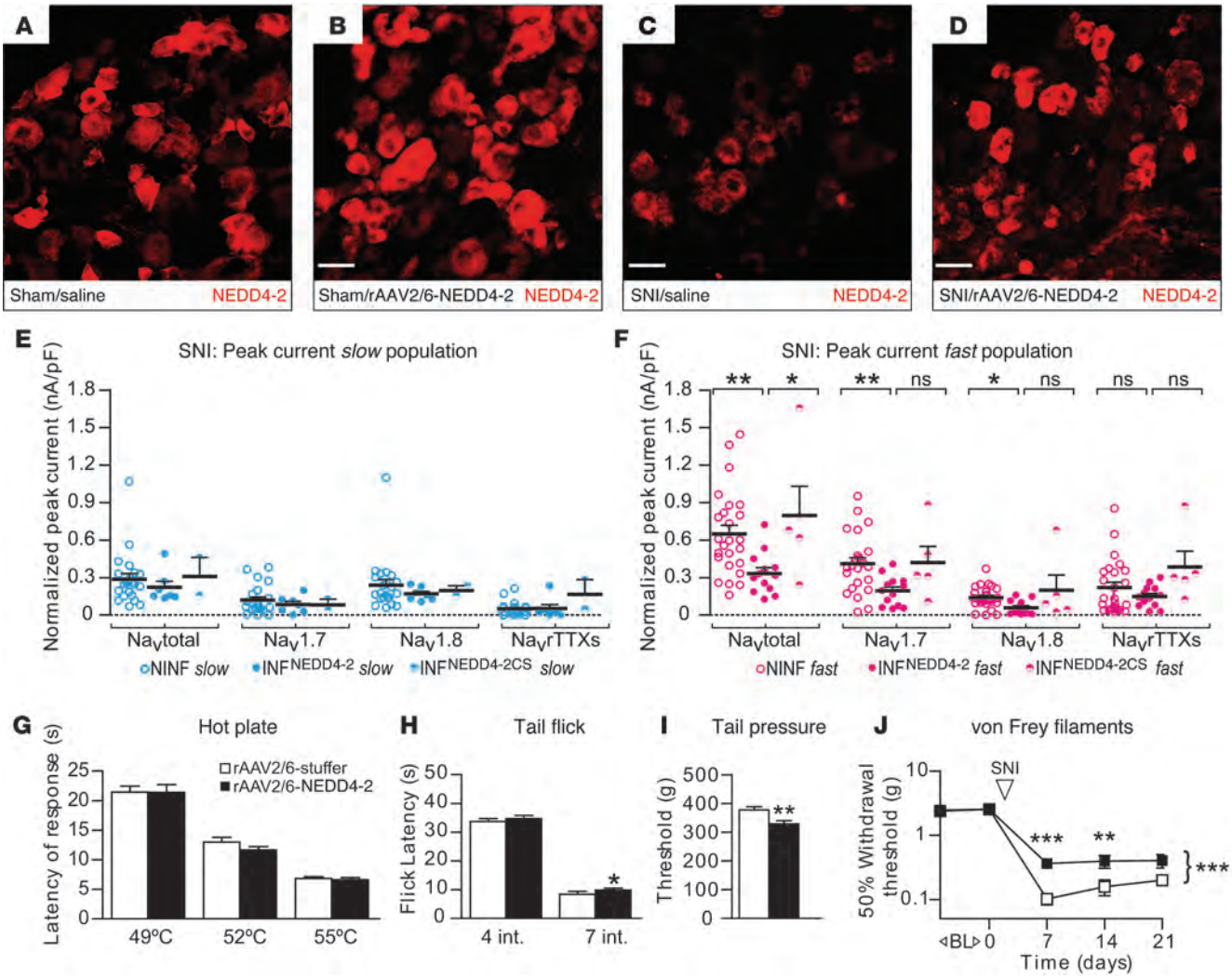

Figure 6

Delivery of rAAV2/6-NEDD4-2 viral vector decreases functional currents after SNI and alleviates mechanical allodynia. (**A**–**D**) Immunofluorescence of NEDD4-2 in coronal sections of L4 ipsilateral DRG injected with rAAV2/6-NEDD4-2 or saline solution in sham- and SNI-operated mice. Scale bars: 30 μm. (**E** and **F**) Scatter dot plots representing Na$_v$total, Na$_v$1.7, Na$_v$1.8, and Na$_v$rTTXs current densities 1 week after SNI in noninfected DRG neurons (NINF), rAAV2/6-NEDD4-2–infected cells (INF$^{NEDD4-2}$), and in the control group infected with the rAAV2/6-NEDD4-2CS vector (INF$^{NEDD4-2CS}$). *Slow* (**E**, in cyan) and *fast* (**F**, in magenta) neurons are shown. Nonparametric 1-way ANOVA (Kruskal-Wallis test) with Dunn's post-hoc test. See Supplemental Figure 5F for total population, Supplemental Table 5 for biophysical properties and values, and Supplemental Figure 5, A–E. (**G**) Basal thermal sensitivity showed no difference at 49°C ($P = 0.987$), 52°C ($P = 0.186$), or 55°C ($P = 0.673$) in the hot-plate test between the 2 groups. Student's *t* test. (**H**) An increase in tail-flick latency ($P = 0.018$ at intensity 7) for high-intensity stimulation in the rAAV2/6-NEDD4-2 group was observed. Mann-Whitney *U* test. (**I**) Tail pressure sensitivity was increased in mice infected with rAAV2/6-NEDD4-2. $^{**}P = 0.006$, Student's *t* test. (**J**) Basal responses to innocuous mechanical stimulation were not different between the 2 strands, but the development of mechanical allodynia was significantly diminished in rAAV2/6-NEDD4-2–infected mice. $^{***}P < 0.001$ at day 7 and $^{**}P < 0.01$ at day 14; 2-way ANOVA on log values with post-hoc Bonferroni's tests. Data are expressed as the mean ± SEM; $n = 12$–15 for rAAV2/6-stuffer and rAAV2/6-NEDD4-2.

plate test at 52°C after SNI (Figure 5E). *Nedd4L*$^{fl/fl}$ mice did not develop SNI-induced hyperalgesia. The observed thermal hypersensitivity in the *SNS-Nedd4L*$^{-/-}$ mice under basal conditions was not further enhanced after SNI. The response of the hot-plate test depends on the strength applied by the paw to the plate, which may be impeded after SNI surgery due to the transection of motor neurons. To overcome this problem, we performed the plantar test, an alternative thermal sensitivity test independent of strength, at the end of the SNI time course (i.e., 35 days after SNI). As illustrated in Figure 5F, the noninjured paws of *SNS-Nedd4L*$^{-/-}$ mice demonstrated more thermal hypersensitivity than the noninjured paws of *Nedd4L*$^{fl/fl}$ mice. SNI induced thermal hypersensitivity in the injured paws of *Nedd4L*$^{fl/fl}$ mice, but did not further enhance the hypersensitivity in the injured paws of *SNS-Nedd4L*$^{-/-}$ mice. Basal mechanical innocuous sensitivity was not altered in *Nedd4L*$^{fl/fl}$ mice (see baseline [BL] in the von Frey filaments test in Figure 5D). After SNI, the decrease in the withdrawal threshold related to the development of mechanical allodynia–like behavior was indistinguishable between groups. Intraplantar injection of formalin in *SNS-Nedd4L*$^{-/-}$ mice led to an increased and earlier maximal

response (peak at 30.4 ± 1.4 minutes in *SNS-Nedd4L*$^{-/-}$ mice compared with 36.3 ± 1.3 minutes in *Nedd4L*$^{fl/fl}$ mice; $P = 0.039$) during the early second phase as compared with the *Nedd4L*$^{fl/fl}$ mice, suggesting a central consequence of increased peripheral activity due to *Nedd4L* deletion (Figure 5G). Acute nociception during phase 1 of the formalin test was similar between the groups.

Functional effects of in vivo exogenous NEDD4-2 overexpression. To test whether the rescue of NEDD4-2 reduction in DRG may functionally modify Na_v expression and influence the course of SNI-induced hypersensitivity, we generated a recombinant serotype 6 adenoassociated viral vector expressing NEDD4-2 (rAAV2/6-NEDD4-2, Supplemental Figure 5A). Two control vectors were designed: noncoding (stuffer) vectors and those expressing the catalytically inactive form of NEDD4-2 (NEDD4-2CS). The infection efficiency of the viral vector was recently demonstrated for small DRG neurons (presumably nociceptors) after intrathecal delivery, and the transduction efficiency was shown to be entirely preserved after peripheral nerve injury (34). Immunofluorescence experiments showed that rAAV2/6-NEDD4-2 increased NEDD4-2 expression in L4/5 DRG under naive conditions and after SNI (Figure 6, A–D and Supplemental Figure 5B). I_{Na} measurements were taken of small DRG neurons after *Nedd4L* gene delivery, followed by single-cell PCR to identify infected (INF) and noninfected neurons (NINF). In naive animals, NEDD4-2 overexpression altered neither the I_{Na} density, nor the biophysical properties of rAAV2/6-NEDD4-2–infected DRG neurons when compared with cells infected with the control vector ($INF^{NEDD4\text{-}2CS}$) or the NINF neurons (Supplemental Figure 5, C–E, and Supplemental Table 4). In the SNI condition, exogenous expression of NEDD4-2 substantially reduced the I_{Na} densities for Na_vtotal (by 49%), $Na_v1.7$ (by 53%), and $Na_v1.8$ (by 58%) of infected neurons ($INF^{NEDD4\text{-}2}$). This was observed mainly in the *fast* subpopulation of DRG neurons as compared with the controls ($INF^{NEDD4\text{-}2CS}$ and NINF; Figure 6F and Supplemental Table 5), accounting for the tendency observed in the total population (Supplemental Figure 5F). The virus can potentially transduce all types of DRG cells, which may explain why effects were observed only in the *fast* population and not in the *slow* population. Before determining whether restoring NEDD4-2 expression with this viral vector would impact SNI-mediated hypersensitivity, we first tested the basal sensitivity. The response to innocuous mechanical stimuli remained unchanged (see baseline in the von Frey filaments test; Figure 6J). Responses to the hot-plate test (Figure 6G) and the low intensity of the tail-flick tests were not different between rAAV2/6-NEDD4-2 or control vector (rAAV2/6-stuffer) mice (Figure 6H). However, mice infected with rAAV2/6-NEDD4-2 showed mild, but significant, hyposensitivities to the higher stimulus of the tail-flick test, whereas they showed mild, but significant, hypersensitivity to mechanical nociception (tail pressure test; Figure 6I). The development of mechanical allodynia following SNI was repressed in rAAV2/6-NEDD4-2–infected mice as compared with mice infected with the noncoding vector (Figure 6J), highlighting the behavioral consequences of the decrease in I_{Na} current.

Discussion

The present study provides what we believe to be the first in vivo evidence that the ubiquitin ligase NEDD4-2 exerts a strong influence on the neuronal excitability of the sensory system, and that dysregulation of this regulatory mechanism contributes to pain hypersensitivity. This is mainly due to a pathological redistribution of $Na_v1.7$ and $Na_v1.8$ in DRG cells.

Peripheral neuropathic pain develops across different disease states as a result of different mechanisms and depends on multiple etiological factors. In this study, we used the SNI model, a common traumatic nerve injury–induced neuropathic pain animal model (35). Although this may not mimic the mechanisms of other neuropathic pain syndromes, its fast onset and prolonged maintenance of thermal and mechanical hypersensitivity renders it very valuable.

Using this model of neuropathic pain in mice, NEDD4-2 expression was found to be substantially decreased in DRG neurons, with a concomitant increase in $Na_v1.7$ and $Na_v1.8$ current densities. The results also demonstrated that knocking out NEDD4-2 expression in nociceptive neurons increased $Na_v1.7$ and $Na_v1.8$ levels and enhanced basal pain sensitivity. Conversely, the overexpression of NEDD4-2 using rAAV2/6 vectors led to a reduction in $Na_v1.7$ and $Na_v1.8$ current densities and a decrease in neuropathic pain–like allodynia in the SNI model.

The different components of I_{Na} were identified in mouse DRG neurons by the use of specific electrophysiological protocols and toxins. $Na_v1.7$-mediated currents were isolated with the perfusion of ProTxII (26). SNI increased $Na_v1.7$ and $Na_v1.8$ currents, particularly in the *slow* neuron subpopulation. Because the biophysical properties of the different I_{Na} components were not modified in the *slow* subpopulation, it is unlikely that the increased current density encountered after SNI was due to a modification of single-channel properties. The results suggest that an increased number of functional channels at the cell membrane may be responsible, a mechanism to which NEDD4-2 downregulation may contribute. This hypothesis is supported by the results obtained with the *SNS-Nedd4L*$^{-/-}$ mice, in which an increase in $Na_v1.7/1.8$ current densities was also observed in *slow* neurons and is unlikely due to the modification of single-channel properties. The specific roles of *fast*/*slow* neuronal subpopulations are not yet understood, but the present observations suggest a role for the *slow* population in modulating thermal sensation.

The protein levels in DRG result from the large intracellular pool of Na_vs and the small Na_v fraction at the plasma membrane (36). As a consequence, modifications of Na_v expression that would be restricted to the plasma membrane may be below the sensitivity limits of the assay, thus accounting for the lack of observed modification of Na_v expression in DRG. Interestingly, both SNI and *SNS-Nedd4L*$^{-/-}$ mice showed an accumulation of $Na_v1.7$ along the sciatic nerve, suggesting NEDD4-2 involvement in channel axonal trafficking. The generation of *SNS-Nedd4L*$^{-/-}$ mice enabled us to investigate the functional contribution of NEDD4-2 in pain pathways. These mice exhibit an abnormal pain phenotype with increased noxious heat sensitivity, as revealed in both the hot-plate and plantar tests under basal conditions. Interestingly, the increase in thermal hypersensitivity seen with the plantar test in the *SNS-Nedd4L*$^{-/-}$ mice reached similar levels to those seen after SNI in the injured paws of control littermates. This finding suggests that genetic disruption of NEDD4-2 leads to thermal pain hypersensitivity similar to that observed when NEDD4-2 is pathologically decreased after SNI. Because *SNS-Nedd4L*$^{-/-}$ mice did not develop mechanical allodynia under basal conditions, the decrease in NEDD4-2 is probably not sufficient to render these mice mechanically hypersensitive. Neither thermal nor mechanical hypersensitivity was enhanced in *SNS-Nedd4L*$^{-/-}$

mice after SNI, suggesting that a maximum effect of SNI-induced hypersensitivity was reached. This is consistent with the fact that NEDD4-2 cannot be further decreased, or only to a minor extent, in the DRG of *SNS-Nedd4L*$^{-/-}$ mice. Finally, the responses in the early second phase of the formalin test were increased, and the kinetics were accelerated in *SNS-Nedd4L*$^{-/-}$ mice when compared with their controls. This result suggests that the peripheral deletion of NEDD4-2 enhances noxious/nocive inputs in the dorsal horn and that it may be sufficient to impact the global mechanisms of central sensitization (37).

The pain behavior of the *SNS-Cre* mouse line does not differ from that of wild-type littermates (38), suggesting that the observed hypersensitive phenotype is due to the deletion of NEDD4-2 and not to the expression of Cre recombinase in $Na_v1.8$-positive nociceptors. The possibility that these differences may also involve non-nociceptive neurons that are potentially subject to Cre recombination cannot be ruled out, as $Na_v1.8$ expression was recently shown to extend to larger DRG neurons (39).

Major modifications of $Na_v1.8$ and $Na_v1.7$ density and distribution were observed in this study. Despite their well-established roles in nociception, the mechanisms by which $Na_v1.7$ and $Na_v1.8$ isoforms specifically contribute to neuropathic pain are still under debate. On the one hand, knocking down $Na_v1.8$ prevents neuropathic pain in mice (40), $Na_v1.7$ accumulates in human painful dental pulp (15), and gain-of-function mutations of $Na_v1.7$ and $Na_v1.8$ are linked to exaggerated pain in humans (12, 13). A recent simulation study suggested that $Na_v1.7$ and $Na_v1.8$ may act synergistically to increase the amplitude of subthreshold oscillations and increase the frequency of repetitive firing in the periphery (41). Increasing their expression in *slow* neurons might promote hyperexcitability. However, in sensory neuron–specific knockouts of $Na_v1.7$, $Na_v1.8$ or double-knockout mice, neuropathic pain–like behavior still develops after nerve injury (18–20). It must be noted that compensatory effects in the expression of the different Na_v isoforms in genetically modified animals during development cannot be excluded. The accumulation of $Na_v1.7$ and $Na_v1.8$ observed along the sciatic nerve after SNI has already been reported for $Na_v1.8$ in an experimental neuropathic pain model and was reported to contribute to neuropathic pain (14).

In the present study, counteracting the SNI-mediated decrease in NEDD4-2 using gene transfer further supports the functional importance of this ubiquitin ligase in traumatic nerve injury–induced neuropathic pain. Gene transfer has already been successfully used in mice to alleviate pain (42), and clinical trials with vectors engineered to express the preproenkephalin gene for treating cancer pain are underway (43, 44). In this study, rAAV-mediated overexpression of NEDD4-2 led to a decrease in $Na_v1.7$ and $Na_v1.8$ current densities in *fast* DRG neurons, which was concomitant with the prevention of the full development of mechanical allodynia. It may be that rAAV overexpression of NEDD4-2 after nerve injury prevents an excess of abnormal peripheral input and reduces activity-dependent central sensitization. It is unlikely that the effects on mechanical allodynia are due to peripheral changes in the activation threshold of low-threshold mechanical afferent fibers, since basal mechanical sensitivity was minimally or not at all affected by rAAV-NEDD4-2 (nor was it after NEDD4-2 knockout). The unexpected mechanical hypoalgesic effect of rAAV2/6-NEDD4-2 might be due to the ability of ubiquitin ligase to regulate other ion channels, such as voltage-gated potassium or chloride channels (45), which could inversely affect cellular excitability depending on the targeted neuronal subpopulation. Despite its effect on the I_{Na} of *fast* DRG neurons, other effects of the viral vector rAAV2/6 on cells or fibers in the peripheral nerve cannot be ruled out.

NEDD4-2 was identified as a central in vivo posttranslational regulator of $Na_v1.7$ and $Na_v1.8$, whose altered function may contribute to the development of neuropathic pain. Given that the abnormal functioning of sodium channels is a key event in the etiology of neuropathic pain, these results support a new paradigm in the treatment of this pathology. Ubiquitylation-dependent mechanisms have already been implicated in neuropathic pain in a study reporting that the intrathecal delivery of proteasome inhibitors attenuated hyperalgesia in rats (46). Another posttranslational modification of sodium channels induced by the accumulation of the glycolytic metabolite methylglyoxal was recently found to play an important role in diabetic neuropathy (47). Posttranslational modifications of $Na_v1.8$ accounted for small, but significant, changes in the biophysical properties of the channel and were responsible for increased excitability of primary sensory neurons and sensitivity in diabetic mice. These results, together with the findings of this study, strongly support the need to look for agents that can modulate Na_v function and that can act as alternatives to the Na_v blockers currently used to treat neuropathic pain.

The factors that lie upstream of the observed NEDD4-2 decrease remain to be identified. Similar to many downregulated genes after SNI, axonal injury and the deprivation of trophic factors from the target tissue likely influence the transcriptional mechanisms involved in the NEDD4-2 decrease (48).

These results point to NEDD4-2 as a central regulator of nociception and demonstrate that NEDD4-2 dysfunction leads to pathological pain. The enhancement of NEDD4-2 activity may provide a novel mechanistic alternative to sodium channel blockers for the treatment of neuropathic pain. NEDD4-2 may even be involved in other neurological diseases linked to altered Na_v channel activity, such as epilepsy and migraine headaches.

Methods

DNA constructs

Human *Nedd4L* (KIAA0439) cDNA lacking a C2 lipid–binding domain cloned into pcDNA3.1 was a gift from T. Nagase (Kazusa DNA Research Institute, Kisarazu, Japan). $Na_v1.7$ cDNA cloned into pCIN5h was provided by S. Tate (Convergence Pharmaceuticals). The QuickChange mutagenesis kit (Stratagene) was used to generate $Na_v1.7$ and NEDD4-2 mutants. $Na_v1.7$ C-terminal PY mutants were generated as follows: Pro^{1944} was mutated into Ala to generate the PA mutant, Tyr^{1947} into Ala to generate the YA mutant, and Val^{1950} into Ala to generate the VA mutant. The NEDD4-2CS mutant was generated by mutating Cys^{801} into a Ser. shRNA against NEDD4-2 cloned into a pGIPZ lentiviral vector was obtained from Open Biosystems. For pull-down experiments, the cDNAs encoding the 66 last amino acids of $Na_v1.7$, the 3 different PY mutants, and the ubiquitin-binding proteasomal subunit S5A (GST-S5A) were cloned into pGEX-4T1 (Amersham Bioscience) to generate GST fusion proteins.

Western blots, immunofluorescence

See Supplemental Methods.

Pull-down and ubiquitylation experiments

pGEX-4T1 containing GST fused to the 66 last amino acids of $Na_v1.7$ WT and PY mutants, as well as GST fused to ubiquitin-binding proteasomal subunit S5A proteins, were produced (see Supplemental Methods). Pulled-down proteins were analyzed by Western blot.

Cell-surface biotinylation

HEK293 cells were incubated for 30 minutes at 4°C with biotin solution (0.5 mg/ml biotin in cold PBS; Pierce Biotechnology) and then rinsed 2 times with PBS containing 200 mM glycine followed by 2 rinsings with PBS. Cells were then solubilized for 1 hour at 4°C on a wheel, and 50 µl of streptavidin-neutravidin-sepharose beads (Invitrogen) was incubated in this fraction for binding to biotinylated proteins. Samples were analyzed by Western blotting.

Real-time RT-PCR

See Supplemental Methods.

Cell culture and transfection

See Supplemental Methods.

Neuron primary culture

See Supplemental Methods.

Mouse lines

See Supplemental Methods.

Animal surgery

In the SNI experiments, the biceps femoris was incised, exposing the sciatic nerve. The tibial and common peroneal nerves were ligated with a silk suture (Ethicon) and transected (35).

Viral vector and intrathecal injection

See Supplemental Methods.

Behavioral pain tests

Hot-plate assay. The hot-plate assay was conducted by placing the animals on the hot-plate surface set at varying temperatures (49°C, 52°C, and 55°C). The latency of response (in seconds) was determined by a hind paw lick or jump. The cutoff was adjusted for each temperature to avoid tissue damage (60 seconds for 49°C, 30 seconds for 52°C, and 20 seconds for 55°C).

Tail-flick assay. The tail-flick assay was conducted using a tail-flick analgesia meter, and the mice were gently restrained in a conical plastic cloth. The latency of response (in seconds) was recorded at 2 different light beam intensities (4 and 7 AU).

Pincher test. The pincher test consists of a pair of large blunt forceps (15 cm long; flat contact area: 7 mm × 1.5 mm with smooth edges) equipped with 2 strain gauges connected to a modified electronic dynamometer (Bioseb). The tips of the forceps were placed around the tail of the tested mice, and the force applied was incremented by hand until a withdrawal response occurred. The measurement was repeated 3 times, and the mean force (in grams) that induced withdrawal was calculated.

von Frey assay. The von Frey assay was conducted by applying a series of calibrated von Frey filaments on the lateral side of the hind paw's plantar surface (sural nerve territory). Mice were thus placed on a platform with a wire netting floor. The mechanical stimulus producing a 50% likelihood of withdrawal was determined using the up-down method.

Formalin test. The formalin test was conducted by injecting 10 µl of 5% formalin subcutaneously into the left hind paw. The time the animal spent shaking or flinching and licking its paw was recorded at 5-minute intervals for 60 minutes.

Plantar test. The plantar test was conducted by exposing the lateral plantar surface of the paw to a beam of radiant heat through a transparent surface. The heat stimulation was repeated 3 times for each paw, and the mean latency time was calculated.

Electrophysiology

HEK293 cell recordings. The external and internal solutions used were as previously described (ref. 23 and see Supplemental Methods). Data were recorded using a VE-2 amplifier (Alembic Instruments) or an Axon 700A amplifier and analyzed using pClamp software, version 8 (Molecular Devices), KaleidaGraph, version 4.03 (Synergy Software), and MATLAB (The MathWorks). The resistance of the borosilicate pipettes (World Precision Instruments) was 2–6 MΩ. The leakage current was subtracted using the P/4 procedure.

I_{Na} densities (pA/pF) were obtained by dividing the peak I_{Na} by the cell capacitance obtained from the pClamp function. Current densities were normalized to WT $Na_v1.7$ or pcDNA3.1 (empty vector control) in the stable cell line for each day of the experiment. The Na^+ current for the steady-state activation (SSA) curves was evoked from a holding potential of −100 mV to test pulses of 100 ms ranging from −120 mV to +30 mV in increments of 5 mV. Steady-state inactivation (SSI) curves were measured from a holding potential of −120 mV using 500-ms prepulses to the indicated potentials followed by a test pulse to 0 mV. To quantify the voltage dependence of SSA and SSI, data from individual cells were fitted with the Boltzmann relationship, $y\,(Vm) = 1 / (1 + \exp[(Vm - V_{1/2}) / k])$, where y is the normalized current or conductance, Vm is the membrane potential, $V_{1/2}$ is the voltage at which half of the available channels are inactivated, and k is the slope factor.

The recovery from inactivation (RFI or "repriming") curves were obtained with a standard 2-pulse protocol consisting of a depolarizing pulse from a holding potential of −120 mV to 0 mV for 50 ms to inactivate the channels, followed by a variable duration (from 0.5 ms to 3,000 ms) step back to −120 mV to promote recovery. The availability of the channels was assessed with the first standard test pulse at 0 mV, and the normalized currents of the second pulse at 0 mV were plotted versus the recovery interval. We calculated the $t_{1/2}$ (ms), which is the time necessary for half of the channels to recover from the first pulse, by interpolation from a linear relation between the 2 points juxtaposing half recovery ($y_1 < 0.5 < y_2$), using the relation $x = [0.5 - (y_1x_2 - y_2x_1) / (x_2 - x_1)] \times (x_2 - x_1) / (y_2 - y_1)$.

DRG neuron recordings. Twelve hours after plating, we performed whole-cell recordings of small neurons (C_m <30 pF) from L4/5 DRG, thought to be nociceptors (27). We used an EPC-10 amplifier and Patchmaster software (both from HEKA Electronics) for data acquisition and analysis. The external and internal solutions used were as previously described (ref. 49 and see also Supplemental Methods). Pipettes had a resistance of less than 3 MΩ, capacity transients were cancelled, and series resistance was compensated by approximately 90%. We used data only from cells in which the access resistance remained stable throughout the duration of the experiment. The leakage current was digitally subtracted using the P/4 procedure.

I_{Na} densities (pA/pF) were obtained by dividing the peak I_{Na} by the cell capacitance obtained from the HEKA function. Once in whole-cell configuration, cells were held at –60 mV for 5 minutes for the following reasons: (a) to dialyze the cell with CsF solution; (b) to reach equilibrium of $Na_v1.8$ (steady-state activation is shifted to hyperpolarized potentials during the first few minutes because of CsF); and (c) to lastingly inactivate the $Na_v1.9$ current (50) in order to prevent contamination of the $Na_v1.8$ current. Cells were clamped at –80 mV for 2 more minutes before starting the recordings. Activation, SSI, and RFI curves were obtained as described in the in vitro experiments, except that each pulse was preceded by a prepulse of 3 seconds at –120 mV to promote recovery of every Na_vs isoform.

Pharmacological separation of $Na_v1.7$, $Na_v1.8$, and rTTXs sodium currents. Na_vtotal current-voltage (I-V), Na_vtotal SSI, and Na_vtotal RFI curves were obtained as mentioned above for the total Na_v isoform component present in DRG neurons. ProTxII (5 nM; provided by B. Priest, Merck Serono), a selective blocker of $Na_v1.7$, was then perfused, and a test pulse at 0 mM was performed until the diminution of peak amplitude reached its steady state (toxin maximal effect). A 5-nM concentration of the toxin would block over 90% of $Na_v1.7$ and less than 10% of the other isoforms (26). Na_vtotal^{ProTxII} I-V, Na_vtotal^{ProTxII} SSI, and Na_vtotal^{ProTxII} RFI were then recorded. Subtracting the total curves for Na_vtotal I-V, Na_vtotal SSI, and Na_vtotal RFI from those of Na_vtotal^{ProTxII} I-V, Na_vtotal^{ProTxII} SSI, and Na_vtotal^{ProTxII} RFI allowed us to measure $Na_v1.7$ I-V, $Na_v1.7$ SSI, and $Na_v1.7$ RFI. Finally, TTX (300 mM) was added to isolate the $Na_v1.8$ I-V, $Na_v1.8$ SSI, and $Na_v1.8$ RFI curves. Subtracting the $Na_v1.8$ I-V, $Na_v1.8$ SSI, and $Na_v1.8$ RFI curves from those of Na_vtotal^{ProTxII} I-V, Na_vtotal^{ProTxII} SSI, and Na_vtotal^{ProTxII} RFI allowed us to record Na_vrTTXs I-V, Na_vrTTXs SSI, and Na_vrTTXs RFI, representing the remainder of the TTX-sensitive current. For examples of this protocol for I-V curves, see Figure 3A.

Statistics

For in vitro experiments (current densities, biophysical properties, and protein quantification), data were analyzed using an unpaired, 2-tailed Student's *t* test when 2 groups were compared, or 1-way ANOVA for multiple group comparisons. For ex vivo recordings (current densities and biophysical properties) and behavioral pain tests, normality was tested with a D'Agostino-Pearson omnibus test to determine whether parametrical (Student's *t*) or nonparametrical (Mann-Whitney *U*) tests would be used when 2 groups were compared. The same normality test was performed for multiple group comparisons to determine whether a regular 1-way ANOVA and post-hoc Bonferroni's tests, or the nonparametric equivalence test (Kruskal-Wallis and Dunn's post tests) would be performed. For behavioral pain time courses (von Frey filaments, formalin), 2-way ANOVA with repeated measures were performed. The statistical tests used are described in each figure legend. A *P* value less than 0.05 was considered significant.

Study approval

All experimental procedures were approved by the Committee on Animal Experimentation of the Canton de Vaud, Switzerland, in accordance with the Swiss Federal Laws on Animal Welfare and the guidelines of the International Association for the Study of Pain (Zimmermann, 1983). Animals were housed under a 12-hour light/12-hour dark cycle and had free access to food and water.

Acknowledgments

We thank O. Staub (Lausanne University) for providing NEDD4-2 purified antibody and the *Nedd4L$^{fl/fl}$* mouse line; R. Kuner (Heidelberg University) for providing the *SNS-Cre* mouse line; S. Tate and V. Morisset (Convergence Pharmaceuticals) for providing $Na_v1.7$ cDNA cloned into pCIN5h and HEK293 cells stably expressing $Na_v1.7$; and B. Priest (Merck Serono) for providing ProTxII. The monoclonal antibody N68/3 (anti-$Na_v1.7$) was developed by and/or obtained from the UC Davis/NIH NeuroMab Facility, supported by an NIH grant (U24NS050606) and maintained by the Department of Neurobiology, Physiology and Behavior, College of Biological Sciences, University of California, Davis. We thank P. Aebischer (EPFL) for all the work performed in his laboratory and for his scientific advice. We thank M.R. Suter (CHUV and University of Lausanne), R.R. Ji (Duke University), C.J. Woolf (F.M. Kirby Neurobiology Center, Children's Hospital Boston and Harvard Medical School), and A. Felley (La Tour-de-Peilz, Switzerland) for comments on the manuscript. This study was supported by grants from the Swiss National Science Foundation (31003A-124996 to I. Decosterd and 310030B-135693 to H. Abriel), the Synapsis Foundation (to I. Decosterd and H. Abriel), the European Society of Anesthesiology (to I. Decosterd), and the Lemanic Neuroscience Doctoral School PhD Fellowship (to C.J. Laedermann). The contribution of B. Gavillet to the preliminary experiments is acknowledged. We would also like to thank C. Kern (CHUV and University of Lausanne) for his support.

Received for publication January 24, 2013, and accepted in revised form April 19, 2013.

Address correspondence to: Hugues Abriel, Department of Clinical Research, University of Bern, Murtenstrasse 35, 3010 Bern, Switzerland. Phone: 41.31.6320928; Fax: 41.31.6320946; E-mail: Hugues.Abriel@dkf.unibe.ch. Or to: Isabelle Decosterd, Pain Center, University Hospital Center (CHUV) and University of Lausanne, Bugnon 46, 1011 Lausanne, Switzerland. Phone: 41.21.3142040; Fax: 41.21.214 3044; E-mail: Isabelle.Decosterd@chuv.ch.

1. Bouhassira D, Lanteri-Minet M, Attal N, Laurent B, Touboul C. Prevalence of chronic pain with neuropathic characteristics in the general population. *Pain*. 2008;136(3):380–387.
2. Amir R, Michaelis M, Devor M. Membrane potential oscillations in dorsal root ganglion neurons: role in normal electrogenesis and neuropathic pain. *J Neurosci*. 1999;19(19):8589–8596.
3. Nystrom B, Hagbarth KE. Microelectrode recordings from transected nerves in amputees with phantom limb pain. *Neurosci Lett*. 1981;27(2):211–216.
4. Costigan M, Scholz J, Woolf CJ. Neuropathic pain: a maladaptive response of the nervous system to damage. *Annu Rev Neurosci*. 2009;32(1):1–32.
5. Brackenbury WJ, Isom LL. Na channel β subunits: overachievers of the ion channel family. *Front Pharmacol*. 2011;2:53.
6. Payandeh J, Scheuer T, Zheng N, Catterall WA. The crystal structure of a voltage-gated sodium channel. *Nature*. 2011;475(7356):353–358.
7. Ho C, O'Leary ME. Single-cell analysis of sodium channel expression in dorsal root ganglion neurons. *Mol Cell Neurosci*. 2011;46(1):159–166.
8. Fukuoka T, Kobayashi K, Yamanaka H, Obata K, Dai Y, Noguchi K. Comparative study of the distribution of the alpha-subunits of voltage-gated sodium channels in normal and axotomized rat dorsal root ganglion neurons. *J Comp Neurol*. 2008;510(2):188–206.
9. Cox JJ, et al. An SCN9A channelopathy causes congenital inability to experience pain. *Nature*. 2006;444(7121):894–898.
10. Fertleman CR, et al. SCN9A mutations in paroxysmal extreme pain disorder: allelic variants underlie distinct channel defects and phenotypes. *Neuron*. 2006;52(5):767–774.
11. Reimann F, et al. Pain perception is altered by a nucleotide polymorphism in SCN9A. *Proc Natl Acad Sci U S A*. 2010;107(11):5148–5153.
12. Faber CG, et al. Gain of function Nav1.7 mutations in idiopathic small fiber neuropathy. *Ann Neurol*. 2012;71(1):26–39.
13. Faber CG, et al. Gain-of-function Nav1.8 mutations in painful neuropathy. *Proc Natl Acad Sci U S A*. 2012;109(47):19444–19449.
14. Gold MS, et al. Redistribution of NaV1.8 in uninjured axons enables neuropathic pain. *J Neurosci*. 2003;23(1):158–166.
15. Luo S, Perry G, Levinson SR, Henry M. Nav1.7 expression is increased in painful human dental pulp. *Mol Pain*. 2008;4(1):16.
16. Persson AK, Gasser A, Black JA, Waxman SG. NaV1.7 accumulates and co-localizes with phosphorylated ERK1/2 within transected axons in early experimental neuromas. *Exp Neurol*. 2011;230(2):273–279.
17. Liu M, Wood JN. The roles of sodium channels in nociception: implications for mechanisms of neuropathic pain. *Pain Med*. 2011;12:S93–99.
18. Akopian AN, et al. The tetrodotoxin-resistant sodium channel SNS has a specialized function in pain pathways. *Nat Neurosci*. 1999;2(6):541–548.
19. Nassar MA, et al. Nociceptor-specific gene deletion reveals a major role for Nav1.7 (PN1) in acute and inflammatory pain. *Proc Natl Acad Sci U S A*. 2004;101(34):12706–12711.
20. Nassar MA, Levato A, Stirling LC, Wood JN. Neuropathic pain develops normally in mice lacking both Nav1.7 and Nav1.8. *Mol Pain*. 2005;1:24.

21. Abriel H, Staub O. Ubiquitylation of ion channels. *Physiology (Bethesda)*. 2005;20(6):398–407.
22. Abriel H, et al. Defective regulation of the epithelial Na^+ channel by Nedd4 in Liddle's syndrome. *J Clin Invest*. 1999;103(5):667–673.
23. van Bemmelen MX, et al. Cardiac voltage-gated sodium channel Nav1.5 is regulated by Nedd4-2 mediated ubiquitination. *Circ Res*. 2004; 95(3):284–291.
24. Fotia AB, Ekberg J, Adams DJ, Cook DI, Poronnik P, Kumar S. Regulation of neuronal voltage-gated sodium channels by the ubiquitin-protein ligases Nedd4 and Nedd4-2. *J Biol Chem*. 2004;279(28):28930–28935.
25. Cachemaille M, Laedermann CJ, Pertin M, Abriel H, Gosselin RD, Decosterd I. Neuronal expression of the ubiquitin ligase Nedd4-2 in rat dorsal root ganglia: Modulation in the spared nerve injury model of neuropathic pain. *Neuroscience*. 2012;227(0):370–380.
26. Schmalhofer WA, et al. ProTx-II, a selective inhibitor of NaV1.7 sodium channels, blocks action potential propagation in nociceptors. *Mol Pharmacol*. 2008;74(5):1476–1484.
27. Lopez-Santiago LF, et al. Sodium channel beta2 subunits regulate tetrodotoxin-sensitive sodium channels in small dorsal root ganglion neurons and modulate the response to pain. *J Neurosci*. 2006;26(30):7984–7994.
28. Berta T, Poirot O, Pertin M, Ji RR, Kellenberger S, Decosterd I. Transcriptional and functional profiles of voltage-gated $Na(^+)$ channels in injured and non-injured DRG neurons in the SNI model of neuropathic pain. *Mol Cell Neurosci*. 2008;37(2):196–208.
29. Cummins TR, Waxman SG. Downregulation of tetrodotoxin-resistant sodium currents and upregulation of a rapidly repriming tetrodotoxin-sensitive sodium current in small spinal sensory neurons after nerve injury. *J Neurosci*. 1997;17(10):3503–3514.
30. Shi PP, et al. Salt-sensitive hypertension and cardiac hypertrophy in mice deficient in the ubiquitin ligase Nedd4-2. *Am J Physiol Renal Physiol*. 2008;295(2):F462–F470.
31. Agarwal N, Offermanns S, Kuner R. Conditional gene deletion in primary nociceptive neurons of trigeminal ganglia and dorsal root ganglia. *Genesis*. 2004;38(3):122–129.
32. Liu Y, et al. VGLUT2-dependent glutamate release from nociceptors is required to sense pain and suppress itch. *Neuron*. 2010;68(3):543–556.
33. Stirling LC, et al. Nociceptor-specific gene deletion using heterozygous NaV1.8-Cre recombinase mice. *Pain*. 2005;113(1–2):27–36.
34. Towne C, Pertin M, Beggah AT, Aebischer P, Decosterd I. Recombinant adeno-associated virus serotype 6 (rAAV2/6)-mediated gene transfer to nociceptive neurons through different routes of delivery. *Mol Pain*. 2009;5(1):52.
35. Decosterd I, Woolf CJ. Spared nerve injury: an animal model of persistent peripheral neuropathic pain. *Pain*. 2000;87(2):149–158.
36. Schmidt J, Rossie S, Catterall WA. A large intracellular pool of inactive Na channel alpha subunits in developing rat brain. *Proc Natl Acad Sci U S A*. 1985;82(14):4847–4851.
37. McCall WD, Tanner KD, Levine JD. Formalin induces biphasic activity in C-fibers in the rat. *Neurosci Lett*. 1996;208(1):45–48.
38. Agarwal N, et al. Cannabinoids mediate analgesia largely via peripheral type 1 cannabinoid receptors in nociceptors. *Nat Neurosci*. 2007;10(7):870–879.
39. Shields SD, et al. Nav1.8 expression is not restricted to nociceptors in mouse peripheral nervous system. *Pain*. 2012;153(10):2017–2030.
40. Lai J, et al. Inhibition of neuropathic pain by decreased expression of the tetrodotoxin-resistant sodium channel, NaV1.8. *Pain*. 2002;95(1-2):143–152.
41. Choi JS, Waxman SG. Physiological interactions between Nav1.7 and Nav1.8 sodium channels: a computer simulation study. *J Neurophysiol*. 2011;106(6):3173–3184.
42. Huang Y, Liu X, Dong L, Liu Z, He X, Liu W. Development of viral vectors for gene therapy for chronic pain. *Pain Res Treat*. 2011;2011:968218.
43. Diamyd Inc. Registry and results database of clinical studies of human participants around the world. NIH Web site. http://clinicaltrials.gov/ct2/show/NCT00804076. Updated Ocotober 3, 2012. Accessed May 6, 2013.
44. Diamyd Inc. Registery and results database of clinical studies of human participants around the world. NIH web site. http://clinicaltrials.gov/ct2/show/NCT01291901. Updated October 3, 2012. Accessed May 6, 2013.
45. Bongiorno D, Schuetz F, Poronnik P, Adams DJ. Regulation of voltage-gated ion channels in excitable cells by the ubiquitin ligases Nedd4 and Nedd4-2. *Channels (Austin)*. 2011;5(1):79–88.
46. Moss A, et al. A role of the ubiquitin-proteasome system in neuropathic pain. *J Neurosci*. 2002;22(4):1363–1372.
47. Bierhaus A, et al. Methylglyoxal modification of Nav1.8 facilitates nociceptive neuron firing and causes hyperalgesia in diabetic neuropathy. *Nat Med*. 2012;18(6):926–933.
48. Costigan M, et al. Replicate high-density rat genome oligonucleotide microarrays reveal hundreds of regulated genes in the dorsal root ganglion after peripheral nerve injury. *BMC Neurosci*. 2002;3(1):16.
49. Cummins TR, Rush AM, Estacion M, Dib-Hajj SD, Waxman SG. Voltage-clamp and current-clamp recordings from mammalian DRG neurons. *Nat Protoc*. 2009;4(8):1103–1112.
50. Cummins TR, Dib-Hajj SD, Black JA, Akopian AN, Wood JN, Waxman SG. A novel persistent tetrodotoxin-resistant sodium current in SNS-null and wild-type small primary sensory neurons. *J Neurosci*. 1999;19(24):RC43.

Dysregulation of voltage-gated sodium channels by ubiquitin-ligase NEDD4-2 in neuropathic pain

Cédric J Laedermann, Matthieu Cachemaille, Guylène Kirschmann, Marie Pertin, Romain-Daniel Gosselin, Isabelle Chang, Maxime Albesa, Chris Towne, Bernard L Schneider, Stephan Kellenberger, Hugues Abriel, Isabelle Decosterd

Inventory of supplemental data

Supplemental Methods

Western blots:

For *in vitro* experiments, protein extraction was performed 48 hours after transfection. HEK293 cells were lysed (50 mM Tris at pH 7.5, 150 mM NaCl, Complete Protease inhibitor cocktail tablets (Roche), 1 mM PMSF, 1% Triton) and soluble fractions were recovered in supernatants after 15 min of centrifugation at 13,000 x *g* at 4 °C. For *ex vivo* experiments, mice were sacrificed (sodium pentobarbital) and L4/L5 DRGs or sciatic nerve (from the distal trifurcation into sural, common peroneal and tibial to the proximal bifurcation into L4 and L5, neuromas were excluded) were quickly dissected. L4 and L5 DRGs or sciatic nerves from 2 mice were pooled for each sample. Lysis (100 mM Tris HCl at pH 6.8, SDS 2%, Glycerol 20% and Complete Protease inhibitor cocktail tablets) of tissues was done and soluble fractions were recovered in supernatants after 20 min centrifugation at 13,000 x *g* at 4°C. Protein concentration was measured using Bradford test-based CooAssay reagent (Uptima). Proteins were separated on acrylamide SDS-PAGE and then transferred to a nitrocellulose (HEK293) or PVDF (mouse tissue) membrane that were immunoblotted with the following antibodies: antibody to $Na_v1.7$ (1:500, mouse monoclonal clone N68/6, UC Davis/National Institute of Health (NIH) NeuroMab Facility, University of California), antibody to $Na_v1.8$ (1:200, NeuroMab), pan antibody to Na_vs (SP19, 1:500, rabbit polyclonal antibody, Sigma), antibody to NEDD4-2 (1:100, rabbit polyclonal antibody, kindly provided by O. Staub, Lausanne University), antibody to GM130 (1:500, mouse monoclonal clone 35/GM130, BD Transduction Laboratories), antibody to calreticulin (1:2000, rabbit polyclonal antibody, kindly provided by A. Abderrahmani, Lille University), antibody to BiP (1:500, rabbit monoclonal clone C50B12, Cell Signalling Technology), antibody to EEA1 (1:1000, rabbit polyclonal antibody, Abcam), antibody to LAMP1 (1:500, rabbit polyclonal antibody,

Abcam), antibody to alpha 1 subunit of the NaK/ATPase (1:5000, mouse monoclonal clone 464.6, Abcam), antibody to beta 1 subunit of the NaK/ATPase (1:1000, rabbit polyclonal antibody, kindly provided by K. Geering, Lausanne University), antibody to caveolin1 (1:200, rabbit polyclonal antibody, Santa Cruz Biotechnology) and antibody to α-tubulin (1:10,000, mouse monoclonal clone B-5-1-2) or antibody to GAPDH (1:5,000, rabbit polyclonal antibody, Abcam). For HEK293 cells we used infrared IRDyeTM (680 or 800 CW)-linked goat anti-rabbit or anti-mouse IgG (1:15,000, LI-COR Biosciences) and for mouse tissue we used secondary peroxidase-linked goat anti-rabbit or anti-mouse IgG (1:20,000, Pierce) and SuperSignal West Dura Chemiluminescent Substrate (Pierce). Protein quantification was performed using ImageJ software (US NIH).

Immunofluorescence:

Animals were transcardially perfused with saline, followed by 4% paraformaldehyde in PBS. DRGs were dissected and fixed at 4°C for 90 min and then transferred in 20% sucrose in PBS overnight. DRGs were mounted in cryoembedding fluid (Tissue-Tek, Sakura Finetek), cryosectioned at 12 µm thickness and mounted directly onto slides.

NEDD4-2 primary antibody was used at 1:100 and $Na_v1.8$ (rabbit polyclonal antibody provided by S. Tate, GSK) at 1:100. Sections of DRGs were blocked for 30 min at room temperature with normal goat serum (NGS) 10% and PBS 1X-Triton X-100 0.3%. Then primary antibodies were diluted in NGS 5% and PBS 1X-Triton X100 0.1% and placed onto the sections overnight at 4°C. Slides were washed in PBS and incubated at room temperature with secondary antibodies as follows: Fluorescein (FITC)-conjugated anti-rabbit (1: 200, Jackson Immunoresearch Laboratories) for $Na_v1.8$ and Cy3 anti-rabbit (1:400, Jackson Immunoresearch Laboratories) for NEDD4-2, diluted in NGS 1% and PBS 1X-Triton X100 0.1% for 90 min. Slides were washed again in PBS and mounted with Mowiol mounting medium (Calbiochem).

Pulldown and ubiquitylation experiments:

Generation of fusion proteins: pGEX-4T1 containing GST-66 last amino acids of Nav1.7 WT and PY mutants (for pulldown experiment, Figure 3B) as well as GST-S5A (for ubiquitylation experiment, Figure 3D) were expressed in E.coli K12 cells after induction with 0.5 mM IPTG for 2 h at 30°C. Cells were resuspended in lysis buffer (20 mM Tris at pH 7.5, 250 mM NaCl, 0.5% NP40, 1 mM EDTA, 1 mM PMSF, 0.2 mg/ml DNASE I (Roche) and 0.2 mg/ml Lysozyme (Roche)) and rotated for 1 hour in the presence of GSH-Sepharose beads (Amersham Bioscience).

Pulldown: HEK293 cells were lysed for 45 minutes at 4°C with lysis buffer. Following a 15 min centrifugation at 13,000 x *g* at 4°C, soluble fractions were incubated with GSH-sepharose beads containing either GST (as a negative control) or the different GST fusion proteins. Pulled-down proteins were analyzed by Western Blot.

Subcellular fractionation:

HEK293 cells, DRGs and sciatic nerves were homogenized in Tris HCl 10mM, pH7.4 and 0.25M sucrose using a mortar and pestle. The lysate was charged on a sucrose gradient increasing from 15 to 50% concentration (8 fractions of 400 µl in Tris 10mM at pH 7.4) and centrifuged at 200,000 x *g* for 2 hours, 4°C. The whole gradient was further divided into 14 fractions of 250 µl that were analyzed by western blot.

Real time RT-PCR:

DRGs were rapidly dissected and collected in RNA-later solution (Qiagen). mRNA was extracted and purified with RNAeasy Plus Minikit (Qiagen) and quantified using RNA 6000 Nano Assay (Agilent Technologies). TaqMan mRNA Assays, specific to mRNA targets were obtained from Applied Biosystems. qRT-PCR was performed using TaqMan Fast Universal PCR Master Mix on a 7500 Fast Real-Time PCR System according to the manufacturer's

protocol. All samples were run in triplicate. Normalized signal levels for each mRNA were calculated using comparative cycle threshold method (ddCT method) relative to the mean of GAPDH or HPRT following the manufacturer's instructions.

Single cell PCR:

After whole-cell recording, single neurons were harvested and transferred to a PCR tube containing 5 µl of Proteinase K (400 ng/µl) and 17 µM of SDS. The mixture was then incubated at 50°C for 1h and at 99°C for 30 min to inactivate Proteinase K. Real-time PCR amplification and a melting curve peaking at the right temperature using beta-globin primer revealed infected cells.

Cell culture and transfection:

HEK293 cells were cultured as previously described (1). 1 µg of $Na_v1.7$ cDNA or PY mutants were transfected into HEK293 cells, concomitantly with 0.8 µg EBO-pCD-Leu2-CD8 cDNA encoding the CD8 antigen as a reporter gene and 0.8 µg of NEDD4-2 or NEDD4-2CS. For patch clamp experiments, calcium phosphate transfection was used and for biochemistry experiments we used lipofectamine (Invitrogene). Experiments were performed 48 hours after transfection unless otherwise stated.

Neuron primary culture:

Mice (C57BL/6 mice, Charles River Lab) were sacrificed at 4-8 weeks old. L/5 DRGs were harvested and digested in 5 ml of solution containing: Liberase blendzyme TM (Roche) at a concentration of 0.5U/DRG, 12 µM EDTA in oxygenated Complete Saline Solution (CSS composition: 137 mM NaCl, 5.3 mM KCl, MgCl2-6H2O, 25 mM Sorbitol, 10 mM HEPES, 3 mM CaCl2 and pH ajusted to 7.2 with NaOH) for 20 min at 37°C. Neurons were further digested with Liberase blendzyme TL in 5 ml solution (0.5U/DRG, 12 µM EDTA in 5 ml

CSS) + Papaïn (30U/ml) for 10 min. Finally neurons were suspended in 1 ml of DRG medium Mix (89% DMEM/F-12, 10% BSA, 1% penicillin/streptomycin) supplemented with 1.5 mg of trypsin inhibitor and 1.5 mg of purified BSA. Mechanical dissociation was performed using a P1000 pipetman to gently triturate the DRG for 12 strokes. Finally, 80 µl of isolated neurons were plated on poly-D-lysine coated coverslips and incubated 12 hours before recordings to allow recovery and adhesion of neurons. Neurons were only recorded for 12 hours to prevent long-term culture phenotypic changes and neurite outgrowth that degrades space clamp.

Mouse lines:

The floxed *Nedd4L* (2) in C57BL6 background was kindly provided by O. Staub (Lausanne University). Briefly, the *Nedd4L* conditional gene targeting construct was assembled using three PCR fragments covering exons 6 through 10. One loxP site was inserted into intron 5 and the second loxP site was inserted into intron 8; this linearized targeting vector was then electroporated into ES cells to generate the homozygote floxed *Nedd4L* mouse line. This mouse line was crossed with another C57BL6 background transgenic mouse line (*Cre-SNS*) selectively expressing *Cre* recombinase in sensory ganglia using promoter elements of the $Na_v1.8$ gene (3) kindly provided by R. Kuner (Heidelberg University). A 230-kb-large bacterial artificial chromosome (BAC) containing the mouse *SCN10A* locus was identified by PCR. A cassette consisting of the Cre recombinase, β-actin, polyA and 500 bp homologous sequences to SCN10a was injected into mouse pronuclei. The two genetically modified mouse lines were backcrossed with C57BL6 mice (Charles River) for more than 8 generations. Homozygous floxed *Nedd4L* mice were crossed with *Cre* heterozygous mice in order to obtain 50% *SNS-Nedd4L*$^{-/-}$ and 50% *Nedd4L*$^{fl/fl}$ mice, which were then used as test animals and control littermates, respectively. Mice progeny were identified by PCR. *SNS-Cre* mice did not display any overt phenotype and were indistinguishable from wildtype when tested for thermal or mechanical sensing (3).

Viral Vector:

mNedd4L (NP_114087.2) coupled to a s-tag (provided by O. Staub, Lausanne University) was cloned into the multiple cloning site of pAAV-MCS (Stratagene) that lies downstream of the PGK promoter and β-globin intron in order to create rAAV2/6-NEDD4-2 (Figure S3A). Production and titration were performed as previously described (4). Briefly, rAAV2/6 was produced by cotransfection of the pAAV-PGK shuttle plasmid with the pDF6 packaging plasmid into the 293AAV cell line that stably expresses the E1 gene needed for activation of rep and cap promoters (5). We added proteasome inhibitor MG132 to increase viral vector production. Cell lysates were purified by high-pressure liquid chromatography on the HiTrap Heparin column (GE Healthcare Bio-Sciences AB) 48 hr later. The obtained viral suspension was concentrated with Centricon Plus-20 (Regenerated Cellulose 100,000 MWCO, Millipore) and the suspension medium replaced with PBS. The infectivity (transduction units per volume, *tu*) of the virus rAAV2/6 was determined by flow cytometry for direct eGFP fluorescence. The percentage of eGFP-positive cells was quantified 48h after infection of 293T cells with respect to uninfected control cells. The number of transduction events was calculated using the Poisson equation.

Intrathecal Injection:

Intrathecal injection were performed using Omnican U-100 insulin syringes (30Gx1/2", B.Braun). Animals backs were shaved, and mice were restrained in a towel. The needle was inserted between spinal cord L5 and L6 to deliver 3.3 X 10e7 *tu* (transduction units per volume) of rAAV2/6 viruses. A brief tail reflex confirmed that we attained the intrathecal space.

Electrophysiology: solutions

HEK293 cells recordings:

Whole cell patch-clamp recordings were carried-out using an internal solution containing 60 mM CsCl, 70 mM Cs Aspartate, 11 mM EGTA, 1 mM MgCl2, 1 mM CaCl2, 10 mM HEPES, and 5 mM Na2-ATP, pH 7.2 with CsOH and external solution containing 130 mM NaCl, 2 mM CaCl2, 1.2 mM MgCl2, 5 mM CsCl, 10mM HEPES, 5 mM glucose, pH 7.4 with CsOH. For the stable cell line expressing $Na_v1.7$, the extracellular sodium was reduced to 50 mM and n-methyl-D-glutamine was used to substitute for sodium.

DRG neuron recordings:

The pipette solution for whole-cell measurements contained: 140 mM CsF, 10 mM NaCl, MgCl2, 0.1 mM CaCl2, 1.1 mM EGTA, 10 mM HEPES, pH was adjusted to 7.2 with CsOH. Extracellular solutions contained 30 mM NaCl, 110 mM TEA–Cl, 3 mM KCl, 1 mM CaCl2, 1 mM MgCl2, 10 mM HEPES, 10 mM Glucose, 0.1 mM CdCl, pH was adjusted to 7.3 using Tris base.

Supplemental References:

1. van Bemmelen MX, et al. Cardiac Voltage-Gated Sodium Channel Nav1.5 Is Regulated by Nedd4-2 Mediated Ubiquitination. *Circ Res.* 2004;95(3):284-291.
2. Shi PP, et al. Salt-sensitive hypertension and cardiac hypertrophy in mice deficient in the ubiquitin ligase Nedd4-2. *Am J Physiol Renal Physiol.* Aug 2008;295(2):F462-470.
3. Agarwal N, Offermanns S, Kuner R. Conditional gene deletion in primary nociceptive neurons of trigeminal ganglia and dorsal root ganglia. *Genesis.* Mar 2004;38(3):122-129.
4. Dusonchet J, Bensadoun J-C, Schneider BL, Aebischer P. Targeted overexpression of the parkin substrate Pael-R in the nigrostriatal system of adult rats to model Parkinson's disease. *Neurobiol Dis.* 2009;35(1):32-41.
5. Grimm D, Kay MA, Kleinschmidt JA. Helper virus-free, optically controllable, and two-plasmid-based production of adeno-associated virus vectors of serotypes 1 to 6. *Mol Ther.* Jun 2003;7(6):839-850.

Supplemental Results

Endogenous NEDD4-2 and PY-dependence of NEDD4-2 downregulatory effect on $Na_v1.7$ in HEK293 cells (related to Supplemental Figure 2).

Whole-cell Na+ current (I_{Na}) were recorded in HEK293 cells co-transfected with wild-type (WT) $Na_v1.7$ and NEDD4-2. NEDD4-2 decreased $Na_v1.7$ current density by ~80% (Supplemental Figure 2A, left, same as in Figure 2B). Conversely, co-transfection of the catalytically inactive NEDD4-2 mutant (NEDD4-2CS) increased I_{Na} density by ~70%. This effect suggests competition against endogenous NEDD4-2. Accordingly, I_{Na} density was similarly increased by NEDD4-2 silencing using shRNA in HEK293 cells stably expressing $Na_v1.7$ (Supplemental Figure 2B). Because NEDD4-2 is known to interact with the PY-motif located in the C-terminus domain of $Na_v1.7$, an alanine scan of the conserved sequence xP1P2xYxxV was performed (1). When the $Na_v1.7$ P2A (PA) and YA mutants were co-transfected with NEDD4-2, negative regulation was abolished (Supplemental Figure 2C). Conversely, a mutation within the "extended PY motif" (VA mutant) only modestly interfered with the NEDD4-2 effect (bar graph for $Na_v1.7$ WT and $Na_v1.7$ co-expressed with NEDD4-2 is the same as in Figure 2B and Supplemental Figure 2A). Because PA and YA mutants abolished the NEDD4-2 downregulatory effect, the current densities mediated by these mutants should not be subject to endogenous NEDD4-2. However PA and YA mutants current densities were not significantly increased as compared to $Na_v1.7$ WT or VA mutant. This effect is observed when at later time points after transfection. Forty eight hours after transfection, $Na_v1.7$ WT, PA, YA and VA mutants have similar current densities (Supplemental Figure 2D, white bars). When recorded 72 hours transfection, I_{Na} mediated by the PA and YA mutants were significantly increased as compared to $Na_v1.7$ WT and VA mutants, suggesting defective internalization by endogenous NEDD4-2 and accumulation of $Na_v1.7$ PY-motif mutants at the cell surface (Supplemental Figure 2D, black bars). The PY-

dependent interaction between $Na_v1.7$ and NEDD4-2 was further examined by pulldown experiments using GST fused to the furthest 66 C-terminal amino acid residues of $Na_v1.7$ (Supplemental Figure 2E is the extension of Figure 2D). WT $Na_v1.7$ and VA mutant GST-fusion proteins interacted with endogenous and transfected NEDD4-2 (Supplemental Figure 2E), whereas no NEDD4-2 interaction was detected with the PA and YA mutant GST-fusion proteins. Finally, whether ubiquitylation was also dependent on the PY-motif was tested (Supplemental Figure 2F is the extension of Figure 2E). Over-expression of NEDD4-2 substantially increased the GST-S5A-bound $Na_v1.7$ signal for WT $Na_v1.7$ and the VA mutant, but there was only a slight increase with the PA and YA mutants, consistent with the role of the PY-motif in this interaction (Supplemental Figure 2F).

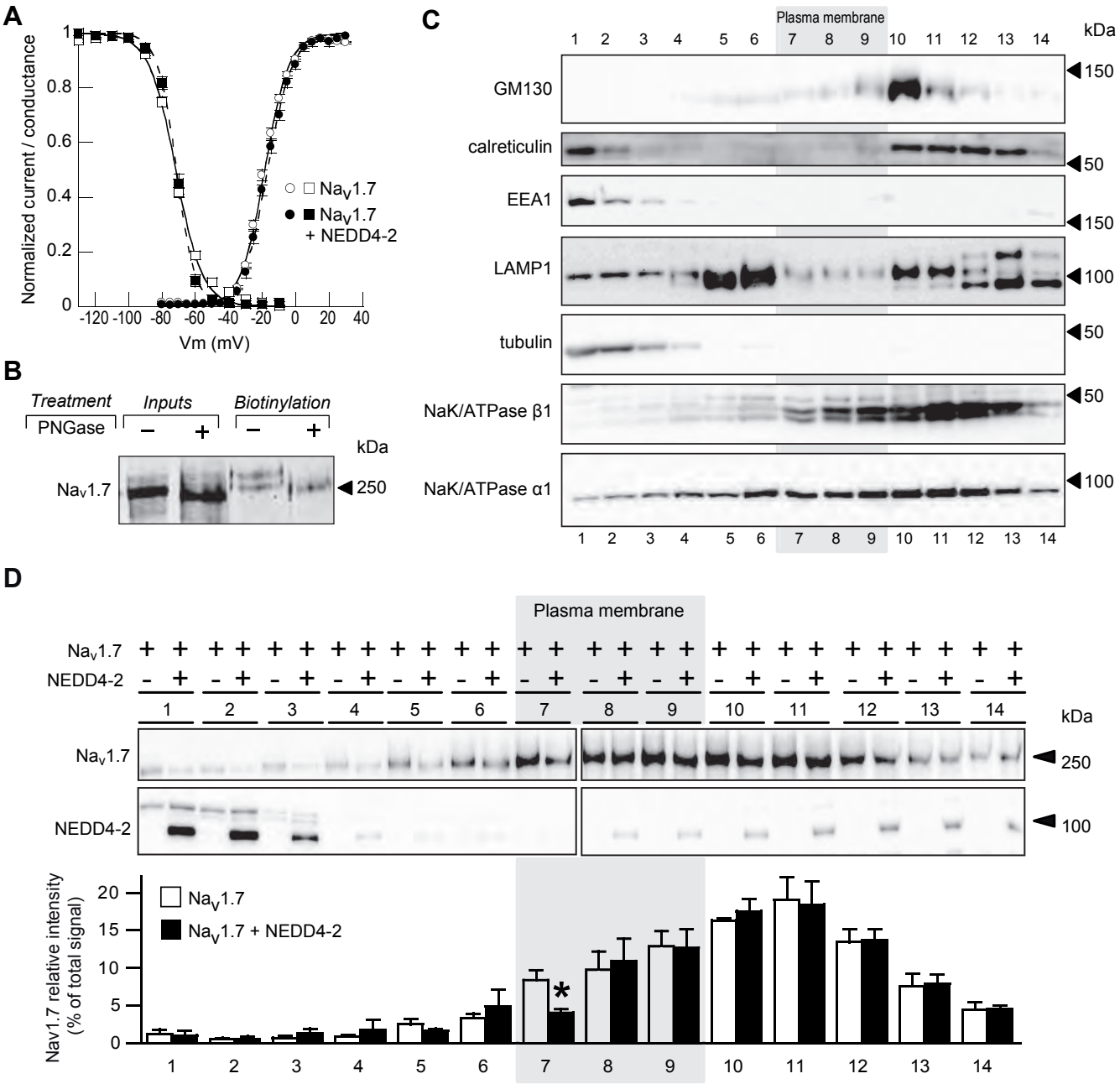

Supplemental Figure 1. NEDD4-2 downregulates Nav1.7 (additional *in vitro* experiments).

(**A**) Biophysical properties of $Na_v1.7$ and $Na_v1.7$ with NEDD4-2 in HEK293 cells. Steady-state activation (circles) and inactivation (square) curves of $Na_v1.7$ either transfected alone or co-transfected with NEDD4-2. See Supplemental Table 1 for values. (**B**) Deglycosylation of biotinylated proteins. Different migration patterns of $Na_v1.7$ in membrane fraction samples were observed. Only the slower migrating band of $Na_v1.7$ (~270 kDa) was down-regulated by NEDD4-2 (Figure 2C), suggesting that the upper band corresponds to the functional maturated channel at the membrane. Inputs signal of $Na_v1.7$ presented a single migrating band at 250 kDa that was not modified when treated with N-Glycosidase F (PGNase F). Deglycosylation of the biotinylated fraction resulted in a merging of the two bands into one faster migrating band. (**C**) Characterization of subcellular fractionation in HEK293 cells. Fractions 7-13 were enriched in plasma membrane (NaK/ATPase β1 and α1-subunit) and an exclusive enrichment was observed in fractions 7-9, where all the other markers were expressed at low levels. Golgi (GM130) was strongly enriched in fraction 10. Lysosomes (LAMP1) were mainly present in fractions 5-6 and 10-14. Lighter fractions were enriched in cytoplasmic (tubulin) and early endosome (EEA1) components. Endoplasmic reticulum (calreticulin) was enriched in fractions 1 and 2 as well as fractions 10-14. Markers had the same distribution with $Na_v1.7$ transfection alone (shown here) or when $Na_v1.7$ was co-transfected with NEDD4-2 (data not shown). (**D**) Subcellular distribution of $Na_v1.7$ and NEDD4-2. HEK293 cells were transfected with either $Na_v1.7$ alone or $Na_v1.7$ and NEDD4-2. Bar graph shows the distribution of $Na_v1.7$ (% of signal in each fraction over the total $Na_v1.7$ signal), with a decrease of 48% (*P = 0.022) in the plasma membrane fraction 7. Fractions exclusively enriched in plasma membrane are highlighted in grey based upon characterization (Supplemental Figure 1C). Data are expressed as means ± SEM Student's t-test, n = 4 independent experiments for each condition.

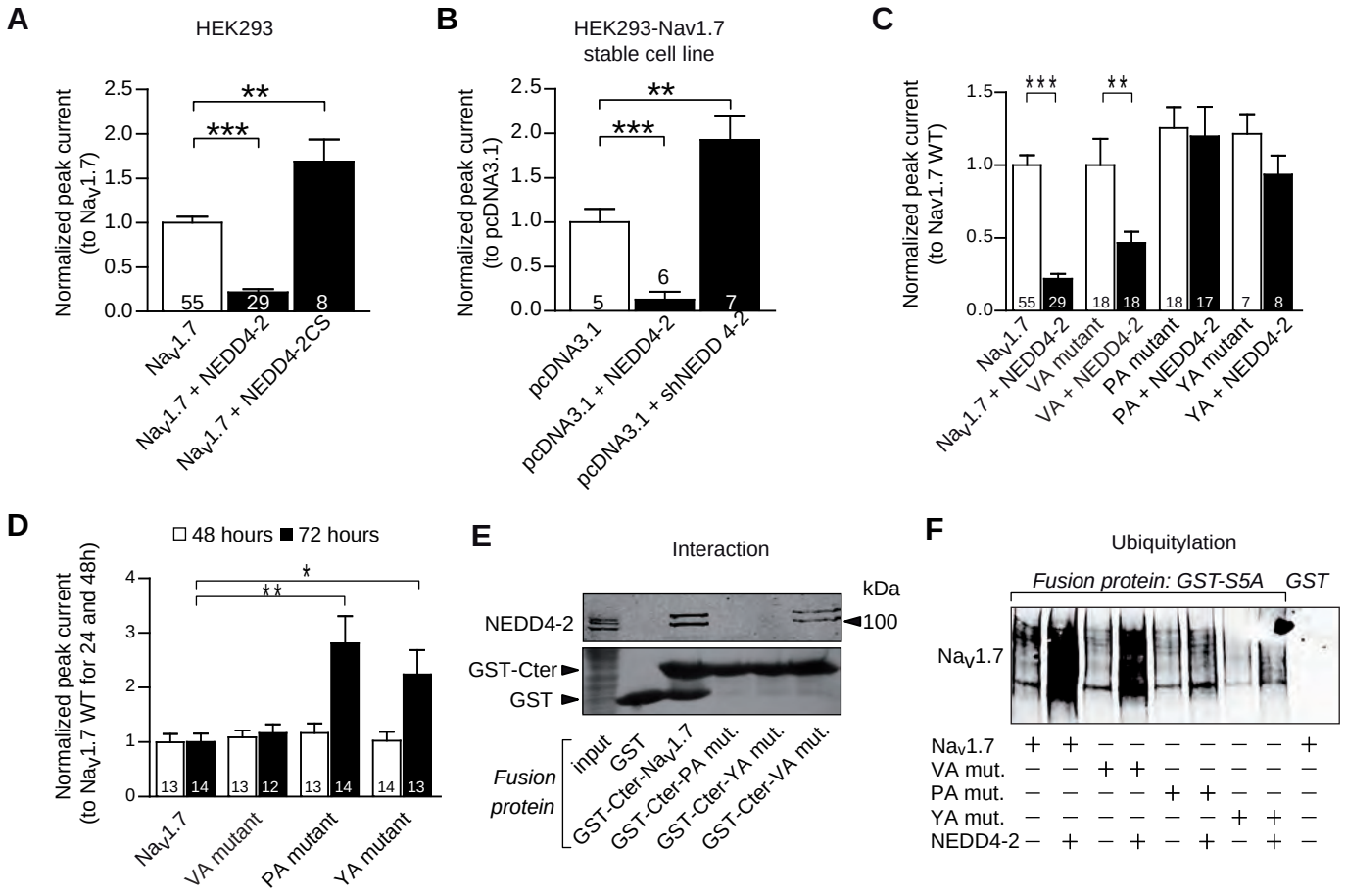

Supplemental Figure 2. NEDD4-2 downregulates Nav1.7 in a PY dependent manner.

(**A**) Effect of NEDD4-2 on Na$_v$1.7 current density in HEK293 cells. NEDD4-2 reduced WT Na$_v$1.7 current density (***P < 0.001), whereas the NEDD4-2CS inactive mutant increased I_{Na} density (**P = 0.001). (**B**) Effect of NEDD4-2 silencing on Na$_v$1.7 current density in Na$_v$1.7 HEK293 stable cell line. NEDD4-2 decreased Na$_v$1.7 current density (***P < 0.001), whereas silencing of NEDD4-2 with shRNA increased I_{Na} density (*P = 0.025). (**C**) Effect of NEDD4-2 co-transfection on WT and mutated Na$_v$1.7 (PY-motif mutants) current densities in HEK293 cells. NEDD4-2-related I_{Na} density downregulation was abolished in PA (P = 0.820) and YA (P = 0.165) PY-motif mutants, but not in the VA (**P = 0.009) mutant. See Supplementary Table 1 for values and biophysical properties. Current densities were normalized to WT Na$_v$1.7 (as in Figure 2B). (**D**) PY-motif - dependent accumulation of Na$_v$1.7 at the membrane. HEK293 cells were transfected with Na$_v$1.7 WT and PY mutants and current densities recorded 48h and 72h post-transfection. Current densities remained similar between Na$_v$1.7 and PY mutants (VA, PA and YA mutants) 48 h after transfection (P > 0.05 for each mutant). 72h after transfection, Na$_v$1.7 and VA mutant current densities decreased compared to 48h post-transfection (by ~58% for Na$_v$1.7 WT and 52% for VA mutant, not visible in the histogram due to data normalization). PA and YA mutant current densities persisted (3% increase for PA and 6% decrease for YA mutant) 72h after transfection and were significantly larger than WT Na$_v$1.7 currents, suggesting a defective internalization by endogenous NEDD4-2 and an accumulation of PA (**P = 0.002) and YA (*P = 0.012) mutants at the cell surface. For A to D, data are expressed as means ± SEM. Student's t-test. Number of recorded cells is indicated in bars. (**E**) GST pulldown experiment showing Na$_v$1.7 PY-motif - dependent interaction with NEDD4-2. HEK293 cells were transfected with NEDD4-2 and soluble fractions were mixed with the respective GST-fusion proteins (GST-Cter-Na$_v$1.7 WT and GST-Cter-PY mutants). Bound NEDD4-2 was analyzed by western blot. (**F**) NEDD4-2-mediated ubiquitylation and PY-motif dependency. HEK293 cells were transfected with Na$_v$1.7 WT, VA, PA and YA mutants alone, or co-transfected with NEDD4-2 and soluble fractions were mixed with GST-S5A proteins. Bound Na$_v$1.7 was analyzed by western blot.

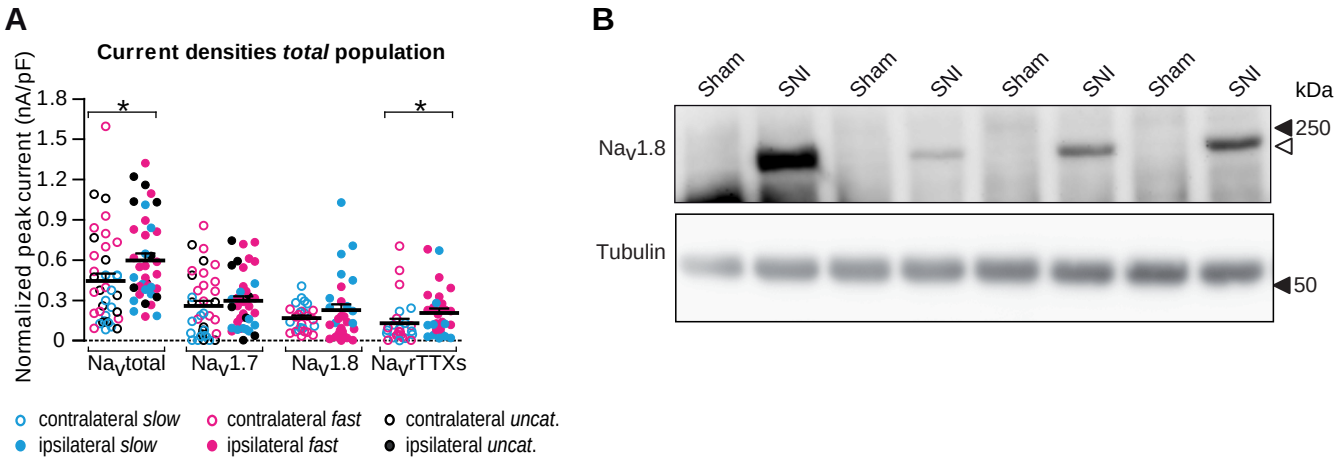

Supplemental Figure 3.

(**A**) Scatter dot plot representing Na_vtotal, Na_v1.7, Na_v1.8 and Na_vrTTXs current densities in contra- and ipsilateral sides recorded in L4/5 DRG neurons one week after SNI. *Slow* (in cyan, see Figure 3B also) and *fast* (in magenta, see Figure 3C also) neurons are distinguishable. In black (*uncat*. for uncategorized) are recordings that did not undergo the entire protocol. Mann Whitney test. See Supplemental Table 2 for values and biophysical properties. (**B**) Western blot of sciatic nerve revealed that Na_v1.8 immunoreactivity is undetectable in sham animals, but SNI induced variable signal intensity (related to Figure 3D). The open arrowheads corresponds to a distinct band of Na_v1.8, observed with lower molecular weight than 250 kDa.

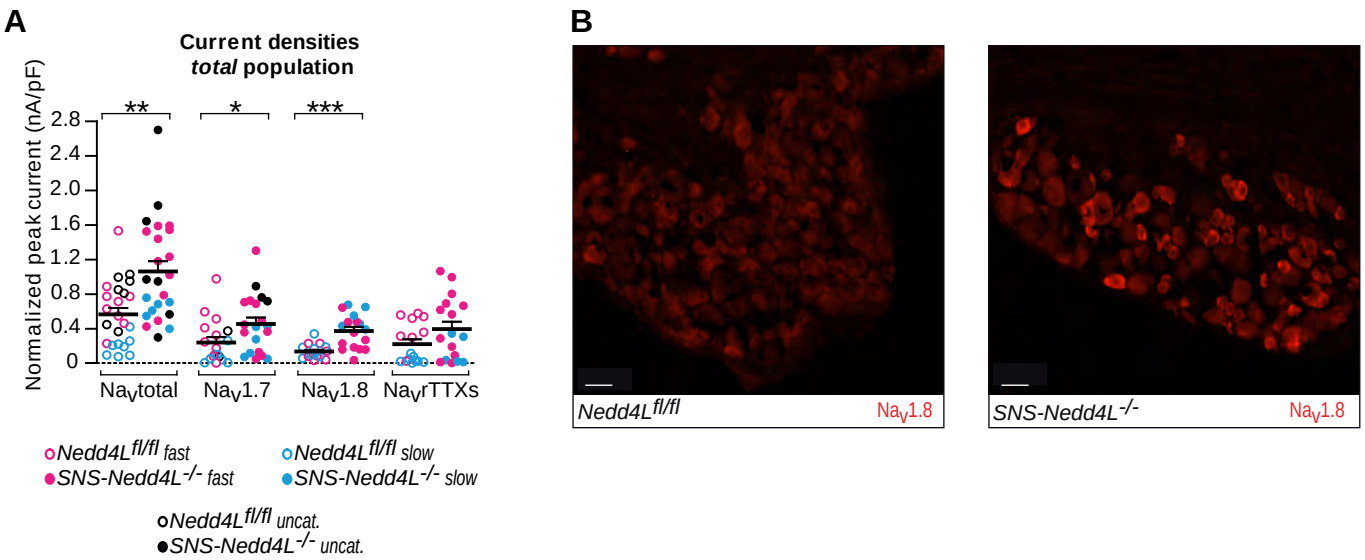

Supplemental Figure 4. Immunofluorescence of $Na_V1.8$ from L4 DRG of *SNS-Nedd4L*$^{-/-}$ mice and control *Nedd4L*$^{fl/fl}$ littermates.

(**A**) Scattered dot plot representing Na_Vtotal, $Na_V1.7$, $Na_V1.8$ and Na_VrTTXs current densities in L4/5 DRG neurons from *SNS-Nedd4L*$^{-/-}$ and *Nedd4L*$^{fl/fl}$ mice. *Slow* (in cyan, see Figure 4F also) and *fast* (in magenta, see Figure 4G also) neurons are distinguishable. In black (*uncat*. for uncategorized) are recordings that did not undergo the entire protocol. Mann Whitney test. See Supplemental Table 3 for values and biophysical properties. (**B**) $Na_V1.8$ immunoreactivity was almost undetectable in control mice using anti-$Na_V1.8$ antibody, while a distinct signal is observed in DRG of *SNS-Nedd4L*$^{-/-}$ mice. Scale bars: 30 µm.

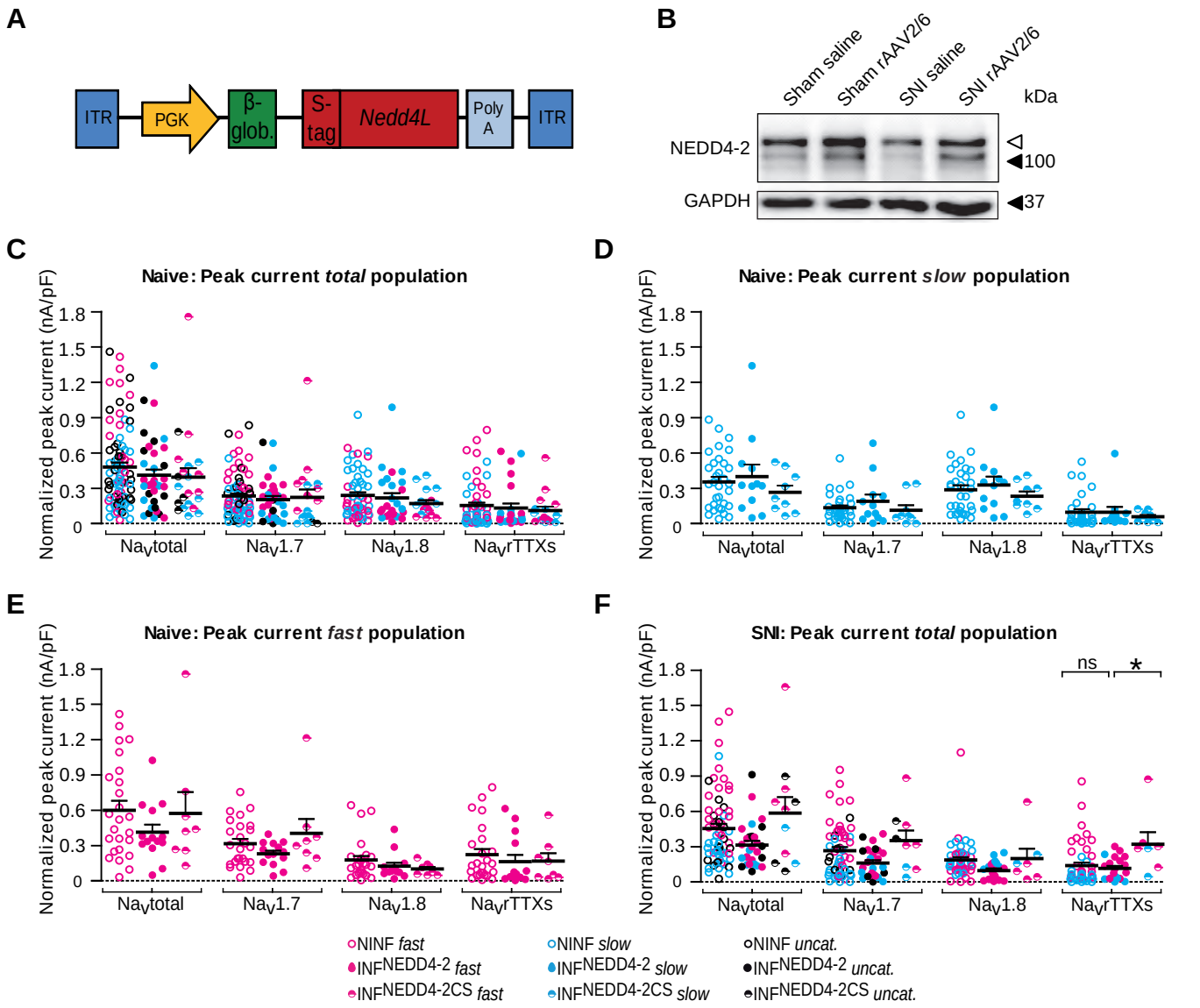

Supplemental Figure 5. Administration of rAAV2/6 viral vector does not modify Na_vs current densities in naive animals.

(**A**) Schematic structure of the recombinant adeno-associated viral vector (rAAV2/6) encoding NEDD4-2 coupled to an s-tag peptide (see Methods). (**B**) Representative western blot of NEDD4-2 in ipsilateral L4 DRG after injection with either rAAV2/6-NEDD4-2 or saline solution. Note that endogenous NEDD4-2 has an apparent molecular weight of 120 kDa, while the virally expressed NEDD4-2 (lacking a C2 domain) migrates at 100 kDa. (**C-E**) Scatter dot plot representing Na_vtotal, Na_v1.7, Na_v1.8 and Na_vrTTXs current densities in non-infected cells (NINF), rAAV2/6-NEDD4-2 infected cells ($INF^{Nedd4-2}$) and in rAAV2/6-NEDD4-2CS ($INF^{Nedd4-2CS}$) in non-operated animals infected with either rAAV2/6-NEDD4-2 or rAAV2/6-NEDD4-2CS. *Slow* (in cyan, see panel D also) and *fast* (in magenta, see panel E also) neurons are distinguishable. In black (*uncat*. for uncategorized) are recordings that did not undergo the entire protocol. Non-parametric one-way analysis of variance (Kruskal-Wallis test) with Dunn *post hoc* test. For values see Supplemental Table 4. (**F**) same as C**,** but after SNI surgery for *total* population. *Slow* and *fast* neurons are shown in Figure 6E and F).

Biophysical properties of Nav1.7, Nav1.7 + NEDD4-2 and PY mutants in HEK293 cells

transfection	WT $Na_v1.7$	WT + NEDD4-2	VA mutant	PA mutant	YA mutant
Activation					
Vm (mV)	-18.6 ± 0.6	-17.2 ± 0.6	-18.4 ± 0.9	-17.0 ± 0.8	-17.1 ± 0.7
slope (mV)	6.9 ± 0.2	7.7 ± 0.3	6.5 ± 0.3	7.3 ± 0.3	7.2 ± 0.5
n	*26*	*9*	*14*	*14*	*9*
Steady-state inactivation					
Vm (mV)	-71.6 ± 0.5	-72.4 ± 1.1	-72.9 ± 0.9	-69.9 ± 0.8	-73.0 ± 0.9
slope (mV)	8.0 ± 0.3	6.8 ± 0.5	7.7 ± 0.5	7.4 ± 0.4	**9.9 ± 1.3 ***
n	*30*	*11*	*15*	*16*	*8*
Recovery from inact.					
$t_{1/2}$ (ms)	7.76 ± 0.38	6.48 ± 0.36	7.79 ± 0.27	7.07 ± 1.12	7.70 ± 0.63
n	*23*	*15*	*15*	*7*	*6*

Supplemental Table 1. Values for $Na_v1.7$, $Na_v1.7$ co-transfected with NEDD4-2 and the PY mutants in HEK cells. The $V_{1/2}$ of steady-state activation and inactivation and their associated slope factors as well as the $t_{1/2}$ of recovery from inactivation (see Methods) under the different conditions were not different from WT $Na_v1.7$, except for the slope factor of inactivation of the YA mutant. *$P < 0.05$, one-way ANOVA, *post hoc* Bonferroni tests between WT $Na_v1.7$ and other conditions for every parameter. Data are expressed as mean ± SEM.

Biophysical properties of Na+ current from ipsi- and contralateral DRG neurons after SNI

		cell type	density (pA/pF)	*n*	Act. Vm (mV)	slope Act (mV)	*n*	Inact. Vm (mV)	*n*	slope Inact (mV)	RFI $t_{1/2}$ (ms)	*n*
Na_vtotal	total	contralateral	444 ± 56	*38*	-28.1 ± 1.4	8.8 ± 0.5	*35*	-63.6 ± 1.7	*33*	10.2 ± 0.5	2.12 ± 0.17	*38*
		ipsilateral	**598 ± 52 ***	*38*	-27.6 ± 1.1	8.8 ± 0.3	*32*	**-71.1 ± 2.1 ****	*33*	**8.6 ± 0.7 ***	1.94 ± 0.18	*35*
	fast	contralateral	584 ± 111	*14*	-32.6 ± 1.4	7.3 ± 0.5	*11*	-70.5 ± 1.5	*12*	9.6 ± 0.8	2.69 ± 0.22	*14*
		ipsilateral	612 ± 72	*18*	-31.1 ± 1.5	7.0 ± 0.3	*14*	**-79.2 ± 1.9 ****	*14*	**7.5 ± 0.6 ***	**2.07 ± 0.18 ***	*15*
	slow	contralateral	265 ± 48	*12*	-22.4 ± 3.0	11.2 ± 0.5	*10*	-57.5 ± 2.3	*10*	11.6 ± 0.8	1.81 ± 0.36	*12*
		ipsilateral	**475 ± 82 ***	*11*	-23.63 ± 1.3	**9.3 ± 0.4 ****	*11*	-61.03 ± 3.2	*11*	10.1 ± 1.6	1.82 ± 0.45	*11*
$Na_v1.7$	total	contralateral	258 ± 40	*36*	-31.2 ± 1.2	6.8 ± 0.4	*25*	-76.1 ± 1.1	*20*	5.8 ± 0.4	2.84 ± 0.33	*18*
		ipsilateral	296 ± 35	*37*	-28.8 ± 1.3	6.2 ± 0.2	*26*	-76.8 ± 1.3	*21*	5.0 ± 0.4	2.24 ± 0.25	*20*
	fast	contralateral	398 ± 62	*14*	-32.0 ± 1.6	6.8 ± 0.6	*11*	-74.8 ± 1.4	*11*	5.2 ± 0.6	2.76 ± 0.32	*11*
		ipsilateral	349 ± 51	*18*	-30.2 ± 1.4	5.7 ± 0.3	*13*	-74.0 ± 1.3	*13*	4.8 ± 0.3	**1.90 ± 0.21 ***	*12*
	slow	contralateral	92 ± 31	*12*	-26.7 ± 3.3	8.9 ± 0.9	*5*	-77.0 ± 3.7	*4*	7.2 ± 0.8	3.64 ± 0.83	*5*
		ipsilateral	**179 ± 40 ***	*11*	-26.4 ± 3.0	7.1 ± 0.6	*7*	-79.8 ± 2.8	*5*	5.3 ± 1.6	3.04 ± 0.63	*6*
$Na_v1.8$	total	contralateral	168 ± 19	*26*	-25.6 ± 1.4	9.6 ± 0.4	*21*	-53.2 ± 1.3	*18*	6.5 ± 0.2	1.13 ± 0.07	*16*
		ipsilateral	227 ± 46	*29*	-24.5 ± 1.8	9.3 ± 0.4	*19*	-50.5 ± 1.1	*18*	**5.7 ± 0.2 ***	**0.82 ± 0.07 ****	*14*
	fast	contralateral	131 ± 21	*14*	-25.9 ± 2.5	9.1 ± 0.5	*8*	-52.6 ± 1.9	*6*	6.4 ± 0.5	1.29 ± 0.10	*7*
		ipsilateral	108 ± 26	*18*	-21.6 ± 2.8	10.0 ± 0.4	*10*	-51.1 ± 1.7	*10*	5.9 ± 0.3	**0.76 ± 10 ****	*8*
	slow	contralateral	209 ± 33	*12*	-24.0 ± 1.6	10.1 ± 0.5	*10*	-53.1 ± 2.0	*10*	6.5 ± 0.2	1.06 ± 0.10	*9*
		ipsilateral	**421 ± 89 ***	*11*	-27.7 ± 2.1	**8.5 ± 0.6 ***	*9*	-50.1 ± 1.7	*7*	**5.5 ± 0.5 ***	0.90 ± 0.08	*6*
Na_vrTTXs	total	contralateral	131 ± 34	*26*	-34.1 ± 2.1	8.2 ± 0.4	*12*	-83.1 ± 2.9	*9*	6.8 ± 1.0	4.81 ± 0.61	*11*
		ipsilateral	**206 ± 33 ***	*29*	-33.9 ± 1.3	7.6 ± 0.3	*18*	-80.7 ± 1.2	*18*	7.0 ± 0.3	**3.09 ± 0.38 ***	*14*
	fast	contralateral	165 ± 61	*14*	-34.2 ± 2.9	7.7 ± 0.4	*6*	-79.5 ± 4.8	*4*	8.5 ± 0.5	4.51 ± 0.32	*6*
		ipsilateral	**249 ± 37 ***	*18*	-34.7 ± 1.4	7.6 ± 0.3	*14*	-80.6 ± 1.6	*13*	**6.8 ± 0.3 ****	**3.08 ± 0.41 ***	*13*
	slow	contralateral	91 ± 23	*12*	-33.1 ± 4.1	9.3 ± 0.5	*5*	-84.6 ± 3.6	*5*	6.5 ± 0.8	5.17 ± 1.37	*5*
		ipsilateral	136 ± 61	*11*	-30.8 ± 3.4	7.7 ± 1.1	*4*	-82.6 ± 2.5	*3*	7.9 ± 2.0	3.3	*1*

Supplemental Table 2. Values for contralateral and ipsilateral DRG neurons after SNI. The capacitance (pF) was not different between the two groups (14.0 ± 0.5 pF, *n* = 38 for the contralateral side; 15.5 ± 0.6 pF, *n* = 38 for ipsilateral side, respectively. *P* = 0.053, Student's t test). The proportions of *fast* (14/26, 54% in contralateral and 18/29, 62% in ipsilateral) and *slow* neurons between groups were not significantly different ($\chi 2$ = 0.12, with 1 degree of freedom *P* = 0.73, chi-square test with Yates correction). SNI had a minor impact on the biophysical properties except for the 7-9 mV hyperpolarizing shift in the $V_{1/2}$ of the steady-state inactivation of Na_vtotal in the *total* population and *fast* subpopulation, and little modification of some slope factors. Recovery from inactivation (RFI) was accelerated for every Na_vs component in the *fast* subpopulation after SNI. Data are expressed as mean ± SEM. Student's *t*-test or Mann Whitney tests.

Biophysical properties of Na+ current from *Nedd4L$^{fl/fl}$* and *SNS-Nedd4L$^{-/-}$* mice DRG neurons

		cell type	density (pA/pF)	*n*	Act. Vm (mV)	slope Act (mV)	*n*	Inact. Vm (mV)	slope Inact (mV)	*n*
Na_vtotal	*total*	*Nedd4L $^{fl/fl}$*	565 ± 78	*24*	-30.8 ± 1.6	7.9 ± 0.4	*23*	-63.0 ± 4.4	7.8 ± 0.5	*14*
		SNS-Nedd4L $^{-/-}$	**1062 ± 121 ****	*24*	**-38.1 ± 2.2 ****	6.9 ± 0.4	*21*	-69.9 ± 4.0	**9.9 ± 0.9 ***	*14*
	fast	*Nedd4L $^{fl/fl}$*	790 ± 125	*8*	-35.5 ± 2.1	7.2 ± 0.4	*8*	-79.3 ± 2.8	7.3 ± 0.4	*6*
		SNS-Nedd4L $^{-/-}$	1166 ± 137	*11*	-38.9 ± 4.5	7.1 ± 0.8	*10*	-77.0 ± 3.6	9.0 ± 1.1	*7*
	slow	*Nedd4L $^{fl/fl}$*	195 ± 43	*8*	-23.7 ± 1.5	9.9 ± 0.4	*6*	-51.0 ± 2.7	8.2 ± 0.9	*6*
		SNS-Nedd4L $^{-/-}$	**617 ± 58 ****	*6*	**-34.2 ± 2.5 ****	**7.1 ± 0.6 ****	*4*	-54.0 ± 3.9	10.5 ± 1.4	*4*
$Na_v1.7$	*total*	*Nedd4L $^{fl/fl}$*	241 ± 63	*18*	-31.9 ± 2.4	6.1 ± 0.4	*15*	-78.7 ± 1.5	7.4 ± 0.9	*6*
		SNS-Nedd4L $^{-/-}$	**455 ± 77 ***	*20*	-36.2 ± 2.7	5.8 ± 0.4	*14*	-80.2 ± 2.0	5.6 ± 0.6	*7*
	fast	*Nedd4L $^{fl/fl}$*	415 ± 108	*8*	-36.7 ± 2.6	5.5 ± 0.5	*7*	-77.2 ± 2.9	8.75 ± 3.7	*2*
		SNS-Nedd4L $^{-/-}$	487 ± 116	*11*	-36.1 ± 3.9	5.9 ± 0.6	*8*	-77.7	3.5	*1*
	slow	*Nedd4L $^{fl/fl}$*	70 ± 33	*8*	-25.4 ± 4.1	7.3 ± 0.6	*6*	-79.5 ± 2.1	6.8 ± 0.5	*4*
		SNS-Nedd4L $^{-/-}$	**487 ± 116 ***	*6*	-27.9 ± 2.0	6.9 ± 0.5	*3*	-79.2 ± 2.4	5.7 ± 0.6	*5*
$Na_v1.8$	*total*	*Nedd4L $^{fl/fl}$*	132 ± 20	*17*	-28.4 ± 1.5	9.8 ± 0.7	*17*	-56.6 ± 1.7	6.7 ± 0.5	*14*
		SNS-Nedd4L $^{-/-}$	**371 ± 50 *****	*17*	-32.9 ± 2.9	11.4 ± 1.3	*12*	-54.6 ± 1.9	**5.4 ± 0.3 ***	*12*
	fast	*Nedd4L $^{fl/fl}$*	117 ± 29	*8*	-28.3 ± 1.8	11.2 ± 0.9	*8*	-54.7 ± 2.7	7.1 ± 0.9	*7*
		SNS-Nedd4L $^{-/-}$	**286 ± 58 ***	*11*	-34.7 ± 5.3	12.5 ± 1.5	*7*	-55.4 ± 3.2	5.8 ± 0.4	*7*
	slow	*Nedd4L $^{fl/fl}$*	152 ± 34	*8*	-27.4 ± 3.3	8.9 ± 1.1	*7*	-58.6 ± 2.5	6.4 ± 0.7	*6*
		SNS-Nedd4L $^{-/-}$	**527 ± 53 *****	*6*	-32.0 ± 3.4	8.3 ± 0.6	*5*	-53.5 ± 1.8	4.8 ± 0.3	*5*
Na_vrTTXs	*total*	*Nedd4L $^{fl/fl}$*	220 ± 59	*16*	-39.7 ± 1.7	6.9 ± 0.5	*10*	-85.0 ± 2.0	8.2 ± 1.0	*6*
		SNS-Nedd4L $^{-/-}$	394 ± 90	*17*	-43.6 ± 2.8	7.1 ± 0.4	*9*	-88.1 ± 1.6	7.4 ± 0.7	*7*
	fast	*Nedd4L $^{fl/fl}$*	399 ± 72	*8*	-40.9 ± 2.1	7.3 ± 0.6	*6*	-84.1 ± 2.2	7.4 ± 0.5	*5*
		SNS-Nedd4L $^{-/-}$	544 ± 112	*11*	-46.6 ± 2.5	7.2 ± 0.4	*7*	-88.4 ± 1.6	7.4 ± 0.8	*5*
	slow	*Nedd4L $^{fl/fl}$*	42 ± 14	*8*	-33.4 ± 4.4	7.2 ± 0.3	*2*	-89.3	12.1	*1*
		SNS-Nedd4L $^{-/-}$	119 ± 71	*6*	-33.2 ± 1.2	6.6 ± 1.5	*2*	-87.5 ± 3.6	7.6 ± 2.7	*2*

Supplemental Table 3. Values for *SNS-Nedd4L$^{-/-}$* and *Nedd4L$^{fl/fl}$* DRG neurons. The capacitance (pF) was not different between the two groups (13.8 ± 0.8 pF, *n* = 24 and 13.5 ± 0.8 pF, *n* = 24, *P* = 0.84, Student's *t* test). *Fast* neurons correspond to 50% of *Nedd4L$^{fl/fl}$* (8/16) and 65% of *SNS-Nedd4L$^{-/-}$* (11/17). The proportion of *fast* and *slow* neurons between genotypes was not different (χ^2 = 0.25, with 1 degree of freedom *P* = 0.62, chi-square test with Yates correction). The two mice lines had the same biophysical properties except for the 10 mV hyperpolarizing shift in the $V_{1/2}$ of activation of Na_vtotal in the *total* population and *slow* subpopulation, and little modification of some slope factors. Data are expressed as mean ± SEM. Student's *t*-test or Mann Whitney tests.

Biophysical properties of Na+ current of DRG neurons from naive mice infected with either rAAV2/6-NEDD4-2 or rAAV2/6-NEDD4-2CS

		cell type	density (pA/pF)	*n*	Act. Vm (mV)	slope Act. (mV)	*n*	Inact. Vm (mV)	slope Inact. (mV)	*n*	RFI $t_{1/2}$ (ms)	*n*
Na_vtotal	*total*	NINF	457 ± 41	*85*	-26.9 ± 0.9	8.3 ± 0.2	*71*	-62.9 ± 1.7	10.3 ± 0.4	*51*	2.35 ± 0.20	*41*
		$INF^{NEDD4-2}$	410 ± 50	*37*	-24.3 ± 1.3	9.0 ± 0.5	*33*	-57.3 ± 2.5	9.7 ± 0.6	*24*	1.86 ± 0.21	*22*
		$INF^{NEDD4-2CS}$	394 ± 80	*22*	-24.6 ± 1.9	8.6 ± 0.5	*20*	-55.2 ± 5.2	**7.4 ± 0.7 *****	*12*	1.46 ± 0.26	*13*
	fast	NINF	600 ± 83	*25*	-30.4 ± 1.5	7.4 ± 0.3	*20*	-69.7 ± 1.9	10.9 ± 0.6	*14*	2.94 ± 0.43	*12*
		$INF^{NEDD4-2}$	413 ± 69	*14*	-27.1 ± 2.0	8.1 ± 0.6	*12*	-69.2 ± 2.5	9.4 ± 0.7	*8*	2.51 ± 0.46	*7*
		$INF^{NEDD4-2CS}$	573 ± 195	*8*	-31.7 ± 2.8	7.3 ± 0.7	*7*	-75.8 ± 2.6	6.5 ± 0.2	*4*	2.41 ± 0.34	*4*
	slow	NINF	356 ± 42	*32*	-22.7 ± 0.9	9.1 ± 0.4	*29*	-53.1 ± 2.1	11.0 ± 0.8	*19*	1.66 ± 0.25	*13*
		$INF^{NEDD4-2}$	399 ± 107	*12*	-24.2 ± 2.3	9.1 ± 0.8	*12*	50.5 ± 4.0	9.0 ± 1.6	*7*	1.56 ± 0.36	*7*
		$INF^{NEDD4-2CS}$	265 ± 61	*9*	-19.62 ± 2.0	9.6 ± 0.7	*9*	-44.9 ± 4.1	8.4 ± 1.7	*4*	1.0 ± 0.22	*4*
$Na_v1.7$	*total*	NINF	235 ± 22	*75*	-27.5 ± 1.0	7.5 ± 0.3	*49*	-75.0 ± 1.0	7.2 ± 0.9	*23*	3.08 ± 0.28	*19*
		$INF^{NEDD4-2}$	205 ± 31	*32*	-28.2 ± 1.8	7.5 ± 0.7	*18*	-74.4 ± 1.4	7.6 ± 0.7	*9*	2.46 ± 0.29	*9*
		$INF^{NEDD4-2CS}$	224 ± 67	*19*	-28.2 ± 2.3	7.7 ± 0.8	*12*	-72.6 ± 1.6	5.3 ± 0.8	*7*	2.27 ± 0.20	*6*
	fast	NINF	317 ± 40	*25*	-29.1 ± 1.5	6.9 ± 0.4	*21*	-73.2 ± 1.8	6.7 ± 0.9	*10*	3.12 ± 0.45	*9*
		$INF^{NEDD4-2}$	230 ± 28	*14*	-28.1 ± 2.5	7.1 ± 0.7	*10*	-74.3 ± 2.5	7.6 ± 0.8	*5*	2.37 ± 0.55	*5*
		$INF^{NEDD4-2CS}$	404 ± 131	*8*	-31.6 ± 3.1	6.5 ± 0.8	*7*	-72.7 ± 3.1	4.3 ± 0.9	*4*	2.21 ± 0.32	*4*
	slow	NINF	137 ± 21	*32*	-23.8 ± 1.5	8.4 ± 0.5	*20*	-75.2 ± 1.6	7.0 ± 1.9	*8*	3.02 ± 0.48	*7*
		$INF^{NEDD4-2}$	188 ± 61	*12*	-29.0 ± 3.9	7.0 ± 1.5	*6*	-73.8 ± 2.2	7.8 ± 2.4	*3*	2.72 ± 0.23	*3*
		$INF^{NEDD4-2CS}$	112 ± 46	*9*	-23.5 ± 2.6	9.3 ± 1.5	*5*	-72.6 ± 0.9	6.7 ± 0.9	*3*	2.3	*1*
$Na_v1.8$	*total*	NINF	239 ± 27	*57*	-25.6 ± 1.0	9.3 ± 0.3	*44*	-47.6 ± 0.7	5.9 ± 0.3	*34*	0.76 ± 0.04	*28*
		$INF^{NEDD4-2}$	218 ± 43	*26*	-25.6 ± 1.5	8.6 ± 0.6	*20*	-48.5 ± 1.0	6.0 ± 0.6	*17*	0.85 ± 0.07	*16*
		$INF^{NEDD4-2CS}$	171 ± 29	*17*	-20.4 ± 1.4	9.8 ± 0.5	*10*	-48.5 ± 0.8	6.2 ± 0.3	*10*	0.71 ± 0.03	*10*
	fast	NINF	177 ± 36	*25*	-27.5 ± 1.5	9.5 ± 0.6	*16*	-49.3 ± 1.1	6.3 ± 0.4	*13*	0.82 ± 0.06	*12*
		$INF^{NEDD4-2}$	124 ± 31	*14*	-22.9 ± 1.2	9.5 ± 0.7	*10*	-49.6 ± 1.6	6.4 ± 1.2	*9*	0.79 ± 0.08	*8*
		$INF^{NEDD4-2CS}$	101 ± 20	*8*	**-19.2 ± 1.6 ****	10.6 ± 0.5	*6*	-50.1 ± 0.8	6.6 ± 0.2	*6*	0.75 ± 0.03	*6*
	slow	NINF	285 ± 38	*32*	-25.1 ± 1.4	9.0 ± 0.5	*26*	-46.6 ± 0.8	5.7 ± 0.3	*21*	0.82 ± 0.06	*16*
		$INF^{NEDD4-2}$	327 ± 76	*12*	-28.2 ± 2.6	7.8 ± 0.9	*10*	-47.3 ± 1.1	5.6 ± 0.4	*8*	0.79 ± 0.08	*7*
		$INF^{NEDD4-2CS}$	234 ± 41	*9*	-22.2 ± 3.0	8.58 ± 0.8	*4*	-46.0 ± 0.7	5.7 ± 0.6	*4*	0.75 ± 0.03	*4*
Na_vrTTXs	*total*	NINF	153 ± 26	*57*	-32.7 ± 1.5	8.3 ± 0.5	*27*	-80.1 ± 1.0	6.9 ± 0.6	*16*	3.37 ± 0.35	*16*
		$INF^{NEDD4-2}$	132 ± 38	*26*	-29.9 ± 2.3	8.4 ± 0.7	*11*	-78.6 ± 2.0	9.5 ± 1.3	*8*	3.41 ± 1.06	*6*
		$INF^{NEDD4-2CS}$	110 ± 35	*17*	-31.3 ± 3.0	9.8 ± 1.0	*8*	-83.6 ± 1.1	6.6 ± 0.7	*5*	3.66 ± 0.72	*4*
	fast	NINF	223 ± 48	*25*	-34.9 ± 2.0	7.9 ± 0.6	*14*	-80.5 ± 1.0	7.7 ± 0.6	*9*	3.64 ± 0.49	*9*
		$INF^{NEDD4-2}$	163 ± 59	*14*	-31.0 ± 1.0	8.1 ± 0.6	*7*	-80.1 ± 0.7	8.9 ± 1.8	*5*	3.93 ± 1.65	*4*
		$INF^{NEDD4-2CS}$	169 ± 70	*8*	-31.5 ± 3.4	9.7 ± 1.1	*7*	-82.9 ± 1.0	6.9 ± 0.7	*4*	3.07 ± 0.35	*3*
	slow	NINF	100 ± 24	*32*	-30.3 ± 2.2	8.7 ± 0.9	*13*	-79.6 ± 2.2	5.9 ± 0.9	*7*	3.02 ± 0.54	*7*
		$INF^{NEDD4-2}$	96 ± 48	*12*	-28.1 ± 7.3	8.9 ± 1.8	*4*	-76.0 ± 6.2	10.4 ± 2.6	*3*	2.37 ± 0.70	*2*
		$INF^{NEDD4-2CS}$	57 ± 16	*9*	-29.4	10.4	*1*	-86.4	5.1	*1*	5.44	*1*

Supplemental Table 4. Values for cells transduced with rAAV2/6-NEDD4-2 ($INF^{NEDD4-2}$) and control cells either transduced with rAAV2/6-NEDD4-2CS ($INF^{NEDD4-2CS}$) or not transduced (NINF) in naive animals. The capacitance (pF) was significantly higher in cells infected with rAAV2/6-NEDD4-2 (15.4 ± 0.4 pF with *n* = 85 for NINF, 17.4 ± 0.7 with *n* = 37 for $INF^{NEDD4-2}$ and 15.5 ± 0.7 pF with *n* = 22 for $INF^{NEDD4-2CS}$, $P < 0.05$ between NINF and $INF^{NEDD4-2}$ cells, Kurskal-Wallis and *post hoc* Dunn tests). NINF cells recorded from each group of vector-injected animals exhibited no differences in the current densities of any of the components and were thus pooled into one group. Data are expressed as mean ± SEM. One-way ANOVA (*post hoc* Bonferroni tests) or Kruskal-Wallis test (Dunn *post hoc* test).

Biophysical properties of Na+ current of DRG neurons from mice infected with either rAAV2/6-NEDD4-2 or rAAV2/6-NEDD4-2CS after SNI

		cell type	density (pA/pF)	*n*	Act. Vm (mV)	slope Act. (mV)	*n*	Inact. Vm (mV)	slope Inact. (mV)	*n*	RFI $t_{1/2}$ (ms)	*n*
Na_vtotal	*total*	NINF	455 ± 41	*63*	-26.4 ± 1.0	8.5 ± 0.3	*55*	-61.0 ± 2.0	8.8 ± 0.4	*46*	1.99 ± 0.13	*45*
		$INF^{NEDD4-2}$	313 ± 37	*28*	-26.0 ± 1.8	8.4 ± 0.4	*25*	-62.5 ± 3.0	7.9 ± 0.5	*21*	2.10 ± 0.18	*19*
		$INF^{NEDD4-2CS}$	585 ± 143	*11*	-31.6 ± 2.1	7.6 ± 0.7	*8*	-70.0 ± 3.0	8.8 ± 1.5	*5*	1.98 ± 0.26	*5*
	fast	NINF	650 ± 69	*25*	-30.2 ± 1.3	7.3 ± 0.3	*24*	-69.5 ± 1.3	9.58 ± 0.5	*20*	2.33 ± 0.12	*20*
		$INF^{NEDD4-2}$	**334 ± 48 ****	*13*	-27.3 ± 1.2	8.1 ± 0.5	*11*	-70.1 ± 0.9	**6.6 ± 0.5 ****	*9*	2.26 ± 0.17	*9*
		$INF^{NEDD4-2CS}$	**798 ± 261 ***	*5*	-33.6 ± 1.9	6.2 ± 0.5	*4*	-72.1 ± 3.7	6.8 ± 1.0	*3*	1.91 ± 0.41	*3*
	slow	NINF	287 ± 46	*22*	-19.5 ± 1.4	10.2 ± 0.5	*18*	-46.9 ± 2.3	8.4 ± 0.6	*15*	1.30 ± 0.18	*14*
		$INF^{NEDD4-2}$	222 ± 52	*7*	-19.7 ± 3.8	9.2 ± 1.3	*7*	-49.7 ± 5.4	7.9 ± 1.0	*5*	1.82 ± 0.39	*4*
		$INF^{NEDD4-2CS}$	309 ± 213	*2*	-25.5 ± 8.0	9.5 ± 1.4	*2*					
$Na_v1.7$	*total*	NINF	266 ± 30	*57*	-26.8 ± 1.1	7.4 ± 0.3	*40*	-73.6 ± 1.0	6.8 ± 0.9	*22*	2.42 ± 0.16	*25*
		$INF^{NEDD4-2}$	160 ± 24	*26*	-25.2 ± 1.3	7.4 ± 0.4	*15*	-70.8 ± 2.7	7.0 ± 1.5	*5*	**1.68 ± 0.18 ***	*9*
		$INF^{NEDD4-2CS}$	351 ± 92	*9*	-30.2 ± 2.3	7.0 ± 0.7	*6*	-71.8 ± 2.3	4.1 ± 0.7	*2*	1.68 ± 0.45	*3*
	fast	NINF	412 ± 47	*25*	-29.8 ± 1.1	6.5 ± 0.3	*23*	-73.7 ± 1.0	6.1 ± 0.4	*15*	2.31 ± 0.16	*15*
		$INF^{NEDD4-2}$	**193 ± 34 ****	*13*	-26.3 ± 1.3	7.4 ± 0.4	*10*	-69.6 ± 3.1	7.3 ± 1.9	*4*	**1.53 ± 0.22 ***	*6*
		$INF^{NEDD4-2CS}$	421 ± 145	*5*	-37.3 ± 2.6	6.1 ± 0.4	*4*	-71.8 ± 2.3	4.1 ± 0.7	*2*	1.68 ± 0.45	*3*
	slow	NINF	120 ± 25	*22*	-22.9 ± 1.7	8.2 ± 0.5	*11*	-74.9 ± 3.9	9.9 ± 4.1	*5*	3.14 ± 0.22	*7*
		$INF^{NEDD4-2}$	85 ± 28	*7*	-20.49 ± 3.5	7.3 ± 1.3	*3*					
		$INF^{NEDD4-2CS}$	83 ± 63	*2*	-22.5	9.4	*1*					
$Na_v1.8$	*total*	NINF	187 ± 25	*46*	-25.0 ± 1.1	9.5 ± 0.3	*33*	-48.4 ± 0.7	5.9 ± 0.2	*31*	0.86 ± 0.05	*29*
		$INF^{NEDD4-2}$	**98 ± 18 ***	*20*	-25.0 ± 1.8	9.6 ± 0.8	*10*	-50.7 ± 1.1	5.7 ± 0.3	*10*	0.85 ± 0.06	*9*
		$INF^{NEDD4-2CS}$	199 ± 92	*7*	-28.9 ± 1.9	9.5 ± 0.7	*5*	-51.1 ± 1.4	5.6 ± 0.4	*4*	0.71 ± 0.06	*5*
	fast	NINF	140 ± 18	*25*	-26.0 ± 1.5	9.9 ± 0.4	*17*	-49.8 ± 0.9	6.4 ± 0.5	*15*	0.90 ± 0.06	*15*
		$INF^{NEDD4-2}$	**59 ± 16 ***	*13*	-23.4 ± 2.5	11.2 ± 0.6	*4*	-52.9 ± 0.6	6.2 ± 0.4	*5*	0.86 ± 0.08	*5*
		$INF^{NEDD4-2CS}$	199 ± 137	*5*	-29.4 ± 1.8	9.7 ± 1.4	*3*	-52.3 ± 1.1	5.9 ± 0.2	*2*	0.71 ± 0.10	*3*
	slow	NINF	239 ± 46	*22*	-23.6 ± 1.7	9.0 ± 0.6	*14*	-47.1 ± 1.1	5.4 ± 0.2	*16*	0.82 ± 0.07	*16*
		$INF^{NEDD4-2}$	170 ± 22	*7*	-26.1 ± 2.8	8.5 ± 1.1	*6*	-48.5 ± 1.7	5.1 ± 0.2	*5*	0.83 ± 0.12	*4*
		$INF^{NEDD4-2CS}$	197 ± 53	*2*	-21.1 ± 6.6	9.3 ± 0.2	*2*	-49.9 ± 3.4	5.3 ± 0.8	*2*	0.72 ± 0.17	*2*
Na_vrTTXs	*total*	NINF	142 ± 27	*46*	-31.5 ± 1.5	8.7 ± 0.5	*21*	-80.0 ± 1.5	7.5 ± 0.5	*21*	3.80 ± 0.31	*19*
		$INF^{NEDD4-2}$	116 ± 22	*20*	-32.3 ± 1.3	8.5 ± 0.5	*13*	-79.9 ± 1.6	7.2 ± 0.7	*6*	3.56 ± 0.49	*8*
		$INF^{NEDD4-2CS}$	**322 ± 108 ***	*7*	**-39.3 ± 1.4 ***	6.7 ± 0.9	*6*	-81.6 ± 2.7	6.4 ± 0.3	*3*	2.38 ± 0.41	*2*
	fast	NINF	220 ± 44	*25*	-32.6 ± 1.8	8.6 ± 0.6	*16*	-79.2 ± 2.0	8.1 ± 0.6	*15*	3.80 ± 0.42	*13*
		$INF^{NEDD4-2}$	149 ± 25	*13*	-32.2 ± 1.6	8.9 ± 0.6	*10*	-79.1 ± 1.6	6.7 ± 0.6	*5*	3.56 ± 0.49	*8*
		$INF^{NEDD4-2CS}$	384 ± 143	*5*	-39.6 ± 1.4	6.2 ± 1.0	*4*	-81.6 ± 2.7	6.4 ± 0.3	*3*	2.38 ± 0.41	*2*
	slow	NINF	50 ± 12	*22*	-26.5 ± 2.6	9.1 ± 1.1	*4*	-81.9 ± 1.9	6.4 ± 0.8	*6*	3.81 ± 0.44	*6*
		$INF^{NEDD4-2}$	54 ± 33	*7*	-33.0 ± 2.6	7.3 ± 0.5	*3*	-84.0	9.8	*1*		
		$INF^{NEDD4-2CS}$	166 ± 169	*2*	-38.9 ± 5.6	7.9 ± 2.3	*2*					

Supplemental Table 5. Values for cells transduced with rAAV2/6-Nedd4-2 ($INF^{NEDD4-2}$) and control cells either transduced with rAAV2/6-Nedd4-2CS ($INF^{NEDD4-2CS}$) or not transduced (NINF) after SNI. The capacitance (pF) was not significantly different between groups (15.9 ± 0.5 pF with *n* = 63 for NINF, 16.4 ± 0.8 with n = 28 for $INF^{NEDD4-2}$ and 15.3 ± 1.0 pF with *n* = 11 for $INF^{NEDD4-2CS}$, *P* = 0.832. NINF cells recorded from animals injected with rAAV2/6-NEDD4-2 or rAAV2/6-NEDD4-2CS exhibited no difference in the peak I_{Na} densities and were thus pooled in one group. Data are expressed as mean ± SEM. One-way ANOVA (*post hoc* Bonferroni tests) or Kruskal-Wallis test (Dunn *post hoc* test).

2.2. β1- and β3- voltage-gated sodium channel subunits modulate cell surface expression and glycosylation of $Na_v1.7$ in HEK293 cells

This article is published in *Frontiers in Cellular Neuroscience* (Laedermann, Syam et al. 2013).

The core findings in this study is that voltage-gated sodium channels (Na_vs) β1- and β3-subunits enhance the membrane expression of two distinct and differentially glycosylated forms of $Na_v1.7$ when expressed in HEK293 cells. This effect is concomitant to an increase of $Na_v1.7$-mediated current and modification of its biophysical properties.

Na_vs β-subunits are well known protein carrying multiple functions. In particular, they are known to regulate the gating of Na_vs α-subunits, maturation, and stabilization at the cell membrane. Glycosylation, an important process for protein biosynthesis, also influences Na_vs α-subunit gating. This led us to hypothesize that β-subunits could directly influence $Na_v1.7$ glycosylation.

In this manuscript, we found that each β-subunit influences the kinetics of $Na_v1.7$ when co-expressed in HEK293 cells. We also observed that only Na_vs β1- and β3-subunits can modify biophysical properties as well as the current density of $Na_v1.7$. Biotinylation of cell surface confirmed that the increase in current density is, at least partially, due to an increase of expression at the plasma membrane. This approach also revealed for the first time that β1- and β3-subunits are able to modulate the glycosylation pattern of membrane $Na_v1.7$, highlighting a new function for these subunits.

In this manuscript, I performed electrophysiological recordings in HEK293 cells. I also contributed to biochemistry and performed qRT-PCR. I wrote the first draft and corrected versions of the manuscript.

frontiers in
CELLULAR NEUROSCIENCE

ORIGINAL RESEARCH ARTICLE
published: 30 August 2013
doi: 10.3389/fncel.2013.00137

β1- and β3- voltage-gated sodium channel subunits modulate cell surface expression and glycosylation of $Na_v1.7$ in HEK293 cells

Cédric J. Laedermann[1,2†], Ninda Syam[2†], Marie Pertin[1], Isabelle Decosterd[1,3‡] and Hugues Abriel[2*‡]

[1] *Pain Center, Department of Anesthesiology, University Hospital Center and University of Lausanne, Lausanne, Switzerland*
[2] *Department of Clinical Research, University of Bern, Bern, Switzerland*
[3] *Department of Fundamental Neurosciences, University of Lausanne, Lausanne, Switzerland*

Edited by:
Dieter Wicher, Max Planck Institute for Chemical Ecology, Germany

Reviewed by:
Stefan H. Heinemann, Friedrich-Schiller-Universität, Germany
Todd Scheuer, University of Washington School of Medicine, USA

****Correspondence:***
Hugues Abriel, Department of Clinical Research, University of Bern, Murtenstrasse 35, 3010 Bern, Switzerland
e-mail: hugues.abriel@dkf.unibe.ch
† These authors have contributed equally to this work and should be considered as co-first authors.
‡ These authors contributed equally to this work and should be considered as co-last authors.

Voltage-gated sodium channels (Na_vs) are glycoproteins composed of a pore-forming α-subunit and associated β-subunits that regulate Na_v α-subunit plasma membrane density and biophysical properties. Glycosylation of the Na_v α-subunit also directly affects Na_vs gating. β-subunits and glycosylation thus comodulate Na_v α-subunit gating. We hypothesized that β-subunits could directly influence α-subunit glycosylation. Whole-cell patch clamp of HEK293 cells revealed that both β1- and β3-subunits coexpression shifted $V_{½}$ of steady-state activation and inactivation and increased $Na_v1.7$-mediated I_{Na} density. Biotinylation of cell surface proteins, combined with the use of deglycosydases, confirmed that $Na_v1.7$ α-subunits exist in multiple glycosylated states. The α-subunit intracellular fraction was found in a core-glycosylated state, migrating at ∼250 kDa. At the plasma membrane, in addition to the core-glycosylated form, a fully glycosylated form of $Na_v1.7$ (∼280 kDa) was observed. This higher band shifted to an intermediate band (∼260 kDa) when β1-subunits were coexpressed, suggesting that the β1-subunit promotes an alternative glycosylated form of $Na_v1.7$. Furthermore, the β1-subunit increased the expression of this alternative glycosylated form and the β3-subunit increased the expression of the core-glycosylated form of $Na_v1.7$. This study describes a novel role for β1- and β3-subunits in the modulation of $Na_v1.7$ α-subunit glycosylation and cell surface expression.

Keywords: voltage-gated sodium channels (Na_vs), Na_vs β-subunits, glycosylation, biophysical properties, trafficking

INTRODUCTION

Voltage-gated sodium channels (Na_vs) are large glycoprotein complexes responsible for the initial rising phase of the action potential in excitable cells. They are composed of a highly processed α-subunit and are associated to one or more β-subunits (Brackenbury and Isom, 2011). The α-subunit is the pore-forming unit of the channel through which the Na^+ ions pass (Catterall, 2000). Nine genes encoding Na_v α-subunits have been found in the human genome. In addition, four genes coding for the different Na_v β-subunits have been identified: *SCN1B* (Isom et al., 1992; Kazen-Gillespie et al., 2000), *SCN2B* (Isom et al., 1995a), *SCN3B* (Morgan et al., 2000) and *SCN4B* (Yu et al., 2003) coding for β1- to β4-subunits, respectively. The α-subunit is composed of four homologous domains (Noda et al., 1984). Each of these domains contains six α-helical transmembrane domains (S1–S6). S1–S4 form the voltage-sensing domains and thus regulate α-subunit opening. S5 and S6 form the pore of the channel (Guy and Seetharamulu, 1986; Payandeh et al., 2011). The pore-forming α-subunit permits the flow of Na^+, but its biophysical properties are modulated by the β-subunits (Isom et al., 1995b), most likely via direct interference with gating (Zimmer and Benndorf, 2002). The influence of β-subunits on the biophysical properties of the recorded sodium current (I_{Na}) vary with cell type, possibly due to different endogenous β-subunit expression and the presence of different partner proteins (Meadows and Isom, 2005). The β-subunits also participate in cell–cell adhesion and cell migration via the interaction with the extracellular matrix and cytoskeletal molecules. They also serve as important signaling molecules (Isom, 2001). Naturally occurring genetic variants in humans and genetically modified animal models have shown that β-subunits are implicated in numerous diseases, i.e., pain, epilepsy, migraines and cardiac arrhythmias (Brackenbury and Isom, 2011). This highlights their importance in the regulation of cellular excitability. The β-subunits are composed of an extracellular immunoglobulin-like domain in the N-terminal region, a single transmembrane segment and an intracellular carboxy-terminus tail (Isom et al., 1992). β1- and β3-subunits interact with the α-subunit via a non-covalent bond (Hartshorne et al., 1982), while β2- and β4-subunits are covalently linked to the α-subunit via disulfide bonds (Hartshorne et al., 1982; Messner and Catterall, 1985; Yu et al., 2003).

Out of the total pool of Na_vs, most of the α-subunits are localized intracellularly: in the endoplasmic reticulum (ER) for synthesis, in the Golgi where post-translational modifications

occur and in the secretory pathway where they are trafficked to the plasma membrane to exert their main functions (Schmidt et al., 1985; Ritchie et al., 1990; Okuse et al., 2002). In the ER and the Golgi, Na_v α-subunits undergo extensive sequential glycosylation (Waechter et al., 1983; Schmidt and Catterall, 1987), a process involving the addition of N-acetylglucosamine capped by sialic acid residues and the sequential addition of oligosaccharide chains. Glycosylation can account for up to 30% of the α-subunit molecular weight (Messner and Catterall, 1985). Protein glycosylation serves various functions such as protein folding, cell signaling, protection from proteases, cell-cell adhesion and regulation. It has also been implicated in development and immunity (Moremen et al., 2012). Glycosylation modifies the gating properties of the Na_v α-subunits (Recio-Pinto et al., 1990; Bennett et al., 1997; Zhang et al., 1999; Tyrrell et al., 2001), most likely by interfering with the electric field near the gating sensors (Bennett et al., 1997; Cronin et al., 2005; Ednie and Bennett, 2012).

Because both β-subunits and glycosylation modify the intrinsic biophysical properties of the Na_v α-subunit, we hypothesized that β-subunits might directly influence α-subunit glycosylation. This study investigated the effect of the four β-subunits on the $Na_v1.7$-mediated current when co-expressed in HEK293 cells. Each of the four β-subunits influenced the biophysical properties and kinetics of the $Na_v1.7$-mediated current to varying degrees, but only the β1- and β3-subunits increased $Na_v1.7$ current density. Cell surface biotinylation and subsequent deglycosylation of the samples revealed the presence of differentially glycosylated forms of $Na_v1.7$ in the cell; a core-glycosylated and a fully-glycosylated form of $Na_v1.7$. β1- and β3-subunits mediated the differentially glycosylated form of $Na_v1.7$ and enhanced its expression at the membrane. This suggests that the increase in $Na_v1.7$ I_{Na} may be explained by a glycosylation-dependent stabilization of $Na_v1.7$ at the cell membrane. This work reveals a novel mechanism by which Na_v β-subunits modulate α-subunit glycosylation and cell surface density.

MATERIALS AND METHODS

DNA CONSTRUCTS

$Na_v1.7$, β1-, β2-, and β4-subunit cDNA cloned into pCINh and β3-subunit cloned into pFBM were provided by Dr. S. Tate (Convergence Pharmaceuticals, Cambridge, UK).

CELL CULTURE AND TRANSFECTION

Human embryonic kidney (HEK293) cells were cultured in DMEM medium supplemented with 10% FBS, 4 mM Glutamine and 20 μg/ml Gentamicin, at 37°C in a 5% CO2 incubator (Life Technologies Inc.). For patch clamp experiments, 1 μg of $Na_v1.7$ cDNA concomitantly with 0.4 μg of a β-subunit and 0.8 μg EBO-pCD-Leu2-CD8 cDNA encoding CD8 antigen as a reporter gene were transfected using the Ca^{2+}-phosphate method in a T25 ($\sim 2 \times 10^6$ cells). For biotinylation and deglycosylation assays, HEK293 cells were transiently co-transfected with 6 μg of $Na_v1.7$ and 6 μg of each β-subunit or empty vector mixed with 30 μl JetPEI (Polyplus-Transfection) and 250 μl 150 mM NaCl in a P100 dish ($\sim 9 \times 10^6$ cells, BD Falcon). For a negative control, the cells were transfected with 12 μg of empty vector. The cells were used in patch clamp or biochemical experiments 48 h post transfection.

CELL SURFACE BIOTINYLATION ASSAY

HEK293 cells transiently co-transfected were treated with 0.5 mg/ml EZ-link™ Sulfo-NHS-SS-Biotin (Thermo Scientific) in cold 1X PBS for 15 min at 4°C. The cells were then washed twice with 200 mM Glycine in cold 1X PBS to inactivate biotin, and twice with cold 1X PBS to remove excess biotin. The cells were then lysed with 1X lysis buffer [50 mM HEPES pH 7.4; 150 mM NaCl; 1.5 mM $MgCl_2$; 1 mM EGTA pH 8; 10% Glycerol; 1% Triton X-100; 1X Complete Protease Inhibitor Cocktail (Roche)] for 1 h at 4°C. Whole cell lysates were centrifuged at 16,000 *g* at 4°C for 15 min. 2 mg of the supernatant was incubated with 50 μl Streptavidin Sepharose High Performance beads (GE Healthcare) for 2 h at 4°C, and the remaining supernatant was kept as input. The beads were subsequently washed five times with 1X lysis buffer before elution with 50 μl of 2X NuPAGE sample buffer (Invitrogen) and 100 mM DTT at 37°C for 30 min. These biotinylated fractions were analyzed as $Na_v1.7$ expression at the cell surface. The input fractions, representing total expression of $Na_v1.7$, were resuspended with 4X NuPAGE sample buffer plus 100 mM DTT to give a concentration of 1 mg/ml (60 μg/well) and were then incubated at 37°C for 30 min.

DEGLYCOSYLATION ASSAY

For the total fractions, 60 μg of proteins of whole cell lysates were denatured at 37°C for 30 min in the presence of 1X Glycoprotein denaturing buffer. The denatured protein lysates were subsequently incubated at 37°C for 1 h with 1500 units PNGaseF (New England Biolabs) in the presence of 1X NP-40 and 1X G7 buffer to cleave most of the high mannose, hybrid and complex oligosaccharides from N-linked glycoproteins. The reaction was stopped by adding 4X NuPAGE sample buffer plus 100 mM DTT and incubating them at 37°C for 30 min. For the biotinylated fractions, 35 μl ddH_2O were added into Streptavidin Sepharose High Performance beads previously incubated with whole cell lysate and denatured at 37°C for 30 min in the presence of 1X glycoprotein denaturing buffer. The denatured proteins bound to Streptavidin beads were subsequently incubated at 37°C for 1 h with 2000 units of PNGaseF in the presence of 1X NP-40 and 1X G7 buffer. Following this incubation step, the beads were washed five times with the same lysis buffer used in the biotinylation assay and eluted with 2X NuPAGE sample buffer and 100 mM DTT at 37°C for 30 min.

WESTERN BLOTS

Protein samples were separated on a 5–15% polyacrylamide gradient gel and blotted onto a nitrocellulose membrane using TransBlot Turbo transfer system (Biorad, Hercules). Antibody detections were performed in the SNAP i.d. system (Millipore) using the following antibodies: mouse monoclonal anti-$Na_v1.7$ clone N68/6 (UC Davis/National Institute of Health (NIH) NeuroMab Facility, University of California), mouse monoclonal clone 464.6 anti-Na^+/K^+ ATPase α-1 (Abcam), rabbit polyclonal anti-actin A2066 (Sigma) and rabbit polyclonal anti-β4 (EnoGene). Rabbit polyclonal homemade anti-β1, anti-β2 and

anti-β3 antibodies were provided by Dr. S. Tate (Convergence Pharmaceuticals, Cambridge, UK). Infrared IRDyeTM (680 or 800 CW)-linked goat anti-rabbit or anti-mouse IgG (LI-COR Biosciences) was used as secondary antibody. The blots were revealed and quantified with Odyssey Li-Cor (Lincoln).

ELECTROPHYSIOLOGY

Twenty-four hours after transfection, cells were split at low density and whole-cell recordings were performed 48 h after transfection. Anti-CD8 beads (Dynal, Oslo, Norway) were used to identify transfected cells. Whole cell patch-clamp recordings were carried-out using an internal solution containing 60 mM CsCl, 70 mM Cs Aspartate, 11 mM EGTA, 1 mM $MgCl_2$, 1 mM $CaCl_2$, 10 mM HEPES, and 5 mM Na_2-ATP, pH 7.2 with CsOH and an external solution containing 130 mM NaCl, 2 mM $CaCl_2$, 1.2 mM $MgCl_2$, 5 mM CsCl, 10 mM HEPES, 5 mM glucose, pH 7.4 with CsOH. Data were recorded with a VE-2 amplifier (Alembic Instruments, Montreal, Canada) or an Axon amplifier 700A and analyzed using pClamp software (version 8, Molecular Devices), Kaleidagraph (version 4.03) and MatLab. The sampling interval was set to 5 μs (200 kHz) and low-pass filtering to 5.0 kHz. Resistance of the borosilicate pipettes (World Precision Instruments, Sarasota, FL, USA) was 2–6 MΩ. Leakage current was subtracted using the P/4 procedure. I_{Na} densities (pA/pF) were obtained by dividing the peak I_{Na} by the cell capacitance obtained from the pClamp function. Voltage dependence of activation (SSA) curves were determined from *I/V* curves where the Na^+ current was evoked from a holding potential of −100 mV to test pulses of 100 ms ranging from −120 to +30 mV in increments of 5 mV. The linear ascending segment of the *I/V* relationship was used to estimate the reversal potential for each trace. Time constant of inactivation was determined by fitting the current decay with the Levenberg-Marquardt single exponential function. The time constant was plotted against the test voltage, with $I = A * \exp(-t/\tau) + C$: where I is the current, A is the percentage of channel inactivation with the time constant τ, t is time and C if the steady-state asymptote. Steady-state inactivation curves (SSI) were measured from a holding potential of −120 mV using 500 ms prepulses to the indicated potentials, followed by a test pulse to 0 mV. To quantify the voltage-dependence of SSA and SSI, data from individual cells were fitted with the Boltzmann relationship, $y\,(V_m) = 1/(1 + \exp[(V_m - V_{½})/k])$, in which y is the normalized current or conductance, V_m is the membrane potential, $V_{½}$ is the voltage at which half of the available channels are inactivated and k is the slope factor.

Recovery from inactivation curves (RFI or "repriming") were obtained with a standard two-pulse protocol consisting of a depolarizing pulse from a holding potential of −120 to 0 mV for 50 ms to inactivate the channels, followed by a variable duration (from 0.5 to 3000 ms) step back to −120 mV to promote recovery. Channel availability was assessed with the first standard test pulse at 0 mV. The normalized currents of the second pulse at 0 mV were plotted against the recovery interval. We calculated $t_{½}$ (ms), the time necessary for half of the channels to recover from the first pulse, by interpolation from a linear relation between the 2 points juxtaposing half recovery ($y_1 < 0.5 < y_2$), using the equation $x = [0.5 - (y_1x_2 - y_2x_1)/(x_2 - x_1)]^*(x_2 - x_1)/(y_2 - y_1)$.

QUANTITATIVE REAL-TIME REVERSE TRANSCRIPTION PCR (qRT-PCR)

HEK293 cells transfected with $Na_v1.7$ (1 μg) alone or with each of β-subunits (0.4 μg) were collected in RNA-later solution (Qiagen, Basel, Switzerland). mRNA was extracted and purified with RNeasy Plus Mini kit (Qiagen) and quantified using RNA 6000 Nano Assay (Agilent Technologies AG, Basel, Switzerland). A total of 600 ng of RNA was reverse transcribed for each sample using Omniscript reverse transcriptase (Qiagen). $Na_v1.7$ primer's sequence is as follow; 5′-TCTGTCTGAGTGTGTTTGCACTAA-3′ and 5′-AAGTCTTCTTCACTCTCTAGGGTATTC-3′. We used GAPDH as reference gene to normalize $Na_v1.7$ mRNA expression. Gene-specific mRNA analyses were performed using the iQ SYBR-green Supermix (BioRad, Reinach, Switzerland) and the iQ5 real-time PCR detection system (BioRad). Only reactions with appropriate amplification and melting curves determining the amplicon specificity were analyzed. For all conditions tested we used $n = 3$ samples. All samples were run in triplicate.

STATISTICS

For electrophysiological experiments (current densities and biophysical properties) normality with D'Agostino-Pearson was tested to determine whether a regular One-Way ANOVA and *post-hoc* Bonferroni tests, or the non-parametric equivalent test (Kruskal-Wallis test and Dunn *post-hoc* tests), should be performed. For RFI, a Two-Way ANOVA was used to compare $Na_v1.7$ alone with $Na_v1.7$ co-transfected with each β-subunit, and the impact of the voltage on this comparison. Biochemical experiments and transcriptional quantification data were analyzed using bilateral Student's *t*.

RESULTS

The functional impact of the co-expression of the four β-subunits on $Na_v1.7$-mediated I_{Na} was studied by performing whole cell patch-clamp experiments in HEK293 cells. Each β-subunit was independently co-transfected with $Na_v1.7$ and then compared to $Na_v1.7$ expressed alone. **Figure 1A** shows typical traces of $Na_v1.7$ I_{Na} obtained with a current-voltage protocol. A hastening of the $Na_v1.7$ current decay kinetics was observed with each of the β-subunits tested (**Figure 1B**). The shortening of the $Na_v1.7$ time constant of current decay was observed for a wide range of voltages and showed voltage-dependency for every β-subunit (**Figure 1B**). The shortening was particularly prominent for the β3-subunit. In addition, β1- and β3-subunits also significantly increased (∼2-fold) $Na_v1.7$-mediated current density as compared to $Na_v1.7$ alone or to $Na_v1.7$ co-expressed with β2- or β4-subunits (**Figure 1C** and **Table 1**). We also observed that β2 and β4-subunits did not antagonize β1 and β3-subunits-dependent up-regulation, and that the two latter have additive positive effect on $Na_v1.7$-mediated current (data not shown).

Whether the I_{Na} density increase mediated by both β1- and β3-subunits was also accompanied by alterations of other $Na_v1.7$ biophysical properties was also assessed. The voltage dependence of macroscopic I_{Na} activation and inactivation (see Materials and Methods) of $Na_v1.7$ in the absence and presence of each β-subunit was recorded and analyzed. The co-transfection of the β1-subunit significantly shifted the $V_{½}$ of steady-state inactivation

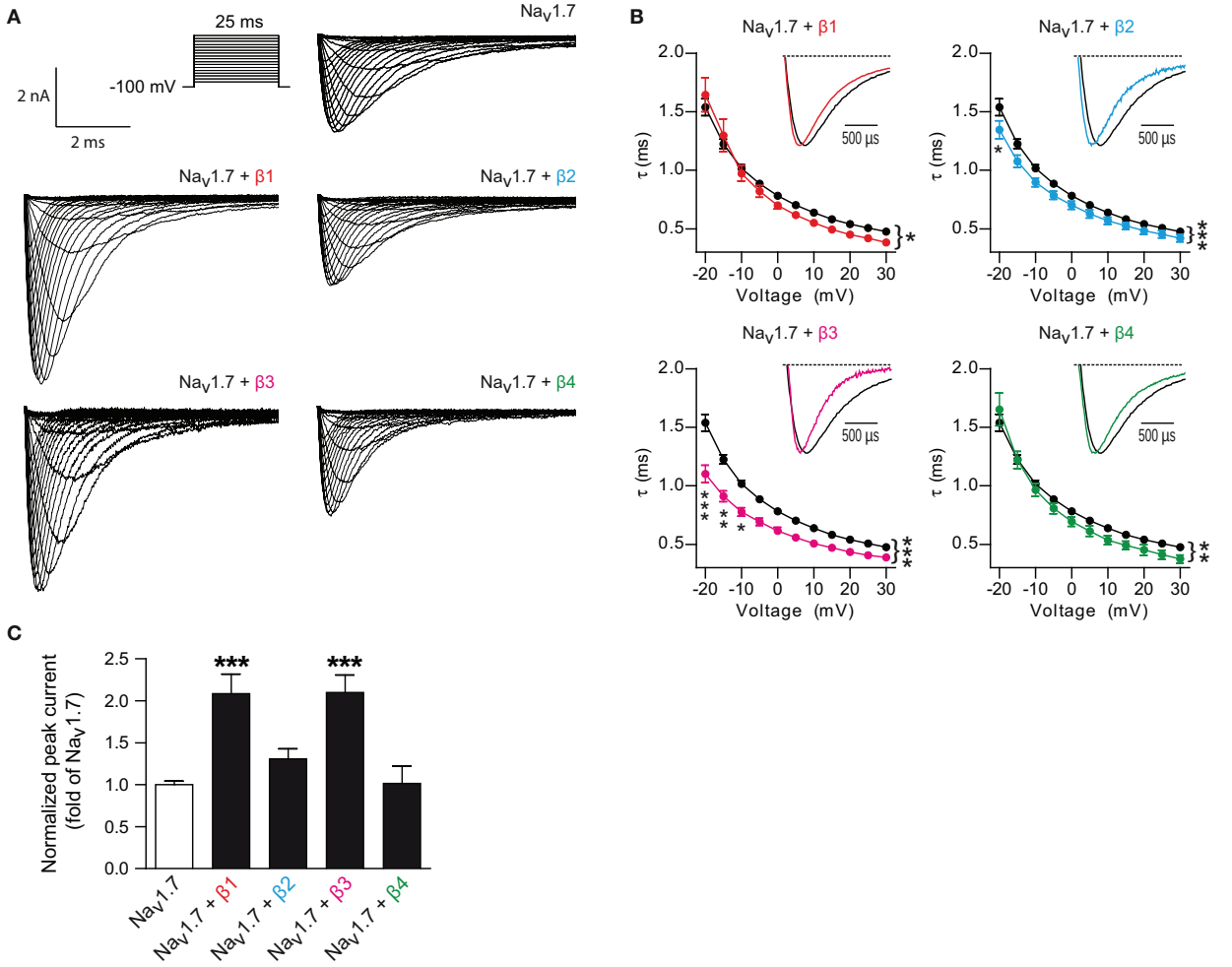

FIGURE 1 | β-subunits regulate Na$_v$1.7 currents. (A) Typical whole-cell Na^+ currents of HEK293 cells transfected with Na$_v$1.7 alone or Na$_v$1.7 co-expressed with individual β-subunits elicited with a typical current-voltage protocol. **(B)** Voltage-dependence of current decay of Na$_v$1.7 alone compared to Na$_v$1.7 with each individual β-subunit. *Inset*: Normalized representative current traces of Na$_v$1.7 elicited by test pulses at 0 mV. Co-transfection of the β1- ($p = 0.011$, $n = 39$), β2- ($p < 0.0001$, $n = 25$), β3- ($p < 0.0001$, $n = 16$), and β4-subunit ($p = 0.006$, $n = 13$) decreased the time constant decay as compared to Na$_v$1.7 alone ($n = 81$). Two-Ways ANOVA and Bonferroni *post-hoc* tests. Data are expressed as mean ± s.e.m. **(C)** I_{Na} densities from HEK293 cells transfected with Na$_v$1.7 alone or co-transfected with individual β-subunits. β1- ($n = 55$) and β3-subunits ($n = 34$), but not β2- ($n = 67$) nor β4-subunits ($n = 27$), increased the Na$_v$1.7 current densities. $p < 0.0001$ for β1- and β3-subunits with One-Way ANOVA followed by Bonferroni *post-hoc* tests. Data are expressed as mean ± s.e.m. and were normalized to Na$_v$1.7 alone for each experiments. Values can be found in **Table 1**. $^*p < 0.05$, $^{**}p < 0.01$ and $^{***}p < 0.001$.

toward depolarized potentials by ∼5.8 mV, but had no influence on $V_{½}$ of activation (**Figure 2A** and **Table 1**). The β3-subunit shifted the $V_{½}$ of inactivation toward depolarized potentials by ∼3.5 mV and the $V_{½}$ of activation toward hyperpolarized potentials by ∼3.7 mV (**Figure 2C** and **Table 1**). Neither the β2- nor β4-subunits affected Na$_v$1.7 voltage dependence of activation or inactivation (**Figures 2B,D** and **Table 1**).

The influence of the β-subunits on recovery from inactivation (RFI) was also tested. Because the RFI relationships could not always be fitted with the exponential functions to the same degree, an interpolation from a linear relation between the 2 points juxtaposing half recovery to obtain the half-time ($t_{½}$) of RFI was used. Only the β1-subunit significantly hastened $t_{½}$ of RFI to 6.19 vs. 7.55 ms for the control (**Figures 3A–D** and **Table 1**).

As only minor modifications of the I_{Na} biophysical properties were observed, it is unlikely that the 2-fold increase in the Na$_v$1.7 current density mediated by β1- and β3-subunits is only due to alterations of the single channel properties. Whether the increase of the Na$_v$1.7 current may have been due to an increase in channel synthesis was investigated. Na$_v$1.7 mRNA levels remained unchanged with β-subunit co-transfection, as observed by q-RT-PCR (**Figure 4**), discounting this hypothesis.

Table 1 | Biophysical properties of Na$_v$1.7 alone or upon β-subunit co-transfection in HEK293 cells.

	Current density		Activation			Inactivation			Recovery	
	normalized pA/pF	*n*	$V_{½}$ (mV)	slope k_v	*n*	$V_{½}$ (mV)	slope k_v	*n*	$t_{½}$ (ms)	*n*
Na$_v$1.7	1.00 ± 0.04	140	−18.6 ± 0.4	6.8 ± 0.2	81	−70.9 ± 0.5	8.1 ± 0.3	92	7.55 ± 0.21	72
Na$_v$1.7 + β1	2.08 ± 0.23***	55	−17.4 ± 0.8	5.8 ± 0.2***	39	−65.7 ± 0.5***	7.0 ± 0.2*	51	6.19 ± 0.23**	27
Na$_v$1.7 + β2	1.31 ± 0.12	67	−18.2 ± 0.9	6.2 ± 0.3	25	−70.9 ± 0.6	7.5 ± 0.2	43	7.03 ± 0.34	34
Na$_v$1.7 + β3	2.10 ± 0.21***	34	−22.3 ± 1.0*	5.4 ± 0.3***	17	−67.4 ± 0.8***	7.0 ± 0.3	18	6.69 ± 0.25	16
Na$_v$1.7 + β4	1.02 ± 0.21	27	−16.1 ± 1.1	7.1 ± 0.3	13	−70.8 ± 0.5	7.2 ± 0.5	20	7.38 ± 0.33	19

*Values for Na$_v$1.7 and Na$_v$1.7 co-transfected with β-subunits. The $V_{½}$ of steady-state activation and inactivation and their associated slope factors, as well as the $t_{½}$ of recovery from inactivation, were obtained as described in the Materials and Methods. *p < 0.05, **p < 0.01, and *** p < 0.001, One-Way ANOVA, post-hoc Bonferroni tests or Kruskal–Wallis with Dunn post-hoc test between Na$_v$1.7 and Na$_v$1.7 with each β-subunit. Data are expressed as mean ± s.e.m.*

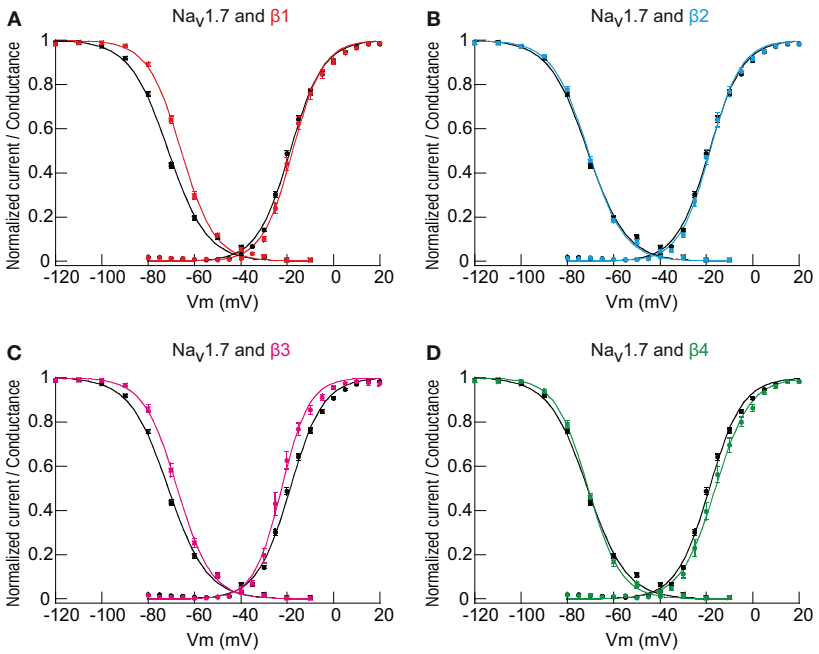

FIGURE 2 | The influence of β1- and β3-subunits on Na$_v$1.7 voltage-dependence of activation and inactivation. (A–D) Normalized currents for both activation and steady-state inactivation (see Materials and Methods) are plotted against the test potential. Each panel compares Na$_v$1.7 alone to Na$_v$1.7 co-expressed with individual β-subunits. A minor but significant effect on the $V_{½}$ of activation was observed for β3-subunit ($n = 17$, hyperpolarizing shift, $p < 0.05$) co-expression as compared to Na$_v$1.7 alone ($n = 81$). β1- ($n = 39$), β2- ($n = 25$) and β4-subunits ($n = 13$) did not modify the $V_{½}$ of activation of Na$_v$1.7. The effect on the $V_{½}$ of inactivation was highly significant for β1- ($n = 51$, depolarizing shift with $p < 0.0001$) and β3-subunit ($n = 18$, depolarizing shift with $p < 0.0001$) compared to Na$_v$1.7 alone ($n = 92$); whereas β2- ($n = 43$) and β4-subunits ($n = 20$) had no effect. Individual points are the mean ± s.e.m. of the normalized current at each voltage point. The smooth curves are Boltzmann fits whose equations give both the $V_{½}$ of activation and inactivation (midpoints) and their associated slope factors (see Materials and Methods). The $V_{½}$ of steady-state activation and inactivation comparing Na$_v$1.7 alone vs. the co-expression with each subunit were tested by One-Way ANOVA followed by Bonferroni's multiple comparison tests. Values and statistics can be found in **Table 1**.

Whether the Na$_v$1.7-mediated I_{Na} upregulation could be due to an increase of Na$_v$1.7 protein density at the cell membrane was investigated by performing biotinylation of plasma membrane proteins. After lysis, proteins were sampled under reducing conditions known to dissociate the covalently bound β2- and β4-subunits from α-subunits (Messner and Catterall, 1985). Co-transfection of β1-, β2-, and β4-subunits significantly decreased Na$_v$1.7 protein expression in the total cell lysate fraction (input, **Figure 5A**). The quantification revealed a ∼2-fold decrease for each of these three subunits. Co-transfection of the β3-subunit had no effect on Na$_v$1.7 expression in the total cell lysate fraction. In the biotinylated membrane fraction two bands at different apparent molecular weights were observed when Na$_v$1.7 was expressed alone (white and black arrow heads in **Figure 5A**). These bands correspond to different glycosylated states of Na$_v$1.7 as demonstrated by using deglycosylating enzymes (**Figure 5B**). Endoglycosidase H (EndoH) only cleaves core N-glycans from proteins whereas Peptide-N-Glycosidase F (PNGaseF) does not discriminate between full and core glycosylated proteins. Of the two bands of biotinylated Na$_v$1.7, only

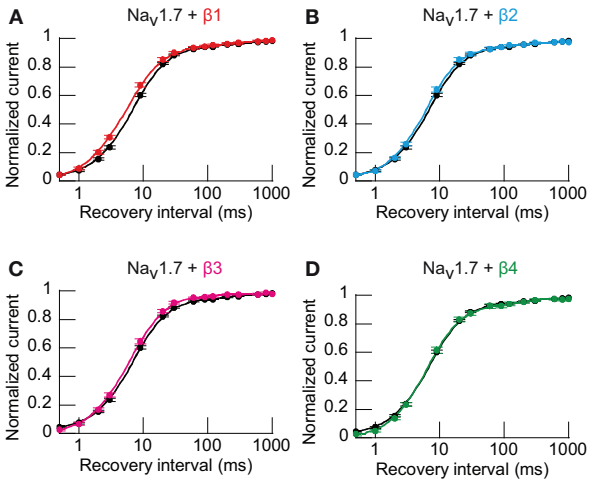

FIGURE 3 | Only β1-subunit significantly increases Na$_v$1.7 recovery from inactivation (RFI). (A–D) RFI from HEK293 cells transfected with Na$_v$1.7 alone or co-transfected with individual β-subunits. Smooth curves were fitted incorporating a geometric weight to arrive at the final curve (no equation) and the $t_{½}$ was calculated by interpolation on the *x*-axis from a linear relation between the 2 points juxtaposing half recovery ($y_1 < 0.5 < y_2$, see Materials and Methods). Only when co-expressed with β1-subunit ($n = 27$, $p < 0.01$) was Na$_v$1.7 RFI significantly faster as compared to Na$_v$1.7 alone ($n = 72$). β2- ($n = 34$), β3- ($n = 16$), and β4-subunits ($n = 19$) did not significantly alter RFI when co-expressed with Na$_v$1.7. Individual points are the mean ± s.e.m. of the normalized current at each time point. Non-parametric One-Way analysis of variance (Kruskal-Wallis test) with Dunn *post-hoc* tests to compare each subunit co-expressed with Na$_v$1.7 vs. Na$_v$1.7 alone.

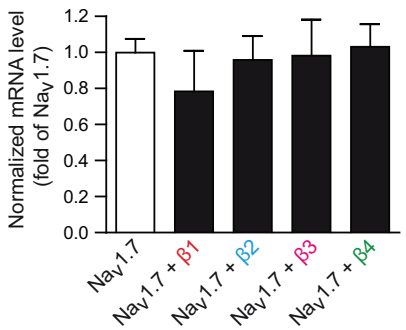

FIGURE 4 | Na$_v$1.7 transcripts upon β-subunit co-transfection. Bar graph showing transcriptional levels of Na$_v$1.7 in control conditions (co-transfected with empty vector) over Na$_v$1.7 levels when cells were co-transfected with each individual β-subunit. Transcripts were normalized to *GAPDH* and run in triplicate. Data represent the mean ± s.e.m., $n = 3$ independent transfections for every condition.

the lower was sensitive to EndoH and was shifted to an apparent lower molecular weight band (compare white arrowhead in the first lane to gray arrowhead in the third lane), indicating that this band corresponds to the core-glycosylated form of the channel (**Figure 5B**). Because PNGaseF was able to digest both bands, it can be proposed that the higher band corresponds to the fully-glycosylated form of Na$_v$1.7. The lower band of biotinylated Na$_v$1.7 migrates at the same apparent molecular weight as the band observed in the input fraction (white arrow heads in **Figure 5A**) suggesting that most of Na$_v$1.7 in the intracellular pool is core-glycosylated. This is consistent with the channel being early and rapidly, but only partially, glycosylated after its synthesis. The upper band in the total cell lysate fraction was faint and blurry (**Figure 5A**), suggesting that the fully-glycosylated channel only represents a small fraction of the total Na$_v$1.7 cellular pool. It was only by enriching the membrane proteins through the precipitation of the biotinylated membrane fraction (the ratio between the amount of lysate protein loaded and the amount of streptavidin beads needed to precipitate biotinylated proteins was ∼1:30) that the upper band was distinctly observed. Co-expression of the β1-subunit reproducibly shifted the upper band to an intermediate migrating band of lower apparent molecular weight. This suggests that the β1-subunit mediates an alternative glycosylated form of Na$_v$1.7. When comparing the β1-subunit-modified intermediate band with the upper band of the control condition (Na$_v$1.7 alone), a significant increase in signal intensity was observed (**Figure 5A**, quantification), which is consistent with the increase in the Na$_v$1.7 current density (**Figure 1C**). Co-transfection of the β2-subunit neither modified the glycosylation pattern nor the expression of any of the two bands, consistent with the fact that the current density was not modified. β3-subunit expression also altered the Na$_v$1.7 band pattern in the biotinylated fractions. The upper band overlapped with the lower band under the migrating conditions used. The β3-subunit significantly increased (∼7-fold) the intensity of the lower band as compared to the lower band of control, consistent with the increase of the Na$_v$1.7 current density elicited by the β3-subunit (**Figure 1C**). Finally, β4-subunit co-transfection led to a small but significant decrease of the lower band.

To confirm that the different bands observed when β-subunits are coexpressed, particularly β1 and β3-subunits, represent alternative glycosylated form of Na$_v$1.7, we again incubated the input and biotinylated fractions with PNGaseF. A small but consistent shift of the Na$_v$1.7 band into a lower apparent molecular weight band in the total cell lysate fraction was observed (the white arrow heads shifted to the gray arrow heads, **Figure 6**). Furthermore, when incubating the biotinylated fraction of β-subunit and Na$_v$1.7 co-expression experiments with PNGaseF, all of the Na$_v$1.7 bands shifted to a single band (gray arrow heads) of the same molecular weight. This confirms that the β1- and β3-subunits modulate differential glycosylation patterns on Na$_v$1.7 (**Figure 6**, black and white arrow heads). Noteworthy, when comparing the single band of Na$_v$1.7 when samples are treated with PNGaseF in the input fraction with the one in the biotinylated fraction, it seems that this band migrates slower in the input as compared to biotinylated fraction when β-subunits are coexpressed (compare bands highlighted by gray arrows for each blots). This may be due to other post-translational modification such as sialylation or palmitoylation of the channel. Further experiments using desialylation or depalmitoylation treatment are needed to confirm this possibility.

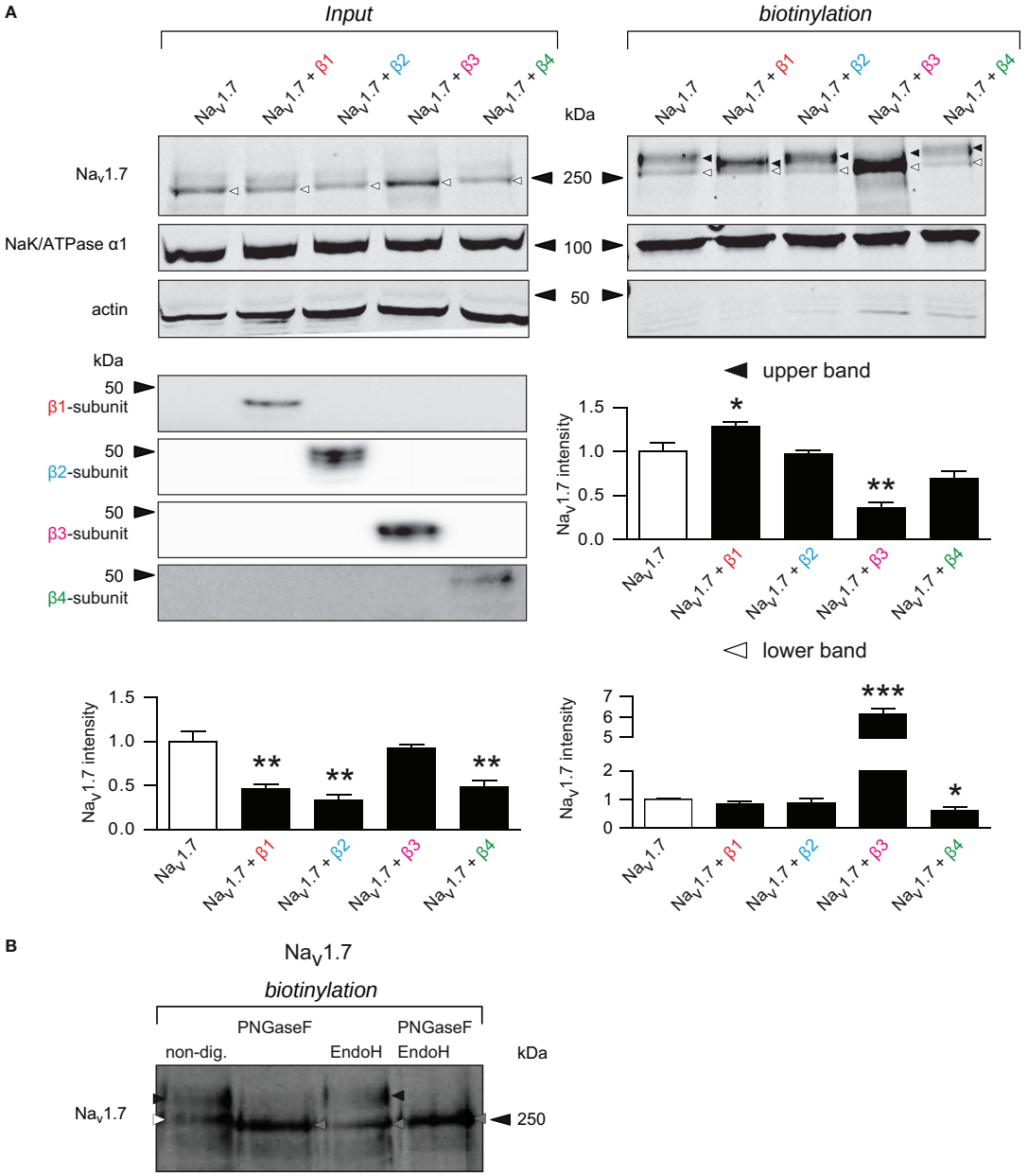

FIGURE 5 | β1- and β3-subunit mediate differential forms of $Na_V1.7$ whose expression is increased at the membrane. (A) Representative western blot of a biotinylation assay with total lysate (*input*, left) and cell surface (*biotinylation*, right) fractions from HEK293 cells transiently transfected with $Na_V1.7$ alone, or co-expressed with each individual β-subunit and the associated quantifications. *Input:* $Na_V1.7$ is detected in two forms: a fast migrating band (~250 kDa, that will be referred to as lower band) that consist mostly of the $Na_V1.7$ immunoreactive signal and a slow migrating band (~280 kDa, that will be referred to as upper band). β1- ($p = 0.006$), β2- ($p = 0.003$), and β4-subunits ($p = 0.009$) significantly decreased $Na_V1.7$ expression, whereas the β3-subunit had no effect ($p = 0.570$). Because the upper band was below the sensitivity threshold, both bands were quantified together. *Biotinylation:* $Na_V1.7$ membrane protein is detected in three forms. When expressed alone, one lower band (white triangle, ~250 kDa) and one upper band (black triangle, ~280 kDa) were present (for identification of these bands, see Panel **B**). When the β1-subunit is co-expressed, the upper band was clearly shifted into an intermediate migrating band (~260 kDa) with increased expression ($p = 0.047$). β2- and β4-subunits revealed the same pattern as when $Na_V1.7$ was transfected alone and did not change its expression, except for the small decrease of the lower band when the β4-subunit is co-transfected ($p = 0.020$). The β3-subunit clearly increased $Na_V1.7$ immunoreactivity of the lower band ($p < 0.0001$). For *input* and *biotinylation* fractions, actin and the α1-subunit of NaK-ATPase were used as biotin leakiness and loading controls, respectively. Data represent mean ± s.e.m, $n = 4$ independent experiments. Student's unpaired *t*-test, each condition being compared with $Na_V1.7$. $^*p < 0.05$, $^{**}p < 0.01$ and $^{***}p < 0.001$. **(B)** Representative western blot and identification of glycosylation state of $Na_V1.7$ in biotinylated fraction from HEK293 cells transiently transfected with $Na_V1.7$. EndoH only cleaves the lower band of biotinylated $Na_V1.7$, demonstrating that this band represents the core-glycosylated form of the channel. The upper band is digested by PNGaseF, demonstrating that it corresponds to fully-glycosylated form of the channel. PNGaseF can also digest the core-glycosylated form of $Na_V1.7$.

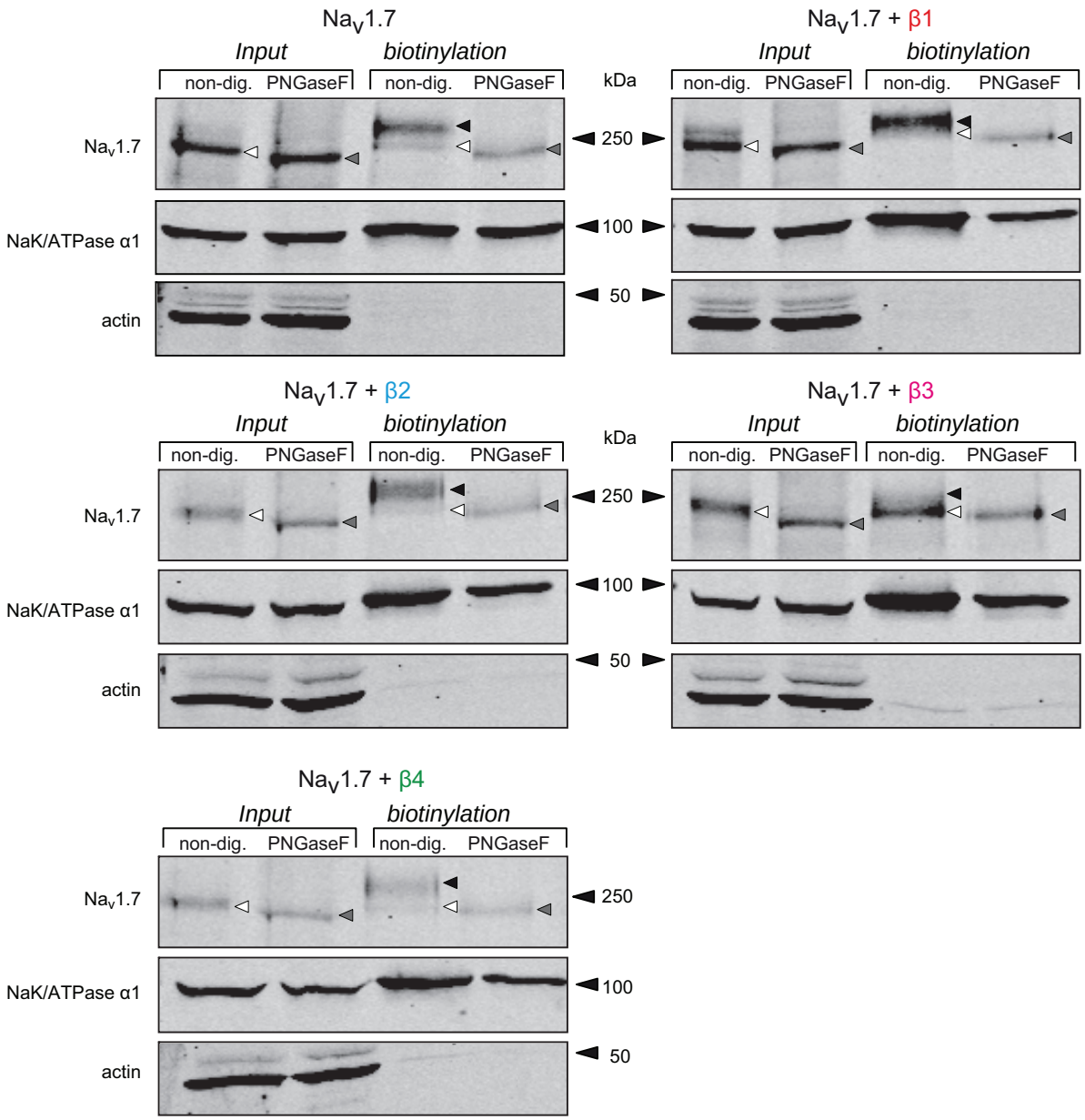

FIGURE 6 | The different forms of Na$_v$1.7 observed with β-subunits are due to differential glycosylation patterns. Western blot of a biotinylation assay followed by deglycosylation with total lysate and cell surface fractions from HEK293 cells transiently transfected with Na$_v$1.7 alone, or co-expressed with each individual β-subunit. Samples were non-treated or treated with Peptide: N-Glycosidase F (PNGaseF) to remove glycosylated residues of the protein. The total lysate Na$_v$1.7 band (black/white triangle) was slightly shifted to an apparent lower molecular weight (gray triangle) when treated with PNGaseF. In the biotinylation fraction, the pattern of Na$_v$1.7 glycosylation by the β-subunits was the same as in **Figure 4**.(black and white triangles). When treated with PNGaseF, all the different bands shifted to the lower band of the same apparent molecular weight, irrespective of the β-subunit co-expressed.

DISCUSSION

This study demonstrates that Na$_v$ β1- and β3-subunits modulate the cell surface expression and glycosylation patterns of Na$_v$1.7 when co-expressed in HEK293 cells. It also confirms that the β-subunits differentially modulate the biophysical properties of Na$_v$1.7.

The observation that β1- and β3-subunits strongly increased Na$_v$1.7 I_{Na} density contrasts with several recent studies. The study performed by Ho et al. (2012) showed no impact of any of the β-subunits on Na$_v$1.7 current density in HEK293 cells. The other studies showed no impact using different cell expression systems (Sangameswaran et al., 1997; Morgan et al., 2000; Vijayaragavan

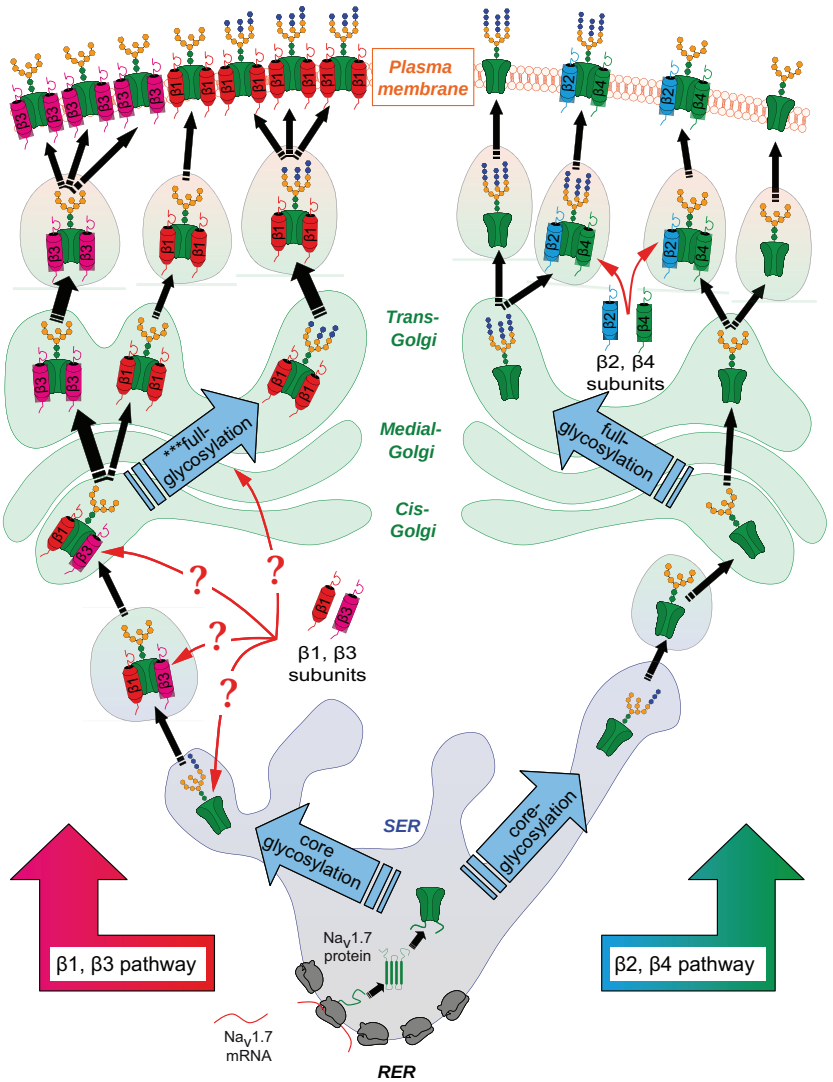

FIGURE 7 | Proposed scheme of the different intracellular pathways of α-subunits depending on the presence of different β-subunits. After synthesis in the rough endoplasmic reticulum (RER), α-subunits are rapidly folded and undergo a first step of glycosylation in the smooth endoplasmic reticulum (SER). It is known that N-acetylglucosamine and oligosaccharide chains are bound on Asp residues of the protein, a process known as core-glycosylation. Newly synthesized glycoproteins are then translocated into the Golgi network, where they are subject to a second step of more complex glycosylation, involving many different enzymes. Once matured, proteins eventually translocate to the plasma membrane. The present findings suggest that core-glycosylated proteins can also be found anchored at the membrane. By some yet undefined mechanism, the β1-subunit interferes with the second glycosylation step (***full-glycosylation on the scheme) which leads to a modification of the glycosylation pattern of the α-subunits. The β1-subunit enhances the core-glycosylated form of $Na_v1.7$. This suggests that the β1- and β3-subunits already interact with the α-subunits before the step of full-glycosylation of the channel occurring in the Golgi network. By enhancing the differential glycosylation pattern of $Na_v1.7$, it can be proposed that the β1- and β3-subunits promote stabilization of the channel at the plasma membrane. On the contrary, it is likely that the β2- and β4-subunits, which have no effect on the glycosylation nor the anchoring, only briefly interact with the α-subunits before translocation of the channel to the plasma membrane. For sake of simplicity, the shown glycosylation patterns are arbitrary. $Na_v1.7$ is depicted as being "freely" expressed in ER/Golgi and membrane networks for easier interpretation of the scheme. However, $Na_v1.7$ is embedded in the membranes of the different organelles.

et al., 2001, 2004). These discrepant observations underline the influence of the cellular background when studying Na_vs α-subunit regulation by β-subunits. Even though this study and the one by Ho et al. (2012) both used HEK293 cells, Ho et al., used a clonal cell line stably expressing rat $Na_v1.7$ cDNA, whereas the present study used transiently transfected human $Na_v1.7$ cDNA. In a stable cell line, it is likely that a significant fraction of α-subunits are already anchored at the plasma membrane; thus it is possible that the ones interacting with the transfected β-subunits only reflect a small fraction of membrane Na_vs α-subunits. Under the conditions of transient transfection, all the membrane Na_vs α-subunits are synthesised *de novo* and are thus more likely to

interact with β-subunits. It is also possible that other differences, such as the origin of the HEK293 cells or even passage numbers, may play a significant role in the observed effects. Other studies have shown, however, that β1- and β3-subunits can increase the current density of several other Na_v isoforms (Nuss et al., 1995; Smith and Goldin, 1998; Fahmi et al., 2001; Zimmer and Benndorf, 2002).

A significant shortening of the time constant of current decay was observed when $Na_v1.7$ was co-expressed with each individual subunit. A rapid rate of inactivation tends to reduce the refractory period of $Na_v1.7$, meaning that β-subunits can enhance cell excitability via this mechanism. The hastening of RFI by the β1-subunit might also reduce the duration of the refractory periods, allowing for faster repetitive firing of neurons.

The β1-subunit shifted $V_{½}$ of inactivation toward more depolarized potentials, which should increase the number of channels available for opening in response to depolarization at a given voltage near the resting membrane potential (approximately −60 to −70 mV). The β3-subunit similarly influenced this parameter, and also shifted the $V_{½}$ of activation toward hyperpolarized potentials, rendering the channel more likely to open at hyperpolarized voltages. These results are consistent with the findings of Ho et al., and account for the shift toward a hyperexcitable state.

The fact that the β1- and β3-subunits strongly increased $Na_v1.7$ current density, but only modestly influenced the biophysical properties, suggests that the single-channel conductance is not altered. In line with the previous, single-channel recordings revealed that β1-subunit did not change the $Na_v1.5$ open probability despite an important increase in current density (Nuss et al., 1995). As a consequence, it was hypothesized that these two subunits also increase $Na_v1.7$ channel density at the cell surface. Biotinylation of cell surface proteins was performed and a strong decrease of the $Na_v1.7$ signal in the input fraction when β1-, β2-, and β4-subunits were co-transfected was observed. This decrease was in contrast with the increase or lack of modification of the $Na_v1.7$ current density. The reason for this decrease remains to be identified, but one can speculate that the expression of the β-subunits may decrease the ratio of intracellular Na_vs to plasma membrane Na_vs by hastening forward trafficking and stabilizing the channel at the cell surface. Furthermore, one of the important functions of glycosylation is the proper folding and protection of proteins with respect to proteolysis (Parodi, 2000). The thus far not observed role of β-subunits in altering $Na_v1.7$ glycosylation might influence the degradation by the proteasome, accounting for the decrease in input. The β-subunits have also been proposed to act as chaperon proteins (Valdivia et al., 2010), further supporting a potential effect on degradation by the proteasome.

The analysis of the $Na_v1.7$ protein at the plasma membrane and the subsequent treatment with the deglycosylating enzyme led to three novel findings: (1) Under normal conditions, $Na_v1.7$ is present in two glycosylated forms, a core-glycosylated form with a molecular weight of ∼250 kDa and a fully-glycosylated form with a molecular weight of ∼280 kDa; (2) The β1-subunit can further mediate a third and intermediate migrating band, which likely represents an alternative fully-glycosylated form of $Na_v1.7$; and (3) the β1-subunit increases the membrane expression of this alternative fully-glycosylated form of $Na_v1.7$; whereas the β3-subunit increases the membrane expression of the core-glycosylated form.

In studies using chimeras between the β1- and β3-subunits, it was proposed that different parts of these subunits were involved in the modulation of gating by direct interaction with the α-subunits (Zimmer and Benndorf, 2002). The observation in this study that the β1- and β3-subunits can mediate the differential glycosylation of $Na_v1.7$, and despite the well-documented causal link demonstrating that differential glycosylation leads to a modification of Na_vs α-subunit gating (Bennett et al., 1997; Zhang et al., 1999; Tyrrell et al., 2001), does not allow us to conclude that the β-subunit-mediated glycosylation of the α-subunit is responsible for the modulation of $Na_v1.7$ gating. Further studies to identify the potential glycosylation site of $Na_v1.7$ are necessary to determine whether the effects of the β-subunits on the biophysical properties of $Na_v1.7$ are also dependent on this mechanism. Nevertheless, the observation that the β1- and β3-subunits influence the gating properties of $Na_v1.7$ and alter its glycosylation pattern, while the β2- and β4-subunits do not, supports this hypothesis.

It was recently proposed that only the upper band of biotinylated $Na_v1.7$ may reflect the functional fully-glycosylated form of the channel, whereas the lower band represents an intermediate and/or immature glycosylated form of the channel which does not participate in Na^+ conductance (Laedermann et al., 2013). The upregulation of expression of the core-glycosylated form of $Na_v1.7$ when the β3-subunit is co-transfected, along with the associated 2-fold increase in the $Na_v1.7$ current density, suggests that there is no such dichotomy and that the link between the glycosylation and functionality of the channel is more complex. It is possible that these distinctly glycosylated forms of $Na_v1.7$ differentially participate in Na^+ conductance, but their relative contribution to the overall sodium current has yet to be determined. For instance, quantification of the shifted upper band when the β1-subunit was present revealed an increased signal intensity of ∼30%, which is less important than the 100% increase of I_{Na} measured using the patch clamp approach. This underlines that, in addition to an increased stabilization of the channel, modification of single channel conductance by the intermediate glycosylated form of $Na_v1.7$ may also partially contribute to the functional 2-fold increase in I_{Na}. This point, in addition to the fact that β-subunits have the ability to shift bands from one glycosylated state to another, demonstrates that quantification of biotinylated proteins needs to be interpreted with caution. It cannot be excluded that due to these shifts, some bands might contaminate the signal of another band.

General kinetic models of biosynthesis (Schmidt and Catterall, 1987) have proposed that the β2-subunit interacts with the α-subunit right before anchoring at the membrane. The present findings are consistent with such a model since both β2- and β4-subunits did not influence $Na_v1.7$ glycosylation, and most likely interacted after the Golgi network (**Figure 7**). The α-β1 complex was previously shown to associate in the ER, enhancing the trafficking to the plasma membrane (Zimmer et al., 2002). Another study demonstrated that β1- and β3-subunits increase the efficiency of channel trafficking from the ER to the plasma

membrane (Fahmi et al., 2001). The β3-subunit has also been shown to mask the ER-retention signal (Zhang et al., 2008). The results of the present work confirm earlier demonstrated interactions between the β- and α-subunits, and suggest an additional function of both: β1- and β3-subunits interact with the α-subunit in the ER/Golgi, where they regulate the differential glycosylation of Na_v α-subunits, which in turn modulates the stabilization of the channel at the cell membrane (**Figure 7**). The mechanisms underlying their interaction and mediation of α-subunit glycosylation, as well as the identification of other potential isoforms that would be subject to such regulation, remain to be investigated.

PHYSIOLOGICAL RELEVANCE

These results were obtained in cellular expression system. Whether such mechanisms also occur in native cells remain to be investigated. This study used the $Na_v1.7$ isoform, an important contributor to pain processing (Lampert et al., 2010). The electrophysiological results show that β1- and β3-subunits are able to increase $Na_v1.7$ excitability, as demonstrated by the increase in peak current, kinetics, voltage-availability and repriming rate. $Na_v1.7$ is expressed in high levels in all types of sensory neurons (Ho and O'leary, 2011). β-subunits are also expressed in sensory neurons, but to a variable extent depending on cell type (Takahashi et al., 2003; Ho et al., 2012). Furthermore, β1- and β3-subunit expression has been reported to be increased in pathological pain (Shah et al., 2000; Coward et al., 2001), where they have been implicated in the generation of hyperexcitability. It remains to be determined if Na_v function is mediated by an altered pattern of α-subunit glycosylation, which is an important regulatory process of excitability in dorsal root ganglia neurons (Tyrrell et al., 2001).

ACKNOWLEDGMENTS

We thank S. Tate and V. Morisset (Convergence Pharmaceuticals) for providing $Na_v1.7$ cDNA cloned into pCIN5h and β1-, β2-, and β4-subunits cDNA cloned into pCINh, as well as β3-subunit cloned into pFBM and the polyclonal antibodies anti-β1-, anti-β2-, and anti-β3-subunit. The monoclonal antibody N68/3 (anti-$Na_v1.7$) was developed by and/or obtained from the UC Davis/NIH NeuroMab Facility, supported by NIH grant U24NS050606 and maintained by the Department of Neurobiology, Physiology and Behavior, College of Biological Sciences, University of California, Davis, CA 95616. This study was supported by grants from the Swiss National Science Foundation (31003A–124996 to Isabelle Decosterd and 310030B-135693 to Hugues Abriel), the Synapsis Foundation (to Isabelle Decosterd and Hugues Abriel), the European Society of Anesthesiology (to Isabelle Decosterd and Hugues Abriel) and the Lemanic Neuroscience Doctoral School Ph.D. Fellowship (to Cédric J. Laedermann). We thank Dr. A. Felley for her comments on the manuscript. We would like to thank Prof. C. Kern, head of the Anesthesiology Department at CHUV for his support.

SUPPLEMENTARY MATERIAL

The Supplementary Material for this article can be found online at: http://www.frontiersin.org/Cellular_Neuroscience/10.3389/fncel.2013.00137/abstract

REFERENCES

Bennett, E., Urcan, M. S., Tinkle, S. S., Koszowski, A. G., and Levinson, S. R. (1997). Contribution of sialic acid to the voltage dependence of sodium channel gating. a possible electrostatic mechanism. *J. Gen. Physiol.* 109, 327–343. doi: 10.1085/jgp.109.3.327

Brackenbury, W. J., and Isom, L. L. (2011). Na channel beta subunits: overachievers of the ion channel family. *Front. Pharmacol.* 2:53. doi: 10.3389/fphar.2011.00053

Catterall, W. A. (2000). From ionic currents to molecular mechanisms: the structure and function of voltage-gated sodium channels. *Neuron* 26, 13–25. doi: 10.1016/S0896-6273(00)81133-2

Coward, K., Jowett, A., Plumpton, C., Powell, A., Birch, R., Tate, S., et al. (2001). Sodium channel beta 1 and beta 2 subunits parallel SNS/PN3 alpha-subunit changes in injured human sensory neurons. *Neuroreport* 12, 483–488. doi: 10.1097/00001756-200103050-00012

Cronin, N. B., O'reilly, A., Duclohier, H., and Wallace, B. A. (2005). Effects of deglycosylation of sodium channels on their structure and function. *Biochemistry* 44, 441–449. doi: 10.1021/bi048741q

Ednie, A. R., and Bennett, E. S. (2012). Modulation of voltage-gated ion channels by sialylation. *Compr. Physiol.* 2, 1269–1301. doi: 10.1002/cphy.c110044

Fahmi, A. I., Patel, M., Stevens, E. B., Fowden, A. L., John, J. E., Lee, K., et al. (2001). The sodium channel -subunit SCN3b modulates the kinetics of SCN5a and is expressed heterogeneously in sheep heart. *J. Physiol.* 537, 693–700. doi: 10.1113/jphysiol.2001.012691

Guy, H. R., and Seetharamulu, P. (1986). Molecular model of the action potential sodium channel. *Proc. Natl. Acad. Sci. U.S.A.* 83, 508–512. doi: 10.1073/pnas.83.2.508

Hartshorne, R. P., Messner, D. J., Coppersmith, J. C., and Catterall, W. A. (1982). The saxitoxin receptor of the sodium channel from rat brain. evidence for two nonidentical beta subunits. *J. Biol. Chem.* 257, 13888–13891.

Ho, C., and O'leary, M. E. (2011). Single-cell analysis of sodium channel expression in dorsal root ganglion neurons. *Mol. Cell Neurosci.* 46, 159–166. doi: 10.1016/j.mcn.2010.08.017

Ho, C., Zhao, J., Malinowski, S., Chahine, M., and O'leary, M. E. (2012). Differential expression of sodium channel beta subunits in dorsal root ganglion sensory neurons. *J. Biol. Chem.* 287, 15044–15053. doi: 10.1074/jbc.M111.333740

Isom, L., De Jongh, K., Patton, D., Reber, B., Offord, J., Charbonneau, H., et al. (1992). Primary structure and functional expression of the beta 1 subunit of the rat brain sodium channel. *Science* 256, 839–842. doi: 10.1126/science.1375395

Isom, L. L. (2001). Sodium channel beta subunits: anything but auxiliary. *Neuroscientist* 7, 42–54. doi: 10.1177/107385840100700108

Isom, L. L., Ragsdale, D. S., De Jongh, K. S., Westenbroek, R. E., Reber, B. F. X., Scheuer, T., et al. (1995a). Structure and function of the β2 subunit of brain sodium channels, a transmembrane glycoprotein with a CAM motif. *Cell* 83, 433–442. doi: 10.1016/0092-8674(95)90121-3

Isom, L. L., Scheuer, T., Brownstein, A. B., Ragsdale, D. S., Murphy, B. J., and Catterall, W. A. (1995b). Functional co-expression of the beta 1 and type IIA alpha subunits of sodium channels in a mammalian cell line. *J. Biol. Chem.* 270, 3306–3312. doi: 10.1074/jbc.270.7.3306

Kazen-Gillespie, K. A., Ragsdale, D. S., D'andrea, M. R., Mattei, L. N., Rogers, K. E., and Isom, L. L. (2000). Cloning, localization, and functional expression of sodium channel beta1A subunits. *J. Biol. Chem.* 275, 1079–1088. doi: 10.1074/jbc.275.2.1079

Laedermann, C. J., Cachemaille, M., Kirschmann, G., Pertin, M., Gosselin, R. D., Chang, I., et al. (2013). Dysregulation of voltage-gated sodium channels by ubiquitin-ligase NEDD4-2 in neuropathic pain. *J. Clin. Invest.* 123, 3002–3013. doi: 10.1172/JCI68996

Lampert, A., O'reilly, A. O., Reeh, P., and Leffler, A. (2010). Sodium

channelopathies and pain. *Pflugers Arch.* 460, 249–263. doi: 10.1007/s00424-009-0779-3

Meadows, L. S., and Isom, L. L. (2005). Sodium channels as macromolecular complexes: implications for inherited arrhythmia syndromes. *Cardiovasc. Res.* 67, 448–458. doi: 10.1016/j.cardiores.2005.04.003

Messner, D. J., and Catterall, W. A. (1985). The sodium channel from rat brain. separation and characterization of subunits. *J. Biol. Chem.* 260, 10597–10604.

Moremen, K. W., Tiemeyer, M., and Nairn, A. V. (2012). Vertebrate protein glycosylation: diversity, synthesis and function. *Nat. Rev. Mol. Cell Biol.* 13, 448–462. doi: 10.1038/nrm3383

Morgan, K., Stevens, E. B., Shah, B., Cox, P. J., Dixon, A. K., Lee, K., et al. (2000). Beta 3: an additional auxiliary subunit of the voltage-sensitive sodium channel that modulates channel gating with distinct kinetics. *Proc. Natl. Acad. Sci. U.S.A.* 97, 2308–2313. doi: 10.1073/pnas.030362197

Noda, M., Shimizu, S., Tanabe, T., Takai, T., Kayano, T., Ikeda, T., et al. (1984). Primary structure of Electrophorus electricus sodium channel deduced from cDNA sequence. *Nature* 312, 121–127. doi: 10.1038/312121a0

Nuss, H. B., Chiamvimonvat, N., Perez-Garcia, M. T., Tomaselli, G. F., and Marban, E. (1995). Functional association of the beta 1 subunit with human cardiac (hH1) and rat skeletal muscle (mu 1) sodium channel alpha subunits expressed in Xenopus oocytes. *J. Gen. Physiol.* 106, 1171–1191. doi: 10.1085/jgp.106.6.1171

Okuse, K., Malik-Hall, M., Baker, M. D., Poon, W. Y., Kong, H., Chao, M. V., et al. (2002). Annexin II light chain regulates sensory neuron-specific sodium channel expression. *Nature* 417, 653–656. doi: 10.1038/nature00781

Parodi, A. J. (2000). Protein glucosylation and its role in protein folding. *Annu. Rev. Biochem.* 69, 69–93. doi: 10.1146/annurev.biochem.69.1.69

Payandeh, J., Scheuer, T., Zheng, N., and Catterall, W. A. (2011). The crystal structure of a voltage-gated sodium channel. *Nature* 475, 353–358. doi: 10.1038/nature10238

Recio-Pinto, E., Thornhill, W. B., Duch, D. S., Levinson, S. R., and Urban, B. W. (1990). Neuraminidase treatment modifies the function of electroplax sodium channels in planar lipid bilayers. *Neuron* 5, 675–684. doi: 10.1016/0896-6273(90)90221-Z

Ritchie, J. M., Black, J. A., Waxman, S. G., and Angelides, K. J. (1990). Sodium channels in the cytoplasm of Schwann cells. *Proc. Natl. Acad. Sci. U.S.A.* 87, 9290–9294. doi: 10.1073/pnas.87.23.9290

Sangameswaran, L., Fish, L. M., Koch, B. D., Rabert, D. K., Delgado, S. G., Ilnicka, M., et al. (1997). A novel tetrodotoxin-sensitive, voltage-gated sodium channel expressed in rat and human dorsal root ganglia. *J. Biol. Chem.* 272, 14805–14809. doi: 10.1074/jbc.272.23.14805

Schmidt, J., Rossie, S., and Catterall, W. A. (1985). A large intracellular pool of inactive Na channel alpha subunits in developing rat brain. *Proc. Natl. Acad. Sci. U.S.A.* 82, 4847–4851. doi: 10.1073/pnas.82.14.4847

Schmidt, J. W., and Catterall, W. A. (1987). Palmitylation, sulfation, and glycosylation of the alpha subunit of the sodium channel. Role of post-translational modifications in channel assembly. *J. Biol. Chem.* 262, 13713–13723.

Shah, B. S., Stevens, E. B., Gonzalez, M. I., Bramwell, S., Pinnock, R. D., Lee, K., et al. (2000). beta3, a novel auxiliary subunit for the voltage-gated sodium channel, is expressed preferentially in sensory neurons and is upregulated in the chronic constriction injury model of neuropathic pain. *Eur. J. Neurosci.* 12, 3985–3990. doi: 10.1046/j.1460-9568.2000.00294.x

Smith, R. D., and Goldin, A. L. (1998). Functional analysis of the rat I sodium channel in xenopus oocytes. *J. Neurosci.* 18, 811–820.

Takahashi, N., Kikuchi, S., Dai, Y., Kobayashi, K., Fukuoka, T., and Noguchi, K. (2003). Expression of auxiliary beta subunits of sodium channels in primary afferent neurons and the effect of nerve injury. *Neuroscience* 121, 441–450. doi: 10.1016/S0306-4522(03)00432-9

Tyrrell, L., Renganathan, M., Dib-Hajj, S. D., and Waxman, S. G. (2001). Glycosylation alters steady-state inactivation of sodium channel Nav1.9/NaN in dorsal root ganglion neurons and is developmentally regulated. *J. Neurosci.* 21, 9629–9637.

Valdivia, C. R., Medeiros-Domingo, A., Ye, B., Shen, W. K., Algiers, T. J., Ackerman, M. J., et al. (2010). Loss-of-function mutation of the SCN3B-encoded sodium channel citation{beta}3 subunit associated with a case of idiopathic ventricular fibrillation. *Cardiovasc. Res.* 86, 392–400. doi: 10.1093/cvr/cvp417

Vijayaragavan, K., O'leary, M. E., and Chahine, M. (2001). Gating properties of Nav1.7 and Nav1.8 peripheral nerve sodium channels. *J. Neurosci.* 21, 7909–7918.

Vijayaragavan, K., Powell, A. J., Kinghorn, I. J., and Chahine, M. (2004). Role of auxiliary beta1-, beta2-, and beta3-subunits and their interaction with Na(v)1.8 voltage-gated sodium channel. *Biochem. Biophys. Res. Commun.* 319, 531–540. doi: 10.1016/j.bbrc.2004.05.026

Waechter, C. J., Schmidt, J. W., and Catterall, W. A. (1983). Glycosylation is required for maintenance of functional sodium channels in neuroblastoma cells. *J. Biol. Chem.* 258, 5117–5123.

Yu, F. H., Westenbroek, R. E., Silos-Santiago, I., McCormick, K. A., Lawson, D., Ge, P., et al. (2003). Sodium channel β4, a new disulfide-linked auxiliary subunit with similarity to β2. *J. Neurosci.* 23, 7577–7585.

Zhang, Y., Hartmann, H. A., and Satin, J. (1999). Glycosylation influences voltage-dependent gating of cardiac and skeletal muscle sodium channels. *J. Membr. Biol.* 171, 195–207. doi: 10.1007/s002329900571

Zhang, Z. N., Li, Q., Liu, C., Wang, H. B., Wang, Q., and Bao, L. (2008). The voltage-gated Na+ channel Nav1.8 contains an ER-retention/retrieval signal antagonized by the beta3 subunit. *J. Cell Sci.* 121, 3243–3252. doi: 10.1242/jcs.026856

Zimmer, T., and Benndorf, K. (2002). The human heart and rat brain IIA Na+ channels interact with different molecular regions of the beta1 subunit. *J. Gen. Physiol.* 120, 887–895. doi: 10.1085/jgp.20028703

Zimmer, T., Biskup, C., Bollensdorff, C., and Benndorf, K. (2002). The beta1 subunit but not the beta2 subunit colocalizes with the human heart Na+ channel (hH1) already within the endoplasmic reticulum. *J. Membr. Biol.* 186, 13–21. doi: 10.1007/s00232-001-0131-0

Conflict of Interest Statement: The authors declare that the research was conducted in the absence of any commercial or financial relationships that could be construed as a potential conflict of interest.

Received: 24 May 2013; paper pending published: 22 June 2013; accepted: 07 August 2013; published online: 30 August 2013.

Citation: Laedermann CJ, Syam N, Pertin M, Decosterd I and Abriel H (2013) β1- and β3- voltage-gated sodium channel subunits modulate cell surface expression and glycosylation of $Na_v1.7$ in HEK293 cells. Front. Cell. Neurosci. 7:137. doi: 10.3389/fncel.2013.00137

This article was submitted to the journal Frontiers in Cellular Neuroscience.

3. Discussion

In the two next chapters, I will discuss the results obtained in the two research papers separately and what they added in terms of mechanisms in the current literature about Na_vs regulation and neuropathic pain. I will discuss the questions that these studies raised and the future perspectives they opened. Finally, I will discuss the limitations of the work.

3.1. Nedd4-2 project

The role of Na_vs has been extensively studied in different animal models of neuropathic pain and led to contradictory results. However, and because the use of sodium channel blockers in the clinics and animal models alleviate pain symptoms, it is likely that Na_vs are implicated in the generation of neuropathic pain-associated hyperexcitability. Besides the multiple mutations that were shown to increase $Na_v1.7$ function and that were linked to exaggerated pain sensitivity (Dib-Hajj, Rush et al. 2005; Waxman and Dib-Hajj 2005; Fertleman, Baker et al. 2006; Novella, Hisama et al. 2007; Cheng, Dib-Hajj et al. 2008), and $Na_v1.7$/$Na_v1.8$ mutations associated with painful peripheral neuropathy (Faber, Hoeijmakers et al. 2012; Faber, Lauria et al. 2012), these channels were demonstrated to be important in acquired types of pain syndromes by accumulating in different location of the primary afferent (Gold, Weinreich et al. 2003; Hong, Morrow et al. 2004; Luo, Perry et al. 2008; Thakor, Lin et al. 2009; Persson, Gasser et al. 2011). The mechanisms that regulate Na_vs trafficking are multiple (Shao, Okuse et al. 2009). However, only few studies investigated whether such mechanisms could be responsible for Na_vs dysregulation in neuropathic pain. The protein kinase pathways were demonstrated to be implicated in Na_vs trafficking and consequentially to have a role in cellular hyperexcitability associated with neuropathic pain (Villarreal, Sachs et al. 2009; Kakimura, Zheng et al. 2010) indicating the potential involvement of post-translational regulations. Here, we reported for the first time the importance of the ubiquitylation pathway in the primary afferent for pain processing. We highlighted the E3 ubiquitin ligase Nedd4-2 as a potent regulator of $Na_v1.7$ and $Na_v1.8$, which downregulation contributes to neuropathic pain-associated hyperexcitability. By using a tissue specific knockout of Nedd4-2, and by rescuying its expression after SNI, we were able to demonstrate both the necessity and the sufficiency of a well-balanced expression of this ubiquitin ligase for maintaining an appropriate cellular excitability in sensory neurons. However these observations also raised several questions:

How is Nedd4-2 downregulated?

In the present study, we observed a downregulation of Nedd4-2 expression in terms of both mRNA and protein. The fact that the decrease of protein level was more important than that of mRNA level, leaves open a downregulation occuring at both stages.

The up- or downregulation of hundreds of gene transcripts in DRGs after peripheral injury is a well-known process (Costigan, Befort et al. 2002), and is largely connected to neuronal survival and regeneration of injured axons. It is also due to the loss of trophic factors from peripheral target organs and novel signalling molecules secreted around the injury such as inflammatory cytokines. Thus, these transcriptional changes lead to both adaptative and maladaptive responses that might ultimately be responsible for generating cellular hyperexcitability.

Ubiquitin ligases of the Nedd4 family have been shown to be important for axonal guidance, axonal branching and development of synaptic structure and function (Myat, Henry et al. 2002; Sieburth, Ch'ng et al. 2005; Drinjakovic, Jung et al. 2010). Interestingly, Nedd4-2 can be secreted in extracellular microvesicles when interacting with Nedd4 Family-interacting protein 1 (Ndfip1) (Putz, Howitt et al. 2008). Both proteins have been implicated in neuronal survival (Sang, Kim et al. 2006; Lackovic, Howitt et al. 2012). In the context of peripheral nerve injury, it is thus possible that Nedd4-2 would similarly be secreted from injured primary afferents promoting cell survival or axonal regeneration after injury. Altogether, this raises the possibility that the adaptive response of Nedd4-2 exosomal secretion could at the same time lead to the maladaptive decrease of its expression, and as a consequence increases Na_v expression.

The regulation of Nedd4-2 at a post-translational level was already largely studied in the kidney where phosphorylation of Nedd4-2 was shown to be of central importance. The mineralocorticoid hormone aldosterone induces the transcription of serum and glucocorticoid-induced kinase (SGK1) (Snyder, 2009), which further binds (via the WW motif), phosphorylates and prevents Nedd4-2 activity, leading to an increase of ENaC activity. Conversely, vasopressin activates adenylate cyclase to increase cAMP, which in turn activates another kinase, PKA (Debonneville et al., 2001). Strikingly these two kinases phophorylate the same consensus sequence RxRxx(S/T) at three different sites (Ser 221, Thr 246 and Ser 327) and modulate Nedd4-2 ability to bind to ENaC making this motif a convergent point for different regulating pathway. Preliminary results from our laboratory (*unpublished data from T. Berta*) indicate that SGK1 mRNA is upregulated in DRG after SNI, which might diminish Nedd4-2 activity. The fate of Nedd4-2 after being phosphorylated is unknown. Because we observed a downregulation of Nedd4-2 protein, answering whether phosphorylation could lead to degradation of the protein remains to be investigated.

It is well described that in inflammatory processes, cytokines are implicated in a complex pathway leading to NF-κB activation. By phosphorylation, they first activate IκB [inhibitor of nuclear factor κB (NF-κB)] kinase (IKK), which in turn phosphorylates and inactivates IκB inhibitory proteins.

The transcription factor NF-κB is no longer inhibited and can trigger its anti-apoptotic function (Delhase et al., 1999). More recently, a subunit of IKK, IKKβ was also reported to phosphorylate Ser327 of Nedd4-2 (Edinger et al., 2009) resulting in an enhanced ENaC function in the kidney. IKK is also enriched in unmyelinated nerves and its activation by pro-inflammatory molecules could possibly act as a negative regulator of Nedd4-2 in these neurons following inflammation. Strikingly, we also observed an important downregulation of Nedd4-2 in early time points after surgery in sham animals (6 hours, see Appendix 1) that, unlike SNI animals, goes back to normal within a couple of days. This raises the possibility that Nedd4-2 downregulation is triggered by inflammation inherent to surgery procedure and which remains persistent only if the nerve is severed.

Finally, nerve growth factor (NGF), is a key player in nociceptor sensitization (Leung and Cahill 2010; Dogrul, Gul et al. 2011; Gaudet, Popovich et al. 2011) by its ability to modulate Na_vs, even though the precise mechanisms are unknown (Waxman et al., 1999). Interestingly, NGF binding to TrkA recpetor leads to Nedd4-2 phosphorylation, which may modulate Na_v membrane expression (Arévalo, Waite et al. 2006).

Are there other mechanisms that regulate Nedd4-2?

Nedd4-2 target proteins can also be regulated by deubiquitylating (DUB) enzymes (Amerik and Hochstrasser 2004) allowing the removal of ubiquitin from targeted proteins. For instance a study (Fakitsas et al., 2007) showed that the deubiquitylating enzyme Usp2-45 can increase ENaC function by deubiquitylation of the channel. However, whether similar mechanisms could occur for Na_vs regulation remains to be investigated.

What is the relevance of the PY motif in Nedd4-2 regulatory effect? Are there other motifs?

The hydrophobic core surrounded by β-sheets of WW domains interacts with the canonical minimal sequence (L/P)PxY (Kasanov, Pirozzi et al. 2001) via a polyproline type II helix. We demonstrated the importance of the PY motif in Nedd4-2-downregulatory function by mutating Proline or Tyrosine of this motif. This led to the abolishment of Nedd4-2 downregulatory effect on $Na_v1.7$-mediated current in a cellular expression system, highlighting the importance of the PY-motif. Demonstrating that $Na_v1.9$ (and also $Na_v1.4$, even though it is not expressed in sensory neurons), devoid of PY motif, is not subject to Nedd4-2 downregulation would further confirm this PY-motif dependent pathway.

The hydrophobic residue Tyrosine of the PY motif (Tyrosine +3) is involved in the binding to the WW-domain pocket, providing additional binding energy, and is thus considered as an “extended PY-motif” (Kanelis, Rotin et al. 2001; Henry, Kanelis et al. 2003) as demonstrated with ENaC. Interestingly, the consensus sequence P/LPxYxxV is observed in every containing-PY-motif Na_vs.

Strikingly, mutation of the Valine of this “extended PY-motif” (in Tyrosine +3) did not alter, or only minimally, the affinitiy between $Na_v1.7$ and Nedd4-2. $Na_v1.7$ mutation of Valine also led to a less pronounced downregulatory effect of Nedd4-2 as highlighted in whole-cell patch clamp experiments. Another study obtained similar results for $Na_v1.5$ and $Na_v1.8$ (Fotia, Ekberg et al. 2004; van Bemmelen, Rougier et al. 2004). This suggests that unlike ENaC, the extended PY motif is not required, or only minimally, for Nedd4-2 to downregulate Na_vs.

The use of an inactive Nedd4-2 mutant (Nedd4-2CS) in HEK293 cells led to an increase $Na_v1.7$-mediated current as compared to control condition. Because Nedd4-2 is highly expressed in HEK293 cell (*unpublished data*, see Appendix 2) we hypothesized that Nedd4-2CS upregulation of $Na_v1.7$ was due to competition with endogenous Nedd4-2. We confirmed this hypothesis by silencing Nedd4-2, which led to similary increase of $Na_v1.7$ current as with Nedd4-2CS. However, because Nedd4-1 can also downregulate $Na_v1.7$ (*data not shown*), the silencing of this ubiquitin ligase is the next experimental control that needs to be performed. The PY motif importance for this competitive regulation to occur was demonstrated by showing that 72 hours after transfection, PY motifs mutants were not subject to endogenous downregulation whereas wild-type $Na_v1.7$ was downregulated.

As mentioned above, PY mutations in ENaC led to hypertensive diseases. The importance of this motif in both cardiac and neuronal Na_vs isoforms (Fotia, Ekberg et al. 2004; Rougier, van Bemmelen et al. 2005) suggests that mutations in its sequence could have important pathophysiological issues. In line with this, the mutation Y1977N, inside the PY-motif of $Na_v1.5$, has been proposed to cause congenital long QT syndrome (Kapa, Tester et al. 2009; Rougier, Albesa et al. 2012).

The regulation of Na_vs by Nedd4-2 might even extend beyond PY motif, involving other binding motifs under the dependence of other intracellular pathways. WW domains also have the ability to bind to alternative motifs (Sudol and Hunter 2000), such as phosphorylated Px(pS/T)P motifs. Accordingly, Gasser et al. (Gasser et al., 2010) showed that $Na_v1.6$ is regulated by Nedd4-2 not only by the interaction with the PY motif, but also by a Pro-Gly-Ser-Pro motif in an intracellular loop (L1) of the channel. This motif is phosphorylated by p-p38 (activated stress-induced p38 MAPK) converting it into a Px(pS)P, thus making it a recognizable for Nedd4-2. The authors reported that both sites are necessary for Nedd4-2 to downregulate $Na_v1.6$.

Was Nedd4-2 already identified as responsible for diseases involving cellular excitability?

Because of the accumulating evidence of Nedd4-2 being able to regulate multiple target proteins and particularly ion channels (Persaud, Alberts et al. 2009), an interest for Nedd4-2 mutations or polymorphism has arisen. Thus far no mutations were identified, but several polymorphisms were

linked to hypertensive diseases (Dunn, Ishigami et al. 2002; Fouladkou, Alikhani-Koopaei et al. 2004; Araki, Umemura et al. 2008; Luo, Wang et al. 2009). Interestingly, one of these naturally occurring Nedd4-2 variant was reported to have impaired downregulatory activity on ENaC *in vitro* (Fouladkou, Alikhani-Koopaei et al. 2004).

With respect to Na_v regulation, another study suggested a role for Nedd4-2 in photosensitive generalized epilepsy (IGE). In a study involving the screening of more than 250 families (Dibbens, Ekberg et al. 2007), the authors identified three rare Nedd4-2 gene variants; one missense mutation, one intronic mutation and one substitution mutation, all being located in the WW motif of Nedd4-2. However, the authors reported no loss of efficiency in Nedd4-2 downregulatory of $Na_v1.2$ in *Xenopus* oocytes. It would be of interest to investigate whether these mutants have intact downregulatory effects on other Na_vs, as for instance $Na_v1.1$ was reported to important in epilepsy (Catterall, Kalume et al. 2010).

In the present study, rather than mutations of Nedd4-2, we reported a decrease of expression. There is some evidence suggesting that such an altered level of expression of Nedd4-2 could generate other pathological state, driven by erratic Na_v expression. For instance, the human strongly metastatic breast cancer MDA-MB-231 cells show an increase Nedd4-2 mRNA compared to weakly/non-metastatic MCF-7 cells (Kuratomi et al., 2005) and it is also known that metastatic potential in cells lines is correlated with altered Na_v expression such as $Na_v1.5$ (Fraser et al., 2005). However, no relation between these observations has been proposed so far.

What are potential other targets of Nedd4-2?

Nedd4-2 regulates many other voltage-gated ion channels such as potassium (K_vs/KCNQs) and choride (ClCs) which also modulate electrical excitability in neurons (Bongiorno et al., 2011). Moreover Nedd4-2 regulation is not restricted to voltage-gated ion channels, but also interacts with amino acid, dopamine and glutamate transporters, adaptor proteins and kinases (Yang and Kumar, 2009). Here again, identifying whether Nedd4-2 mutants could be associated with pathologies showing dysregluation of the above-mentioned proteins would be of interest.

I will now discuss the limitations of the study.

What is the relevance of the two populations?

In this study, we segregated neuronal subpopulation based on the ratio of $Na_v1.8/Na_v$total current as it was already performed in several studies (Abdulla and Smith 2002; Lopez-Santiago, Pertin et al. 2006). *Slow* neurons had a ratio >0.5 whereas *fast* neurons ratio was <0.5. However, the authors did not propose any physiological functions for these two subpopulations. Based on our observations on Nedd4-2 knockout mice, we could only speculate that *slow* neurons are underlying thermal modality.

We initially made the assumption that *slow* and *fast* neurons could represent non-peptidergic and peptidergic neurons, which was based on the relative amount of $Na_v1.8$ current recorded in small DRG neurons. Several studies reported an important co-localisation of IB4 positive neurons and $Na_v1.8$ (Benn, Costigan et al. 2001; Fukuoka, Kobayashi et al. 2008) in DRG and that slower kinetics in these cells was due to TTX resistant currents (Stucky and Lewin 1999; Wu and Pan 2004). However, a recent study suggested that $Na_v1.9$, and not $Na_v1.8$, is the most relevant co-marker of non-peptidergic neurons (Fang, Djouhri et al. 2006). Furthermore, we characterized the cells based on the ratio of $Na_v1.8$ current density to the Na_vtotal current, but the absolute amount of $Na_v1.8$ current is only slightly smaller in *fast* compared to *slow* neurons (refer to the $Na_v1.8$ density between *slow* and *fast* neurons of control conditions in Supplemental Table 2, 3, 4). Furthermore, non-peptidergic neurons are most likely involved in mechanical rather than thermal sensitivity (Abrahamsen, Zhao et al. 2008; Scherrer, Imamachi et al. 2009), which is in apparent contradiction with our observations.

Altogether, these observations leave open the classification of *slow* and *fast* neurons into specific DRG neuronal populations with specific functions and highlight the necessity for further investigations.

The distinction between intact and severed neurons: underestimation of the effect?

In this study we used the SNI model of neuropathic pain, where severed and intact nerves are found to be intermingled in the same DRG, hence allowing cross-excitation between cell bodies (Devor and Wall 1990; Amir and Devor 1996) as well as ephaptic cross-excitation along the fibers (Lisney and Pover 1983). In a previous study from our group, we used fluorogold retrolabelling to identify injured from intact neurons in the rat (Berta, Poirot et al. 2008). This distinction highlighted different results in terms of mRNA, peak current and biophysical properties depending on the injured/non-injured identity, with the most important changes occurring in the injured neurons. Because we did not perform this distinction in the present study, it is possible that some of the observed effects are underestimated. In line with the previous assumption, the stronger downregulation of Nedd4-2 in the injured L4 DRG using the SNL model suggests that reduction of Nedd4-2 influencing on Na_vs mainly takes place in injured neurons. Thus, the next step would be to study Na_vs expression in L4 SNL to confirm this hypothesis. Noteworthy, in a previous study performed in our research group using immunofluorescence in the rat, we observed a similar decrease of Nedd4-2 in injured and non-injured neurons (Cachemaille, Laedermann et al. 2012). The previous highlights the need for further investigations to study the effect of axotomy on Nedd4-2 regulation.

The controversy of $Na_v1.7$ and $Na_v1.8$ implication in neuropathic pain.

We already discussed in the introduction the controversial role of $Na_v1.7$ and $Na_v1.8$ in neuropathic pain. In humans, recent identifications of mutations in $Na_v1.7$ and $Na_v1.8$ in nerve fiber neuropathy clearly point out these two sodium channels isoform as important candidates implicated in neuropathic pain. However, animal studies gave inconsistent observations. Knocking out $Na_v1.7$, $Na_v1.8$, or both, using Cre recombinase and loxP sites (Agarwal, Offermanns et al. 2004), does not alter development of neuropathic pain symptoms (Akopian, Souslova et al. 1999; Kerr, Souslova et al. 2001; Nassar, Stirling et al. 2004; Nassar, Levato et al. 2005). One of the possible explanations is that upon gene deletion, some other genes might be modulated and compensate the deleted gene (Barbaric, Miller et al. 2007). The attenuation of neuropathic pain symptoms when these isoforms are silenced rather than knocked out (Lai, Gold et al. 2002; Yeomans, Levinson et al. 2005; Dong, Goregoaker et al. 2007), which is maybe less robust in terms of expression but more precise in a temporal manner, supports this possibility. It is also possible that $Na_v1.7$ and $Na_v1.8$ are differentially implicated in neuropathic pain depending on the species; knocking out genes is generally used in mice whereas knocking down genes is rather used in rats, at least in the pain research field.

Sensory neuron specific Nedd4-2 knockout mouse lines.

We have just discussed the limitation of the use of knockout mouse lines, which could account for the lack of effect of $Na_v1.7$ and $Na_v1.8$ deletion on neuropathic pain development. We used similar knockout mouse lines that may lack both spatial and temporal resolution. “Temporal” because the Cre recombinase expression starts early in development, which might allow for compensatory mechanisms to take place. “Spatial” because $Na_v1.8$ (the promoter for Cre recombinase), which was initially thought to be exclusively expressed in small nociceptive neurons (Shields, Ahn et al. 2012), was recently reported to be expressed more broadly in DRG cells. One way to overcome this problem would be the use of inducible knockout mouse lines, such as tamoxifen induced recombination mice (Friedel, Wurst et al. 2011). To our knowledge, these mice have never been used to study Na_vs implication (directly, or via regulatory proteins) in neuropathic pain. An alternative approach would be the use of viral vector expressing Cre recombination. Thus, the viral vector delivery might be performed at any time point and as precisely as the injection allows.

Limitations of the SNI model.

It has to be acknowledged that the spared nerve injury (SNI) model used in the present study might not perfectly reflect the pathophysiological mechanisms of all type of neuropathic pain encountered in clinical practice. However and as already mentioned previously, among neuropathic pain conditions, mononeuropathy has the highest incidence rate (Dieleman, Kerklaan et al. 2008), highlighting the importance of single nerve injury. The development of animal models for nerve

injury–induced neuropathic pain has significantly contributed to the discovery of mechanisms that contribute to neuropathic pain syndromes.

In the present study, we used the SNI model because (*1*) it produces robust thermal and mechanical hypersensitivity that lasts for an extended period of time (more than 6 months), and (*2*) we have long-standing experience with it. Under our experimental conditions, 100% of the mice that undergo SNI surgery develop mechanical allodynia, which corresponds well to the high percentage (50-70%) of patients developing neuropathic pain after traumatic nerve injury (Flores 2006; Ciaramitaro, Mondelli et al. 2010). Furthermore, the involvement and regulation of Na_vs in these models have been extensively studied. However, studying Nedd4-2 impact on Na_vs regulation in other neuropathic pain models such as the streptozotocin or other chemically-induced neuropathic pain models will give further insight on the role of Nedd4-2 in this pathology.

Limitation of DRG culture and whole cell patch clamp.

Recording sodium currents from neuronal primary culture is another limitation of this study. Neurons are undergoing an important traumatic stress after dissociation. It is possible that changes induced by treatment (SNI, knockout of Nedd4-2 or viral rescuing of Nedd4-2) will be biased in the effect mediated by the dissociation procedure itself. In native tissue, neurons are surrounded by connective tissue, make synapses with other neurons, communicate with satellite cells, interact with extracellular matrix proteins and so on. Freshly dissociated neuronal culture, by loosing connectivity with these other actors, will most likely undergo important molecular changes. Furthermore, proteolytic enzymes, such as collagenase and protease, are required to obtain cell preparations and might also impact on membrane protein expression. In the present study, if Nedd4-2 reduction in SNI is due to the injury itself as we postulated, then the axotomy resulting from dissociation can *per se* trigger Nedd4-2 downregulation. However, immunofluorescence on dissociated DRG neurons 36 hours post-dissociation reveals that Nedd4-2 expression is still lower in knockout animals than in control littermates, somehow discarding this possibility. Presumably, this should also be the case after SNI. Another important issue is that we are recording only electrical activity in the cell body of the primary afferent, leaving aside the rest of the nerve, where most of the current is processed. Alternative electrophysiological recordings should be carried on, such as skin nerve preparations, in order to study the conduction of AP along the axons in the context of Nedd4-2 regulation.

In this study, we made the assumption that Na_vs current density reflects the excitability of the cell. However recent evidence shows that increasing sodium conductance does not necessarily lead to increased excitability (Kispersky, Caplan et al. 2012) and performing current clamp to record action potentials properties should be carried in the future.

3.2. β-subunits project

Glycosylation and β-subunit-dependent regulation of Na_v α-subunits are two well-described processes that significantly contribute to modulation of Na_v gating. In this study, I described a new role for two out of the four β-subunits, namely β1 and β3-subunits, as modulators of $Na_v1.7$ glycosylation while β2 and β4-subunits do not. It is likely that such mechanisms are also occurring for other Na_v isoform, but remains to be demonstrated. We also confirmed that β-subunits modulates $Na_v1.7$ membrane expression and gating. Thus, we highlighted that two known regulatory mechanisms, glycosylation and β-subunits regulation, are converging into one single pathway.

Is the β-subunits-mediated glycosylation of α-subunit responsible for the modulation of gating?

The modification of Na_v gating by α-subunit sialylation was already demonstrated (Bennett, Urcan et al. 1997; Zhang, Hartmann et al. 1999). The effect of β-subunits on Na_vs α-subunit gating is thought to be mediated by direct interference of the subunit with gating sensors (Zimmer and Benndorf 2002). In the present study, we proposed that, in addition to modulating gating of α-subunit via direct physical interference, the β-subunit-mediated glycosylation of the α-subunit might be responsible for the modification of the biophysical properties. To answer this question, a starting point would involve the use of a cell line deficient for glycosylating enzyme or the inhibition of glycosylation using treatment such as tuncamycin. Determining whether β-subunit modification of gating is abolished when all the cellular process of glycosylation are hindered would allow confirming or infirming the causal link between β-subunits-mediated glycosylation of the α-subunit and modification of the biophysical properties by these subunits. Obviously, this approach might lack specificity for a given mechanisms because all the glycosylation processes, crucial for the proper cell function, would be impaired in the cell. Thus, the next step would be the identification of the amino acid(s) on the α-subunit that is (are) alternatively glycosylated upon β1 and β3-subunit co-expression. Mutating this site would definitively allow to demonstrate the potential causality between β-subunits-mediated glycosylation and modification of the biophysical properties.

Glycosylation of β-subunits?

Interestingly, β-subunits are themselves substrates for glycosylation (Isom, De Jongh et al. 1992). β-subunits and glycosylation were already proposed to collaborate for modulating α-subunit function. In a study, authors proposed a *trans* effect of β-subunit glycosylation on α-subunit gating (Johnson, Montpetit et al. 2004; Johnson and Bennett 2006); in short, the glycosylation of β-subunit

itself impacts on α-subunit gating. To show this, the authors used a cell line deficient in glycosylating enzyme and demonstrated that β-subunit effect on gating was no longer effective. However, it is possible that β-subunit ineffectiveness was due to altered α-subunit glycosylation rather than β-subunit defective glycosylation.

How do β1 and β3 mediate differential glycosylation?

In our model, we proposed that β-subunits interact, directly or indirectly, with the α-subunit early after synthesis and before exiting the Golgi network. Thus, demonstrating that an interaction or a co-localisation is already occurring in the ER/Golgi would be the next step for further investigation of the β-subunits effects on glycosylation. The experimental approaches could include the use of powerful microscopy (confocal, correlative light and electron microscopy) and use of ER/Golgi markers. Split-luciferase complementation assays (Shavkunov, Panova et al. 2012) would allow studying temporal interaction between β-subunits and α-subunits whereas pull-down experiments could be used to study physical interaction between the two proteins.

To our knowledge there are no known mechanisms explaining how β-subunits could modify the glycosylation of α-subunit. Thus, investigating whether β-subunits modulate glycosylation by direct interaction with the α-subunit, or by interfering with glycosylating/deglycosylating enzymes or by other mechanisms remains to be done.

Modulation of I_{Na} current; conflicting results.

Our first observation that β1 strongly increased $Na_v1.7$ I_{Na} density contrasted with another study performed by Ho et al. revealing no influence of any of the β-subunits on $Na_v1.7$ current density using the same cultured cell lines (Ho, Zhao et al. 2012) and also with another study using *Xenopus* oocytes (Sangameswaran, Fish et al. 1997; Vijayaragavan, O'Leary et al. 2001). Nevertheless, other studies already reported increased current density of other Na_vs isoforms by β-subunits (Nuss, Chiamvimonvat et al. 1995; Smith and Goldin 1998; Fahmi, Patel et al. 2001; Zimmer and Benndorf 2002). The unaltered $Na_v1.7$ current upon expression of β2 and β4 subunits are in accordance with a previous study also using HEK293 cells (Ho, Zhao et al. 2012) and also in other recipient cells and Na_vs isoforms (Malhotra, Chen et al. 2001; Vijayaragavan, Powell et al. 2004; Aman, Grieco-Calub et al. 2009). The strong upregulatory effect of β3 subunits on $Na_v1.7$ current density is also in contradiction with the study from Ho. et al. and other studies (Morgan, Stevens et al. 2000; Vijayaragavan, Powell et al. 2004), but here again, other groups also already reported and increase of $Na_v1.7$ peak current (Fahmi, Patel et al. 2001).

This is possibly due to different cell background, involving differential endogenous β-subunits expression as well as other partners (Meadows and Isom 2005). Comparing our results with the results obtained by Ho et al., revealed that very subtle differences (both studies were carried with

HEK293 cells, but Ho and colleagues used a stable cell line expressing rat $Na_v1.7$ cDNA, whereas we used transient transfection of human $Na_v1.7$ cDNA) are already sufficient to generate differences in β-subunit effects on $Na_v1.7$.

Physiological relevance.

Naturally occurring genetic variants in humans and genetically modified animal models have shown that β-subunits are implicated in numerous diseases such as pain, epilepsy, migraines or cardiac arrhythmias (Brackenbury and Isom 2011). However, whether α-subunit glycosylation would be altered in the presence of dysfunctional β-subunits has never been investigated. I already discussed the potential effect of β-subunits modulating $Na_v1.7$ in the pain pathway in the discussion of the article. *SCN2B* knockout animals show altered I_{Na} current and altered pain phenotype. This is presumably due to their regulation of both stabilization and gating of the α-subunit. The next step is the investigation of the state of glycosylation of this isoform, as well as others, in these mouse lines.

Limitations of in vitro patch clamp recording.

I am aware of the limitations of using HEK293 cells to study the physiological function of proteins. The transfection of cDNAs is by itself problematic because it may saturate all the translation machinery, and fine mechanisms of regulations are probably very different than they are in native tissue. Furthermore, it is likely that many partner proteins are missing. In my research work, I focussed on Na_vs regulation in neuronal cell and using HEK293 cells, which are defined as being of renal origin, is also questionable. However, there is evidence that HEK293 cells are of neuronal origin (Shaw, Morse et al. 2002). Nevertheless, it would be more relevant to work on *ex vivo* samples, such as DRGs neurons. Using *SCNB* knockout mice or electroporation of β-subunits cDNA would allow the investigation of these subunits influence on different Na_vs component.

3.3. General Discussion

Na_vs are central players in electrical processing in the nervous system and carry an important role in normal and pathological pain. During the past decade, numerous mutations of $Na_v1.7$ and $Na_v1.8$ were identified and are incriminated in several different pain pathologies such as neuropathic pain. These mutations were often linked with alterations of Na_v sodium conductance and a shift toward hyperexcitable state of the channels. However, thus far, post-translational modulation of Na_v by regulatory proteins, which can also lead to modification of the sodium conductance, has been more sparsely investigated.

The purpose of my thesis was the investigation of Na_vs regulation by two important players, Nedd4-2 and β-subunits and was done in the specific perspective of neuropathic pain disorder.

We confirmed that Nedd4-2 downregulates $Na_v1.7$ in mammalian cells and further extensively investigated the ubiquitylation of $Na_v1.7$ and the motifs incriminated in the interaction with Nedd4-2. The major contribution of the first article of my thesis research work was the demonstration that Nedd4-2 downregulation after SNI is sufficient to alter Na_vs expression and to generate pain hypersensitivity. To our knowledge, this represents the first evidence of a physiological role for Nedd4-2 in regulating Na_vs *in vivo*. We used a known regulatory mechanism that allowed us to highlight a novel physiological relevance of the ubiquitylation pathway. In addition, targeting a mechanism of dysregulation of Na_vs might open new avenues for a mechanism-based treatment of neuropathic pain.

In the second part of my thesis research work, I did the opposite; we highlighted a novel mechanism of Na_vs α-subunit regulation *in vitro,* but whether this has any physiological implication remains to be investigated. Obviously, β-subunit regulation of Na_vs α-subunit is not novel, but the fact that such regulation can be driven by β-subunit dependent glycosylation has never been reported. This paves avenues for studying glycosylation of Na_vs in *SCNB* knockout animals, or in animals that underwent SNI and that show increased levels of β-subunit expression.

As shown in the Figure 9 of the introduction, β-subunits and Nedd4-2 have opposite effects on Na_vs membrane expression. Because there is a tight balance between internalization and stabilization processes, I wondered whether these two mechanisms could compete one with another. To answer this question, I first tested whether β-subunits co-expression could impair Nedd4-2 potency to downregulate $Na_v1.7$ (see Appendix 3). Nedd4-2 downregulated $Na_v1.7$ to the same extent when β1 or β3-subunits were co-transfected as it did with $Na_v1.7$ alone (~70% decrease), suggesting that β-subunits are not competing with Nedd4-2. Conversely, I also demonstrated that Nedd4-2 does not compete with β-subunits upregulatory effect on $Na_v1.7$. To do so, I showed that β-subunits have the

same upregulatory effect on $Na_v1.7$ than on YA mutant of $Na_v1.7$, which is not subject to Nedd4-2 regulation. Together, these results suggest that both pathways are independent.

Altogether, I dissected out Na_vs regulatory processes, demonstrated Nedd4-2 *in vivo* significance and highlighted a new regulatory mechanism of glycosylation mediated by β-subunits *in vitro*.

For an efficient treatment of neuropathic pain, there is a clear need for a better control of sensory neurons hyper-excitability. Much hope was coming from the development of new Na_v blockers (Priest and Kaczorowski 2007). However, the progresses have been slow because of the great difficulty to design selective Na_vs subtype blockers that would generate fewer side effects. Only a few examples of such selective Na_vs blockers are found in the scientific literature or in the pharmaceutical press releases (Bhattacharya, Wickenden et al. 2009). Based on our studies, we propose that targeting post-translational mechanisms, which regulate Na_vs density at the cell membrane, could be used as an alternative to Na_v blockers to modulate neuronal excitability. However, how to target ubiquitylation or glycosylation mechanisms remains a challenging task. In a recent study (Ernst, Avvakumov et al. 2013), a strategy for modulating enzymes of the ubiquitin system has been proposed; using ubiquitin variants the authors could compete with or boost ubiquitylation processes. Strikingly, the authors were able to enhance Nedd4 activity. This approach, in addition to gene therapy, could be used to rescue Nedd4-2 activity after peripheral nerve injury and thus reduce cellular excitability.

4. References

Abdulla, F. A. and P. A. Smith (2002). "Changes in Na(+) channel currents of rat dorsal root ganglion neurons following axotomy and axotomy-induced autotomy." J Neurophysiol **88**(5): 2518-2529.

Abrahamsen, B., J. Zhao, et al. (2008). "The Cell and Molecular Basis of Mechanical, Cold, and Inflammatory Pain." Science **321**(5889): 702-705.

Abriel, H. and R. S. Kass (2005). "Regulation of the voltage-gated cardiac sodium channel Nav1.5 by interacting proteins." Trends Cardiovasc Med **15**(1): 35-40.

Abriel, H., J. Loffing, et al. (1999). "Defective regulation of the epithelial Na+ channel by Nedd4 in Liddle's syndrome." J Clin Invest **103**(5): 667-673.

Abriel, H. and O. Staub (2005). "Ubiquitylation of ion channels." Physiology (Bethesda) **20**(6): 398-407.

Agarwal, N., S. Offermanns, et al. (2004). "Conditional gene deletion in primary nociceptive neurons of trigeminal ganglia and dorsal root ganglia." genesis **38**(3): 122-129.

Akil, H., D. Mayer, et al. (1976). "Antagonism of stimulation-produced analgesia by naloxone, a narcotic antagonist." Science **191**(4230): 961-962.

Akil, H., D. J. Mayer, et al. (1972). "[Comparison in the rat between analgesia induced by stimulation of periacqueducal gray matter and morphine analgesia]." C R Seances Acad Sci D **274**(26): 3603-3605.

Akopian, A. N., L. Sivilotti, et al. (1996). "A tetrodotoxin-resistant voltage-gated sodium channel expressed by sensory neurons." Nature **379**(6562): 257-262.

Akopian, A. N., V. Souslova, et al. (1999). "The tetrodotoxin-resistant sodium channel SNS has a specialized function in pain pathways." Nat Neurosci **2**(6): 541-548.

Akopian, A. N., V. Souslova, et al. (1997). "Structure and distribution of a broadly expressed atypical sodium channel." FEBS Letters **400**(2): 183-187.

Almeida, T. F., S. Roizenblatt, et al. (2004). "Afferent pain pathways: a neuroanatomical review." Brain Research **1000**(1â€“2): 40-56.

Aman, T. K., T. M. Grieco-Calub, et al. (2009). "Regulation of Persistent Na Current by Interactions between β Subunits of Voltage-Gated Na Channels." The Journal of Neuroscience **29**(7): 2027-2042.

Amaya, F., H. Wang, et al. (2006). "The voltage-gated sodium channel Na(v)1.9 is an effector of peripheral inflammatory pain hypersensitivity." J Neurosci **26**: 12852-12860.

Amerik, A. Y. and M. Hochstrasser (2004). "Mechanism and function of deubiquitinating enzymes." Biochimica Et Biophysica Acta **1695**(1-3): 189-207.

Amir, R. and M. Devor (1996). "Chemically Mediated Cross-Excitation in Rat Dorsal Root Ganglia." The Journal of Neuroscience **16**(15): 4733-4741.

Amir, R., J. D. Kocsis, et al. (2005). "Multiple interacting sites of ectopic spike electrogenesis in primary sensory neurons." J Neurosci **25**(10): 2576-2585.

Amir, R., M. Michaelis, et al. (1999). "Membrane potential oscillations in dorsal root ganglion neurons: role in normal electrogenesis and neuropathic pain." J Neurosci **19**(19): 8589-8596.

Apkarian, A. V., M. C. Bushnell, et al. (2005). "Human brain mechanisms of pain perception and regulation in health and disease." European Journal of Pain **9**(4): 463-484.

Araki, N., M. Umemura, et al. (2008). "Expression, transcription, and possible antagonistic interaction of the human Nedd4L gene variant: implications for essential hypertension." Hypertension **51**(3): 773-777.

Arévalo, J. C., J. Waite, et al. (2006). "Cell Survival through Trk Neurotrophin Receptors Is Differentially Regulated by Ubiquitination." Neuron **50**(4): 549-559.

Bair Mj, R. R. L. K. W. K. K. (2003). "Depression and pain comorbidity: A literature review." Archives of Internal Medicine **163**(20): 2433-2445.

Barbaric, I., G. Miller, et al. (2007). "Appearances can be deceiving: phenotypes of knockout mice." Briefings in Functional Genomics & Proteomics **6**(2): 91-103.
Basbaum, A. I., D. M. Bautista, et al. (2009). "Cellular and Molecular Mechanisms of Pain." Cell **139**(2): 267-284.
Beggs, S. and M. W. Salter (2007). "Stereological and somatotopic analysis of the spinal microglial response to peripheral nerve injury." Brain, Behavior, and Immunity **21**(5): 624-633.
Beneski, D. A. and W. A. Catterall (1980). "Covalent labeling of protein components of the sodium channel with a photoactivable derivative of scorpion toxin." Proceedings of the National Academy of Sciences **77**(1): 639-643.
Benn, S. C., M. Costigan, et al. (2001). "Developmental Expression of the TTX-Resistant Voltage-Gated Sodium Channels Nav1.8 (SNS) and Nav1.9 (SNS2) in Primary Sensory Neurons." The Journal of Neuroscience **21**(16): 6077-6085.
Bennett, E., M. S. Urcan, et al. (1997). "Contribution of Sialic Acid to the Voltage Dependence of Sodium Channel Gating." The Journal of General Physiology **109**(3): 327-343.
Bennett, G. and Y. Xie (1988). "A peripheral mononeuropathy in rat that produces disorders of pain sensation like those seen in man." Pain **33**: 87 - 107.
Bennett, V. and A. J. Baines (2001). "Spectrin and Ankyrin-Based Pathways: Metazoan Inventions for Integrating Cells Into Tissues." Physiological Reviews **81**(3): 1353-1392.
Berta, T., O. Poirot, et al. (2008). "Transcriptional and functional profiles of voltage-gated Na(+) channels in injured and non-injured DRG neurons in the SNI model of neuropathic pain." Mol Cell Neurosci **37**(2): 196-208.
Bhattacharya, A., A. Wickenden, et al. (2009). "Sodium channel blockers for the treatment of neuropathic pain." Neurotherapeutics **6**(4): 663-678.
Biswas, S., I. Deschênes, et al. (2008). "Calmodulin Regulation of NaV1.4 Current: Role of Binding to the Carboxyl Terminus." The Journal of General Physiology **131**(3): 197-209.
Black, J. A., T. R. Cummins, et al. (1999). "Upregulation of a silent sodium channel after peripheral, but not central, nerve injury in DRG neurons." Journal of Neurophysiology **82**: 2776-2785.
Black, J. A., S. Liu, et al. (2004). "Changes in the expression of tetrodotoxin-sensitive sodium channels within dorsal root ganglia neurons in inflammatory pain." Pain **108**(3): 237-247.
Boivie, J., G. Leijon, et al. (1989). "Central post-stroke pain — a study of the mechanisms through analyses of the sensory abnormalities." Pain **37**(2): 173-185.
Bouhassira, D., M. Lanteri-Minet, et al. (2008). "Prevalence of chronic pain with neuropathic characteristics in the general population." Pain **136**(3): 380-387.
Brackenbury, W. J. and L. L. Isom (2011). "Na Channel beta Subunits: Overachievers of the Ion Channel Family." Front Pharmacol **2**: 53.
Braz, J. M., M. A. Nassar, et al. (2005). "Parallel “Pain” Pathways Arise from Subpopulations of Primary Afferent Nociceptor." Neuron **47**(6): 787-793.
Brower, V. (2000). "New paths to pain relief." Nat Biotech **18**(4): 387-391.
Cachemaille, M., C. J. Laedermann, et al. (2012). "Neuronal expression of the ubiquitin ligase Nedd4-2 in rat dorsal root ganglia: modulation in the spared nerve injury model of neuropathic pain." Neuroscience **227**(0): 370-380.
Cantrell, A., V. Tibbs, et al. (2002). "Molecular mechanism of convergent regulation of brain Na(+) channels by protein kinase C and protein kinase A anchored to AKAP-15." Mol Cell Neurosci **21**: 63 - 80.
Cao, Y.-Q. (2006). "Voltage-gated calcium channels and pain." Pain **126**(1–3): 5-9.
Carr, D. B., M. Day, et al. (2003). "Transmitter Modulation of Slow, Activity-Dependent Alterations in Sodium Channel Availability Endows Neurons with a Novel Form of Cellular Plasticity." Neuron **39**(5): 793-806.
Caterina, M., M. Schumacher, et al. (1997). "The capsaicin receptor: a heat-activated ion channel in the pain pathway." Nature **389**: 816 - 824.

Catterall, W. A. (1992). "Cellular and molecular biology of voltage-gated sodium channels." Physiological Reviews **72**(suppl 4): S15-S48.
Catterall, W. A., F. Kalume, et al. (2010). "NaV1.1 channels and epilepsy." J Physiol **588**(Pt 11): 1849-1859.
Catterall, W. A., E. Perez-Reyes, et al. (2005). "International Union of Pharmacology. XLVIII. Nomenclature and Structure-Function Relationships of Voltage-Gated Calcium Channels." Pharmacological Reviews **57**(4): 411-425.
Chahine, M., R. Ziane, et al. (2005). "Regulation of Nav channels in sensory neurons." Trends in Pharmacological Sciences **26**(10): 496-502.
Chen, C., J. D. Calhoun, et al. (2012). "Identification of the Cysteine Residue Responsible for Disulfide Linkage of Na+ Channel α and β2 Subunits." Journal of Biological Chemistry **287**(46): 39061-39069.
Chen, Y., F. H. Yu, et al. (2006). "Neuromodulation of Na+ Channel Slow Inactivation via cAMP-Dependent Protein Kinase and Protein Kinase C." Neuron **49**(3): 409-420.
Cheng, X., S. Dib-Hajj, et al. (2008). "Mutation I136V alters electrophysiological properties of the NaV1.7 channel in a family with onset of erythromelalgia in the second decade." Molecular Pain **4**(1): 1.
Ciaramitaro, P., M. Mondelli, et al. (2010). "Traumatic peripheral nerve injuries: epidemiological findings, neuropathic pain and quality of life in 158 patients." Journal of the Peripheral Nervous System **15**(2): 120-127.
Ciechanover, A. (2005). "Proteolysis: from the lysosome to ubiquitin and the proteasome." Nat Rev Mol Cell Biol **6**(1): 79-87.
Cordell, W. H., K. K. Keene, et al. (2002). "The high prevalence of pain in emergency medical care." The American Journal of Emergency Medicine **20**(3): 165-169.
Costigan, M., K. Befort, et al. (2002). "Replicate high-density rat genome oligonucleotide microarrays reveal hundreds of regulated genes in the dorsal root ganglion after peripheral nerve injury." BMC Neurosci **3**(1): 16.
Coull, J. A. M., D. Boudreau, et al. (2003). "Trans-synaptic shift in anion gradient in spinal lamina I neurons as a mechanism of neuropathic pain." Nature **424**(6951): 938-942.
Courteix, C., A. Eschalier, et al. (1993). "Streptozocin-induced diabetic rats: behavioural evidence for a model of chronic pain." Pain **53**(1): 81-88.
Coward, K., A. Aitken, et al. (2001). "Plasticity of TTX-sensitive sodium channels PN1 and Brain III in injured human nerves." NeuroReport **12**(3).
Coward, K., A. Jowett, et al. (2001). "Sodium channel beta 1 and beta 2 subunits parallel SNS/PN3 alpha-subunit changes in injured human sensory neurons." NeuroReport **12**(3): 483-488.
Cox, J. J., F. Reimann, et al. (2006). "An SCN9A channelopathy causes congenital inability to experience pain." Nature **444**(7121): 894-898.
Cregg, R., A. Momin, et al. (2010). "Pain channelopathies." The Journal of Physiology **588**(11): 1897-1904.
Cronin, N. B., A. O'Reilly, et al. (2004). "Effects of Deglycosylation of Sodium Channels on Their Structure and Function†." Biochemistry **44**(2): 441-449.
Cummins, T. R., F. Aglieco, et al. (2001). "Nav1.3 Sodium Channels: Rapid Repriming and Slow Closed-State Inactivation Display Quantitative Differences after Expression in a Mammalian Cell Line and in Spinal Sensory Neurons." The Journal of Neuroscience **21**(16): 5952-5961.
Cummins, T. R., S. D. Dib-Hajj, et al. (1999). "A novel persistent tetrodotoxin-resistant sodium current in SNS-null and wild-type small primary sensory neurons." J Neurosci **19**(24): RC43.
Cummins, T. R., J. R. Howe, et al. (1998). "Slow closed-state inactivation: a novel mechanism underlying ramp currents in cells expressing the hNE/PN1 sodium channel." J Neurosci **18**: 9607-9619.

Cummins, T. R. and S. G. Waxman (1997). "Downregulation of tetrodotoxin-resistant sodium currents and upregulation of a rapidly repriming tetrodotoxin-sensitive sodium current in small spinal sensory neurons after nerve injury." J Neurosci **17**(10): 3503-3514.

Cusdin, F. S., J. J. Clare, et al. (2008). "Trafficking and Cellular Distribution of Voltage-Gated Sodium Channels." Traffic **9**(1): 17-26.

de Leon, J., V. Santoro, et al. (2012). "Interactions between antiepileptics and second-generation antipsychotics." Expert Opinion on Drug Metabolism & Toxicology **8**(3): 311-334.

Decosterd, I., R. R. Ji, et al. (2002). "The pattern of expression of the voltage-gated sodium channels Na(v)1.8 and Na(v)1.9 does not change in uninjured primary sensory neurons in experimental neuropathic pain models." Pain **96**: 269-277.

Decosterd, I. and C. J. Woolf (2000). "Spared nerve injury: an animal model of persistent peripheral neuropathic pain." Pain **87**(2): 149-158.

Devor, M., R. Govrin-Lippmann, et al. (1993). "Na+ channel immunolocalization in peripheral mammalian axons and changes following nerve injury and neuroma formation." The Journal of Neuroscience **13**(5): 1976-1992.

Devor, M. and P. D. Wall (1990). "Cross-excitation in dorsal root ganglia of nerve-injured and intact rats." Journal of Neurophysiology **64**(6): 1733-1746.

Dib-Hajj, S. D., A. M. Binshtok, et al. (2009). "Voltage-gated sodium channels in pain states: Role in pathophysiology and targets for treatment." Brain Research Reviews **60**(1): 65-83.

Dib-Hajj, S. D., T. R. Cummins, et al. (2010). "Sodium Channels in Normal and Pathological Pain." Annual Review of Neuroscience **33**(1): 325-347.

Dib-Hajj, S. D., A. M. Rush, et al. (2005). "Gain-of-function mutation in NaV1.7 in familial erythromelalgia induces bursting of sensory neurons." Brain **128**: 1847-1854.

Dib-Hajj, S. D., L. Tyrrell, et al. (1998). "NaN, a novel voltage-gated Na channel, is expressed preferentially in peripheral sensory neurons and down-regulated after axotomy." Proc Natl Acad Sci U S A **95**: 8963-8968.

Dibbens, L. M., J. Ekberg, et al. (2007). "NEDD4-2 as a potential candidate susceptibility gene for epileptic photosensitivity." Genes Brain Behav **6**(8): 750-755.

Dick, I. E., R. M. Brochu, et al. (2007). "Sodium Channel Blockade May Contribute to the Analgesic Efficacy of Antidepressants." The Journal of Pain **8**(4): 315-324.

Dickenson, A. H., E. A. Matthews, et al. (2002). "Neurobiology of neuropathic pain: mode of action of anticonvulsants." European Journal of Pain **6**: 51-60.

Dieleman, J. P., J. Kerklaan, et al. (2008). "Incidence rates and treatment of neuropathic pain conditions in the general population." Pain **137**(3): 681-688.

Diss, J. K. J., S. P. Fraser, et al. (2004). "Voltage-gated Na+ channels: multiplicity of expression, plasticity, functional implications and pathophysiological aspects." European Biophysics Journal **33**(3): 180-193.

Djouhri, L., S. Koutsikou, et al. (2006). "Spontaneous Pain, Both Neuropathic and Inflammatory, Is Related to Frequency of Spontaneous Firing in Intact C-Fiber Nociceptors." The Journal of Neuroscience **26**(4): 1281-1292.

Dogrul, A., H. Gul, et al. (2011). "Systemic and spinal administration of etanercept, a tumor necrosis factor alpha inhibitor, blocks tactile allodynia in diabetic mice." Acta Diabetologica **48**(2): 135-142.

Dong, X. W., S. Goregoaker, et al. (2007). "Small interfering RNA-mediated selective knockdown of NaV1.8 tetrodotoxin-resistant sodium channel reverses mechanical allodynia in neuropathic rats." Neuroscience **146**(2): 812-821.

Drew, L. J., D. K. Rohrer, et al. (2004). "Acid-sensing ion channels ASIC2 and ASIC3 do not contribute to mechanically activated currents in mammalian sensory neurones." The Journal of Physiology **556**(3): 691-710.

Drinjakovic, J., H. Jung, et al. (2010). "E3 Ligase Nedd4 Promotes Axon Branching by Downregulating PTEN." Neuron **65**(3): 341-357.

Dubin, A. E. and A. Patapoutian (2010). "Nociceptors: the sensors of the pain pathway." The Journal of Clinical Investigation **120**(11): 3760-3772.
Ducreux, D., N. Attal, et al. (2006). "Mechanisms of central neuropathic pain: a combined psychophysical and fMRI study in syringomyelia." Brain **129**(4): 963-976.
Dunn, D. M., T. Ishigami, et al. (2002). "Common variant of human NEDD4L activates a cryptic splice site to form a frameshifted transcript." J Hum Genet **47**(12): 665-676.
Dworkin, R. H., A. B. O'Connor, et al. (2007). "Pharmacologic management of neuropathic pain: Evidence-based recommendations." Pain **132**(3): 237-251.
Ednie, A. R. and E. S. Bennett (2011). Modulation of Voltage-Gated Ion Channels by Sialylation. Comprehensive Physiology, John Wiley & Sons, Inc.
England, J. D., F. Gamboni, et al. (1993). "Sodium-Channels Accumulate at the Tips of Injured Axons." Neurology **43**(4): A232-A232.
England, J. D., L. T. Happel, et al. (1996). "Sodium channel accumulation in humans with painful neuromas." Neurology **47**(1): 272-276.
Ernst, A., G. Avvakumov, et al. (2013). "A strategy for modulation of enzymes in the ubiquitin system." Science **339**(6119): 590-595.
Faber, C. G., J. G. Hoeijmakers, et al. (2012). "Gain of function Nanu1.7 mutations in idiopathic small fiber neuropathy." Ann Neurol **71**(1): 26-39.
Faber, C. G., G. Lauria, et al. (2012). "Gain-of-function Nav1.8 mutations in painful neuropathy." Proc Natl Acad Sci U S A **109**(47): 19444-19449.
Fahmi, A. I., M. Patel, et al. (2001). "The sodium channel -subunit SCN3b modulates the kinetics of SCN5a and is expressed heterogeneously in sheep heart." The Journal of Physiology **537**(3): 693-700.
Fang, X., L. Djouhri, et al. (2006). "Intense Isolectin-B4 Binding in Rat Dorsal Root Ganglion Neurons Distinguishes C-Fiber Nociceptors with Broad Action Potentials and High Nav1.9 Expression." The Journal of Neuroscience **26**(27): 7281-7292.
Fertleman, C. R., M. D. Baker, et al. (2006). "SCN9A mutations in paroxysmal extreme pain disorder: allelic variants underlie distinct channel defects and phenotypes." Neuron **52**(5): 767-774.
Firsov, D., L. Schild, et al. (1996). "Cell surface expression of the epithelial Na channel and a mutant causing Liddle syndrome: A quantitativeâ€‰approach." Proceedings of the National Academy of Sciences of the United States of America **93**(26): 15370-15375.
Flores, L. P. (2006). "Estudo epidemiológico das lesões traumáticas de plexo braquial em adultos." Arquivos de Neuro-Psiquiatria **64**: 88-94.
Foley, K. M. (2003). "Opioids and Chronic Neuropathic Pain." New England Journal of Medicine **348**(13): 1279-1281.
Fotia, A. B., A. Dinudom, et al. (2003). "The role of individual Nedd4-2 (KIAA0439) WW domains in binding and regulating epithelial sodium channels." FASEB J **17**(1): 70-72.
Fotia, A. B., J. Ekberg, et al. (2004). "Regulation of neuronal voltage-gated sodium channels by the ubiquitin-protein ligases Nedd4 and Nedd4-2." J Biol Chem **279**(28): 28930-28935.
Fouladkou, F., R. Alikhani-Koopaei, et al. (2004). "A naturally occurring human Nedd4-2 variant displays impaired ENaC regulation in Xenopus laevis oocytes." Am J Physiol Renal Physiol **287**(3): F550-561.
Fox, A., C. Eastwood, et al. (1999). "Critical evaluation of the streptozotocin model of painful diabetic neuropathy in the rat." Pain **81**(3): 307-316.
Friedel, R., W. Wurst, et al. (2011). Generating Conditional Knockout Mice. Transgenic Mouse Methods and Protocols. M. H. Hofker and J. Deursen, Humana Press. **693:** 205-231.
Fukuoka, T., K. Kobayashi, et al. (2008). "Comparative study of the distribution of the alpha-subunits of voltage-gated sodium channels in normal and axotomized rat dorsal root ganglion neurons." J Comp Neurol **510**(2): 188-206.

Fukuoka, T. and K. Noguchi (2011). "Comparative study of voltage-gated sodium channel alpha-subunits in non-overlapping four neuronal populations in the rat dorsal root ganglion." Neurosci Res **70**(2): 164-171.

Fukuoka, T., A. Tokunaga, et al. (2002). "VR1, but not P2X3, increases in the spared L4 DRG in rats with L5 spinal nerve ligation." Pain **99**(1–2): 111-120.

Fukuoka, T., H. Yamanaka, et al. (2012). "Re-evaluation of the phenotypic changes in L4 dorsal root ganglion neurons after L5 spinal nerve ligation." Pain **153**(1): 68-79.

Gammaitoni, A. R., N. A. Alvarez, et al. (2003). "Safety and Tolerability of the Lidocaine Patch 5%, a Targeted Peripheral Analgesic: A Review of the Literature." The Journal of Clinical Pharmacology **43**(2): 111-117.

Gasser, A., X. Cheng, et al. (2010). "Two Nedd4-binding motifs underlie modulation of sodium channel Nav1.6 by p38 MAPK." J Biol Chem **285**(34): 26149-26161.

Gaudet, A., P. Popovich, et al. (2011). "Wallerian degeneration: gaining perspective on inflammatory events after peripheral nerve injury." Journal of Neuroinflammation **8**(1): 110.

Gaumann, D. M., P. C. Brunet, et al. (1992). "Clonidine Enhances the Effects of Lidocaine on Câ€ Fiber Action Potential." Anesthesia & Analgesia **74**(5): 719-725.

Gavillet, B., J.-S. Rougier, et al. (2006). "Cardiac Sodium Channel Nav1.5 Is Regulated by a Multiprotein Complex Composed of Syntrophins and Dystrophin." Circulation Research **99**(4): 407-414.

Gebhart, G. F. (2004). "Descending modulation of pain." Neuroscience & Biobehavioral Reviews **27**(8): 729-737.

Gee, S., R. Madhavan, et al. (1998). "Interaction of muscle and brain sodium channels with multiple members of the syntrophin family of dystrophin-associated proteins." J Neurosci **18**: 128 - 137.

Gold, M. S., D. Weinreich, et al. (2003). "Redistribution of NaV1.8 in Uninjured Axons Enables Neuropathic Pain." The Journal of Neuroscience **23**(1): 158-166.

Gosselin, R.-D., M. R. Suter, et al. (2010). "Glial Cells and Chronic Pain." The Neuroscientist **16**(5): 519-531.

Gould, H. J., T. N. Gould, et al. (2000). "A possible role for nerve growth factor in the augmentation of sodium channels in models of chronic pain." Brain Research **854**(1-2): 19-29.

Hartshorne, R. P., D. J. Messner, et al. (1982). "The saxitoxin receptor of the sodium channel from rat brain. Evidence for two nonidentical beta subunits." J Biol Chem **257**(23): 13888-13891.

Harvey, K. F., A. Dinudom, et al. (1999). "All three WW domains of murine Nedd4 are involved in the regulation of epithelial sodium channels by intracellular Na+." Journal of Biological Chemistry **274**(18): 12525-12530.

Harvey, K. F. and S. Kumar (1999). "Nedd4-like proteins: an emerging family of ubiquitin-protein ligases implicated in diverse cellular functions." Trends Cell Biol **9**(5): 166-169.

Henry, P. C., V. Kanelis, et al. (2003). "Affinity and specificity of interactions between Nedd4 isoforms and the epithelial Na+ channel." J Biol Chem **278**(22): 20019-20028.

Herzog, R. I., T. R. Cummins, et al. (2001). "Persistent TTX-resistant Na+ current affects resting potential and response to depolarization in simulated spinal sensory neurons." Journal of Neurophysiology **86**: 1351-1364.

Hicke, L., H. L. Schubert, et al. (2005). "Ubiquitin-binding domains." Nat Rev Mol Cell Biol **6**(8): 610-621.

Hilaire, C., B. Campo, et al. (2005). "K+ current regulates calcium-activated chloride current-induced afterdepolarization in axotomized sensory neurons." European Journal of Neuroscience **22**(5): 1073-1080.

Ho, C. and M. E. O'Leary (2011). "Single-cell analysis of sodium channel expression in dorsal root ganglion neurons." Mol Cell Neurosci **46**(1): 159-166.

Ho, C., J. Zhao, et al. (2012). "Differential expression of sodium channel beta subunits in dorsal root ganglion sensory neurons." J Biol Chem **287**(18): 15044-15053.

Hodgkin, A. L. and A. F. Huxley (1952). "A quantitative description of membrane current and its application to conduction and excitation in nerve." The Journal of Physiology **117**(4): 500-544.

Hong, S., L. Agresta, et al. (2008). "The TRPV1 receptor is associated with preferential stress in large dorsal root ganglion neurons in early diabetic sensory neuropathy." Journal of Neurochemistry **105**(4): 1212-1222.

Hong, S., T. J. Morrow, et al. (2004). "Early Painful Diabetic Neuropathy Is Associated with Differential Changes in Tetrodotoxin-sensitive and -resistant Sodium Channels in Dorsal Root Ganglion Neurons in the Rat." Journal of Biological Chemistry **279**(28): 29341-29350.

Hucho, T. B., O. A. Dina, et al. (2005). "Epac Mediates a cAMP-to-PKC Signaling in Inflammatory Pain: An Isolectin B4(+) Neuron-Specific Mechanism." The Journal of Neuroscience **25**(26): 6119-6126.

Hudson, L. J., S. Bevan, et al. (2001). "VR1 protein expression increases in undamaged DRG neurons after partial nerve injury." European Journal of Neuroscience **13**(11): 2105-2114.

Huibregtse, J. M., M. Scheffner, et al. (1995). "A family of proteins structurally and functionally related to the E6-AP ubiquitin-protein ligase." Proceedings of the National Academy of Sciences **92**(11): 5249.

Ingham, R. J., G. Gish, et al. (2004). "The Nedd4 family of E3 ubiquitin ligases: functional diversity within a common modular architecture." Oncogene **23**(11): 1972-1984.

Isom, L., K. De Jongh, et al. (1992). "Primary structure and functional expression of the beta 1 subunit of the rat brain sodium channel." Science **256**(5058): 839-842.

Isom, L. L. (2001). "Sodium channel beta subunits: anything but auxiliary." Neuroscientist **7**(1): 42-54.

Isom, L. L., D. S. Ragsdale, et al. (1995). "Structure and function of the β2 subunit of brain sodium channels, a transmembrane glycoprotein with a CAM motif." Cell **83**(3): 433-442.

Isom, L. L., T. Scheuer, et al. (1995). "Functional co-expression of the beta 1 and type IIA alpha subunits of sodium channels in a mammalian cell line." J Biol Chem **270**(7): 3306-3312.

James, W. M. and W. S. Agnew (1987). "Multiple oligosaccharide chains in the voltage-sensitive Na channel from Electrophorus electricus: Evidence for α-2,8-linked polysialic acid." Biochemical and Biophysical Research Communications **148**(2): 817-826.

Jarecki, B. W., A. D. Piekarz, et al. (2010). "Human voltage-gated sodium channel mutations that cause inherited neuronal and muscle channelopathies increase resurgent sodium currents." The Journal of Clinical Investigation **120**(1): 369-378.

Jentsch, T. J. (2000). "Neuronal KCNQ potassium channels:physislogy and role in disease." Nat Rev Neurosci **1**(1): 21-30.

Ji, R.-R., T. Kohno, et al. (2003). "Central sensitization and LTP: do pain and memory share similar mechanisms?" Trends in Neurosciences **26**(12): 696-705.

Jin, X. and R. W. Gereau (2006). "Acute p38-Mediated Modulation of Tetrodotoxin-Resistant Sodium Channels in Mouse Sensory Neurons by Tumor Necrosis Factor-+Ý." The Journal of Neuroscience **26**(1): 246-255.

Johnson, D. and E. S. Bennett (2006). "Isoform-specific Effects of the β2 Subunit on Voltage-gated Sodium Channel Gating." Journal of Biological Chemistry **281**(36): 25875-25881.

Johnson, D., M. L. Montpetit, et al. (2004). "The Sialic Acid Component of the β1 Subunit Modulates Voltage-gated Sodium Channel Function." Journal of Biological Chemistry **279**(43): 44303-44310.

Joshi, S. K., J. P. Mikusa, et al. (2006). "Involvement of the TTX-resistant sodium channel Nav 1.8 in inflammatory and neuropathic, but not post-operative, pain states." Pain **123**: 75-82.

Julius, D. and A. I. Basbaum (2001). "Molecular mechanisms of nociception." Nature **413**(6852): 203-210.

Kakimura, J.-i., T. Zheng, et al. (2010). "Regulation of the Spontaneous Augmentation of NaV1.9 in Mouse Dorsal Root Ganglion Neurons: Effect of PKA and PKC Pathways." Marine Drugs **8**(3): 728-740.

Kalso, E., M. R. Tramer, et al. (1998). "Systemic local-anaesthetic-type drugs in chronic pain: a systematic review." European Journal of Pain-London **2**(1): 3-14.
Kamynina, E., C. Debonneville, et al. (2001). "A novel mouse Nedd4 protein suppresses the activity of the epithelial Na+ channel." FASEB J **15**(1): 204-214.
Kanelis, V., D. Rotin, et al. (2001). "Solution structure of a Nedd4 WW domain-ENaC peptide complex." Nat Struct Biol **8**(5): 407-412.
Kapa, S., D. J. Tester, et al. (2009). "Genetic testing for long-QT syndrome: distinguishing pathogenic mutations from benign variants." Circulation **120**(18): 1752-1760.
Kasanov, J., G. Pirozzi, et al. (2001). "Characterizing Class I WW domains defines key specificity determinants and generates mutant domains with novel specificities." Chem Biol **8**(3): 231-241.
Kazarinova-Noyes, K., J. D. Malhotra, et al. (2001). "Contactin Associates with Na+ Channels and Increases Their Functional Expression." Journal of Neuroscience **21**(19): 7517-7525.
Kazen-Gillespie, K. A., D. S. Ragsdale, et al. (2000). "Cloning, localization, and functional expression of sodium channel beta1A subunits." J Biol Chem **275**(2): 1079-1088.
Kerr, B. J., V. Souslova, et al. (2001). "A role for the TTX-resistant sodium channel Nav 1.8 in NGF-induced hyperalgesia, but not neuropathic pain." NeuroReport **12**(14): 3077-3080.
Kim, D. S., J. O. Choi, et al. (2002). "Downregulation of voltage-gated potassium channel α gene expression in dorsal root ganglia following chronic constriction injury of the rat sciatic nerve." Molecular Brain Research **105**(1–2): 146-152.
Kim, S. and J. Chung (1992). "An experimental model for peripheral neuropathy produced by segmental spinal nerve ligation in the rat." Pain **50**: 355 - 363.
Kispersky, T. J., J. S. Caplan, et al. (2012). "Increase in Sodium Conductance Decreases Firing Rate and Gain in Model Neurons." The Journal of Neuroscience **32**(32): 10995-11004.
Klugbauer, N., L. Lacinova, et al. (1995). "Structure and Functional Expression of a New Member of the Tetrodotoxin-Sensitive Voltage-Activated Sodium-Channel Family from Human Neuroendocrine Cells." EMBO Journal **14**(6): 1084-1090.
Kretschmer, T., D. H. Nguyen, et al. (2002). "Painful human neuromas: a potential role for a structural transmembrane protein, ankyrin G." Journal of Neurosurgery **97**(6): 1424-1431.
Lackovic, J., J. Howitt, et al. (2012). "Differential regulation of Nedd4 ubiquitin ligases and their adaptor protein Ndfip1 in a rat model of ischemic stroke." Experimental Neurology **235**(1): 326-335.
LaCroix-Fralish, M. L. and J. S. Mogil (2009). "Progress in Genetic Studies of Pain and Analgesia." Annual Review of Pharmacology and Toxicology **49**(1): 97-121.
Laedermann, C. J., M. Cachemaille, et al. (2013). "Dysregulation of voltage-gated sodium channels by ubiquitin ligase NEDD4-2 in neuropathic pain." J Clin Invest **123**(7): 3002-3013.
Laedermann, C. J., N. Syam, et al. (2013). "ß1- and ß3- voltage-gated sodium channel subunits modulate cell surface expression and glycosylation of Nav1.7 in HEK293 cells." Frontiers in Cellular Neuroscience **7**.
Lai, J., M. S. Gold, et al. (2002). "Inhibition of neuropathic pain by decreased expression of the tetrodotoxin-resistant sodium channel, NaV1.8." Pain **95**(1-2): 143-152.
Lang, P. M., J. Fleckenstein, et al. (2008). "Retigabine reduces the excitability of unmyelinated peripheral human axons." Neuropharmacology **54**(8): 1271-1278.
Langford, D. J., A. L. Bailey, et al. (2010). "Coding of facial expressions of pain in the laboratory mouse." Nat Meth **7**(6): 447-449.
Latremoliere, A. and C. J. Woolf (2009). "Central Sensitization: A Generator of Pain Hypersensitivity by Central Neural Plasticity." The Journal of Pain **10**(9): 895-926.
Lawson, K. (2006). "Potassium Channels as Targets for the Management of Pain." Central Nervous System Agents in Medicinal Chemistry(Formerly Current Medicinal Chemistry - Central Nervous System Agents) **6**(2): 119-128.

Lee, D. H., L. Chang, et al. (2005). "Hyperpolarization-Activated, Cation-Nonselective, Cyclic Nucleotide-Modulated Channel Blockade Alleviates Mechanical Allodynia and Suppresses Ectopic Discharge in Spinal Nerve Ligated Rats." The Journal of Pain **6**(7): 417-424.
Lee, Y.-C. and P.-P. Chen (2010). "A review of SSRIs and SNRIs in neuropathic pain." Expert Opinion on Pharmacotherapy **11**(17): 2813-2825.
Leo, S., R. D'Hooge, et al. (2010). "Exploring the role of nociceptor-specific sodium channels in pain transmission using Nav1.8 and Nav1.9 knockout mice." Behavioural Brain Research **208**(1): 149-157.
Leung, L. and C. Cahill (2010). "TNF-alpha and neuropathic pain - a review." Journal of Neuroinflammation **7**(1): 27.
Levine, J. D., N. C. Gordon, et al. (1978). "The narcotic antagonist naloxone enhances clinical pain." Nature **272**(5656): 826-827.
Lisney, S. J. W. and C. M. Pover (1983). "Coupling between Fibers Involved in Sensory Nerve Neuromata in Cats." Journal of the Neurological Sciences **59**(2): 255-264.
Liu, C.-N., P. D. Wall, et al. (2000). "Tactile allodynia in the absence of C-fiber activation: altered firing properties of DRG neurons following spinal nerve injury." Pain **85**(3): 503-521.
Liu, M. and J. N. Wood (2011). "The roles of sodium channels in nociception: implications for mechanisms of neuropathic pain." Pain Med **12 Suppl 3**: S93-99.
Loeser, J. D. and R.-D. Treede (2008). "The Kyoto protocol of IASP Basic Pain Terminology." Pain **137**(3): 473-477.
Lopez-Santiago, L. F., W. J. Brackenbury, et al. (2011). "Na+ Channel Scn1b Gene Regulates Dorsal Root Ganglion Nociceptor Excitability in Vivo." Journal of Biological Chemistry **286**(26): 22913-22923.
Lopez-Santiago, L. F., M. Pertin, et al. (2006). "Sodium channel beta2 subunits regulate tetrodotoxin-sensitive sodium channels in small dorsal root ganglion neurons and modulate the response to pain." J Neurosci **26**(30): 7984-7994.
Lu, P.-J., X. Z. Zhou, et al. (1999). "Function of WW Domains as Phosphoserine- or Phosphothreonine-Binding Modules." Science **283**(5406): 1325-1328.
Luo, F., Y. B. Wang, et al. (2009). "A Functional Variant of NEDD4L Is Associated With Hypertension, Antihypertensive Response, and Orthostatic Hypotension." Hypertension **54**(4): 796-801.
Luo, S., G. Perry, et al. (2008). "Nav1.7 expression is increased in painful human dental pulp." Molecular Pain **4**(1): 16.
Ma, C., Y. Shu, et al. (2003). "Similar Electrophysiological Changes in Axotomized and Neighboring Intact Dorsal Root Ganglion Neurons." Journal of Neurophysiology **89**(3): 1588-1602.
Malcangio, M., M. S. Ramer, et al. (2000). "Abnormal substance P release from the spinal cord following injury to primary sensory neurons." European Journal of Neuroscience **12**(1): 397-399.
Malhotra, J. D., C. Chen, et al. (2001). "Characterization of Sodium Channel α- and β-Subunits in Rat and Mouse Cardiac Myocytes." Circulation **103**(9): 1303-1310.
Malhotra, J. D., K. Kazen-Gillespie, et al. (2000). "Sodium Channel +Ý Subunits Mediate Homophilic Cell Adhesion and Recruit Ankyrin to Points of Cell-Cell Contact." Journal of Biological Chemistry **275**(15): 11383-11388.
Malik-Hall, M., O. A. Dina, et al. (2005). "Primary afferent nociceptor mechanisms mediating NGF-induced mechanical hyperalgesia." European Journal of Neuroscience **21**(12): 3387-3394.
Mantyh, P. W., M. Koltzenburg, et al. (2011). "Antagonism of Nerve Growth Factor-TrkA Signaling and the Relief of Pain." Anesthesiology **115**(1): 189-204 110.1097/ALN.1090b1013e31821b31821ac31825.
Mao, J. and L. L. Chen (2000). "Systemic lidocaine for neuropathic pain relief." Pain **87**(1): 7-17.

Marmigere, F. and P. Ernfors (2007). "Specification and connectivity of neuronal subtypes in the sensory lineage." Nature Reviews. Neuroscience **8**(2): 114-127.
Massotte, D. and B. L. Kieffer (1999). "A molecular basis for opiate action." Essays in Biochemistry, Vol 33 **33**: 65-77.
Matzner, O. and M. Devor (1994). "Hyperexcitability at sites of nerve injury depends on voltage-sensitive Na+ channels." Journal of Neurophysiology **72**(1): 349-359.
McCormick, K. A., L. L. Isom, et al. (1998). "Molecular Determinants of Na+ Channel Function in the Extracellular Domain of the β1 Subunit." Journal of Biological Chemistry **273**(7): 3954-3962.
McEwen, D. P., L. S. Meadows, et al. (2004). "Sodium Channel β1 Subunit-mediated Modulation of Nav1.2 Currents and Cell Surface Density Is Dependent on Interactions with Contactin and Ankyrin." Journal of Biological Chemistry **279**(16): 16044-16049.
Meadows, L., J. D. Malhotra, et al. (2001). "The intracellular segment of the sodium channel β1 subunit is required for its efficient association with the channel α subunit." Journal of Neurochemistry **76**(6): 1871-1878.
Meadows, L. S. and L. L. Isom (2005). "Sodium channels as macromolecular complexes: implications for inherited arrhythmia syndromes." Cardiovasc Res **67**(3): 448-458.
Melzack, R. and P. D. Wall (1965). "Pain Mechanisms - a New Theory." Science **150**(3699): 971-&.
Messinger, R. B., A. K. Naik, et al. (2009). "In vivo silencing of the CaV3.2 T-type calcium channels in sensory neurons alleviates hyperalgesia in rats with streptozocin-induced diabetic neuropathy." Pain **145**(1–2): 184-195.
Messner, D. J. and W. A. Catterall (1985). "The sodium channel from rat brain. Separation and characterization of subunits." J Biol Chem **260**(19): 10597-10604.
Micó, J. A., D. Ardid, et al. (2006). "Antidepressants and pain." Trends in Pharmacological Sciences **27**(7): 348-354.
Milligan, E. D. and L. R. Watkins (2009). "Pathological and protective roles of glia in chronic pain." Nat Rev Neurosci **10**(1): 23-36.
Minett, M. S., M. A. Nassar, et al. (2012). "Distinct Nav1.7-dependent pain sensations require different sets of sensory and sympathetic neurons." Nat Commun **3**: 791.
Moore, K. A., T. Kohno, et al. (2002). "Partial Peripheral Nerve Injury Promotes a Selective Loss of GABAergic Inhibition in the Superficial Dorsal Horn of the Spinal Cord." The Journal of Neuroscience **22**(15): 6724-6731.
Moremen, K. W., M. Tiemeyer, et al. (2012). "Vertebrate protein glycosylation: diversity, synthesis and function." Nat Rev Mol Cell Biol **13**(7): 448-462.
Morgan, K., E. B. Stevens, et al. (2000). "β3: An additional auxiliary subunit of the voltage-sensitive sodium channel that modulates channel gating with distinct kinetics." Proceedings of the National Academy of Sciences **97**(5): 2308-2313.
Myat, A., P. Henry, et al. (2002). "Drosophila Nedd4, a Ubiquitin Ligase, Is Recruited by Commissureless to Control Cell Surface Levels of the Roundabout Receptor." Neuron **35**(3): 447-459.
Nagasako, E. M., A. L. Oaklander, et al. (2003). "Congenital insensitivity to pain: an update." Pain **101**(3): 213-219.
Nagy, J. I. and S. P. Hunt (1982). "Fluoride-resistant acid phosphatase-containing neurones in dorsal root ganglia are separate from those containing substance P or somatostatin." Neuroscience **7**(1): 89-97.
Nassar, M. A., M. D. Baker, et al. (2006). "Nerve injury induces robust allodynia and ectopic discharges in Nav1.3 null mutant mice." Mol Pain **2**(1): 33.
Nassar, M. A., A. Levato, et al. (2005). "Neuropathic pain develops normally in mice lacking both Nav1.7 and Nav1.8." Mol Pain **1**: 24.

Nassar, M. A., L. C. Stirling, et al. (2004). "Nociceptor-specific gene deletion reveals a major role for Nav1.7 (PN1) in acute and inflammatory pain." Proc Natl Acad Sci U S A **101**(34): 12706-12711.
Novella, S. P., F. M. Hisama, et al. (2007). "A case of inherited erythromelalgia." Nat Clin Pract Neurol **3**: 229-234.
Nuss, H. B., N. Chiamvimonvat, et al. (1995). "Functional association of the beta 1 subunit with human cardiac (hH1) and rat skeletal muscle (mu 1) sodium channel alpha subunits expressed in Xenopus oocytes." J Gen Physiol **106**(6): 1171-1191.
Ossipov, M. H., G. O. Dussor, et al. (2010). "Central modulation of pain." The Journal of Clinical Investigation **120**(11): 3779-3787.
Pabbidi, R., S.-Q. Yu, et al. (2008). "Influence of TRPV1 on diabetes-induced alterations in thermal pain sensitivity." Molecular Pain **4**(1): 9.
Park, J. and Z. D. Luo (2010). "Calcium channel functions in pain processing." Channels **4**(6): 510-517.
Passmore, G. M., A. A. Selyanko, et al. (2003). "KCNQ/M Currents in Sensory Neurons: Significance for Pain Therapy." The Journal of Neuroscience **23**(18): 7227-7236.
Payandeh, J., T. Scheuer, et al. (2011). "The crystal structure of a voltage-gated sodium channel." Nature **475**(7356): 353-358.
Perquin, C. W., A. A. J. M. Hazebroek-Kampschreur, et al. (2000). "Pain in children and adolescents: a common experience." Pain **87**(1): 51-58.
Perret, D. and Z. D. Luo (2009). "Targeting voltage-gated calcium channels for neuropathic pain management." Neurotherapeutics **6**(4): 679-692.
Persaud, A., P. Alberts, et al. (2009). "Comparison of substrate specificity of the ubiquitin ligases Nedd4 and Nedd4-2 using proteome arrays." Mol Syst Biol **5**.
Persson, A. K., A. Gasser, et al. (2011). "NaV1.7 accumulates and co-localizes with phosphorylated ERK1/2 within transected axons in early experimental neuromas." Experimental Neurology **230**(2): 273-279.
Pertin, M., R.-R. Ji, et al. (2005). "Upregulation of the Voltage-Gated Sodium Channel β2 Subunit in Neuropathic Pain Models: Characterization of Expression in Injured and Non-Injured Primary Sensory Neurons." The Journal of Neuroscience **25**(47): 10970-10980.
Pickart, C. M. (2001). "Mechanisms underlying ubiquitination." Annu Rev Biochem **70**(1): 503-533.
Pradhan, A. A., M. L. Smith, et al. (2012). "Ligand-directed signalling within the opioid receptor family." British Journal of Pharmacology **167**(5): 960-969.
Price, M. P., G. R. Lewin, et al. (2000). "The mammalian sodium channel BNC1 is required for normal touch sensation." Nature **407**(6807): 1007-1011.
Price, M. P., S. L. McIlwrath, et al. (2001). "The DRASIC Cation Channel Contributes to the Detection of Cutaneous Touch and Acid Stimuli in Mice." Neuron **32**(6): 1071-1083.
Priest, B. T. and G. J. Kaczorowski (2007). "Blocking sodium channels to treat neuropathic pain." Expert Opinion on Therapeutic Targets **11**(3): 291-306.
Putz, U., J. Howitt, et al. (2008). "Nedd4 Family-interacting Protein 1 (Ndfip1) Is Required for the Exosomal Secretion of Nedd4 Family Proteins." Journal of Biological Chemistry **283**(47): 32621-32627.
Qu, Y., J. C. Rogers, et al. (1999). "Functional Roles of the Extracellular Segments of the Sodium Channel α Subunit in Voltage-dependent Gating and Modulation by β1 Subunits." Journal of Biological Chemistry **274**(46): 32647-32654.
Ragsdale, D., J. McPhee, et al. (1994). "Molecular determinants of state-dependent block of Na+ channels by local anesthetics." Science **265**(5179): 1724-1728.
Raman, I. M. and B. P. Bean (1997). "Resurgent Sodium Current and Action Potential Formation in Dissociated Cerebellar Purkinje Neurons." The Journal of Neuroscience **17**(12): 4517-4526.

Ranscht, B. (1988). "Sequence of contactin, a 130-kD glycoprotein concentrated in areas of interneuronal contact, defines a new member of the immunoglobulin supergene family in the nervous system." The Journal of Cell Biology **107**(4): 1561-1573.

Recio-Pinto, E., W. B. Thornhill, et al. (1990). "Neuraminidase treatment modifies the function of electroplax sodium channels in planar lipid bilayers." Neuron **5**(5): 675-684.

Renganathan, M., T. R. Cummins, et al. (2001). "Contribution of Na(v)1.8 sodium channels to action potential electrogenesis in DRG neurons." Journal of Neurophysiology **86**: 629-640.

Reynolds, D. V. (1969). "Surgery in the Rat during Electrical Analgesia Induced by Focal Brain Stimulation." Science **164**(3878): 444-445.

Ritchie, J. M., J. A. Black, et al. (1990). "Sodium channels in the cytoplasm of Schwann cells." Proc Natl Acad Sci U S A **87**(23): 9290-9294.

Rivera-Arconada, I. and J. A. Lopez-Garcia (2006). "Retigabine-induced population primary afferent hyperpolarisation in vitro." Neuropharmacology **51**(4): 756-763.

Rizo, J. and T. C. Sudhof (1998). "C2-domains, structure and function of a universal Ca2+-binding domain." J Biol Chem **273**(26): 15879-15882.

Rougier, J. S., M. Albesa, et al. (2012). "Long QT syndrome type 3 caused by a PY-motif mutation leading to altered ubiquitylation and increased expression of Nav1.5 in knock-in mice." Faseb Journal **26**.

Rougier, J. S., M. X. van Bemmelen, et al. (2005). "Molecular determinants of voltage-gated sodium channel regulation by the Nedd4/Nedd4-like proteins." Am J Physiol Cell Physiol **288**(3): C692-701.

Rush, A. M., M. J. Craner, et al. (2005). "Contactin regulates the current density and axonal expression of tetrodotoxin-resistant but not tetrodotoxin-sensitive sodium channels in DRG neurons." European Journal of Neuroscience **22**(1): 39-49.

Rush, A. M., T. R. Cummins, et al. (2007). "Multiple sodium channels and their roles in electrogenesis within dorsal root ganglion neurons." The Journal of Physiology **579**(1): 1-14.

Sang, Q., M. H. Kim, et al. (2006). "Nedd4-WW Domain-Binding Protein 5 (Ndfip1) Is Associated with Neuronal Survival after Acute Cortical Brain Injury." The Journal of Neuroscience **26**(27): 7234-7244.

Sangameswaran, L., L. M. Fish, et al. (1997). "A novel tetrodotoxin-sensitive, voltage-gated sodium channel expressed in rat and human dorsal root ganglia." J Biol Chem **272**: 14805-14809.

Sangameswaran, L., L. M. Fish, et al. (1997). "A novel tetrodotoxin-sensitive, voltage-gated sodium channel expressed in rat and human dorsal root ganglia." J Biol Chem **272**(23): 14805-14809.

Sazuka, T., Y. Tomooka, et al. (1992). "Identification of a Developmentally Regulated Gene in the Mouse Central-Nervous-System Which Encodes a Novel Proline Rich Protein." Biochimica Et Biophysica Acta **1132**(3): 240-248.

Scherrer, G., N. Imamachi, et al. (2009). "Dissociation of the Opioid Receptor Mechanisms that Control Mechanical and Heat Pain." Cell **137**(6): 1148-1159.

Schild, L., Y. Lu, et al. (1996). "Identification of a PY motif in the epithelial Na channel subunits as a target sequence for mutations causing channel activation found in Liddle syndrome." EMBO Journal **15**(10): 2381-2387.

Schmidt, J., S. Rossie, et al. (1985). "A large intracellular pool of inactive Na channel alpha subunits in developing rat brain." Proc Natl Acad Sci U S A **82**(14): 4847-4851.

Schmidt, J. W. and W. A. Catterall (1987). "Palmitylation, sulfation, and glycosylation of the alpha subunit of the sodium channel. Role of post-translational modifications in channel assembly." J Biol Chem **262**(28): 13713-13723.

Scholz, J., D. C. Broom, et al. (2005). "Blocking Caspase Activity Prevents Transsynaptic Neuronal Apoptosis and the Loss of Inhibition in Lamina II of the Dorsal Horn after Peripheral Nerve Injury." Journal of Neuroscience **25**(32): 7317-7323.

Scholz, J., R. J. Mannion, et al. (2009). "A Novel Tool for the Assessment of Pain: Validation in Low Back Pain." PLoS Med **6**(4): e1000047.
Shah, B. S., E. B. Stevens, et al. (2000). "beta3, a novel auxiliary subunit for the voltage-gated sodium channel, is expressed preferentially in sensory neurons and is upregulated in the chronic constriction injury model of neuropathic pain." European Journal of Neuroscience **12**(11): 3985-3990.
Shao, D., K. Okuse, et al. (2009). "Protein–protein interactions involving voltage-gated sodium channels: Post-translational regulation, intracellular trafficking and functional expression." The International Journal of Biochemistry & Cell Biology **41**(7): 1471-1481.
Shavkunov, A., N. Panova, et al. (2012). "Bioluminescence Methodology for the Detection of Protein-Protein Interactions Within the Voltage-Gated Sodium Channel Macromolecular Complex." Assay and Drug Development Technologies **10**(2): 148-160.
Shaw, G., S. Morse, et al. (2002). "Preferential transformation of human neuronal cells by human adenoviruses and the origin of HEK 293 cells." The FASEB Journal.
Shields, S. D., H. S. Ahn, et al. (2012). "Nav1.8 expression is not restricted to nociceptors in mouse peripheral nervous system." Pain **153**(10): 2017-2030.
Shih, S. C., K. E. Sloper-Mould, et al. (2000). "Monoubiquitin carries a novel internalization signal that is appended to activated receptors." EMBO J **19**(2): 187-198.
Sieburth, D., Q. Ch'ng, et al. (2005). "Systematic analysis of genes required for synapse structure and function." Nature **436**(7050): 510-517.
Smith, R. D. and A. L. Goldin (1998). "Functional analysis of the rat I sodium channel in xenopus oocytes." J Neurosci **18**(3): 811-820.
Snider, W. D. and S. B. McMahon (1998). "Tackling Pain at the Source: New Ideas about Nociceptors." Neuron **20**(4): 629-632.
Staub, O. and D. Rotin (1996). "WW domains." Structure **4**(5): 495-499.
Staub, O. and D. Rotin (2006). "Role of ubiquitylation in cellular membrane transport." Physiol Rev **86**(2): 669-707.
Stucky, C. L. and G. R. Lewin (1999). "Isolectin B4-Positive and -Negative Nociceptors Are Functionally Distinct." J Neurosci **19**(15): 6497-6505.
Sudol, M. and T. Hunter (2000). "NeW wrinkles for an old domain." Cell **103**(7): 1001-1004.
Suter, M. R., G. Kirschmann, et al. (2013). "Rufinamide Attenuates Mechanical Allodynia in a Model of Neuropathic Pain in the Mouse and Stabilizes Voltage-gated Sodium Channel Inactivated State." Anesthesiology **118**(1): 160-172 110.1097/ALN.1090b1013e318278cade.
Suter, M. R., M. Papaloïzos, et al. (2003). "Development of Neuropathic Pain in the Rat Spared Nerve Injury Model Is Not Prevented by a Peripheral Nerve Block." Anesthesiology **99**(6): 1402-1408.
Tate, S., S. Benn, et al. (1998). "Two sodium channels contribute to the TTX-R sodium current in primary sensory neurons." Nat Neurosci **1**(8): 653-655.
Tateyama, M., J. Kurokawa, et al. (2003). "Stimulation of Protein Kinase C Inhibits Bursting in Disease-Linked Mutant Human Cardiac Sodium Channels." Circulation **107**(25): 3216-3222.
Taylor, C. P., N. S. Gee, et al. (1998). "A summary of mechanistic hypotheses of gabapentin pharmacology." Epilepsy Research **29**(3): 233-249.
Thakor, D., A. Lin, et al. (2009). "Increased peripheral nerve excitability and local NaV1.8 mRNA up-regulation in painful neuropathy." Molecular Pain **5**(1): 14.
Tracey, I. and M. C. Bushnell (2009). "How Neuroimaging Studies Have Challenged Us to Rethink: Is Chronic Pain a Disease?" The Journal of Pain **10**(11): 1113-1120.
Tulleuda, A., B. Cokic, et al. (2011). "TRESK channel contribution to nociceptive sensory neurons excitability: modulation by nerve injury." Molecular Pain **7**(1): 30.
Turk, D. C., J. Audette, et al. (2010). "Assessment and Treatment of Psychosocial Comorbidities in Patients With Neuropathic Pain." Mayo Clinic Proceedings **85**(3): S42-S50.

Tyrrell, L., M. Renganathan, et al. (2001). "Glycosylation Alters Steady-State Inactivation of Sodium Channel Nav1.9/NaN in Dorsal Root Ganglion Neurons and Is Developmentally Regulated." The Journal of Neuroscience **21**(24): 9629-9637.

Ueda, H. (2006). "Molecular mechanisms of neuropathic pain–phenotypic switch and initiation mechanisms." Pharmacology & Therapeutics **109**(1–2): 57-77.

van Bemmelen, M. X., J. S. Rougier, et al. (2004). "Cardiac Voltage-Gated Sodium Channel Nav1.5 Is Regulated by Nedd4-2 Mediated Ubiquitination." Circulation Research **95**(3): 284-291.

Varga, A., K. Bolcskei, et al. (2006). "Relative roles of protein kinase A and protein kinase C in modulation of transient receptor potential vanilloid type 1 receptor responsiveness in rat sensory neurons in vitro and peripheral nociceptors in vivo." Neuroscience **140**(2): 645-657.

Vijayaragavan, K., M. Boutjdir, et al. (2004). "Modulation of Nav1.7 and Nav1.8 Peripheral Nerve Sodium Channels by Protein Kinase A and Protein Kinase C." Journal of Neurophysiology **91**(4): 1556-1569.

Vijayaragavan, K., M. E. O'Leary, et al. (2001). "Gating Properties of Nav1.7 and Nav1.8 Peripheral Nerve Sodium Channels." The Journal of Neuroscience **21**(20): 7909-7918.

Vijayaragavan, K., A. J. Powell, et al. (2004). "Role of auxiliary beta1-, beta2-, and beta3-subunits and their interaction with Na(v)1.8 voltage-gated sodium channel." Biochem Biophys Res Commun **319**(2): 531-540.

Villarreal, C. F., D. Sachs, et al. (2009). "The peripheral pro-nociceptive state induced by repetitive inflammatory stimuli involves continuous activation of protein kinase A and protein kinase C epsilon and its NaV1.8 sodium channel functional regulation in the primary sensory neuron." Biochemical Pharmacology **77**(5): 867-877.

Waechter, C. J., J. W. Schmidt, et al. (1983). "Glycosylation is required for maintenance of functional sodium channels in neuroblastoma cells." Journal of Biological Chemistry **258**(8): 5117-5123.

Wall, P. D. and M. Devor (1983). "Sensory afferent impulses originate from dorsal root ganglia as well as from the periphery in normal and nerve injured rats." Pain **17**(4): 321-339.

Wall, P. D., M. Devor, et al. (1979). "Autotomy following peripheral nerve lesions: experimental anaesthesia dolorosa." Pain **7**(2): 103-111.

Wang, H. and C. J. Woolf (2005). "Pain TRPs." Neuron **46**(1): 9-12.

Watkins, L., E. Milligan, et al. (2001). "Glial activation: a driving force for pathological pain." Trends Neurosci **24**: 450 - 455.

Watson, P. (1983). "Amitriptyline Versus Placebo in Postherpetic Neuralgia - Reply." Neurology **33**(11): 1530-1531.

Waxman, S. G. and S. Dib-Hajj (2005). "Erythermalgia: molecular basis for an inherited pain syndrome." Trends Mol Med **11**: 555-562.

Waxman, S. G., J. D. Kocsis, et al. (1994). "Type III sodium channel mRNA is expressed in embryonic but not adult spinal sensory neurons, and is reexpressed following axotomy." Journal of Neurophysiology **72**: 466-470.

Wood, J. N. and N. Eijkelkamp (2012). "Noxious mechanosensation – molecules and circuits." Current Opinion in Pharmacology **12**(1): 4-8.

Woolf, C. J. (1983). "Evidence for a Central Component of Post-Injury Pain Hypersensitivity." Nature **306**(5944): 686-688.

Woolf, C. J. (2004). "Dissecting out mechanisms responsible for peripheral neuropathic pain: Implications for diagnosis and therapy." Life Sciences **74**(21): 2605-2610.

Woolf, C. J. and I. Decosterd (1999). "Implications of recent advances in the understanding of pain pathophysiology for the assessment of pain in patients." Pain: S141-S147.

Woolf, C. J. and Q. Ma (2007). "Nociceptorsâ€"Noxious Stimulus Detectors." Neuron **55**(3): 353-364.

Woolf, C. J. and R. J. Mannion (1999). "Neuropathic pain: aetiology, symptoms, mechanisms, and management." The Lancet **353**(9168): 1959-1964.

Woolf, C. J. and M. W. Salter (2000). "Neuronal Plasticity: Increasing the Gain in Pain." Science **288**(5472): 1765-1768.

Wu, G., M. Ringkamp, et al. (2001). "Early Onset of Spontaneous Activity in Uninjured C-Fiber Nociceptors after Injury to Neighboring Nerve Fibers." The Journal of Neuroscience **21**(8): RC140.

Wu, Z.-Z. and H.-L. Pan (2004). "Tetrodotoxin-sensitive and -resistant Na+ channel currents in subsets of small sensory neurons of rats." Brain Research **1029**(2): 251-258.

Yang, B. and S. Kumar (2009). "Nedd4 and Nedd4-2: closely related ubiquitin-protein ligases with distinct physiological functions." Cell Death Differ **17**(1): 68-77.

Yang, Y., Y. Wang, et al. (2004). "Mutations in SCN9A, encoding a sodium channel alpha subunit, in patients with primary erythermalgia." J Med Genet **41**: 171-174.

Yeomans, D. C., S. R. Levinson, et al. (2005). "Decrease in Inflammatory Hyperalgesia by Herpes Vector-Mediated Knockdown of Nav1.7 Sodium Channels in Primary Afferents." Human Gene Therapy **16**(2): 271-277.

Yu, E. J., S.-H. Ko, et al. (2005). "Distinct domains of the sodium channel beta3-subunit modulate channel-gating kinetics and subcellular location." Biochem. J. **392**(3): 519-526.

Yu, F. H., R. E. Westenbroek, et al. (2003). "Sodium Channel β4, a New Disulfide-Linked Auxiliary Subunit with Similarity to β2." The Journal of Neuroscience **23**(20): 7577-7585.

Zhang, H., L. Zhou, et al. (2004). "Acute nerve injury induces long-term potentiation of C-fiber evoked field potentials in spinal dorsal horn of intact rat." Sheng Li Xue Bao **56**: 591 - 596.

Zhang, J. M., D. F. Donnelly, et al. (1997). "Axotomy Increases the Excitability of Dorsal Root Ganglion Cells With Unmyelinated Axons." Journal of Neurophysiology **78**(5): 2790-2794.

Zhang, Y., H. A. Hartmann, et al. (1999). "Glycosylation influences voltage-dependent gating of cardiac and skeletal muscle sodium channels." J Membr Biol **171**(3): 195-207.

Zhou, J., H.-G. Shin, et al. (2002). "Phosphorylation and Putative ER Retention Signals Are Required for Protein Kinase A-Mediated Potentiation of Cardiac Sodium Current." Circulation Research **91**(6): 540-546.

Zimmer, T. and K. Benndorf (2002). "The human heart and rat brain IIA Na+ channels interact with different molecular regions of the beta1 subunit." J Gen Physiol **120**(6): 887-895.

5. Appendices

(1) Figure of time course of Nedd4-2 expression in DRGs after sham and SNI surgery

(2) Figure of constitutive levels of Nedd4/Nedd4-like ubiquitin ligase in HEK293 cells

(3) Figure of competition between Nedd4-2 and β-subunits on $Na_v1.7$ in HEK293 cells.

(4) Manuscript to be soon submitted to *Molecular Pain*: Voltage-gated sodium channels expression in mice DRG after SNI leads to re-evaluation of injured fibers projections. I participated to the conception and design of the experiments. I wrote the first draft of the manuscript and revised versions. I prepared the figures.

(5) Contribution to publications:

a. "Neuronal expression of the ubiquitin ligase Nedd4-2 in rat dorsal root ganglia: modulation in the spared nerve injury model of neuropathic pain" in *Neuroscience* (Cachemaille, Laedermann et al. 2012). I participated to the conception and design of the experiments. I performed some of the biochemical experiments. I revised the manuscript.

b. "Rufinamide attenuates mechanical allodynia in a model of neuropathic pain in the mouse and stabilizes voltage-gated sodium channel inactivated state" in *Anesthesiology* (Suter, Kirschmann et al. 2013). I performed the patch-clamp experiment on dissociated DRG neurons. I revised the manuscript.

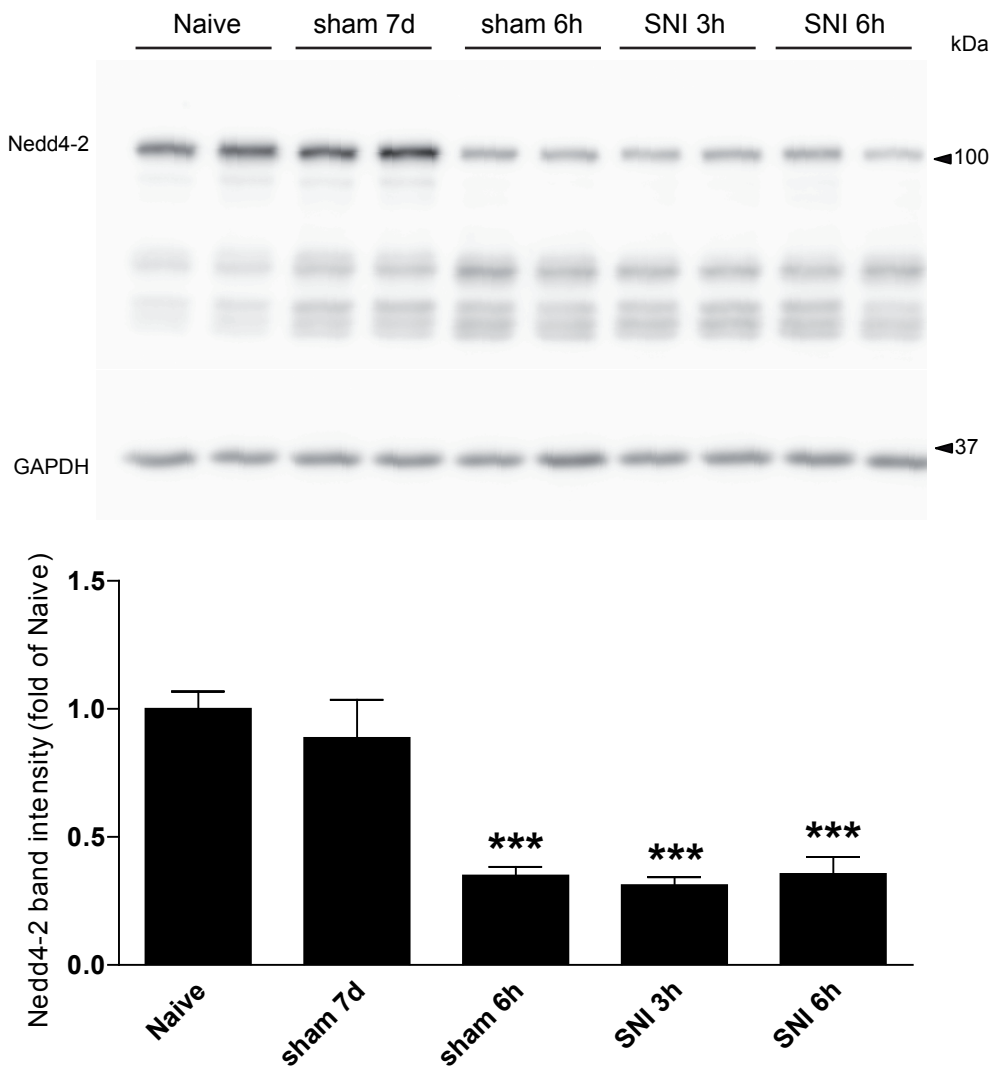

Appendix 1. Nedd4-2 expression in DRGs is reduced in sham and SNI in early time points after surgery.
Representative western blot analysis showing the decrease of Nedd4-2 after 6 hours in both sham and SNI conditions in L4/5 DRGs and its associated quantification. Data are expressed as means ± SEM, $n = 4$ samples for each time point/group. ***$P < 0.001$ by one-way ANOVA, *post hoc* Bonferroni test. Glyceraldehyde 3-phosphate dehydrogenase (GAPDH) was used as a loading control.

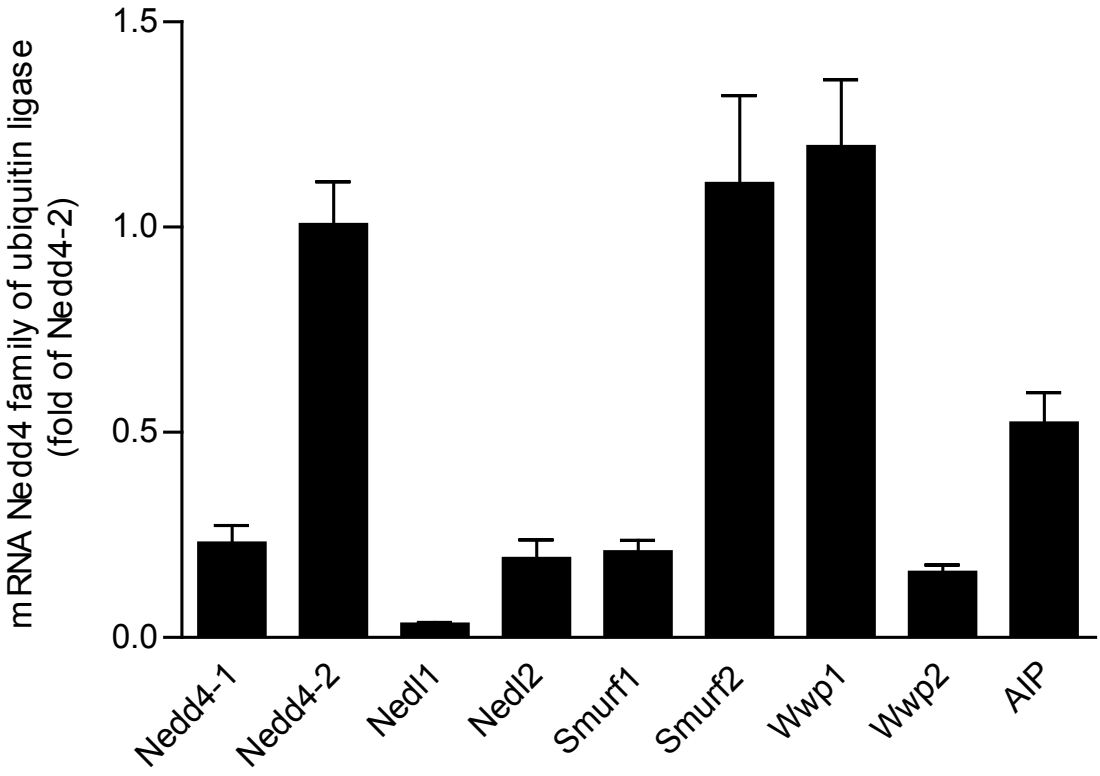

Appendix 2. Constitutive transcript levels of Nedd4/Nedd4-like E3 subfamily members in HEK293 cells. Levels of transcripts were normalized using GAPDH as a reference gene and further normalized to Nedd4-2 levels. Data are expressed as means ± SEM, *n* = 3 samples per group and run in triplicate.

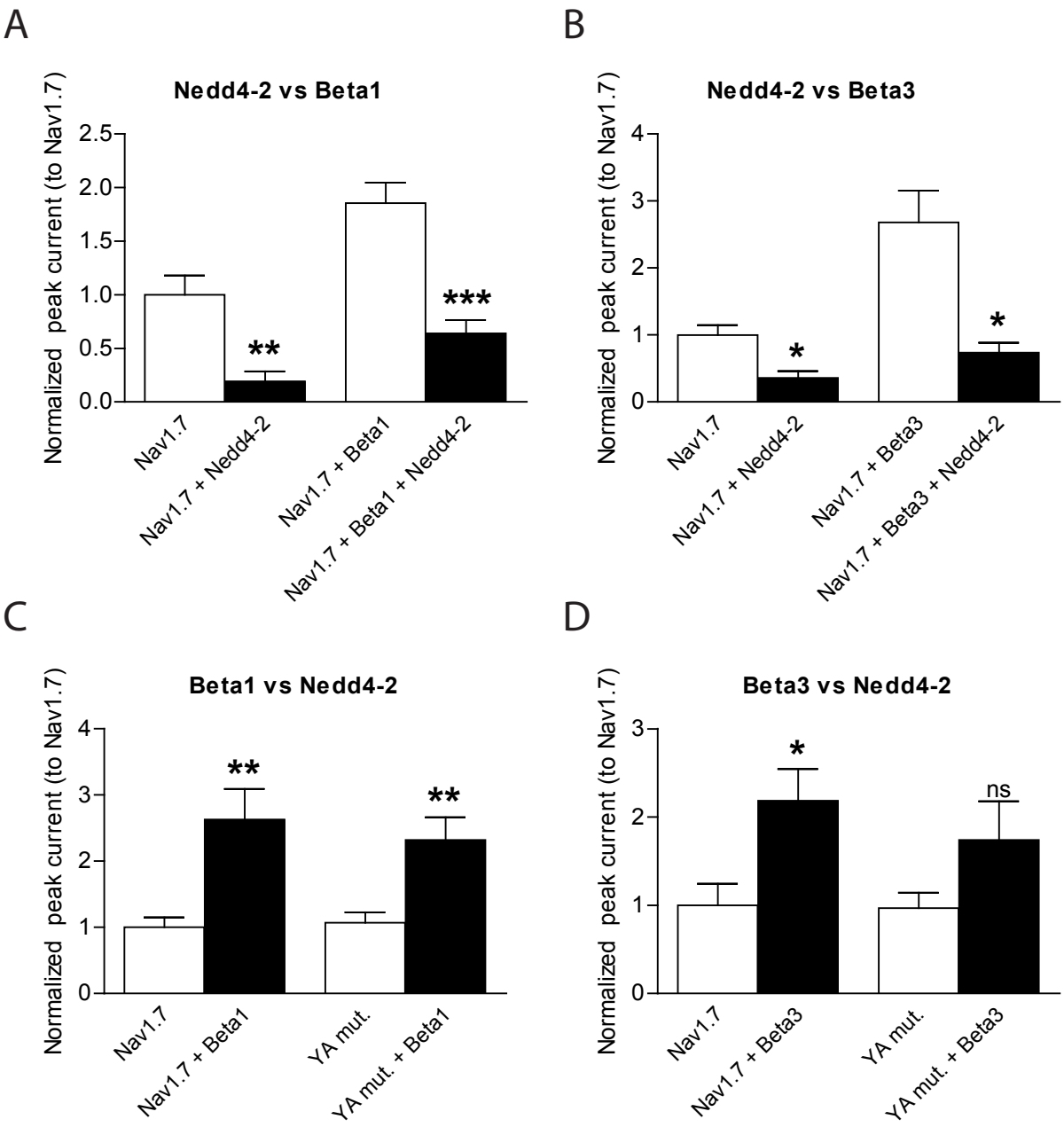

Appendix 3. β-subunits and Nedd4-2 are not competing to regulate $Na_v1.7$ current densities in HEK293 cells. A) Bar graph quantification of $Na_v1.7$ current densities showing that β1-subunit does not hinder Nedd4-2 downregulatory effect (-80% with $Na_v1.7$ alone, and -65% for $Na_v1.7$ co-transfected with β1-subunit). B) Bar graph quantification of $Na_v1.7$ current densites showing that β3-subunit does not hinder Nedd4-2 downregulatory effect (-64% with $Na_v1.7$ alone, and -73% for $Na_v1.7$ co-transfected with β3-subunit). C) Bar graph quantification of $Na_v1.7$ current densities showing that β 1-subunit has similar upregulatory effect on $Na_v1.7$ (+160%) than on YA mutant (+119%). D) Bar graph quantification of $Na_v1.7$ current densites showing that β3-subunit has the same upregulatory effect on $Na_v1.7$ (+119%) than on YA mutant (+81%). These results suggest that these two pathways do not compete one with another. Data are expressed as means ± SEM. Student's *t*-test, *n* = 8-12 for each condition.

Voltage-gated sodium channels expression in mice DRG after SNI leads to re-evaluation of injured fibers projections

Cédric J Laedermann[1,3], Marie Pertin[1,3], Marc R Suter[1],Isabelle Decosterd[1,2]

[1]Pain Center, Department of Anesthesiology, University Hospital Center and University of Lausanne, Lausanne, 1011, Switzerland.
[2]Department of Fundamental Neurosciences, University of Lausanne, Lausanne, 1005, Switzerland.
[3]These authors contributed equally to this work as co-authors

Corresponding author:

Cédric Laedermann
Pain Center, Department of Anesthesiology,
University Hospital Center and University of Lausanne, 1011 Lausanne, Switzerland
Email: cedric.laedermann@unil.ch

Abstract

Electrical activity in nerve fibers is mainly carried by voltage-gated sodium channels (Na_vs), and their dysregulation is suspected to play a major role in hyperexcitability associated with neuropathic pain. We studied the modification in the transcriptional levels of Na_vs in dorsal root ganglia (DRG) in the spared nerve injury (SNI) model of neuropathic pain in mice. This model allows the investigation of Na_vs changes in injured and non-injured neurons, which are intermingled in the same ganglia. We observed a strong downregulation of every Na_vs isoform, even $Na_v1.3$, which was previously shown to be strongly upregulated in rat neuropathic pain models, suggesting differences between these two species. We also used the spinal nerve ligation (SNL), where cell bodies of injured and non-injured fibers are anatomically separated in different DRGs, to evaluate the contribution of the axotomy itself in Na_vs downregulation. Besides the transcription analysis of Na_vs, we performed a careful characterization of axotomized neurons projection to L3, L4 and L5 DRGs after SNI by studying Activating Transcription Factor 3 (ATF3) expression, a known marker of nerve injury. This highlighted another major difference between mice and rats; most injured fibers actually find their cell bodies in L3 and L4 after SNI in mice whereas they were mostly found in L4 and L5 DRGs in the rats. The spared sural nerve, through which the overrated pain signal is transmitted in behavioral studies, mostly finds its origin in L4 and L5 DRGs. Thus, L3 is enriched with injured neurons, L4 with a mixture of injured and non-injured neurons, and L5 is enriched in non-injured neurons after SNI. They should be pooled only with caution in SNI studies in mice. We conclude that the largest Na_vs downregulation occurs in the DRGs harboring axotomized fibers and that there is a rostral shift of the DRGs harboring injured fibers in the C57BL/6J mice as compared to the rat.

Keywords

Voltage-gated sodium channels (Na_vs), qRT-PCR, neuropathic pain, dorsal root ganglia (DRG), sciatic nerve, spared nerve injury (SNI), spinal nerve ligation (SNL), nerve injury, Activating Transcription Factor 3 (ATF3).

Background

Increased electric activity is a major mechanism in the development of neuropathic pain following peripheral nerve injury. Spontaneous discharges can originate from both injured and non-injured nerve fibers or from dorsal root ganglia (DRG) (Wall and Devor 1983; Liu, Wall et al. 2000; Wu, Ringkamp et al. 2001; Ma, Shu et al. 2003; Amir, Kocsis et al. 2005; Djouhri, Koutsikou et al. 2006). Voltage-gated sodium channels (Na_vs) are key players in carrying cellular excitability (Catterall, Goldin et al. 2005) and are capital for pain processing (Liu and Wood 2011). Na_vs are heteromeric protein composed of a large pore-forming α-subunit and small β-auxiliary subunits (Catterall 2000; Brackenbury and Isom 2011). From the nine distinct channel isoforms described ($Na_v1.1$ to $Na_v1.9$), $Na_v1.5$, $Na_v1.8$ and $Na_v1.9$ are resistant to tetrodotoxin (TTX). All isoforms, except $Na_v1.4$ and $Na_v1.5$, are expressed in DRGs, $Na_v1.7$ being the most expressed TTX-sensitive isoform (Black, Dib-Hajj et al. 1996; Rush, Cummins et al. 2007; Berta, Poirot et al. 2008; Fukuoka, Kobayashi et al. 2008; Fukuoka and Noguchi 2011; Ho and O'Leary 2011). Nerve-injury-mediated hyperexcitability has been proposed to result from altered expression of Na_vs (Gold, Weinreich et al. 2003; Chahine, Ziane et al. 2005; Study and Kral 2005). These changes in Na_v expression occur in both injured and non-injured neurons in rats (Decosterd, Ji et al. 2002; Fukuoka and Noguchi 2002; Gold, Weinreich et al. 2003; Pertin, Ji et al. 2005). In different experimental models of neuropathic pain in rats mRNAs of most Na_vs were downregulated in the DRGs (Dib-Hajj, Black et al. 1996; Cummins and Waxman 1997; Dib-Hajj, Tyrrell et al. 1998; Sleeper, Cummins et al. 2000; Berta, Poirot et al. 2008) except for an increase of $Na_v1.3$ transcript (Waxman, Kocsis et al. 1994; Cummins and Waxman 1997; Berta, Poirot et al. 2008). Na_vs changes in mice models of neuropathic pain have, however, seldom been investigated.

The various animal models of neuropathic pain involving nerve transection and/or ligation developed to study the pain mechanisms exhibit different relation between injured and non-injured fibers. The first behavioral model of nerve injury used complete sciatic nerve transection (Wall, Devor et al. 1979). This model did probably not reflect the partial nerve injury observed in most neuropathic pain patients which involve also signals arising from intact sensory neurons (Campbell and Meyer 2006). Since then, models of partial injuries have been described which also allow evoked behavioral testing of the hindpaw. The L5 spinal nerve ligation (SNL) is an experimental neuropathic pain model which displays a clear separation between injured and non-injured cell bodies (Kim and Chung 1992). This model does not allow cross-talk between injured and non-injured cell bodies in respectively L5 and

L4 DRGs. The spared nerve injury model (SNI) (Decosterd and Woolf 2000) involves a lesion of two of the three terminal branches of the sciatic nerve, the common peroneal and tibial nerves, sparing the sural nerve, and induces mechanical and thermal hypersensitivity in the territory of the sural nerve. In this model, severed and intact nerves are intermingled in the same DRG which may allow cross-excitation between cell bodies (Devor and Wall 1990; Amir and Devor 1996) as well as ephaptic cross-talk along the fibers (Lisney and Pover 1983). Originally carried out in rats, the SNI model was further transposed and validated in mice (Bourquin, Süveges et al. 2006). To our knowledge, a careful characterization of injured and non-injured fibers projection to DRGs has not been carried in mice after SNI and the assumption of neuroanatomical similarities between the two species, rat and mice, is possibly not correct (Rigaud, Gemes et al. 2008).

In this study, we investigated the changes in Na_vs transcription in mice DRGs following SNI and SNL surgeries. To correlate Na_vs expression to injury we also studied the projection of injured and intact fibers to L3, L4 and L5 DRGs after SNI.

Results

Expression of Na_vs in mice L4 and L5 DRGs

We first assessed the level of expression of Na_vs in the DRGs of sham operated mice using qRT-PCR (Figure 1). Constitutively, $Na_v1.7$ is the most expressed TTX sensitive isoform in L4 and L5 DRGs as it was in the rat (Berta, Poirot et al. 2008; Fukuoka, Kobayashi et al. 2008; Ho and O'Leary 2011). Consistent with observations in rats, $Na_v1.8$ is also highly expressed in mice L4 and L5 DRGs, but $Na_v1.9$ being the most expressed isoform is specific to mice.

Downregulation of Na_vs expression after SNI injury

Peripheral nerve injury leads to hyperexcitability, which is evidenced by ectopic discharges and is thought to be conducted by Na_vs. We thus analyzed Na_vs mRNA regulation after SNI in mice. In order to reduce the number of animals necessary for experiments, it is common to pool DRGs together. In parallel to what is performed in rats, we pooled L4 and L5 DRGs which we assumed should contain a mixture of cell bodies of injured and non-injured fibers. SNI induced an important downregulation of every isoforms tested (Figure 2A). $Na_v1.1$ was decreased by -45%, $Na_v1.2$ by -17%, $Na_v1.3$ by -26%, $Na_v1.6$ by -34%, $Na_v1.7$ by -31%, $Na_v1.8$ by -38% and $Na_v1.9$ by -40% compared to sham.

How a decrease in Na_vs mRNA in the DRG could contribute to hyperexcitability remains under debate, but several explanations have been proposed; besides the fact that a reduction of mRNA does not necessarily mean a reduction of protein level, a potential reason invoked is a redistribution of the Na_vs mRNA from the cell body to the sciatic nerve where it will be translated and gain its function (Thakor, Lin et al. 2009). It is also possible that an induction of translation to increase *de novo* synthesis of proteins, which will be subsequently redirected along axons, will lead to a reduction of transcriptional levels.

Our results highlight an important difference between mice and rats: whereas $Na_v1.3$ is much increased in rats (Waxman, Kocsis et al. 1994; Black, Cummins et al. 1999; Lindia, Köhler et al. 2005; Berta, Poirot et al. 2008), we observed a downregulation of this isoform in mice after SNI. Despite controversies in the role of sodium channels in neuropathic pain, the upregulation of $Na_v1.3$ is commonly thought to be a main candidate for neuropathic pain-associated hyperexcitability in rats (Cummins and Waxman 1997; Black, Cummins et al. 1999). This was recently confirmed by knocking down this gene in rat after nerve injury which led to an attenuation of nerve injury-induced neuropathic pain symptoms (Samad, Tan et al. 2013). However, our results indicate that the implication of $Na_v1.3$ might be different in

mice; this is corroborated by the normal development of neuropathic pain symptoms in $Na_v1.3$ null mutant mice (Nassar, Baker et al. 2006).

Axotomy is responsible for the downregulation of Na_vs

Because L4 and L5 DRGs contain both injured and adjacent non-injured neurons after SNI and to answer whether axotomy by itself is responsible for change in Na_vs expression, we then performed L5 SNL. We thus compared L4 non-injured and L5 injured DRGs to their homologue DRGs in sham conditions. We observed a highly significant decrease in the mRNA expression of almost every Na_vs in the injured L5 DRG. $Na_v1.1$ was decreased by -61%, $Na_v1.3$ by -47%, $Na_v1.6$ by -63%, $Na_v1.7$ by -53%, $Na_v1.8$ by -74%, $Na_v1.9$ by -68%. Only $Na_v1.2$ remained unchanged in injured L5 DRG (Figure 2B). In contrast, there was no modification in Na_vs expression in the non-injured L4 DRG compared to sham operated animals with the exception of a decrease of $Na_v1.1$ mRNA by -33%.

These results seem to indicate that the modification in Na_vs expression is due to and exclusively occurring in injured fibers, consistent with a previous study performed in the rat SNL model (Fukuoka, Yamanaka et al. 2012). However, this result contrasts with our previous study carried in the rat after SNL (Berta, Poirot et al. 2008) where we observed a small, but significant increase of $Na_v1.6$, $Na_v1.7$, $Na_v1.8$ and $Na_v1.9$ in L4 non-injured DRG.

Regulation of Na_vs in distinct DRGs after SNI leads to re-assess the innervation.

To refine our analysis of DRGs housing injured and non-injured fibers after SNI, we collected L4 and L5 separately after surgery instead of combining them. We also collected L3 DRG, because, as can be observed in our dissection procedure (see Figure 3) and following the description of differential anatomical relationships in mice strains by Rigaud *et al.* (Rigaud, Gemes et al. 2008), this DRG is likely to provide fibers to the sciatic nerve. $Na_v1.1$ mRNA was significantly decreased by -52% in L4 and the same tendency was observed for L3 (-43%, $p = 0.082$) but not in L5 (-9%). $Na_v1.2$, $Na_v1.3$ and $Na_v1.6$ mRNA expression remained unchanged in all three ganglia despite an observable trend to decrease in L3 (-40%, -43% and -32% for $Na_v1.2$, $Na_v1.3$ and $Na_v1.6$, respectively) and L4 (-21%, -36% and -42% for $Na_v1.2$, $Na_v1.3$ and $Na_v1.6$, respectively) whereas no such trend was seen in L5 DRG (-2%, +29% and -11%, for $Na_v1.2$, $Na_v1.3$ and $Na_v1.6$, respectively) (Figure 2C). The high variability, due to the weak endogenous expression of these isoforms (Figure 1) and the necessity to pool the DRGs from 8 animals (see Methods), might be responsible for the lack of statistical significance in the decrease of $Na_v1.1$, $Na_v1.2$, $Na_v1.3$ and $Na_v1.6$. $Na_v1.7$ mRNA was significantly decreased in L3 (-35%), but remained statistically unchanged in L4 (-16%) and L5 (-16%). $Na_v1.8$ mRNA was strongly downregulated in L3 (-47%) and L4 DRGs (-49%)

and was also downregulated in L5 DRG, but to a minor extent (-19%). $Na_v1.9$ mRNA was downregulated in all three ganglia to a similar level (-27% for L3, -37% for L4 and -29% for L5).

Our observations in the SNL model, made us hypothesize that the injury is responsible for the decrease of Na_vs expression. Our results in the SNI model, when analyzing separately each DRG from L3 to L5, consistently shows a more important downregulation of Na_vs expression in L3 and L4 as compared to L5 (even if not always statistically significant). This raises the possibility that L3 and L4 (rather than L4 and L5) harbor most of the injured fibers following SNI surgery.

Identification of L3, L4 and L5 DRGs in C57BL/6J mice

Segmentation of the lumbar vertebral column varies significantly between different mice strains (Green 1941). Rigaud *et al.* recently demonstrated that DBA/2J strain possess five lumbar bony segments, whereas C57BL/6J strain possess six segments (Rigaud, Gemes et al. 2008). Because of this variability between strains, we describe the precise dissecting procedure to harvest L3, L4 and L5 DRGs in C57BL/6J mice.

Figure 3 shows a representative photography of the sciatic nerve, L2 to L6 spinal nerves with their DRGs, and spinal cord of a C57BL/6J mouse after dissection. The sites of SNI, $SNIv_{(cp,t)}$, a SNI variant sparing common peroneal (cp) and tibial (t) nerves (Bourquin, Süveges et al. 2006), and SNL injuries are illustrated on the picture and on the drawn extensions of the sciatic nerve trifurcation into sural, common peroneal and tibial nerves. Following the sciatic nerve into the rostral direction conducts to the first bifurcation heading to L5 spinal nerve and to the branches leading to L4/L3/L2 DRGs. Based on the dissection, it is likely that L3 DRG also receives afferents from the femoral/saphenous nerve, which can help to identify the correct DRGs. Unlike in the rat, the sciatic nerve in the mice does not find any of its fibers originating from the L6 DRG, which seems to confirm a rostral shift in the mice to find homologous DRGs as compared to the rat (Rigaud, Gemes et al. 2008*)*.

Injured fibers in the SNI model in the mice project to L3 and L4

In rats, 98% of sciatic nerve fibers originate from L4-L5 DRGs, whereas the saphenous nerve (part of the femoral nerve) fibers have their cell somas located in the L3 DRG (Swett, Torigoe et al. 1991). This explains that L4 and L5 are the main DRGs of interest in the SNI model in rats. However, Rigaud *et al* demonstrated that rats L4-L5 DRGs rather find their functional and anatomical homologous in the mice L3-L4 DRGs (Rigaud, Gemes et al. 2008). The latter, in addition to our observations that L3 DRG shows a stronger downregulation of Na_vs transcript as compared to L5, suggest that the ganglia likely to be subject to injury-related

phenotypic changes might need to be reconsidered in mice. We consequently investigated the amount of injured fibers received by each ganglion after SNI. Using immunofluorescence (IF), we studied the expression of ATF3, a member of ATF/CREB family and marker of axotomized neurons (Tsujino, Kondo et al. 2000; Tsuzuki, Kondo et al. 2001). In sham operated animals, ATF3-Immunoreactivity (IR) is only weakly observable and reaches a maximum of 8% for L3 (Supplemental Figure 1 and Figure 4B). Because naïve animals showed no IR for ATF3 at all (Supplemental Figure 1), it is likely that surgical exposure by itself already induces the activation of ATF3 expression as it has already been proposed (Shortland, Baytug et al. 2006). Seven days after SNI surgery, the percentage of ATF3 positive cells in L3 (37%) and L4 DRGs (34%) was significantly increased as compared to sham condition (Figure 4A, B) whereas in L5 the low percentage of ATF3 positive cells observed in sham was maintained (3%). This result contrasts with the strong increase of ATF3 expression observed in L5 in rats after SNI (Takahashi, Kikuchi et al. 2003) and clearly confirms that most of the common peroneal and tibial injured fibers have their cell bodies located in L3/L4 rather than in L5 DRGs in mice. We also studied the mRNA expression of ATF3 level in L3 to L5 DRGs using qRT-PCR. This approach supported the dramatic increased of ATF3 in L3 and L4 and the unchanged expression in L5 (Figure 4C).

So what is the relevance of L5 DRG in the mice SNI model? We used the same approach as above, but with the variant of the SNI transecting only the sural nerve ($SNIv_{(cp,t)}$), in order to investigate whether fibers from this nerve would project to L5 DRGs. Sham surgery revealed that the percentage of ATF3-IR cells was 8%, 7% and 4% for L3 to L5 respectively (Figure 5B), which was not different from sham condition of the traditional SNI. After $SNIv_{(cp,t)}$, there was a significant increase of ATF3-IR cells in L4 (17%) and L5 (15%) as compared to sham condition (Figure 5A, 5B). Conversely, the number of injured cells was not increased in L3 (7%). This suggests that sural nerve find its origin in L4 and L5 DRGs.

Even though we did not perform typical anatomical study using for instance retrolabelling, our results seem to confirm that tibial and common-peronal nerves, that represent the injured fibers in the SNI, predominantly find their origins in L3 and L4 DRGs. Nevertheless, the observation that transection of the sural nerves induces an increase of ATF3 postive neurons in L4 and L5, highlights the importance of L5 ganglion in SNI as well. This demonstrates that when using the SNI model in mice, DRGs should be pooled with caution because L3, L4 and L5 DRGs provide very different information. L3 DRGs will be enriched in injured neurons, L4 will present a mixture of injured and non-injured neurons and finally L5 will mostly be enriched in spared sural neurons (Figure 6).

Conclusion

We here showed that the expression of most of Na_vs mRNAs is downregulated in the axotomized lumbar DRGs after SNI and SNL in mice. For SNI, this is similar to rats except for $Na_v1.3$ which is increased in rats. This phenotypic change is mostly due to axotomized neurons in SNI and SNL. Finally, we re-evaluated the projection of injured neurons after SNI. The injured common peroneal and tibial nerves are projecting to L3 and L4 DRGs and the non-injured sural nerve to L4 and L5 DRGs in C57BL/6J mice. This is of great importance when investigating nerve-injury mediated modification in DRGs after SNI in mice. L3 DRG should be harvested for the changes in the injured nerve, L4 for a mixture of injured and non-injured and finally L5 for the non-injured sural nerve.

Methods

Surgery:

All procedures were approved by the Committee on Animal Experimentation for the Canton of Vaud, Switzerland, in accordance with Swiss Federal Law on Animal Welfare and guidelines of the International Association for Study of Pain (Zimmermann 1983).

Spared nerve injury model (SNI) of neuropathic pain was previously described in rats (Decosterd and Woolf 2000; Pertin, Gosselin et al. 2012) and in mice (Bourquin, Süveges et al. 2006). Briefly, adult C57BL/6J mice (Charles River, L'Arbresle, France) were anesthetized with 1.5% isoflurane and after exposure of the sciatic nerve, the common peroneal and tibial nerves were ligated together with a 6.0 silk suture (Ethicon, Johnson and Johnson AG, Zug, Switzerland) and transected. In the SNI variant ($SNIv_{(cp,t)}$) (Bourquin, Süveges et al. 2006) the ligation and transection were performed on the sural nerve, leaving the common peroneal and tibial nerves intact. The incision was closed in distinct layers (muscle and skin). Sham surgery was performed similarly except for the nerve transection.

Spinal nerve ligation surgery (SNL) was adapted from the procedure described by Kim and Chung (Kim and Chung 1992) transposed to mice. Briefly, after skin and muscle incision the L5 transverse process of vertebra was exposed and carefully removed. The L4 and L5 spinal nerves were exposed and the L5 spinal nerve was tightly ligated and transected distal to the ligature. The incision was closed in distinct layers (muscle and skin).

Dissection:

Briefly, mice were terminally anesthetized with sodium pentobarbital (Esconarkon; Streuli Pharma AG, Uznach, Switzerland) and *biceps femoris* muscle of left thigh was incised. The artery *genus descendes* was used as a reference for muscle incision, which further lead to the exposure of the sciatic nerve and trifurcation to the peripheral branches: common peroneal, tibial and sural nerves. The sciatic nerve was followed in the rostral direction, removing muscular tissue, until reaching the vertebral column. Vertebral lamina, pedicles and spinous processes were trimmed away to expose spinal cord and DRGs. For the nomenclature of DRGs, refer to Figure 4.

Quantitative real-time Reverse Transcription PCR (qRT-PCR):

Ipsilateral DRGs were rapidly dissected and collected in RNA-later solution (Qiagen, Basel, Switzerland). For SNI, 2 series of mice were used, one with a pool of L4 and L5 together as

was usually done (4 DRGs pooled from 2 mice per sample) and one series where L3, L4 and L5 were dissected separately (8 DRGs pooled from 8 mice per sample). For SNL we always separate L4 and L5 DRGs (2 DRGs pooled from 2 mice per sample) as they represent respectively non-injured and injured neurons. For all conditions tested we used n = 3-4 samples. mRNA was extracted and purified with RNeasy Plus Mini kit (Qiagen) and quantified using RNA 6000 Nano Assay (Agilent Technologies AG, Basel, Switzerland). A total of 600 ng of RNA was reverse transcribed for each sample using Omniscript reverse transcriptase (Qiagen). Primer's sequences and working concentrations for Na_vs α-subunits, ATF3 and glyceraldehyde-3-phosphate deshydrogenase (GAPDH) can be found in Table 1.
We used GAPDH as reference gene to normalize Na_vs mRNA expression since it is not altered in SNI and SNL conditions (Renganathan, Dib-Hajj et al. 2002). Gene-specific mRNA analyses were performed using the iQ SYBR-green Supermix (BioRad, Reinach, Switzerland) and the iQ5 real-time PCR detection system (BioRad). Only reactions with appropriate amplification and melting curves determining the amplicon specificity were analyzed. All samples were run in triplicate.

Immunofluorescence:

One week after sham, SNI or $SNIv_{(cp,t)}$ surgery, animals were lethally anesthetized with sodium pentobarbital (Esconarkon) and transcardially perfused with saline solution, directly followed by paraformaldehyde 4% diluted in phosphate buffered saline (PBS). L3 to L5 DRGs were dissected and post-fixed at 4°C for 90 min and then transferred in sucrose solution (20% sucrose in PBS) overnight. The following day, tissues were mounted in cryoembedding fluid (Tissue-Tek; Sakura Finetek, Zoeterwoude, Holland), frozen, cryosectioned in 12µm-thick sections and thaw-mounted onto slides.
We used the rabbit anti-ATF3 antibody (1:300, Santa Cruz Biotechnology, Heidelberg, Germany) as nuclear marker of injured neurons and the goat anti-HuD antibody (Elav like proteins, 1:50, Santa Cruz Biotechnology) as marker of total neuron number. Secondary antibodies were as follow: Cy3-conjugated anti-rabbit (1:400, Jackson ImmunoResearch, Suffolk, UK) for ATF3 and AlexaFluor 488-conjugated anti-goat (Molecular Probes, Basel, Switzerland) for HuD. Standard protocols for fluorescent immunohistochemistry were used. Sections of DRGs were blocked for 30 min at room temperature (RT) with normal horse serum (NHS) 10% and PBS 1X-Triton X-100 0.3%. Primary antibodies were diluted in NHS 5% and PBS 1X-Triton X-100 0.1% and incubated on sections overnight at 4°C. Slides were

washed in PBS 1X and then incubated for 90 min at RT with the corresponding secondary antibody diluted in NHS 1% and PBS 1X-Triton X-100 0.1%. Slides were washed in PBS 1X and mounted in Mowiol medium (Calbiochem, Merck Millipore, Darmstadt, Germany).
Fluorescence was detected using an epifluorescent microscope (AxioVision, Carl Zeiss, Feldbach, Switzerland). Images were taken at 20× magnification, with the same parameters used between experimental conditions. The complete DRG images were reconstructed by juxtaposing the different images using Photoshop CS4 software (11.0, Sun Microsystems, Redwood City, CA). Mean cell counts from each DRG are the average of 4 to 7 sections. The first section was randomly selected and the next ones were chosen every 72 um from the series of consecutive cut sections. Four animals were analyzed per condition. Percentage of injured neurons was expressed as the number of ATF3-IR neurons over the total cell number (HuD-IR neurons). Note that the percentage of ATF3 positive cells is probably a slight under-estimation of the actual proportion of injured cells because it represents the ratio of ATF3 positive cells over HuD positive cells, which were counted independently to the presence or absence of the nucleus (one cell might have been counted twice in different stack).

Statistical analysis:

For immunofluorescence experiments, number of positive cells in sham and SNI were tested for statistical difference using bilateral unpaired Student's *t* test. For qPCR, normalized transcripts from 3 to 4 samples were compared in sham versus treated conditions using bilateral, unpaired Student's *t* test.

List of abbreviations

Voltage-gated sodium channels (Na_vs), dorsal root ganglia (DRG), spared nerve injury (SNI), spinal nerve ligation (SNL), activating transcription factor 3 (ATF3), immuno-reactivity (IR), tetrodotoxin (TTX),

Author contributions

The authors declare no competing interests.

Author contributions

M.P. performed SNI, $SNIv_{(cp,t)}$, immunofluorescence, cell counting and qPCR. C.J.L. wrote the manuscript and supervised experimental approach. M.R.S analyzed data and corrected the manuscript. I.D. supervised experimental approach and corrected the manuscript.

Acknowledgments

We thank Guylène Kirschmann for performing SNL surgery. This study was supported by grants from the Swiss National Science Foundation (31003A-124996 to I.D.) We would like to thank Prof. C. Kern, head of the Anesthesiology Department at CHUV, for his support.

Figure Legends

Figure 1:

Constitutive mRNA expression of Na_vs isoforms in sham mice DRGs.

Constitutive levels of mRNA were determined by qPCR and normalized using GAPDH as a reference gene. qPCR efficiencies were obtained by the standard curve method (Pertin, Ji et al. 2005) and integrated for calculation of the relative expression. Data are expressed as mean ± SEM, $n = 4$ samples (2 animals per sample).

Figure 2:

SNI and SNL modulate Na_vs mRNA expression in mice DRGs.

Transcription profile: (A) one week after SNI in pooled L4/L5 DRGs. $Na_v1.1$ ($p < 0.0001$), $Na_v1.2$ ($p = 0.0171$), $Na_v1.3$ ($p = 0.003$), $Na_v1.6$ ($p = 0.001$), $Na_v1.7$ ($p < 0.0001$), $Na_v1.8$ ($p < 0.0001$) and $Na_v1.9$ ($p < 0.0001$) are all downregulated after SNI. (B) One week after SNL in L4 and L5 DRGs. In injured L5 DRG (black bars), $Na_v1.1$ ($p = 0.005$), $Na_v1.3$ ($p = 0.017$), $Na_v1.6$ ($p = 0.006$), $Na_v1.7$ ($p = 0.011$), $Na_v1.8$ ($p = 0.001$) and $Na_v1.9$ ($p = 0.004$) were significantly decreased and only $Na_v1.2$ was unchanged ($p = 0.362$). In non-injured L4 DRG (white bars), only $Na_v1.1$ was decreased ($p = 0.045$) but $Na_v1.2$ ($p = 0.982$), $Na_v1.3$ ($p = 0.172$), $Na_v1.6$ ($p = 0.247$), $Na_v1.7$ ($p = 0.593$), $Na_v1.8$ ($p = 0.731$) and $Na_v1.9$ ($p = 0.378$) remained unchanged. (C) One week after SNI in separated L3, L4 and L5 DRGs. $Na_v1.1$ was only significantly downregulated in L4 (L3, $p = 0.082$; L4, $p = 0.023$; L5, $p = 0.253$). $Na_v1.2$ (L3, $p = 0.145$; L4, $p = 0.333$; L5, $p = 0.944$), $Na_v1.3$ (L3, $p = 0.139$, L4, $p = 0.189$, L5, $p = 0.344$), $Na_v1.6$ (L3, $p = 0.171$, L4, $p = 0.051$, L5, $p = 0.168$) remained statistically unchanged

in every DRG tested. $Na_v1.7$ was only significantly downregulated in L3 (L3, $p = 0.005$, L4, $p = 0.138$, L5, $p = 0.104$). $Na_v1.8$ (L3, $p = 0.001$, L4, $p < 0.001$, L5, $p = 0.021$) and $Na_v1.9$ (L3, $p = 0.031$; L4, $p = 0.006$; L5, $p = 0.046$) were downregulated in all three DRGs.

For A, B and C, mRNA levels are expressed as ratio of level in SNI/Sham or SNL/sham. Data are expressed as mean ± SEM, n = 3-4 samples, Student's t test to compare sham to SNI or SNL.

Figure 3:

Representative postero-lateral view of mouse DRGs dissection.

On the photography, L3, L4 and L5 spinal nerves (black arrows) linked to L3, L4 and L5 DRGs respectively, are the main contributors of the sciatic nerve. L6 does not contribute to the sciatic nerve. Sites of SNI, $SNIv_{(cp,t)}$ and SNL lesions are shown. SNI: Spared Nerve Injury; SNIv (cp,t): Spared Nerve Injury variant , sparing common peroneal (cp) and tibial (t) nerves; SNL: Spinal Nerve Ligation

Figure 4:

ATF3 expression increases in mice L3, and L4 but not L5 DRG neurons after SNI. (A) Representative immunofluorescence showing that ATF3 (marker of injured neurons, red) is up-regulated in L3 and L4 DRG neurons (HuD positive cells, green) after SNI. Scale bar = 50 µm. (B) Quantification of ATF3-Immunoreactivity (IR) in L3, L4 and L5 DRG neurons one week after SNI or sham surgery. ATF3-IR is increased in L3 ($p < 0.0001$) and L4 ($p < 0.0001$) after SNI but remained the same in L5 ($p = 0.986$). Data are expressed as mean ± SEM, $n = 4$ animals in each group. Student's t test. (C) mRNA levels of ATF3 one week after SNI compared to sham surgery in L3, L4 and L5 DRGs. ATF3 mRNA is increased in L3 ($p = 0.0003$) and L4 ($p = 0.0003$) but not in L5 ($p = 0.987$) after SNI. Levels of transcripts were first normalized to GAPDH as a reference gene and then to sham for each DRG. Data are expressed as mean ± SEM, n = 3-4 animals in each group. Student's t test. SNI: Spared Nerve Injury

Figure 5:

ATF3 expression increases in mice L4 and L5 but not L3 DRG neurons after $SNIv_{(cp,t)}$. Representative immunofluorescence showing that ATF3 (marker of injured neurons, red) is mostly upregulated in L4 and L5 DRG neurons (HuD positive cells, green). Scale bar = 50

μm. (B) Quantification of ATF3-IR in L3, L4 and L5 DRG neurons one week after $SNIv_{(cp,t)}$ or sham surgery. ATF3 is increased in L4 ($p < 0.002$) and L5 ($p < 0.002$) after $SNIv_{(cp,t)}$ but not in L5 ($p = 0.291$). Data are expressed as mean ± SEM, n = 4 animals in each group. Student's *t* test. $SNIv_{(cp,t)}$: Spared Nerve Injury variant , sparing common peroneal (cp) and tibial (t) nerves

Figure 6:

Schematic view of sciatic nerve branches with projections of injured fibers into DRGs. On the scheme, we show that tibial and common peroneal nerves predominantly originate in L3 and L4 DRGs (red fibers) while the sural mainly originate from L4 and L5 (blue fibers). SNI: Spared Nerve Injury; $SNIv_{(cp,t)}$: Spared Nerve Injury variant , sparing common peroneal (cp) and tibial (t) nerves.

Supplemental Figure 1:

Sham surgery increases ATF3 expression in L3, L4 and L5 mice DRG neurons. Representative immunofluorescence showing that ATF3 is also expressed in every DRG tested after sham surgery (see Figure 5B for quantification). Conversely, naïve animals show no ATF3-IR in any of the DRG tested (only L4 is shown). Scale bar = 50 μm.

Table 1:

Primer List.

References:

Amir, R. and M. Devor (1996). "Chemically Mediated Cross-Excitation in Rat Dorsal Root Ganglia." The Journal of Neuroscience **16**(15): 4733-4741.

Amir, R., J. D. Kocsis, et al. (2005). "Multiple interacting sites of ectopic spike electrogenesis in primary sensory neurons." J Neurosci **25**(10): 2576-2585.

Berta, T., O. Poirot, et al. (2008). "Transcriptional and functional profiles of voltage-gated Na(+) channels in injured and non-injured DRG neurons in the SNI model of neuropathic pain." Mol Cell Neurosci **37**(2): 196-208.

Black, J. A., T. R. Cummins, et al. (1999). "Upregulation of a Silent Sodium Channel After Peripheral, but not Central, Nerve Injury in DRG Neurons." Journal of Neurophysiology **82**(5): 2776-2785.

Black, J. A., S. Dib-Hajj, et al. (1996). "Spinal sensory neurons express multiple sodium channel alpha-subunit mRNAs." Brain Res Mol Brain Res **43**(1-2): 117-131.

Bourquin, A.-F., M. Süveges, et al. (2006). "Assessment and analysis of mechanical allodynia-like behavior induced by spared nerve injury (SNI) in the mouse." Pain **122**(1–2): 14.e11-14.e14.

Brackenbury, W. J. and L. L. Isom (2011). "Na Channel beta Subunits: Overachievers of the Ion Channel Family." Front Pharmacol **2**: 53.

Campbell, J. N. and R. A. Meyer (2006). "Mechanisms of Neuropathic Pain." Neuron **52**(1): 77-92.

Catterall, W. A. (2000). "From ionic currents to molecular mechanisms: the structure and function of voltage-gated sodium channels." Neuron **26**: 13-25.

Catterall, W. A., A. L. Goldin, et al. (2005). "International Union of Pharmacology. XLVII. Nomenclature and structure-function relationships of voltage-gated sodium channels." Pharmacol Rev **57**: 397-409.

Chahine, M., R. Ziane, et al. (2005). "Regulation of Nav channels in sensory neurons." Trends in Pharmacological Sciences **26**(10): 496-502.

Cummins, T. R. and S. G. Waxman (1997). "Downregulation of tetrodotoxin-resistant sodium currents and upregulation of a rapidly repriming tetrodotoxin-sensitive sodium current in small spinal sensory neurons after nerve injury." J Neurosci **17**(10): 3503-3514.

Decosterd, I., R. R. Ji, et al. (2002). "The pattern of expression of the voltage-gated sodium channels Na(v)1.8 and Na(v)1.9 does not change in uninjured primary sensory neurons in experimental neuropathic pain models." Pain **96**: 269-277.

Decosterd, I. and C. J. Woolf (2000). "Spared nerve injury: an animal model of persistent peripheral neuropathic pain." Pain **87**(2): 149-158.

Devor, M. and P. D. Wall (1990). "Cross-excitation in dorsal root ganglia of nerve-injured and intact rats." Journal of Neurophysiology **64**(6): 1733-1746.

Dib-Hajj, S., J. A. Black, et al. (1996). "Down-regulation of transcripts for Na channel alpha-SNS in spinal sensory neurons following axotomy." Proc Natl Acad Sci USA **93**: 14950-14954.

Dib-Hajj, S. D., L. Tyrrell, et al. (1998). "NaN, a novel voltage-gated Na channel, is expressed preferentially in peripheral sensory neurons and down-regulated after axotomy." Proc Natl Acad Sci U S A **95**: 8963-8968.

Djouhri, L., S. Koutsikou, et al. (2006). "Spontaneous Pain, Both Neuropathic and Inflammatory, Is Related to Frequency of Spontaneous Firing in Intact C-Fiber Nociceptors." The Journal of Neuroscience **26**(4): 1281-1292.

Fukuoka, T., K. Kobayashi, et al. (2008). "Comparative study of the distribution of the alpha-subunits of voltage-gated sodium channels in normal and axotomized rat dorsal root ganglion neurons." J Comp Neurol **510**(2): 188-206.

Fukuoka, T. and K. Noguchi (2002). "Contribution of the spared primary afferent neurons to the pathomechanisms of neuropathic pain." Molecular Neurobiology **26**(1): 57-67.

Fukuoka, T. and K. Noguchi (2011). "Comparative study of voltage-gated sodium channel alpha-subunits in non-overlapping four neuronal populations in the rat dorsal root ganglion." Neurosci Res **70**(2): 164-171.

Fukuoka, T., H. Yamanaka, et al. (2012). "Re-evaluation of the phenotypic changes in L4 dorsal root ganglion neurons after L5 spinal nerve ligation." Pain **153**(1): 68-79.

Gold, M. S., D. Weinreich, et al. (2003). "Redistribution of NaV1.8 in Uninjured Axons Enables Neuropathic Pain." The Journal of Neuroscience **23**(1): 158-166.

Green, E. L. (1941). "GENETIC AND NON-GENETIC FACTORS WHICH INFLUENCE THE TYPE OF THE SKELETON IN AN INBRED STRAIN OF MICE." Genetics **26**(2): 192-222.

Ho, C. and M. E. O'Leary (2011). "Single-cell analysis of sodium channel expression in dorsal root ganglion neurons." Mol Cell Neurosci **46**(1): 159-166.

Kim, S. H. and J. M. Chung (1992). "An experimental model for peripheral neuropathy produced by segmental spinal nerve ligation in the rat." Pain **50**(3): 355-363.

Lindia, J. A., M. G. Köhler, et al. (2005). "Relationship between sodium channel NaV1.3 expression and neuropathic pain behavior in rats." Pain **117**(1–2): 145-153.
Lisney, S. J. W. and C. M. Pover (1983). "Coupling between Fibers Involved in Sensory Nerve Neuromata in Cats." Journal of the Neurological Sciences **59**(2): 255-264.
Liu, C.-N., P. D. Wall, et al. (2000). "Tactile allodynia in the absence of C-fiber activation: altered firing properties of DRG neurons following spinal nerve injury." Pain **85**(3): 503-521.
Liu, M. and J. N. Wood (2011). "The roles of sodium channels in nociception: implications for mechanisms of neuropathic pain." Pain Med **12 Suppl 3**: S93-99.
Ma, C., Y. Shu, et al. (2003). "Similar Electrophysiological Changes in Axotomized and Neighboring Intact Dorsal Root Ganglion Neurons." Journal of Neurophysiology **89**(3): 1588-1602.
Nassar, M. A., M. D. Baker, et al. (2006). "Nerve injury induces robust allodynia and ectopic discharges in Nav1.3 null mutant mice." Mol Pain **2**(1): 33.
Pertin, M., R.-D. Gosselin, et al. (2012). The Spared Nerve Injury Model of Neuropathic Pain. Pain Research. Z. D. Luo, Humana Press. **851:** 205-212.
Pertin, M., R.-R. Ji, et al. (2005). "Upregulation of the Voltage-Gated Sodium Channel β2 Subunit in Neuropathic Pain Models: Characterization of Expression in Injured and Non-Injured Primary Sensory Neurons." The Journal of Neuroscience **25**(47): 10970-10980.
Renganathan, M., S. Dib-Hajj, et al. (2002). "Nav1.5 underlies the â€˜third TTX-R sodium currentâ€™ in rat small DRG neurons." Molecular Brain Research **106**(1â€“2): 70-82.
Rigaud, M., G. Gemes, et al. (2008). "Species and strain differences in rodent sciatic nerve anatomy: Implications for studies of neuropathic pain." Pain **136**(1–2): 188-201.
Rush, A. M., T. R. Cummins, et al. (2007). "Multiple sodium channels and their roles in electrogenesis within dorsal root ganglion neurons." The Journal of Physiology **579**(1): 1-14.
Samad, O. A., A. M. Tan, et al. (2013). "Virus-mediated shRNA Knockdown of Nav1.3 in Rat Dorsal Root Ganglion Attenuates Nerve Injury-induced Neuropathic Pain." Molecular Therapy **21**(1): 49-56.
Shortland, P. J., B. Baytug, et al. (2006). "ATF3 expression in L4 dorsal root ganglion neurons after L5 spinal nerve transection." European Journal of Neuroscience **23**(2): 365-373.
Sleeper, A. A., T. R. Cummins, et al. (2000). "Changes in expression of two tetrodotoxin-resistant sodium channels and their currents in dorsal root ganglion neurons after sciatic nerve injury but not rhizotomy." J Neurosci **20**: 7279-7289.
Study, R. E. and M. G. Kral (2005). "Spontaneous action potential activity in isolated dorsal root ganglion neurons from rats with a painful neuropathy." Pain **65**(2-3): 235-242.
Swett, J. E., Y. Torigoe, et al. (1991). "Sensory neurons of the rat sciatic nerve." Experimental Neurology **114**(1): 82-103.
Takahashi, N., S. Kikuchi, et al. (2003). "Expression of auxiliary β subunits of sodium channels in primary afferent neurons and the effect of nerve injury." Neuroscience **121**(2): 441-450.
Thakor, D., A. Lin, et al. (2009). "Increased peripheral nerve excitability and local NaV1.8 mRNA up-regulation in painful neuropathy." Molecular Pain **5**(1): 14.
Tsujino, H., E. Kondo, et al. (2000). "Activating Transcription Factor 3 (ATF3) Induction by Axotomy in Sensory and Motoneurons: A Novel Neuronal Marker of Nerve Injury." Molecular and Cellular Neuroscience **15**(2): 170-182.

Tsuzuki, K., E. Kondo, et al. (2001). "Differential regulation of P2X3 mRNA expression by peripheral nerve injury in intact and injured neurons in the rat sensory ganglia." Pain **91**(3): 351-360.

Wall, P. D. and M. Devor (1983). "Sensory afferent impulses originate from dorsal root ganglia as well as from the periphery in normal and nerve injured rats." Pain **17**(4): 321-339.

Wall, P. D., M. Devor, et al. (1979). "Autotomy following peripheral nerve lesions: experimental anaesthesia dolorosa." Pain **7**(2): 103-111.

Waxman, S. G., J. D. Kocsis, et al. (1994). "Type III sodium channel mRNA is expressed in embryonic but not adult spinal sensory neurons, and is reexpressed following axotomy." Journal of Neurophysiology **72**: 466-470.

Wu, G., M. Ringkamp, et al. (2001). "Early Onset of Spontaneous Activity in Uninjured C-Fiber Nociceptors after Injury to Neighboring Nerve Fibers." The Journal of Neuroscience **21**(8): RC140.

Zimmermann, M. (1983). "Ethical guidelines for investigations of experimental pain in conscious animals." Pain **16**(2): 109-110.

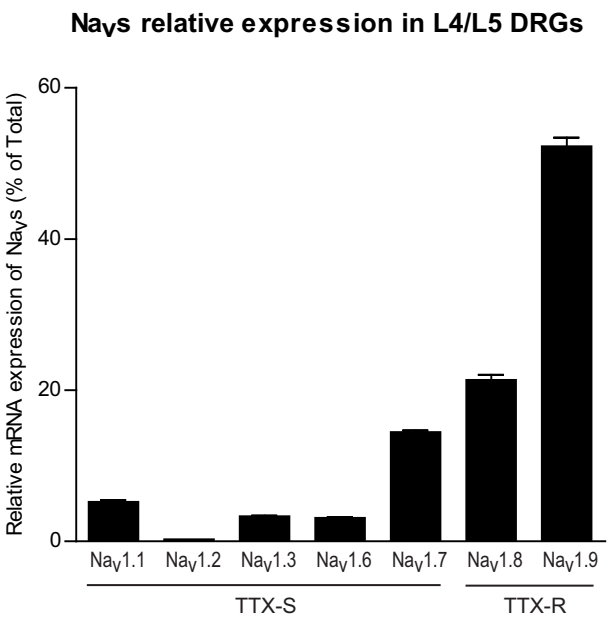
Na$_V$s relative expression in L4/L5 DRGs
Relative mRNA expression of Na$_V$s (% of Total)
60
40
20
0
Na$_V$1.1
Na$_V$1.2
Na$_V$1.3
Na$_V$1.6
Na$_V$1.7
Na$_V$1.8
Na$_V$1.9
TTX-S
TTX-R

Figure 1

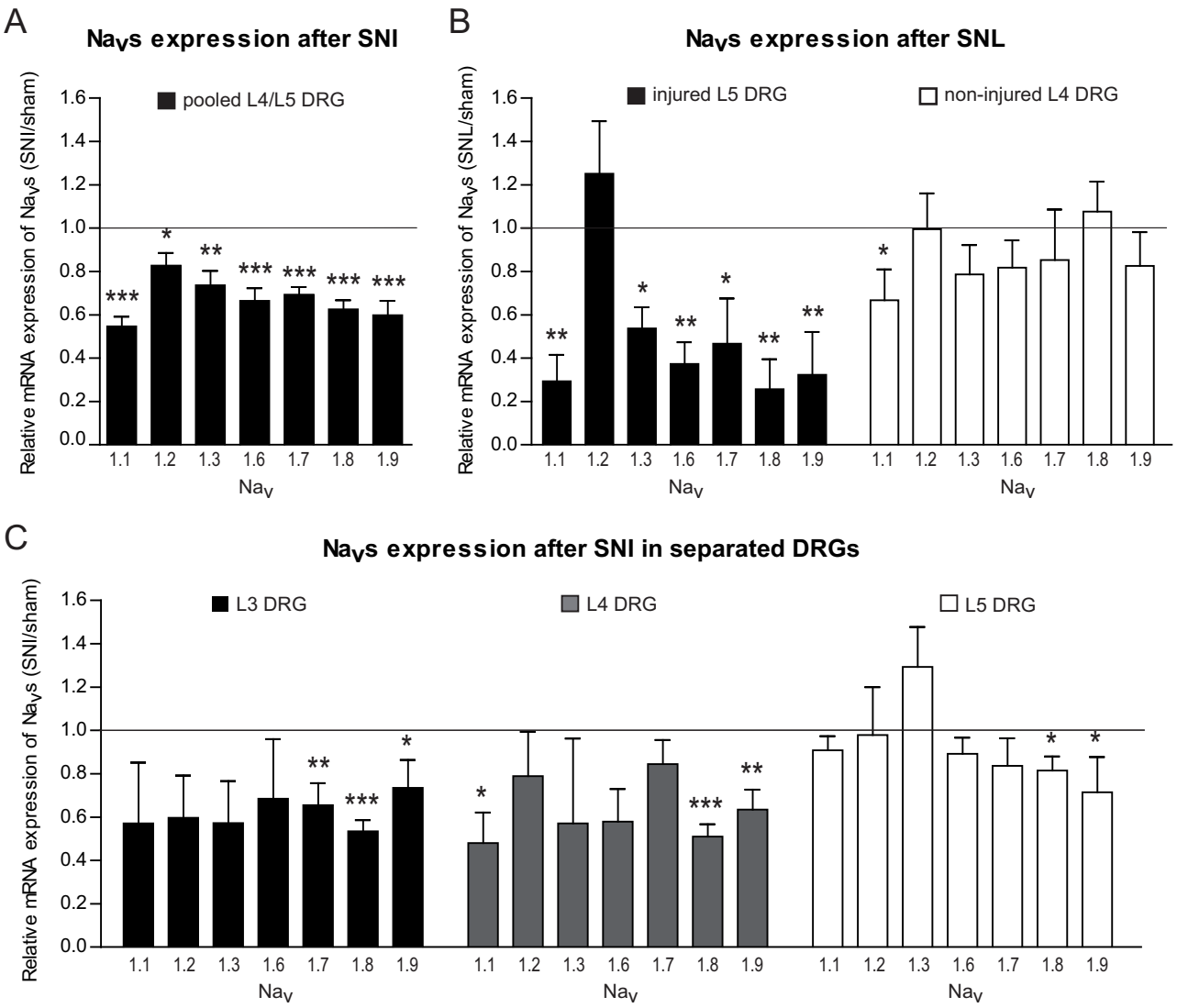
A
Na$_V$s expression after SNI
pooled L4/L5 DRG
Relative mRNA expression of Na$_V$s (SNI/sham)
1.6
1.4
1.2
1.0
0.8
0.6
0.4
0.2
0.0
1.1 1.2 1.3 1.6 1.7 1.8 1.9
Na$_V$
B
Na$_V$s expression after SNL
injured L5 DRG
non-injured L4 DRG
Relative mRNA expression of Na$_V$s (SNL/sham)
C
Na$_V$s expression after SNI in separated DRGs
L3 DRG
L4 DRG
L5 DRG
Relative mRNA expression of Na$_V$s (SNI/sham)

Figure 2

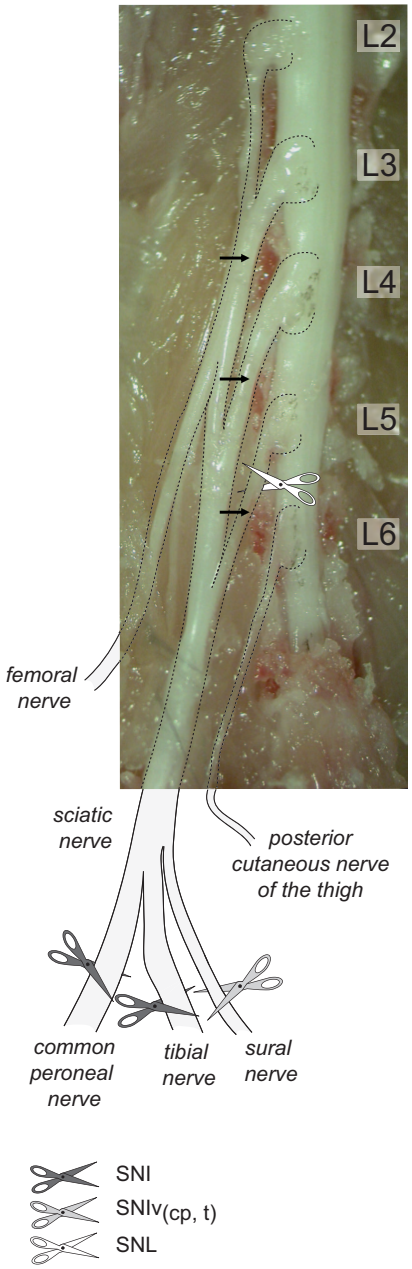
L2
L3
L4
L5
L6
femoral nerve
sciatic nerve
posterior cutaneous nerve of the thigh
common peroneal nerve
tibial nerve
sural nerve
SNI
SNIv(cp, t)
SNL

Figure 3

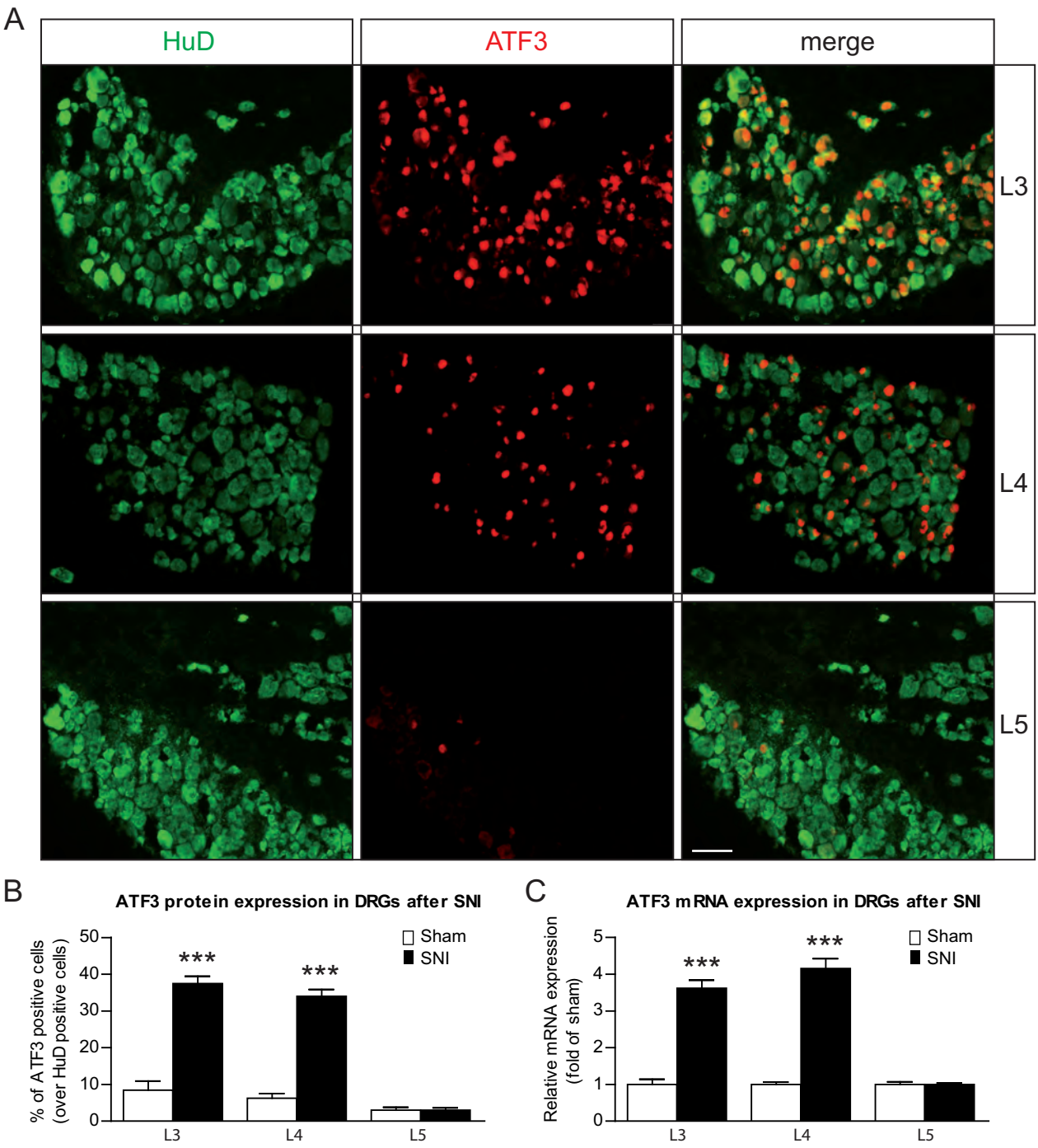
A
HuD
ATF3
merge
L3
L4
L5
B
ATF3 protein expression in DRGs after SNI
% of ATF3 positive cells
(over HuD positive cells)
Sham
SNI
***
***
L3
L4
L5
C
ATF3 mRNA expression in DRGs after SNI
Relative mRNA expression
(fold of sham)
Sham
SNI
***
***
L3
L4
L5

Figure 4

A

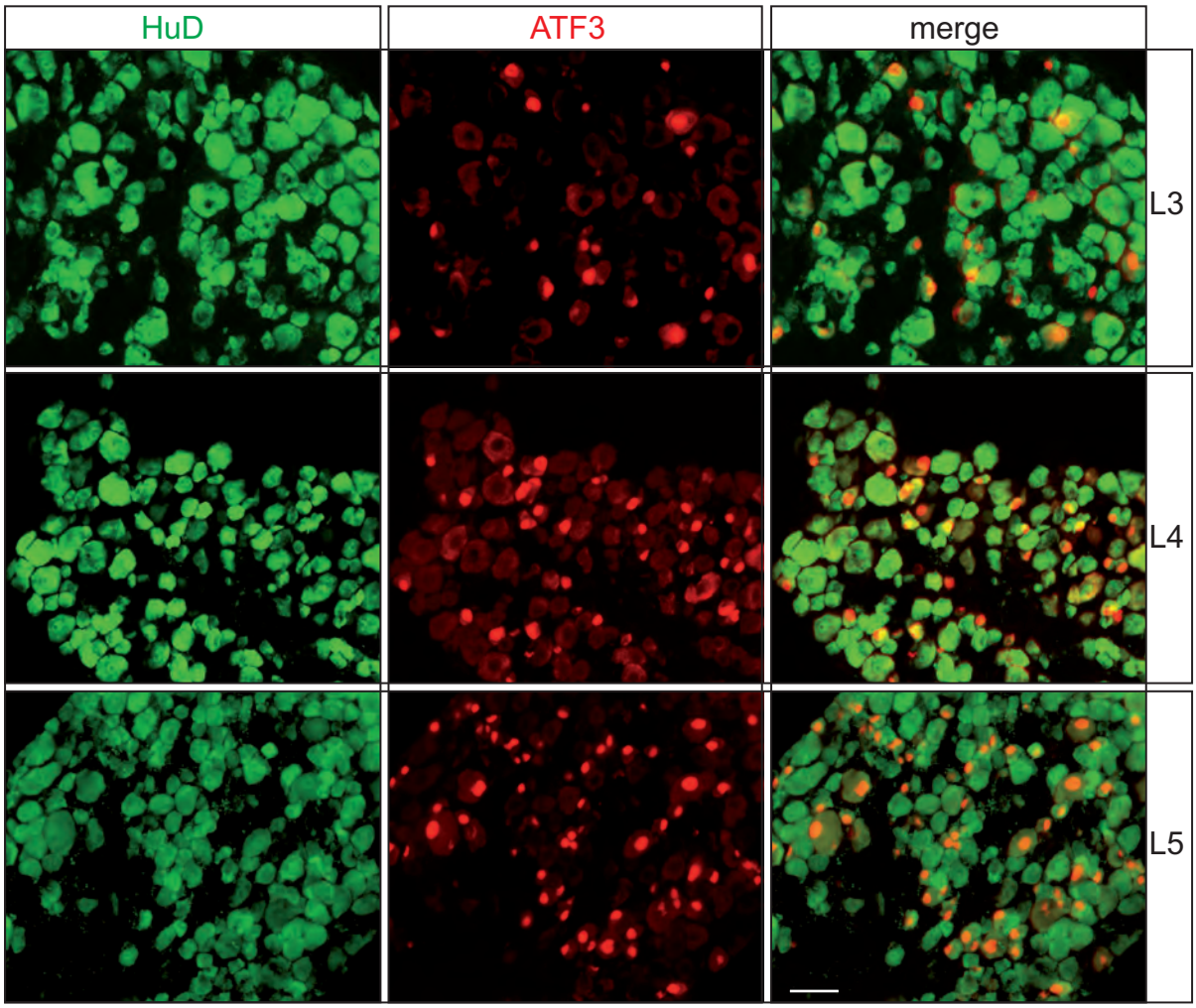
HuD
ATF3
merge
L3
L4
L5

B

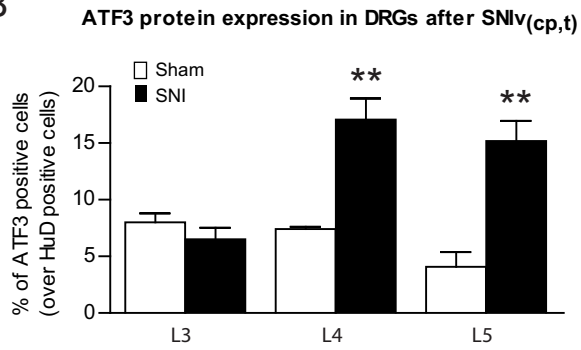
ATF3 protein expression in DRGs after SNIv(cp,t)
Sham
SNI
% of ATF3 positive cells
(over HuD positive cells)
20
15
10
5
0
**
**
L3
L4
L5

Figure 5

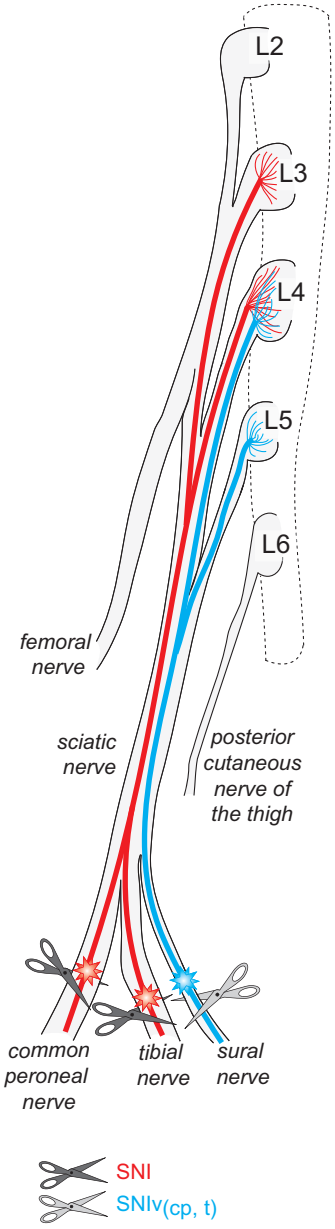
L2
L3
L4
L5
L6
femoral nerve
sciatic nerve
posterior cutaneous nerve of the thigh
common peroneal nerve
tibial nerve
sural nerve
SNI
SNIv(cp, t)

Figure 6

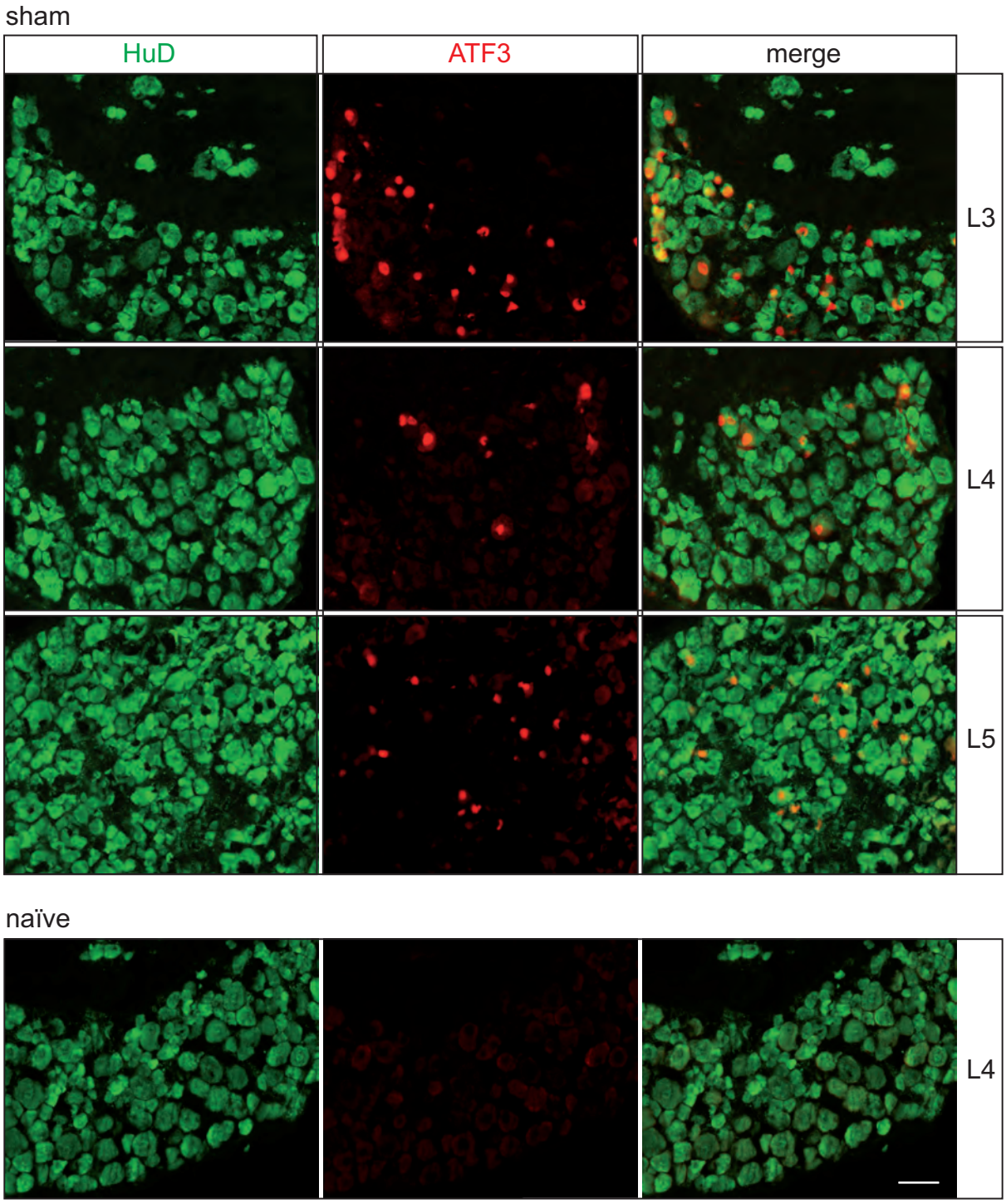

Supplemental Figure 1

Table 1
List of primers sequences

gene name	Primer sequence 5'-3'	Primer concentration
GAPDH	(Fw) TCCATGACAACTTTGGCATTG (Rev) CAGTCTTCTGGGTGGCAGTGA	200 nM
ATF3	(Fw) AGCTGAGATTCGCCATCCAGAA (Rev) CTCGCCGCCTCCTTTTCCT	200 nM
Nav1.1	(Fw) AACAAGCTTGATTCACATACAATAAG (Rev) AGGAGGGCGGACAAGCTG	200 nM
Nav1.2	(Fw) GGGAACGCCCATCAAAGAAG (Rev) ACGCTATCGTAGGAAGGTGG	100 nM
Nav1.3	(Fw) AGGCATGAGGGTGGTTGTGAACG (Rev) CAGAAGATGAGGCACACCAGTAGC	300 nM
Nav1.6	(Fw) AGTAACCCTCCAGAATGGTCCAA (Rev) GTCTAACCAGTTCCACGGGTCT	200 nM
Nav1.7	(Fw) TCCTTTATTCATAATCCCAGCCTCAC (Rev) GATCGGTTCCGTCTCTCTTTGC	200 nM
Nav1.8	(Fw) ACCGACAATCAGAGCGAGGAG (Rev) ACAGACTAGAAATGGACAGAATCACC	200 nM
Nav1.9	(Fw) TGAGGCAACACTACTTCACCAATG (Rev) AGCCAGAAACCAAGGTACTAATGATG	300 nM

Neuroscience 227 (2012) 370–380

NEURONAL EXPRESSION OF THE UBIQUITIN LIGASE NEDD4-2 IN RAT DORSAL ROOT GANGLIA: MODULATION IN THE SPARED NERVE INJURY MODEL OF NEUROPATHIC PAIN

M. CACHEMAILLE, [a,b]* **C. J. LAEDERMANN,** [a,b,c] **M. PERTIN,** [a,b] **H. ABRIEL,** [c] **R.-D. GOSSELIN** [a,b] **AND I. DECOSTERD** [a,b]

[a] *Pain Center, Department of Anesthesiology, University Hospital Center (CHUV) and University of Lausanne (UNIL), Lausanne, Switzerland*

[b] *Department of Fundamental Neurosciences (DNF), University of Lausanne, Lausanne, Switzerland*

[c] *Department of Clinical Research, University of Bern, Bern, Switzerland*

Abstract—Neuronal hyperexcitability following peripheral nerve lesions may stem from altered activity of voltage-gated sodium channels (VGSCs), which gives rise to allodynia or hyperalgesia. *In vitro*, the ubiquitin ligase Nedd4-2 is a negative regulator of VGSC α-subunits (Na_v), in particular $Na_v1.7$, a key actor in nociceptor excitability. We therefore studied Nedd4-2 in rat nociceptors, its co-expression with $Na_v1.7$ and $Na_v1.8$, and its regulation in pathology. Adult rats were submitted to the spared nerve injury (SNI) model of neuropathic pain or injected with complete Freund's adjuvant (CFA), a model of inflammatory pain. L4 dorsal root ganglia (DRG) were analyzed in sham-operated animals, seven days after SNI and 48 h after CFA with immunofluorescence and Western blot. We observed Nedd4-2 expression in almost 50% of DRG neurons, mostly small and medium-sized. A preponderant localization is found in the non-peptidergic sub-population. Additionally, 55.7 ± 2.7% and 55.0 ± 3.6% of Nedd4-2-positive cells are co-labeled with $Na_v1.7$ and $Na_v1.8$ respectively. SNI significantly decreases the proportion of Nedd4-2-positive neurons from 45.9 ± 1.9% to 33.5 ± 0.7% ($p < 0.01$) and the total Nedd4-2 protein to 44% ± 0.13% of its basal level ($p < 0.01$, $n = 4$ animals in each group, mean ± SEM). In contrast, no change in Nedd4-2 was found after peripheral inflammation induced by CFA. These results indicate that Nedd4-2 is present in nociceptive neurons, is downregulated after peripheral nerve injury, and might therefore contribute to the dysregulation of Na_vs involved in the hyperexcitability associated with peripheral nerve injuries.

Key words: Nedd4-2, neuropathic pain, voltage-gated sodium channels, $Na_v1.7$, $Na_v1.8$, dorsal root ganglion.

INTRODUCTION

Neuropathic pain affects a high proportion of the world population (Bouhassira et al., 2008) and originates from a maladaptive plasticity caused by a lesion in the somatosensory system (Woolf and Salter, 2000; Costigan et al., 2009). Clinically, it is associated with sensory dysfunctions referred as spontaneous pain, allodynia and hyperalgesia (Woolf and Decosterd, 1999). Convergent studies have shown that after a peripheral nerve lesion, ectopic activity, potentially accounting for pain symptoms, arises in injured and non-injured Aβ (normally non-nociceptive), Aδ and C-fibers (nociceptive) and in dorsal root ganglion (DRG) (Ma et al., 2003; Wu et al., 2001; Devor, 2009). Membrane hyperexcitability is thought to cause such abnormal generation of action potentials in DRG neurons (Amir et al., 2005) with the dysregulation of voltage-gated sodium channels (VGSCs) being the cornerstone of this regulation (Rush et al., 2007; Sheets et al., 2008).

Increased membrane ion permeability during action potential relies on the pore forming α-subunit (Na_v) of VGSCs, and its inhibition explains conduction blockade by local anesthetics (Catterall, 2000). Remarkably, the stability and internalization of ion channels are under the control of post-translational modifications, especially their ubiquitylation by E3 ubiquitin ligases driving their routing to degradation (Abriel and Staub, 2005). In particular the Nedd4 family of E3 proteins are potent regulators of channels, including Na_v (Abriel et al., 1999; Harvey and Kumar, 1999; van Bemmelen et al., 2004; Kabra et al., 2008). Most of the ten Na_v isoforms are expressed in DRG neurons and contribute to electrogenesis, with a specific expression for $Na_v1.7$, $Na_v1.8$ and $Na_v1.9$ in the peripheral nervous system (Black et al., 2002; Rush et al., 2007; Ho and O'Leary, 2011). Interestingly, mutations leading to loss or gain of $Na_v1.7$ function result in congenital insensitivity to pain or lead to severe familial pain disorders (Raouf et al., 2010). Mice with selective knock out of $Na_v1.7$, $Na_v1.8$

*Correspondence to: M. Cachemaille, Pain Center, Department of Anesthesiology, University Hospital Center (CHUV) and University of Lausanne (UNIL), Bugnon 46, 1011 Lausanne, Switzerland. Tel: +41-21-314-11-11; fax: +41-21-314-20-04.
E-mail address: Matthieu.Cachemaille@chuv.ch (M. Cachemaille).

Abbreviations: ATF-3, Activating Transcription Factor 3; CFA, complete Freund's adjuvant; DRG, dorsal root ganglion; GAPDH, glyceraldehyde-3-phosphate dehydrogenase; HEK293, Human Embryonic Kidney cells; IB4, isolectin B4; IR, immunoreactivity; NGS, normal goat serum; RT, room temperature; SNI, spared nerve injury; VGSCs, voltage-gated sodium channels.

0306-4522/12 $36.00 © 2012 IBRO. Published by Elsevier Ltd. All rights reserved.
http://dx.doi.org/10.1016/j.neuroscience.2012.09.044

and $Na_v1.9$ in DRG neurons have reduced pain sensitivity or diminished response to inflammatory pain (Nassar et al., 2004). These data suggest a key role of peripheral Na_vs in basal nociception, and also a possible impact of the regulation of nociceptor-specific Na_v in pathological pain. Various reports have indicated that inflammatory and neuropathic pain are associated with changes in $Na_v1.7$, $Na_v1.8$ and $Na_v1.9$ expression at both the mRNA and the protein levels in DRG neurons (Cummins and Waxman, 1997; Berta et al., 2008; Strickland et al., 2008; Thakor et al., 2009) but the mechanism leading to the selective alteration of some Na_v currents in neuropathic pain is still unclear (Berta et al., 2008). One theory posits the existence of refined mechanisms at the post-translational level leading to change in Na_v function or trafficking. In this context Nedd4-2, a well-described Nedd4 member, can interact with all Na_vs expressed in DRG neurons (except $Na_v1.9$) via their C-terminal PY motive. Indeed, *Xenopus oocytes* exogenously coexpressing Nedd4-2 with $Na_v1.2$, 1.7 and 1.8 present a reduction of their respective currents (Fotia et al., 2004). However, despite the apparent importance of Na_v regulation by Nedd4-2, the expression of Nedd4-2 in the nociceptive pathway has not been studied so far.

The aim of the present study is first to investigate *in vivo* the expression of Nedd4-2 in rat DRG and characterize its localization in the different subpopulations of primary sensory neurons using specific markers. In addition, we have assessed Nedd4-2 modulation in rodent models of neuropathic and inflammatory pain. Our results indicate that Nedd4-2 immunoreactivity (IR) is present in small diameter nociceptive neurons together with $Na_v1.7$ and $Na_v1.8$ and that this expression is down-regulated after nerve injury.

EXPERIMENTAL PROCEDURES

Surgery

All procedures were approved by the Committee on Animal Experimentation for the Canton of Vaud, Switzerland, in accordance with Swiss Federal Law on Animal Welfare and guidelines of the International Association for Study of Pain (IASP) (Zimmermann, 1983). We used the spared nerve injury (SNI) model of neuropathic pain as previously described (Decosterd and Woolf, 2000). Briefly, adult Sprague–Dawley rats were deeply anesthetized using 1.5% isoflurane and, after exposure of the sciatic nerve, the common peroneal and tibial nerves were ligated with 5.0 silk sutures and transected while the sural nerve was left intact. Muscle and skin were closed in two distinct layers with 5.0 silk thread and wound clips. Sham surgery was performed similarly, although without nerve damage, as the control condition. Eight animals were used for SNI ($n = 4$ for immunolabeling and $n = 4$ for Western blot) and a similar group of eight rats was used for sham surgery.

For experiments with complete Freund's adjuvant (CFA), rats were injected with 50 µl of CFA (Sigma, St. Louis MO, USA, $n = 4$) or NaCl 0.9% ($n = 4$), in the dorsal part of the left hindpaw, under isoflurane anesthesia (1.5% isoflurane). Animals were kept for 48 h and tissues dissected at this time-point for further analysis (Nagakura et al., 2003).

Immunohistochemistry

One week after the SNI surgery or 48 h after CFA injection, animals were lethally anesthetized with sodium pentobarbital and transcardially perfused with saline, followed by paraformaldehyde 4% in PBS. L4 DRGs (Hammond et al., 2004) were dissected and post-fixed at 4 °C for 90 min and then transferred in 20% sucrose in PBS overnight. The following day, tissues were mounted in cryoembedding fluid (Tissue-Tek; Sakura Finetek, Zoeterwoude, Holland). Then samples were frozen, cryosectioned in 12-µm thick sections and thaw-mounted onto slides.

Nedd4-2 was revealed using a specific rabbit anti-Nedd4-2 antibody (Nedd4-2, 1:100, generously provided by Olivier Staub, Department of Pharmacology and Toxicology, University of Lausanne, Switzerland). For the colocalization experiments, antibodies were as follows: mouse anti-peripherin (Peripherin; 1:500, Chemicon International, Billerica, MA, USA), mouse anti-neurofilament 200 (NF200, 1:400, Sigma, St. Louis, MO, USA), rat anti-Substance P (1:400, BD Bioscience, Basel, Switzerland), mouse anti-$Na_v1.7$ (1:100, Neuromab, Davis, CA, USA), mouse anti-$Na_v1.8$ (1:100, Neuromab, Davis, CA, USA), rabbit anti-Activating Transcription Factor 3 (ATF-3, 1:200, Santa Cruz Biotechnology, Heidelberg, Germany). Secondary antibodies were as follows: Cy3-conjugated anti-rabbit (1:400, Jackson ImmunoResearch, Suffol, UK) for Nedd4-2, Cy3-conjugated anti-mouse (1:300, Jackson ImmunoResearch) for $Na_v1.7$, FITC-conjugated anti-rabbit (1:200, Jackson ImmunoResearch, Suffol) for ATF-3, FITC-conjugated anti-rat (1:200, Jackson ImmunoResearch, Suffol) for Substance P, Alexa 488 anti-rabbit (1:500, Molecular Probes, Basel, Switzerland) for Nedd4-2 and Alexa 488 anti-mouse (1:1000, Molecular Probes) for peripherin, NF200, $Na_v1.8$. Non-peptidergic neurons were stained using biotinylated griffonia simplicifolia Isolectin B4 (IB4) (1:100, Vector Laboratories, Burlingame, CA) followed by AMCA-conjugated streptavidin (1:50; Jackson ImmunoResearch). Standard protocols for fluorescent immunohistochemistry were used. Sections of DRGs were blocked for 30 min at room temperature (RT) with 10% normal goat serum (NGS) and 0.3% PBS 1X-Triton X-100. Primary antibodies were diluted in 5% NGS and 0.1% PBS 1X-Triton X-100, and incubated on sections overnight at 4 °C. For ATF-3/Nedd4-2 dual labeling, the sequence of the protocol started with the primary and secondary incubations for ATF-3 followed by primary and secondary probing for Nedd4-2 (Pertin et al., 2005; Fukuoka et al., 2012). Control experiments were performed to rule out the possibility of a nuclear presence of Nedd4-2. Slides were washed in PBS and then incubated at RT with the corresponding secondary antibody or AMCA-conjugated streptavidin diluted in NGS 1% and PBS 1X-Triton X-100 0.1% for 90 min. Slides were washed in PBS and mounted in Mowiol medium (Calbiochem, Gibbstown, NJ).

Pictures and counting

Fluorescence was detected using an epifluorescent microscope (AxioPlan and AxiVision, Carl Zeiss, Feldbach, Switzerland). Images were taken at 20× magnification, with the same parameters used between experimental conditions, saved as TIFF files and then juxtaposed as one picture using Photoshop CS4 software (11.0, Sun Microsystems, Redwood City, CA) in order to reconstruct a complete DRG. The same parameters for image capture were used between experimental conditions and ganglia from four animals were analyzed per condition. Mean cell counts from each animal were the average of four sections selected 60 µm apart. The first slide was randomly selected and the three next ones were chosen every five slides from the series of consecutive cut sections. In all conditions, only neurons in which the nucleus was visible were counted. The observer was blinded to experimental groups. Counts of

labeled neuronal profiles were expressed as a percentage of the total number of labeled and unlabeled neuronal profiles. Neuronal cross-sectional areas were measured in μm^2 and the mean gray value of each cell was recorded based on mean pixel intensity using ImageJ software (1.42, National Institute of Mental Health, Bethesda, MD, USA). Groups for cell area were as follows: 0–600 μm^2 for small neurons, 600–1200 μm^2 for medium-sized neurons and >1200 μm^2 for large neurons (Harper and Lawson, 1985; Noguchi et al., 1993).

Threshold of detection for IR-positive cells

Positively labeled cells were identified on acquired digital images by the experimenter. The accuracy of detection was verified for each condition by determining the signal/background threshold as follows (King et al., 2009). Ten pictures were randomly chosen in images libraries of four independent markers (Nedd4-2, $Na_v1.7$, peripherin and NF-200). Background intensities were measured and averaged. The final threshold of mean gray values was calculated by adding two standard deviations, giving a value of 18. Twenty out of 718 Nedd4-2-positive cells (sham) and 42 out of 616 positive cells (SNI) were below the detection threshold. For $Na_v1.7$ counting, all positive cells were above the detection threshold.

Cell transfection

Human Embryonic Kidney cells (HEK293) were cultured in DMEM (Gibco, Life Technologies, Zug, Switzerland) supplemented with 10% fetal bovine serum, 0.2% glutamine and gentamicin (20 mg/mL) at 37 °C in a 5% CO_2 incubator. For control of antibodies, cells were transfected, using calcium phosphate, with 0.8 µg of truncated human Nedd4-2 cDNA (without the amino-terminal C2 domain) cloned into pcDNA3.1 (generously provided by Olivier Staub, Department of Pharmacology and Toxicology, Lausanne, Switzerland) or 1 µg of $Na_v1.7$ cDNA cloned into pCIN5h and provided by Dr. Simon Tate (Convergence Pharmaceuticals, Cambridge, UK). Protein extraction was performed 48 h after transfection.

Western blotting

Animals were sacrificed 7 days after Sham or SNI surgery, or 48 h after CFA injection. L4 and L5 DRGs were quickly dissected and kept at −80 °C until use. HEK293 transfected cells were detached using dissociation buffer (Invitrogen, Life Technologies), centrifuged at 2000*g* for 2 min at RT and supernatants were removed. Homogenization of DRGs or HEK cells was done in 100 mM Tris–HCl (pH 6.8), SDS 2%, glycerol 20%, NaCl and complete protease inhibitor cocktail tablets (Roche, Basel, Switzerland). Samples were centrifuged at 14,000 rpm for 20 min at 4 °C and proteins in the supernatants were quantified using Bradford assays. Protein samples (15–20 µg) were separated by SDS–PAGE and transferred onto PVDF membranes (BioRad, Hercules, CA). Blots were blocked with non fat dry milk 5% for 30 min at RT and then incubated overnight at 4 °C with the appropriate antibody: rabbit anti-Nedd4-2 (1:100) (Flores et al., 2005), mouse anti-$Na_v1.7$ (1:400, Neuromab) or mouse anti-Glyceraldehyde-3-phosphate dehydrogenase (GAPDH, 1:500,000, Abcam, Cambridge, UK). These blots were further incubated with horseradish peroxydase-conjugated secondary antibody anti-mouse or anti-rabbit (1:2000, Dako, Heverlee, Belgium), developed in Super Signal Solution (Pierce, Rockford, IL, USA) and revealed with LAS-4000-Mini Fujifilm (Bucher Biotec, Basel, Switzerland). Pixel intensities were quantified with ImageJ. Results were expressed as the ratio of the signal of interest over sham after normalization by GAPDH loading control.

Statistics

Data are represented as mean ± SEM. Comparisons between groups were performed using Student's *t* test or a one-way ANOVA followed by Dunnett's Multiple Comparison Test for Fig. 3F. Statistical analyses were done with JMP statistical software (5.01, SAS institute, Cary, NC). Differences were considered significant at *p*-values below 0.05.

RESULTS

Nedd4-2 is present in nociceptive neurons

Nedd4-2 IR is widely distributed in rat DRG neurons (Fig. 1A). Western blot analysis (Fig. 1B) reveals one major band in DRG at approximately 120 kDa corresponding to the endogenous form of Nedd4-2 (lane 1). In HEK293 cells, the endogenous form of Nedd4-2 corresponds to a slightly lower band (~115 kDa), in line with species differences (van Bemmelen et al., 2004; Rougier et al., 2005). In DRG, we inconstantly observed one additional band between 100 and 120 kDa, which is known to be a splice variant (Itani et al., 2003; Hryciw et al., 2004) (see Figs. 3A and 5B). As a positive control, the analysis of HEK293 cells transfected with a truncated form of human Nedd4-2 cDNA showed a robust protein level at 100 kDa, in line with the size of the construct (Kamynina et al., 2001).

We thoroughly explored the molecular identity of Nedd4-2-immunopositive DRG neurons using dual immunofluorescence (Fig. 2). The six sets of counting performed throughout our study gave overall percentages of Nedd4-2-expressing neurons ranging

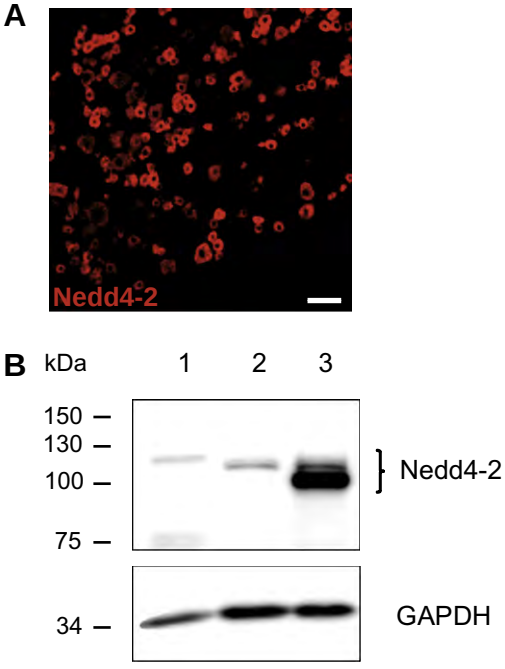

Fig. 1. Protein expression of Nedd4-2 in rat DRG. (A) Nedd4-2-immunoreactivity (IR) in rat L4 DRG (scale bar = 100 µm). (B) Western blot analysis of Nedd4-2. Lane 1: rat L4 DRG; lane 2: HEK293 cells; lane 3: Nedd4-2 transfected HEK293 cells; GAPDH was used as a loading control.

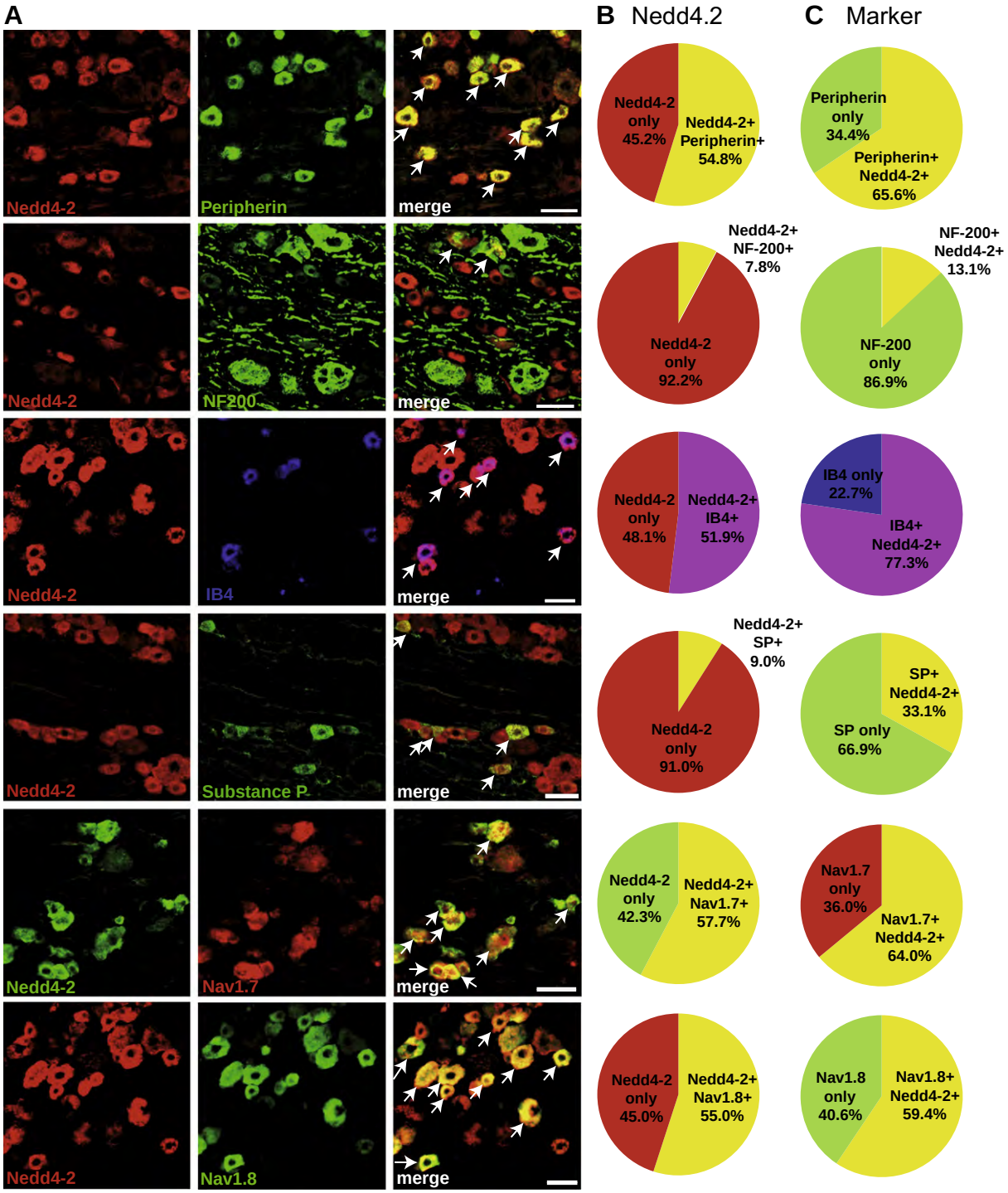

Fig. 2. Nedd4-2 is mainly present in nociceptive DRG neurons and colocalizes with the sodium channels $Na_v1.7$ and $Na_v1.8$. (A) Representative double immunofluorescence for Nedd4-2 (first column) with the markers peripherin, NF-200, IB4, Substance P, or with $Na_v1.7$ and $Na_v1.8$ (second column) and merged images (third column, arrows) in rat DRG neurons (sham group). (B) Quantitative analysis of Nedd4-2-IR with the different markers. Among all Nedd4.-2-positive neurons, 54.8 ± 3.8% co-stained for peripherin, 7.8 ± 2.7% for NF-200, 51.9 ± 2.2% for IB4, 9.0 ± 1.2% for Substance P, 57.7 ± 2.7% for $Na_v1.7$ and 55.0 ± 3.6% for $Na_v1.8$. (C) Among the following markers, many co-stained with Nedd4-2: peripherin (65.6 ± 3.2%), NF-200 (13.1 ± 3.7%), IB4 (77.3 ± 4.6%), Substance P (33.1 ± 2.8%), $Na_v1.7$ (64.0 ± 2.9%) and $Na_v1.8$ (59.4 ± 4.9%). Data are presented as mean ± SEM. $n = 4$. Scale bar = 50 µm.

from 43.3 ± 2.6% to 49.6 ± 0.9% of total neurons ($n = 4$). Peripherin, an intermediate filament selective for small sensory neurons presumably nociceptive, is found in about half of neurons with Nedd4-2-IR (Fig. 2B) and conversely Nedd4-2-IR is present in a large majority of peripherin-positive neurons (Fig. 2C). Nedd4.2 is weakly expressed in the NF200-postive large myelinated fiber cell population. Within the subpopulations of

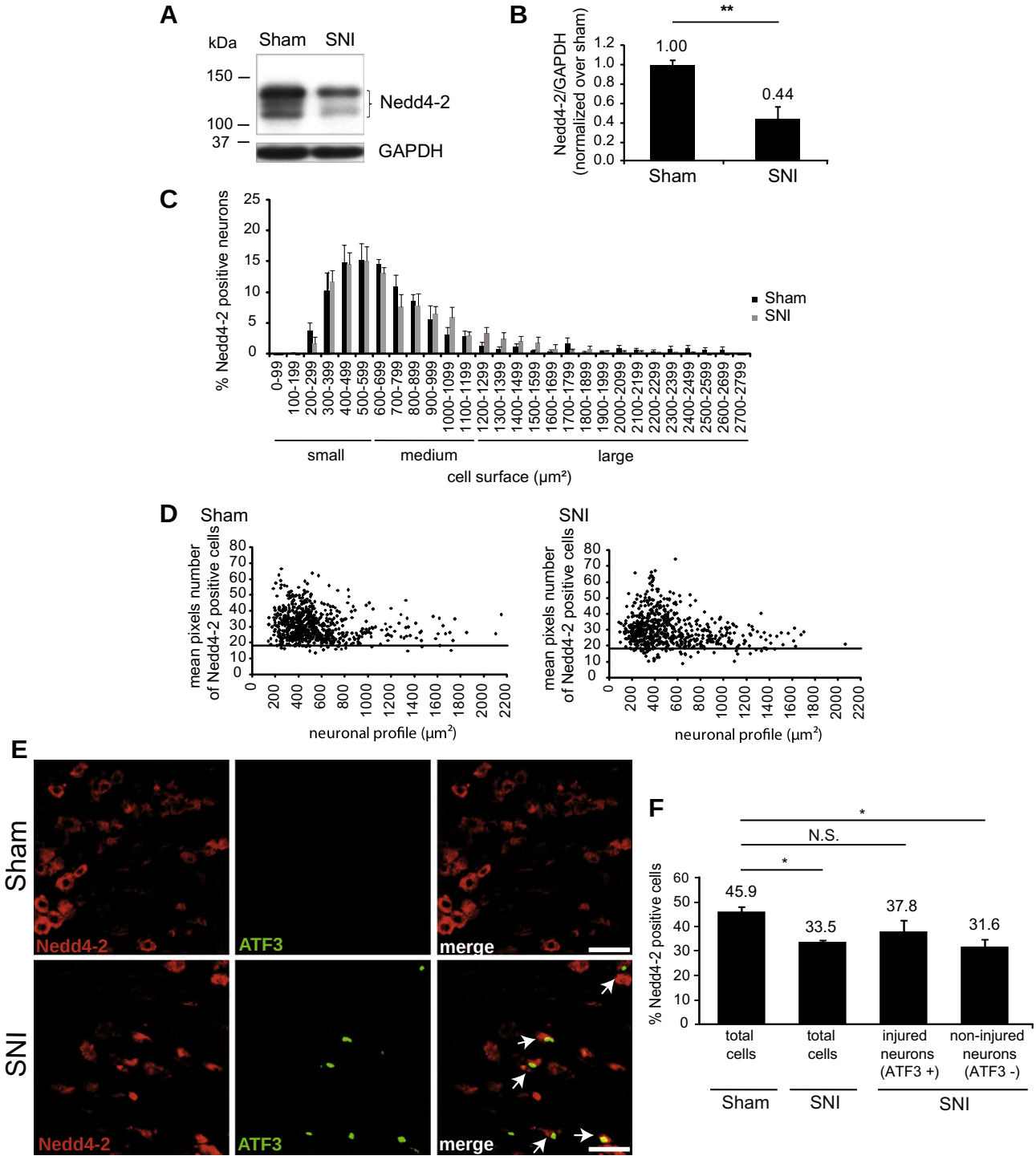

Fig. 3. Peripheral nerve injury decreases Nedd4-2 in DRG neurons. (A) Representative Western blot analysis one week after sham or SNI surgeries. (B) Quantification of Nedd4-2 protein content indicates a downregulation of Nedd4-2 in L4 DRG after SNI (quantifications are expressed as ratio over sham signal after normalization to GAPDH signal). (C) Distribution of cross-sectional area of Nedd4-2-positive neurons in the L4 DRG; 0–600 µm^2 indicates small DRG neurons, 600–1200 µm^2 medium DRG neurons, >1200 µm^2 represents the large DRG neurons (Noguchi et al., 1993). 507 Nedd4-2-positive neurons were measured in the sham group, 438 in the SNI group. (D) Representation of mean pixel number (intensity) of all Nedd4-2-IR profiles according to their size. The horizontal line at 18 represents the threshold between positive and negative neurons. (E) Representative immunofluorescence showing Nedd4-2 (red) in both neurons expressing ATF-3 (green), a marker of injured neurons, and ATF-3 immuno-negative cells in L4 DRG. (F) Quantification of Nedd4.2-IR one week after SNI or sham surgery, in injured/ATF-3-positive profiles. Results are expressed in mean ± SEM, $n = 4$ animals in each group for all panels. $^{**}p < 0.01$, $^{*}p < 0.05$. N.S., non-significative. Student's t test. One-way ANOVA followed by Dunnett's Multiple Comparison Test for Fig. 3F. Scale bar = 50 µm.

small neurons, Nedd4-2-positive cells are mainly represented in the non-peptidergic neurons (IB4 positive) while less than 10% of Nedd4-2 immunoreactive cells are positive for the neuropeptide Substance P.

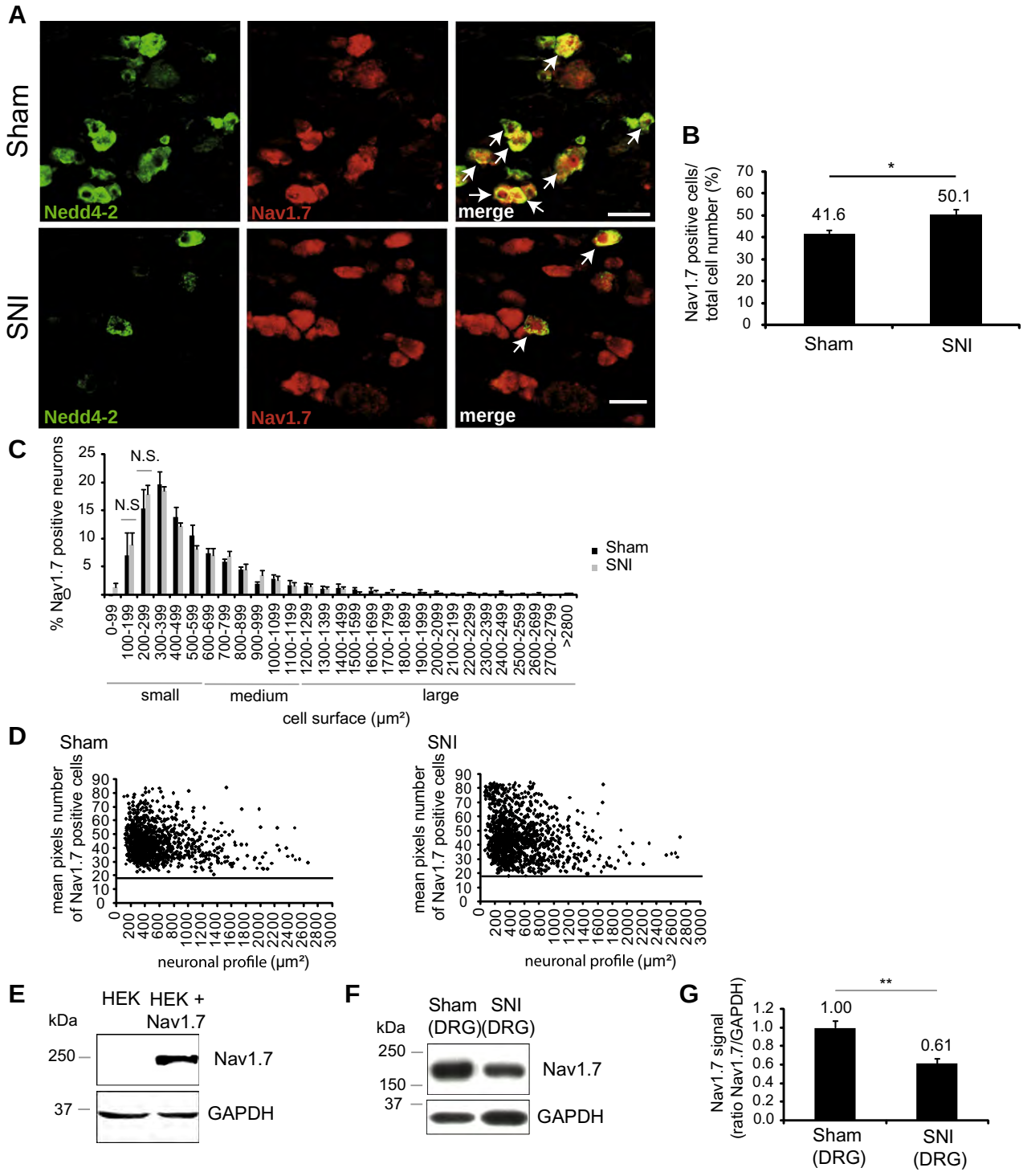

Fig. 4. Nedd4-2-IR and $Na_v1.7$ expression one week after SNI. (A) Immunofluorescence showing the colocalization (right panel, arrows) between Nedd4-2 immunosignal (green, left panel) and $Na_v1.7$ (red, middle panel) in rat lumbar DRG. Scale bar = 50 µm. (B) Quantification of $Na_v1.7$-immunoreactive cells. (C) Cell-size of $Na_v1.7$-IR profiles in L4 DRG, expressed as the percentage of $Na_v1.7$-positive cells in total cells. 0–600 μm^2 indicates small neurons, 600–1200 μm^2 medium neurons, > 1200 μm^2 represents large neurons. 1040 $Na_v1.7$-positive neurons were measured in the sham group and 1304 in the SNI group. (D) Representation of mean pixel number of all $Na_v1.7$-positive cells according to their size. The horizontal line at 18 represents the threshold between $Na_v1.7$-positive and -negative neurons. (E) Control of $Na_v1.7$ antibody by Western blot analysis in HEK293 cells. The first lane represents native HEK cells and the right lane HEK cells transfected with $Na_v1.7$ cDNA. GAPDH was used as a loading control. (F) Representative Western blot of $Na_v1.7$ one week after sham and SNI surgery DRG. GAPDH was used as a loading control. (G) Quantification of Western blot analysis. A significant decrease of $Na_v1.7$ expression was observed when compared to sham. Quantifications are expressed as ratio over sham after normalization to GAPDH. Results are expressed in mean ± SEM and $n = 4$ animals in all panels. $^{*}p < 0.05$, $^{**}p < 0.01$, Student's t test.

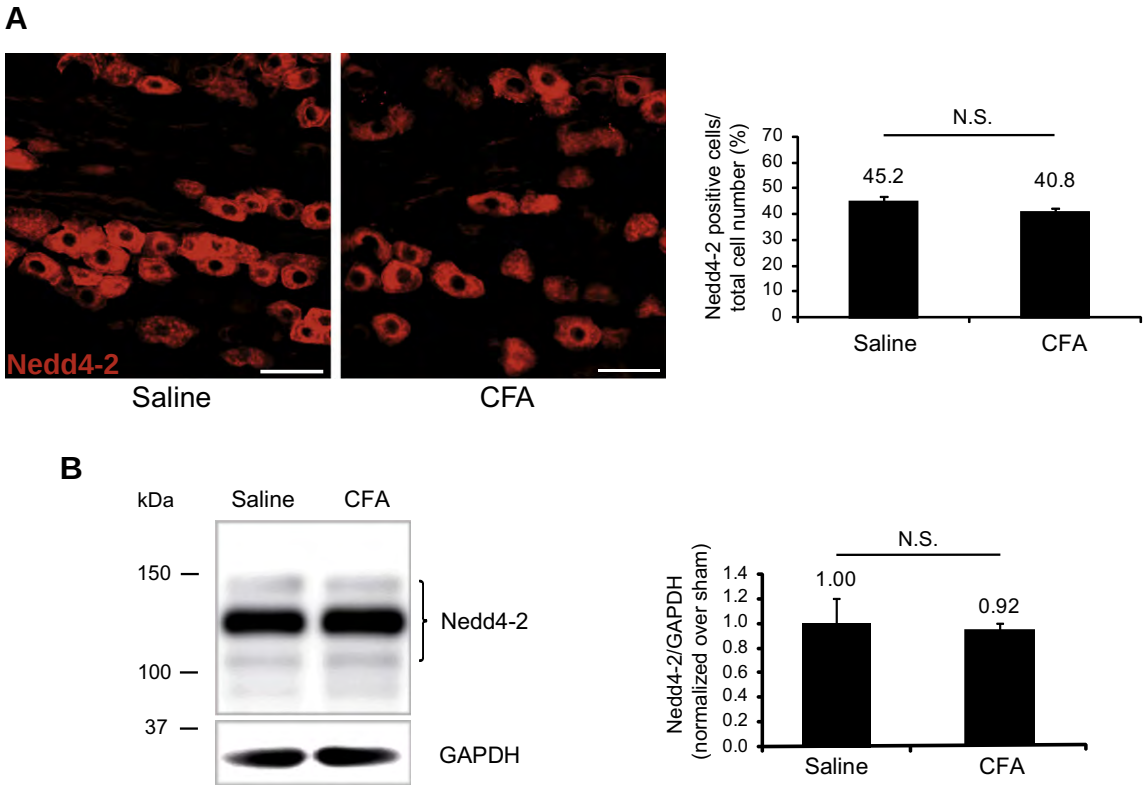

Fig. 5. Peripheral inflammation does not induce changes in Nedd4-2 expression in the DRG. (A) Representative immunofluorescence from L4 DRG showing the absence of significative difference in Nedd4-2 signal between saline or CFA-treated rats. Right bar histogram shows the quantification of Nedd4-2-immunoreactive profiles in total neuronal profiles. (B) Western-blot analysis of rat L4 DRG after saline or CFA administration. Quantifications are expressed as ratio over GAPDH signal, normalized over sham signal. Results are expressed as mean ± SEM, $n = 4$ animals in each group. N.S., non-significative, Student's t test. Scale bar = 50 μm.

Together, these results indicate that Nedd4-2 is expressed in DRG neurons and is predominantly localized in small diameter sensory neurons, which include many nociceptive neurons.

Nedd4-2-IR is decreased after SNI

In order to test the hypothesis that Nedd4-2 plays a role in the hyperexcitability associated with neuropathic pain in rats, we explored the regulation of its expression following peripheral nerve injury. Using Western blot analysis of L4 DRG (Fig. 3A and B), we observed a decrease of about 56% in Nedd4-2 protein content after SNI. Similar results were observed using immunofluorescence on DRG (Fig. 3E and F): quantification indicated a decrease in the number of Nedd4-2-IR cell profiles after SNI. In addition, we evaluated whether Nedd4-2 signal could be shifted to another DRG neurons subpopulation after nerve injury (Fig. 3C). The distribution of Nedd4-2-positive neurons in DRG cells of different sizes confirms an expression mainly in small neurons ($< 600\ \mu m^2$), but no significant difference was detected between sham and SNI groups. The reduction of Nedd4-2-IR observed after SNI is not associated with a decrease of mean pixel intensity calculated for individual neurons (Fig. 3D), but rather with a reduced number of Nedd4-2-expressing neurons (Fig. 3F).

We therefore investigated whether the downregulation of Nedd4-2-IR occurs in injured DRG neurons (injured afferents of the tibial and peroneal nerves) after SNI, which are known to be positive for the transcription factor ATF-3 (Tsujino et al., 2000; Miyoshi et al., 2011). As anticipated, the proportion of immunoreactive neurons for ATF-3 in SNI rats is higher than in the sham group (34.8 ± 2.8% as compared to 4.8 ± 0.2%), yet a detailed analysis shows that downregulation of Nedd4-2 occurs in both injured (ATF positive) and the remaining non-injured (ATF negative) neurons present in the DRG (Fig. 3F). This suggests that neuronal deterioration and in turn the previously reported neuronal death following nerve section (Tandrup et al., 2000; McKay Hart et al., 2002) is unlikely to account for the reduction of Nedd4-2 IR, in line with the reported absence of neuronal death in neuropathic pain without axonal injury (Schaeffer et al., 2010).

Nedd4-2-IR colocalizes with sodium channels $Na_v1.7$ and $Na_v1.8$

The regulation of ion channels by Nedd4-2, in particular the voltage-gated sodium channels $Na_v1.7$ and $Na_v1.8$, implies their coexpression in the same DRG neurons. In line with this hypothesis, strong colocalizations between Nedd4-2 and $Na_v1.7$ (Figs. 2 and 4A) or $Na_v1.8$ (Fig. 2) were found. More than 60% of $Na_v1.7$-positive neurons

co-expressed Nedd4-2, a value that dropped concomitantly with Nedd4-2 downregulation after SNI (64.0 ± 2.9% to 40.1 ± 3.0% in sham and SNI groups respectively, $p < 0.01$, $n = 4$ in each group). A significant increase in the number of $Na_v1.7$ immunoreactive neuronal profiles is observed after SNI as compared to sham (Fig. 4B), without any significant change in the distribution of $Na_v1.7$-IR cross-sectional area (Fig. 4C). The enrichment in $Na_v1.7$-IR is mostly observed in small neurons (0–600 μm^2) and a simultaneous increase in mean pixel intensity is observed in individual cells of this category after SNI (Fig. 4D). Remarkably, Western blot quantification shows a decrease in $Na_v1.7$ content in DRG after SNI (Fig. 4F–G).

Many $Na_v1.8$-IR cells express Nedd4-2 (Fig. 2A–C) in a proportion that is not altered by SNI (59.4 ± 4.9% and 59.6 ± 5.3% in sham and SNI groups respectively, $n = 4$). Conversely, 55.0 ± 3.6% of Nedd4-2-IR profiles showed $Na_v1.8$-IR, but this proportion was significantly decreased to 38.6 ± 4.4% after SNI ($p < 0.05$, $n = 4$). This parallels the known downregulation of $Na_v1.8$ after peripheral nerve injury, which is here confirmed by the decrease of cells expressing $Na_v1.8$ in DRG: 46.9 ± 5.2% of total DRG neuronal profiles showed $Na_v1.8$-IR from control rats compared with 21.1 ± 1.7% of DRG neuronal profiles from SNI animals ($p < 0.01$, $n = 4$).

Nedd4-2 IR is not altered by peripheral inflammation

We further tested the hypothesis that Nedd4-2 might be regulated after peripheral inflammation (Fig. 5). As shown in (Fig. 5A and B) 48 h following intraplantar injection of CFA, neither the density of Nedd4-2-positive neurons nor the global Nedd4-2 content was modified.

DISCUSSION

In the present study, we characterized the expression of Nedd4-2 in primary sensory neurons and showed its downregulation after a peripheral nerve lesion. Using immunofluorescence and Western blot, we first established the presence of Nedd4-2-IR in DRG neurons and its main localization in small-diameter neurons. Furthermore, after SNI, we found a significant decrease in Nedd4-2 content in DRG neurons. Finally we demonstrated that the expressions of $Na_v1.7$ and $Na_v1.8$ strongly co-localize with Nedd4-2-IR in the basal condition and after peripheral nerve injury.

The demonstration of a colocalization between Nedd4-2 and $Na_v1.7$ or $Na_v1.8$ immunoreactivities was the first crucial step before postulating an involvement of Nedd4-2 in the regulation of Na_v after peripheral nerve injury. In rat DRG, we found that a large proportion of neurons were immunoreactive for Nedd4-2, a proportion that further increased when we considered the sole population of small neurons that express peripherin. This result, together with the low percentage of Nedd4-2-positive cells in myelinated NF200 immunoreactive neurons (presumably non-nociceptive except the Aδ subpopulation), suggests that Nedd4-2 may have a role to play in the physiology of nociceptive neurons. In addition, the further enrichment of Nedd4-2 in IB4-positive nociceptive neurons (77.3 ± 4.6%) indicates a putative specific role of Nedd4-2 in the excitability of non-peptidergic nociceptors, a cell population described as having longer duration action potentials and expressing a high density of $Na_v1.8$ (Stucky and Lewin, 1999). The marked downregulation of Nedd4-2-IR in DRG neurons following peripheral nerve injury suggests changes in ion channel trafficking and the possible role of this in neuropathic pain is a promising subject for future study. After nerve injury, the reduced proportions of Nedd4-2-positive neurons were not significantly different between injured (ATF-3 positive) and non-injured (ATF-3 negative) DRG neuronal populations. This might imply that Nedd4-2 downregulation contributes to Na_v turnover in both injured (axotomized) and non-injured adjacent neurons.

Sodium channels exist both at the plasma membrane and in intracellular pools (Schmidt et al., 1985; Ritchie et al., 1990). Multiple and complex mechanisms contribute to the forward trafficking of sodium channels – and other voltage-gated ion channels – from the intracellular pool to their subsequent functional insertion in the plasma membrane. In this process, insertion is counter-balanced by various post-translational modifications including ubiquitylation and consequent internalization of the channel (Jenkins and Bennett, 2001; Okuse et al., 2002; Garrido et al., 2003; Mohler et al., 2004; Lopez-Santiago et al., 2006), a phenomenon in which Nedd4-2 has been implicated in transfected cells (Fotia et al., 2004). In SNI, the Nedd4-2 decrease may influence this balance, possibly leading to an accumulation of Na_v at the cell membrane while the total quantity of sodium channels in neurons may remain stable. This mechanism might explain discrepancies that have been reported between the apparent rate of Na_v synthesis and the observed functional current, as in the case of TTX sensitive Na_v isoforms (Berta et al., 2008). In accordance with previous studies on $Na_v1.7$ transcriptional expression (Raymond et al., 2004; Berta et al., 2008), we found a significant reduction in total $Na_v1.7$ protein after SNI. Nevertheless, the number of $Na_v1.7$-IR neurons was increased after SNI. This discrepancy might originate from a redistribution of $Na_v1.7$ protein to a different neuronal compartment more easily accessible to the antibody, such as plasma membrane. It is also possible that following peripheral nerve injury $Na_v1.7$ is upregulated but redistributed from the soma of sensory neurons toward fibers resulting in apparent simultaneous signal reduction in the cell bodies and increase in the total DRG protein content.

Further investigations should be conducted in order to distinguish the membrane and intracellular pools of $Na_v1.7$ using electrophysiological and biochemical approaches. $Na_v1.7$ has so far never been investigated in DRG using patch clamp techniques due to the difficulty to selectively isolate its currents. Interestingly, however, $Na_v1.7$ specific blockers have recently been developed and will allow $Na_v1.7$ exploration (Schmalhofer et al.,

2008; Liu et al., 2012). Furthermore, biochemical strategies might also be employed to quantify the internalization and membrane targeting of Na_v in neuropathic pain and the importance of the specific interaction with Nedd4-2 in this process.

The strong downregulation of $Na_v1.8$, in line with many other studies but in apparent contradiction of our hypothesis, would suggest that a transcriptional downregulatory mechanism predominates regardless of the inhibition by Nedd4-2 of channel internalization. In addition, it was already proposed that the downregulation of $Na_v1.8$ mRNA and protein in DRGs is due to a redistribution of this channel along the axons of injured (Thakor et al., 2009) or uninjured nerves (Gold et al., 2003). Nedd4-2 downregulation in the DRG might also impact $Na_v1.8$ expression at the membrane along the axon and further studies are needed to answer this question.

Nedd4-2 is not the only potential post-translational regulator of Na_v. An interaction between p11 (from the S100 protein family) and $Na_v1.8$ has been reported to facilitate $Na_v1.8$ sorting toward the cell membrane (Okuse et al., 2002). Besides, ankyrin interacts with and upregulates $Na_v1.5$ in cardiac cells (Mohler et al., 2004) as well as $Na_v1.2$ and $Na_v1.6$ at nodes of Ranvier (Jenkins and Bennett, 2001; Garrido et al., 2003). In addition, $Na_v\beta$-subunits fulfill important regulatory functions. In particular, the β2-subunit was shown to modulate mRNA and protein expression of various Na_v (Lopez-Santiago et al., 2006) and is increased after nerve injury (Pertin et al., 2005). Finally, protein kinases such as PKA or PKC also modulate VGSC, with PKA increasing $Na_v1.8$ and decreasing $Na_v1.7$ currents while PKC decreases $Na_v1.8$ and $Na_v1.7$ currents (Vijayaragavan et al., 2004). Nedd4-2 interacts specifically via one of its WW domains (protein–protein interaction modules) with a PY motif situated in the COOH termini of Na_v or ENaC (Harvey et al., 1999; Rougier et al., 2005). Previous studies have established the connection between Nedd4-2 and the Na_v *in vitro* (Fotia et al., 2004; van Bemmelen et al., 2004; Rougier et al., 2005). In cardiac cells, $Na_v1.5$ can be downregulated by Nedd4-2 (Abriel et al., 2000; van Bemmelen et al., 2004) implying a probable modulation of cardiac excitability. With the exception of $Na_v1.4$ and $Na_v1.9$, all Na_v contain the specific PY motif suggesting an interaction with Nedd4-2. These include $Na_v1.6$, whose mRNA is the third most abundant among sodium channels in the DRG (Berta et al., 2008); this channel has recently been reported to be modulated by Nedd4-2 (Gasser et al., 2010). Additionally, $Na_v1.2$, mainly present in the central nervous system, has been shown to be downregulated when associated with Nedd4-2 (Fotia et al., 2004; Rougier et al., 2005). In addition to Na_v, Voltage-gated K+ channels play major roles in modulating electrical excitability in neurons. For instance, KCNQ2/3/5contain a PY motif and is subjected to Nedd4-2 dependent downregulation in a *Xenopus oocyte* expression system (Ekberg et al., 2007; Pongs, 2008; Bongiorno and Poronnik, 2011). This regulation and modulation of K+ channels might also be a key point in the excitability generated after a peripheral nerve injury.

Finally, besides its expression level, Nedd4-2 is regulated by a direct phosphorylation as well (Debonneville et al., 2001; Snyder, 2009). In particular, serum- and glucocorticoid kinase 1 (Debonneville et al., 2001) increases ENaC cell-surface expression through a negative regulation of Nedd4-2 (Alvarez et al., 1999). These findings imply a posttranslational regulation of Nedd4-2 playing therefore a role in Na_v modulation. Upstream regulatory mechanisms of Nedd4-2 might therefore represent other perspectives to explore in the context of peripheral nerve injuries.

CONCLUSION

In summary, we have demonstrated *in vivo* the presence of the ubiquitin ligase Nedd4-2 in the rat DRG. Moreover meticulous analyses of the immunoreactive cell populations showed its presence mainly in small nociceptive neurons, especially the non-peptidergic neurons. We also colocalized Nedd4-2 with $Na_v1.7$ and $Na_v1.8$. In a model of peripheral nerve injury, the decrease of Nedd4-2-positive neurons suggests a putative role in altered Na_v turnover, especially $Na_v1.7$, which could contribute to hyperexcitability. Future studies will shed light on the exact molecular impact of Nedd4-2 on Na_v in nociceptors and pathological pain.

Acknowledgements—The authors would like to thank Pr. Olivier Staub, Pharmacology and Toxicology Department, University of Lausanne (UNIL), Lausanne, Switzerland for his help with Nedd4-2 antibody and immunofluorescence, Pr. Peter Clarke for his helpful comments about the manuscript and Pr. Christian Kern, chairman of the Anesthesiology Department, University Hospital Center (CHUV), Lausanne, Switzerland for his support. This work was financially supported by the Swiss National Science Foundation (Isabelle Decosterd), Synapsis Foundation (Isabelle Decosterd and Hugues Abriel) and the European Society of Anesthesiology (Isabelle Decosterd and Hugues Abriel).

REFERENCES

Abriel H, Kamynina E, Horisberger JD, Staub O (2000) Regulation of the cardiac voltage-gated Na+ channel (H1) by the ubiquitin-protein ligase Nedd4. FEBS Lett 466:377–380.

Abriel H, Loffing J, Rebhun JF, Pratt JH, Schild L, Horisberger JD, Rotin D, Staub O (1999) Defective regulation of the epithelial Na+ channel by Nedd4 in Liddle's syndrome. J Clin Invest 103:667–673.

Abriel H, Staub O (2005) Ubiquitylation of ion channels. Physiology (Bethesda) 20:398–407.

Alvarez dlR, Zhang P, Naray-Fejes-Toth A, Fejes-Toth G, Canessa CM (1999) The serum and glucocorticoid kinase sgk increases the abundance of epithelial sodium channels in the plasma membrane of *Xenopus oocytes*. J Biol Chem 274:37834–37839.

Amir R, Kocsis JD, Devor M (2005) Multiple interacting sites of ectopic spike electrogenesis in primary sensory neurons. J Neurosci 25:2576–2585.

Berta T, Poirot O, Pertin M, Ji RR, Kellenberger S, Decosterd I (2008) Transcriptional and functional profiles of voltage-gated Na(+) channels in injured and non-injured DRG neurons in the SNI model of neuropathic pain. Mol Cell Neurosci 37:196–208.

Black JA, Renganathan M, Waxman SG (2002) Sodium channel Na(v)1.6 is expressed along nonmyelinated axons and it contributes to conduction. Brain Res Mol Brain Res 105:19–28.

Bongiorno D, Schuetz F, Poronnik P, Adams DJ (2011) Regulation of voltage-gated ion channels in excitable cells by the ubiquitin ligases Nedd4 and Nedd4-2. Channels (Austin) 5.

Bouhassira D, Lanteri-Minet M, Attal N, Laurent B, Touboul C (2008) Prevalence of chronic pain with neuropathic characteristics in the general population. Pain 136:380–387.

Catterall WA (2000) From ionic currents to molecular mechanisms: the structure and function of voltage-gated sodium channels. Neuron 26:13–25.

Costigan M, Scholz J, Woolf CJ (2009) Neuropathic pain: a maladaptive response of the nervous system to damage. Annu Rev Neurosci 32:1–32.

Cummins TR, Waxman SG (1997) Downregulation of tetrodotoxin-resistant sodium currents and upregulation of a rapidly repriming tetrodotoxin-sensitive sodium current in small spinal sensory neurons after nerve injury. J Neurosci 17:3503–3514.

Debonneville C, Flores SY, Kamynina E, Plant PJ, Tauxe C, Thomas MA, Munster C, Chraibi A, Pratt JH, Horisberger JD, Pearce D, Loffing J, Staub O (2001) Phosphorylation of Nedd4-2 by Sgk1 regulates epithelial Na(+) channel cell surface expression. EMBO J 20:7052–7059.

Decosterd I, Woolf CJ (2000) Spared nerve injury: an animal model of persistent peripheral neuropathic pain. Pain 87:149–158.

Devor M (2009) Ectopic discharge in Abeta afferents as a source of neuropathic pain. Exp Brain Res 196:115–128.

Ekberg J, Schuetz F, Boase NA, Conroy SJ, Manning J, Kumar S, Poronnik P, Adams DJ (2007) Regulation of the voltage-gated K(+) channels KCNQ2/3 and KCNQ3/5 by ubiquitination. Novel role for Nedd4-2. J Biol Chem 282:12135–12142.

Flores SY, Loffing-Cueni D, Kamynina E, Daidie D, Gerbex C, Chabanel S, Dudler J, Loffing J, Staub O (2005) Aldosterone-induced serum and glucocorticoid-induced kinase 1 expression is accompanied by Nedd4-2 phosphorylation and increased Na+ transport in cortical collecting duct cells. J Am Soc Nephrol 16:2279–2287.

Fotia AB, Ekberg J, Adams DJ, Cook DI, Poronnik P, Kumar S (2004) Regulation of neuronal voltage-gated sodium channels by the ubiquitin-protein ligases Nedd4 and Nedd4-2. J Biol Chem 279:28930–28935.

Fukuoka T, Yamanaka H, Kobayashi K, Okubo M, Miyoshi K, Dai Y, Noguchi K (2012) Re-evaluation of the phenotypic changes in L4 dorsal root ganglion neurons after L5 spinal nerve ligation. Pain 153:68–79.

Garrido JJ, Fernandes F, Moussif A, Fache MP, Giraud P, Dargent B (2003) Dynamic compartmentalization of the voltage-gated sodium channels in axons. Biol Cell 95:437–445.

Gasser A, Cheng X, Gilmore ES, Tyrrell L, Waxman SG, Dib-Hajj SD (2010) Two Nedd4-binding motifs underlie modulation of sodium channel Nav1.6 by p38 MAPK. J Biol Chem 285:26149–26161.

Gold MS, Weinreich D, Kim CS, Wang R, Treanor J, Porreca F, Lai J (2003) Redistribution of Na(V)1.8 in uninjured axons enables neuropathic pain. J Neurosci 23:158–166.

Hammond DL, Ackerman L, Holdsworth R, Elzey B (2004) Effects of spinal nerve ligation on immunohistochemically identified neurons in the L4 and L5 dorsal root ganglia of the rat. J Comp Neurol 475:575–589.

Harper AA, Lawson SN (1985) Conduction velocity is related to morphological cell type in rat dorsal root ganglion neurones. J Physiol 359:31–46.

Harvey KF, Dinudom A, Komwatana P, Jolliffe CN, Day ML, Parasivam G, Cook DI, Kumar S (1999) All three WW domains of murine Nedd4 are involved in the regulation of epithelial sodium channels by intracellular Na+. J Biol Chem 274:12525–12530.

Harvey KF, Kumar S (1999) Nedd4-like proteins: an emerging family of ubiquitin-protein ligases implicated in diverse cellular functions. Trends Cell Biol 9:166–169.

Ho C, O'Leary ME (2011) Single-cell analysis of sodium channel expression in dorsal root ganglion neurons. Mol Cell Neurosci 46:159–166.

Hryciw DH, Ekberg J, Lee A, Lensink IL, Kumar S, Guggino WB, Cook DI, Pollock CA, Poronnik P (2004) Nedd4-2 functionally interacts with ClC-5: involvement in constitutive albumin endocytosis in proximal tubule cells. J Biol Chem 279:54996–55007.

Itani OA, Campbell JR, Herrero J, Snyder PM, Thomas CP (2003) Alternate promoters and variable splicing lead to hNedd4-2 isoforms with a C2 domain and varying number of WW domains. Am J Physiol Renal Physiol 285:F916–F929.

Jenkins SM, Bennett V (2001) Ankyrin-G coordinates assembly of the spectrin-based membrane skeleton, voltage-gated sodium channels, and L1 CAMs at Purkinje neuron initial segments. J Cell Biol 155:739–746.

Kabra R, Knight KK, Zhou R, Snyder PM (2008) Nedd4-2 induces endocytosis and degradation of proteolytically cleaved epithelial Na+ channels. J Biol Chem 283:6033–6039.

Kamynina E, Debonneville C, Bens M, Vandewalle A, Staub O (2001) A novel mouse Nedd4 protein suppresses the activity of the epithelial Na+ channel. FASEB J 15:204–214.

King JW, Thomas S, Corsi F, Gao L, Dina R, Gillmore R, Pigott K, Kaisary A, Stauss HJ, Waxman J (2009) IL15 can reverse the unresponsiveness of Wilms' tumor antigen-specific CTL in patients with prostate cancer. Clin Cancer Res 15:1145–1154.

Liu P, Jo S, Bean BP (2012) Modulation of neuronal sodium channels by the sea anemone peptide BDS-I. J Neurophysiol 107:3155–3167.

Lopez-Santiago LF, Pertin M, Morisod X, Chen C, Hong S, Wiley J, Decosterd I, Isom LL (2006) Sodium channel beta2 subunits regulate tetrodotoxin-sensitive sodium channels in small dorsal root ganglion neurons and modulate the response to pain. J Neurosci 26:7984–7994.

Ma C, Shu Y, Zheng Z, Chen Y, Yao H, Greenquist KW, White FA, LaMotte RH (2003) Similar electrophysiological changes in axotomized and neighboring intact dorsal root ganglion neurons. J Neurophysiol 89:1588–1602.

McKay Hart A, Brannstrom T, Wiberg M, Terenghi G (2002) Primary sensory neurons and satellite cells after peripheral axotomy in the adult rat: timecourse of cell death and elimination. Exp Brain Res 142:308–318.

Miyoshi S, Sekiguchi M, Konno S, Kikuchi S, Kanaya F (2011) Increased expression of vascular endothelial growth factor protein in dorsal root ganglion exposed to nucleus pulposus on the nerve root in rats. Spine 36:E1–E6.

Mohler PJ, Rivolta I, Napolitano C, LeMaillet G, Lambert S, Priori SG, Bennett V (2004) Nav1.5 E1053K mutation causing Brugada syndrome blocks binding to ankyrin-G and expression of Nav1.5 on the surface of cardiomyocytes. Proc Natl Acad Sci U S A 101:17533–17538.

Nagakura Y, Okada M, Kohara A, Kiso T, Toya T, Iwai A, Wanibuchi F, Yamaguchi T (2003) Allodynia and hyperalgesia in adjuvant-induced arthritic rats: time course of progression and efficacy of analgesics. J Pharmacol Exp Ther 306:490–497.

Nassar MA, Stirling LC, Forlani G, Baker MD, Matthews EA, Dickenson AH, Wood JN (2004) Nociceptor-specific gene deletion reveals a major role for Nav1.7 (PN1) in acute and inflammatory pain. Proc Natl Acad Sci U S A 101:12706–12711.

Noguchi K, De Leon M, Nahin RL, Senba E, Ruda MA (1993) Quantification of axotomy-induced alteration of neuropeptide mRNAs in dorsal root ganglion neurons with special reference to neuropeptide Y mRNA and the effects of neonatal capsaicin treatment. J Neurosci Res 35:54–66.

Okuse K, Malik-Hall M, Baker MD, Poon WY, Kong H, Chao MV, Wood JN (2002) Annexin II light chain regulates sensory neuron-specific sodium channel expression. Nature 417:653–656.

Pertin M, Ji RR, Berta T, Powell AJ, Karchewski L, Tate SN, Isom LL, Woolf CJ, Gilliard N, Spahn DR, Decosterd I (2005) Upregulation of the voltage-gated sodium channel beta2 subunit in neuropathic

pain models: characterization of expression in injured and non-injured primary sensory neurons. J Neurosci 25:10970–10980.
Pongs O (2008) Regulation of excitability by potassium channels. Results Probl Cell Differ 44:145–161.
Raouf R, Quick K, Wood JN (2010) Pain as a channelopathy. J Clin Invest 120:3745–3752.
Raymond CK, Castle J, Garrett-Engele P, Armour CD, Kan Z, Tsinoremas N, Johnson JM (2004) Expression of alternatively spliced sodium channel alpha-subunit genes. Unique splicing patterns are observed in dorsal root ganglia. J Biol Chem 279:46234–46241.
Ritchie JM, Black JA, Waxman SG, Angelides KJ (1990) Sodium channels in the cytoplasm of Schwann cells. Proc Natl Acad Sci U S A 87:9290–9294.
Rougier JS, van Bemmelen MX, Bruce MC, Jespersen T, Gavillet B, Apotheloz F, Cordonier S, Staub O, Rotin D, Abriel H (2005) Molecular determinants of voltage-gated sodium channel regulation by the Nedd4/Nedd4-like proteins. Am J Physiol Cell Physiol 288:C692–C701.
Rush AM, Cummins TR, Waxman SG (2007) Multiple sodium channels and their roles in electrogenesis within dorsal root ganglion neurons. J Physiol 579:1–14.
Schaeffer V, Meyer L, Patte-Mensah C, Eckert A, Mensah-Nyagan AG (2010) Sciatic nerve injury induces apoptosis of dorsal root ganglion satellite glial cells and selectively modifies neurosteroidogenesis in sensory neurons. Glia 58:169–180.
Schmalhofer WA, Calhoun J, Burrows R, Bailey T, Kohler MG, Weinglass AB, Kaczorowski GJ, Garcia ML, Koltzenburg M, Priest BT (2008) ProTx-II, a selective inhibitor of NaV1.7 sodium channels, blocks action potential propagation in nociceptors. Mol Pharmacol 74:1476–1484.
Schmidt J, Rossie S, Catterall WA (1985) A large intracellular pool of inactive Na channel alpha subunits in developing rat brain. Proc Natl Acad Sci U S A 82:4847–4851.
Sheets PL, Heers C, Stoehr T, Cummins TR (2008) Differential block of sensory neuronal voltage-gated sodium channels by lacosamide [(2R)-2-(acetylamino)-N-benzyl-3-methoxypropanamide], lidocaine, and carbamazepine. J Pharmacol Exp Ther 326:89–99.
Snyder PM (2009) Down-regulating destruction: phosphorylation regulates the E3 ubiquitin ligase Nedd4-2. Sci Signal 2:pe41.
Strickland IT, Martindale JC, Woodhams PL, Reeve AJ, Chessell IP, McQueen DS (2008) Changes in the expression of NaV1.7, NaV1.8 and NaV1.9 in a distinct population of dorsal root ganglia innervating the rat knee joint in a model of chronic inflammatory joint pain. Eur J Pain 12:564–572.
Stucky CL, Lewin GR (1999) Isolectin B(4)-positive and -negative nociceptors are functionally distinct. J Neurosci 19:6497–6505.
Tandrup T, Woolf CJ, Coggeshall RE (2000) Delayed loss of small dorsal root ganglion cells after transection of the rat sciatic nerve. J Comp Neurol 422:172–180.
Thakor DK, Lin A, Matsuka Y, Meyer EM, Ruangsri S, Nishimura I, Spigelman I (2009) Increased peripheral nerve excitability and local NaV1.8 mRNA up-regulation in painful neuropathy. Mol Pain 5:14.
Tsujino H, Kondo E, Fukuoka T, Dai Y, Tokunaga A, Miki K, Yonenobu K, Ochi T, Noguchi K (2000) Activating transcription factor 3 (ATF3) induction by axotomy in sensory and motoneurons: a novel neuronal marker of nerve injury. Mol Cell Neurosci 15:170–182.
van Bemmelen MX, Rougier JS, Gavillet B, Apotheloz F, Daidie D, Tateyama M, Rivolta I, Thomas MA, Kass RS, Staub O, Abriel H (2004) Cardiac voltage-gated sodium channel Nav1.5 is regulated by Nedd4-2 mediated ubiquitination. Circ Res 95:284–291.
Vijayaragavan K, Boutjdir M, Chahine M (2004) Modulation of Nav1.7 and Nav1.8 peripheral nerve sodium channels by protein kinase A and protein kinase C. J Neurophysiol 91:1556–1569.
Woolf CJ, Decosterd I (1999) Implications of recent advances in the understanding of pain pathophysiology for the assessment of pain in patients. Pain Suppl 6:S141–S147.
Woolf CJ (2000) Salter MW (Neuronal plasticity: increasing the gain in pain. Science 288:1765–1769.
Wu G, Ringkamp M, Hartke TV, Murinson BB, Campbell JN, Griffin JW, Meyer RA (2001) Early onset of spontaneous activity in uninjured C-fiber nociceptors after injury to neighboring nerve fibers. J Neurosci 21:RC140:5.
Zimmermann M (1983) Ethical guidelines for investigations of experimental pain in conscious animals. Pain 16:109–110.

(Accepted 19 September 2012)
(Available online 25 September 2012)

Rufinamide Attenuates Mechanical Allodynia in a Model of Neuropathic Pain in the Mouse and Stabilizes Voltage-gated Sodium Channel Inactivated State

Marc R. Suter, M.D.,* Guylène Kirschmann,† Cedric J. Laedermann, M.Sc.,‡ Hugues Abriel, M.D., Ph.D.,§ Isabelle Decosterd, M.D.‖

ABSTRACT

Background: Voltage-gated sodium channels dysregulation is important for hyperexcitability leading to pain persistence. Sodium channel blockers currently used to treat neuropathic pain are poorly tolerated. Getting new molecules to clinical use is laborious. We here propose a drug already marketed as anticonvulsant, rufinamide.

Methods: We compared the behavioral effect of rufinamide to amitriptyline using the Spared Nerve Injury neuropathic pain model in mice. We compared the effect of rufinamide on sodium currents using *in vitro* patch clamp in cells expressing the voltage-gated sodium channel Nav1.7 isoform and on dissociated dorsal root ganglion neurons to amitriptyline and mexiletine.

Results: In naive mice, amitriptyline (20 mg/kg) increased withdrawal threshold to mechanical stimulation from 1.3 (0.6–1.9) (median [95% CI]) to 2.3 g (2.2–2.5) and latency of withdrawal to heat stimulation from 13.1 (10.4–15.5) to 30.0 s (21.8–31.9), whereas rufinamide had no effect. Rufinamide and amitriptyline alleviated injury-induced mechanical allodynia for 4 h (maximal effect: 0.10 ± 0.03 g (mean ± SD) to 1.99 ± 0.26 g for rufinamide and 0.25 ± 0.22 g to 1.92 ± 0.85 g for amitriptyline). All drugs reduced peak current and stabilized the inactivated state of voltage-gated sodium channel Nav1.7, with similar effects in dorsal root ganglion neurons.

Conclusions: At doses alleviating neuropathic pain, amitriptyline showed alteration of behavioral response possibly related to either alteration of basal pain sensitivity or sedative effect or both. Side-effects and drug tolerance/compliance are major problems with drugs such as amitriptyline. Rufinamide seems to have a better tolerability profile and could be a new alternative to explore for the treatment of neuropathic pain.

What We Already Know about This Topic

- Neuropathic pain remains a poorly treated chronic pain condition
- Rufinamide is an antiepileptic drug that is thought to produce its effect against seizures through reducing sodium channel activity

What This Article Tells Us That Is New

- Rufinamide may produce, in part, an effect against neuropathic pain by interfering with the sodium channel subtype Nav 1.7 implicated in pain transmission

PAIN is essential for survival as it serves as an alert to engage protective behavior. Neuropathic pain, caused by a lesion or disease of the somatosensory nervous system, affects 7% of the population[1] and possesses no protective purpose.

Sodium channels are major targets for the development of new drug to treat neuropathic pain.[2] Nerve injury changes the expression of sodium channels[3] which affects peripheral nerve hyperexcitability and ectopic discharges along the nerve, in the dorsal root ganglion or at the injury site.[4,5] They are composed of a α-pore forming subunit associated to one or two β-modulating subunits. Nine genes encode for the α-subunits, Nav1.1–1.9.[6]

Current therapy for neuropathic pain involves adjuvant medications—not primarily developed for this purpose—such as anticonvulsants, antidepressants, or local anesthetics.[7] Tricyclic antidepressants are considered as first-line treatment in different international guidelines.[8] Their mode of action does not seem to be linked to their antidepressant actions as acknowledged by their faster onset.[9] Amitriptyline was shown to interact with sodium channels as exemplified by its

* Pain Fellow, † Laboratory Technician, Pain Center, Department of Anesthesiology, University Hospital Center and University of Lausanne, Lausanne, Switzerland. ‡ Ph.D. Student, Pain Center, Department of Anesthesiology, University Hospital Center and University of Lausanne, and Department of Clinical Research, University of Bern, Bern, Switzerland. § Professor, Department of Clinical Research, University of Bern. ‖ Associate Professor, Pain Center, Department of Anesthesiology, University Hospital Center and Department of Cell Biology and Morphology, University of Lausanne.

Received from the Pain Center, University Hospital Center and University of Lausanne, Lausanne, Switzerland. Submitted for publication February 2, 2012. Accepted for publication August 23, 2012. Supported by the Swiss National Science Foundation (Swiss Pain Research Consortium, Special Program University Medicine grant, 33CM30-124117, to Drs. Decosterd and Suter and grant 310030B_135693 to Dr. Abriel), Bern, Switzerland; the Swiss Society of Anesthesiology, Bern, Switzerland; and the University of Bern, Bern, Switzerland. Presented at International Association for the Study of Pain meeting, Montreal, Quebec, Canada, August 30, 2010.

Address correspondence to Dr. Suter: Pain Center, Department of Anesthesiology, CHUV, Avenue du Bugnon 46, 1011 Lausanne, Switzerland. marc.suter@chuv.ch. Anesthesiology 2013; 118:160-72

cardiac toxicity and this target could also play a role in pain modulation.[10] Mexiletine, a sodium channel blocker and an oral analog of local anesthetics has been used in the treatment of neuropathic pain[11] but its tolerance on long-term therapy raises considerable questions as shown by a median discontinuation of treatment of 43 days in a recent study.[12] Rufinamide is an antiepileptic drug licensed for Lennox-Gastaut syndrome, a refractory type of epilepsy.[13] It is considered to inhibit sodium channels, stabilizing its inactive form, and reducing the firing of sodium-dependent action potentials.

Since the discovery that loss-of-function mutations in *SCN9A*, the gene encoding for Nav1.7 isoform, are associated with congenital insensitivity to pain,[14] it has become a potential target for treatment. Moreover, gain-of-function mutations *SCN9A* are associated with familial pain syndromes (erythromelalgia and paroxysmal extreme pain disorder)[15] and in subset of patients with idiopathic small nerve fiber neuropathy or generalized pain syndromes.[16,17] Nav1.7 is expressed in sensory, sympathetic, and myenteric fibers.[18–20] It exhibits slower recovery from fast inactivation[21,22] compared with other tetrodotoxin-sensitive channels Nav1.4 and 1.6 and slower inactivation at potentials close to the membrane resting potential, thus contributing to the large ramp current during slow depolarization.[23] Nav1.7 is thought to play an important role in "boosting" the depolarization of small diameter nociceptive neurons.

In the present study, we investigated the analgesic effect of rufinamide on the spared nerve injury (SNI) model of neuropathic pain and amitriptyline was used as a positive control. Our null hypothesis was that treated and control groups show the same behavior. We also explored the effect of rufinamide on heterogeneously expressed Nav1.7 channels and used mexiletine and amitriptyline as control. We finally tested the effect of rufinamide on dorsal root ganglia neurons. For electrophysiological studies, our null hypothesis was that the drugs do not change the measured parameters, which were $V_{1/2}$ of activation and steady-state inactivation, frequency-dependent inhibition and $t_{1/2}$ of recovery from inactivation.

Materials and Methods

Drugs

Rufinamide (R8404), amitriptyline (A8404), and mexiletine (M2727) were purchased from Sigma (Buchs, Switzerland). For behavioral experiment, rufinamide was dissolved in dimethylsulfoxide (DMSO) and then mixed with 1 × phosphate buffered saline to the desired concentration. Control was 30% DMSO in 1 × phosphate buffered saline. Doses (5, 10, 25, 50 mg/kg) were chosen corresponding to the therapeutic ones used in epilepsy models in mice (rufinamide was effective in the maximal electroshock test (effective dose 23.9 mg/kg orally) and in the pentylenetetrazol induced seizure test (54 mg/kg, intraperitoneally).[24] Amitriptyline was dissolved directly in sterile 0.9% saline and doses were chosen according to previous studies in neuropathic pain models. Drugs were administered intraperitoneally.

Animal Experiments

All experiments were approved by the Committee on Animal Experimentation of the Canton de Vaud, Lausanne, Switzerland, in accordance with Swiss Federal law on animal care and the guidelines of the International Association for the Study of Pain.[25] 5-week-old C57BL/6 male mice (Charles River, l'Abresle, France) weighting 20–25 g at the start of experiment were housed in the same room, 5 per cage, at constant temperature of 21°C and a 12/12 dark/light cycle. No other animals were housed in that room. Mice had ad libitum access to water and food.

Surgery

SNI surgery[26,27] on mice[28] was performed under 1.5–2.5% isoflurane (Abott AG, Baar, ZG, Switzerland) anesthesia. Briefly, the left hindlimb was immobilized in a lateral position and slightly elevated. Incision was made at mid-thigh level using the femur as a landmark and a section was made through the biceps femoris in the direction of point of origin of the vascular structure. The three peripheral branches (sural, common peroneal, and tibial nerves) of the sciatic nerve were exposed without stretching nerve structures. Both tibial and common peroneal nerves were ligated using a 6.0 silk suture and transected together. The sural nerve was carefully preserved by avoiding any nerve stretch or nerve contact.

Behavior

For all the behavioral experiments, the observer was blinded to the treatment applied.

Mechanical Sensitivity. Animals were habituated to the testing environment daily for at least 2 days before baseline testing. The room temperature and humidity remained stable for all experiments. For testing mechanical sensitivity, animals were put under inverted plastic boxes on an elevated mesh floor and allowed 10 min for habituation before the threshold testing. Mechanical allodynia was tested using a series of von Frey hairs with logarithmically incrementing stiffness (0.02, 0.04, 0.08, 0.16, 0.32, 0.64, 1.28, and 2.56 g). The filaments were applied perpendicularly to the plantar surface 1–2 s. The 50% withdrawal threshold was determined using Dixon's up–down method.[29]

Heat Sensitivity. The effect of rufinamide and amitriptyline on basal heat sensitivity was assessed with the Hot Plate assay. Briefly, the animals were placed on the hot-plate surface set at 52°C. The latency of response (in seconds) was determined as the time until a hindlimb lick or jump occurred. The cutoff was set at 30 s to avoid tissue damage.

Activity was quantified with the Activ-meter (Bioseb, Vitrolles, France). The total activity (summation of immobile, slow and fast activity given by the software) of naive animals in their home cage was measured during the 4 h

following injection of rufinamide (50 mg/kg) and amitriptyline (10 mg/kg). It was compared with the activity after saline injection. All experiments for activity were performed between 5 and 9 PM.

A five-point sedation score from 0 to 4 points was used for rufinamide (50 mg/kg) and amitriptyline (10 mg/kg), 0 = normal behavior, normal locomotion, 1 = awake, slow locomotion, 2 = no locomotion, eyes half closed, still responding to righting reflex, 3 = asleep, eyes closed, still responding to righting reflex, 4 = no righting reflex, adapted from Boast *et al.*[30]

Experimental Design

For drug effect on naïve animals, eight animals per group were used to assess mechanical withdrawal threshold and heat withdrawal latency. For the Activ-meter, six animals were used in a cross-over design for rufinamide and amitriptyline.

Normal mechanical threshold was assessed before surgery without difference between groups. SNI surgery was performed and 1 week later allodynia-like behavior was tested before intraperitoneal injection of rufinamide. Two series of experiments were done, the first one compared rufinamide 25 mg/kg and 50 mg/kg with DMSO 30% (n = 10 per group, 9 for DMSO) and the second one compared rufinamide 5 mg/kg and 10 mg/kg with DMSO 30% (n = 8 per group) at 20-40-60-120-240 min and 24 h. After a washout period of 1 week the animals of the first series were tested with amitriptyline 10 or 20 mg/kg or saline at 60-120-240 min and 24 h after intraperitoneal injection (n = 9 per group for amitriptyline 20 mg/kg and 10 per group for amitriptyline 10 mg/kg and saline).

Plasma levels of the drug were assessed at 120 min after injection of 50 mg/kg rufinamide. Mice (n = 3) were anesthetized with isoflurane and 1 ml of blood was collected intracardially. Drug levels were analyzed by the pharmaceutical monitoring laboratory of Lavigny, Switzerland.#

Electrophysiology

Rufinamide was dissolved in DMSO at 10 mM as stock solution and diluted daily at desired concentration in the extracellular medium. As control, the same DMSO concentration was used (1% for 100 1% for 100 mM, to 5% for 500 mM). Higher concentration could not be achieved without increasing DMSO content. Amitriptyline and mexiletine were dissolved in extracellular medium directly.

Human embryonic kidney 293 cells stably expressing Nav1.7 were kindly provided by Simon Tate (Ph.D., Chief Scientific Officer, Convergence Pharmaceuticals, Cambridge, United Kingdom) and were cultured in Dulbecco's modified Eagle's medium-F12 + L-Glutamine (Invitrogen, Merelbeke, Belgium) supplemented with 5% fetal bovine serum and geneticin 0.4 mg/ml. Measurements were made at room temperature using pClamp software, version 10.2, and a VE-2 amplifier (Alembic Instruments, Montreal, Quebec, Canada). The sampling rate was 30 kHz. Data were smoothed and analyzed using Clampfit software version 10.2.0.12 (Axon Instruments, Union City, CA) and KaleidaGraph (Synergy Software, Reading, PA). Whole-cell patch clamp recordings were conducted using an internal solution containing (in millimole per liter (mM)) CsCl 60, Cesium aspartate 70, EGTA 11, $MgCl_2$ 1, $CaCl_2$ 1, HEPES 10, and Na_2-adenosine triphosphate 5, pH adjusted to 7.2 with CsOH; and an external solution containing NaCl 50, n-methyl-D-glutamine-Cl 80, $CaCl_2$ 2, $MgCl_2$ 1.2, CsCl 5, HEPES 10, and glucose 5, pH adjusted to 7.4 with CsOH. Holding potential was −100 mV. The values were not corrected for liquid junction potential. Pipette resistance was ranging from 2 to 4 MOhm. Only data from cells having stable access resistance over the duration of the experiment were used; cells for which signs of poor voltage-clamp control, such as delayed inflections of the current or discontinuities in the peak sodium current (I_{Na}) *versus* V_m curve, were not analyzed. Around 15% of sealed cells were lost. Data were filtered after acquisition using Boxcar 9 points. Peak currents were measured with a single 10 ms pulse protocol to −10mV from the holding potential. Percentage inhibition was calculated as $(peak_{vehicle} - peak_{drug})/peak_{vehicle} \times 100$ for each cell and then mean inhibition for each drug and concentration was calculated. Other protocols are shown as inserts in the figures. The linear ascending segment of the current-voltage relationship was used to estimate the reversal potential for each trace before obtaining the voltage-dependent activation curve. Voltage dependence of activation and steady-state inactivation curves were individually fitted with Boltzmann relationships, $y(V_m) = 1/(1 + \exp[(V_m - V_{1/2})/K])$ in which y is the normalized current or conductance, Vm is the membrane potential, $V_{1/2}$ is the voltage at which half of the channels are activated or inactivated, and K is the slope factor. The value of $t_{1/2}$ of recovery from inactivation was calculated by interpolation from a linear relation between the two points juxtaposing half recovery ($y_1 < 0.5 < y_2$), using the relation $x = (0.5-[y_1x_2-y_2x_1]/[x_2-x_1]) \times (x_2-x_1)/(y_2-y_1)$. For use-dependent block, the percentage of decrease of current was calculated between the 1st and 50th pulse.

For *ex-vivo* recordings, dorsal root ganglion neurons were collected from adult C57BL/6 mice (4–8 weeks old). Briefly, L4 and L5 dorsal root ganglion neurons were harvested and digested in Liberase blendzyme thermolysin medium (Roche, Indianapolis, IN) 0.5 U/dorsal root ganglion with 12 μM EDTA in 5 ml Complete Saline Solution (in mM, NaCl 137, KCl 5.3, MgCl2-6H2O 1, Sorbitol 25, HEPES 10, CaCl2 3, and pH adjusted to 7.2 with NaOH) for 20 min at 37°C. Neurons were further digested with Liberase blendzyme TL with EDTA in Complete Saline Solution with papaïn (30 U/ml) for 10 min. Finally neurons were suspended in dorsal root ganglion medium mix (89%

#http://www.ilavigny.ch/html/hopital/laboratoire.php. Accessed June 21, 2012.

DMEM/F-12, 10% bovine serum albumin, 1% penicillin/streptomycin) supplemented with 1.5 mg/ml of trypsin inhibitor and 1.5 mg/ml of purified bovine serum albumin. Mechanical dissociation was performed using a pipetman and neurons were plated on poly-D-lysine-coated coverslips and incubated 12 h before recording to allow recovery and adhesion of neurons. Neurons were only recorded for 12 more hours to prevent long-term culture phenotypic changes and neurite outgrowth that degrades space clamp. Small neurons (diameter < 30 μm) were recorded using an EPC-10 amplifier (HEKA Electronics, Lambrecht, Germany) and Patchmaster/Fitmaster software for data acquisition/analysis. The sampling interval was 20 μs and a 5 kHz filter was used in all experiments. Experiments were carried out in the whole-cell patch clamp configuration. Extracellular solution contained (in mM) NaCl 30, tetraethylammonium–Cl 110, KCl 3, $CaCl_2$ 1, $MgCl_2$ 1, HEPES 10, Glucose 10, CdCl 0.1; pH was adjusted to 7.3 using Tris base, osmolarity was adjusted to 320 mOsm/l with sucrose. The pipette solution contained cerebrospinal fluid 140, NaCl 10, $MgCl_2$ 2, $CaCl_2$ 0.1, EGTA 1.1, HEPES 10, pH was adjusted to 7.2 with CsOH and osmolarity was adjusted to 310 mOsm/l. Pipettes were pulled from Borosilicate glass (World Precision Instruments, Sarasota, FL) and had a resistance < 3 MOhm, when filled with the pipette solution. Capacity transients were canceled and series resistance was compensated to around 90%. Leakage current was digitally subtracted online using hyperpolarizing control pulses, applied after the test pulse, of one-fourth test pulse amplitude (P/4 procedure). For current density measurements, membrane currents were normalized to the membrane capacitance which was calculated from the integral of the transient current in response to a brief hyperpolarizing pulse of 10 mV from the holding potential.

Once in whole-cell configuration, cells were held at −60 mV for 5 min to dialyze the cell with CsF solution (fluoride shifts Nav1.8 steady-state activation and inactivation to hyperpolarized potentials) to reach Nav1.8 stable biophysical properties and to inactivate Nav1.9 current and was further clamped at −80 mV for 2 more minutes. Whole-cell Na currents were elicited by a series of 100 ms test pulses ranging from −80 to +40 mV in increments of 5 mV at a frequency of 0.33 Hz. Test pulses were preceded by a prepulse of 3 s at −120 mV. Normalized conductance (G/Gmax) was fitted as described for *in vitro* recordings and $V_{1/2}$ and slope factor were extracted from the equation. Steady-state inactivation curves were measured from a holding potential of −120 mV using 500 ms prepulses to the indicated potentials followed by a test pulse to 0 mV. Again, $V_{1/2}$ and slope factors were obtained as mentioned for *in vitro* recordings.

Recovery from inactivation curves was obtained with a standard two-pulse protocol consisting of a depolarizing pulse from a holding potential of −120 to 0 mV for 50 ms to inactivate the channels, followed by a variable duration step (from 0.05 to 3276.8 ms) back to −120 mV to promote recovery. The availability of the channels was assessed with a second test pulse at 0 mV and the ratio of the second pulse versus the first was plotted against the recovery interval. The $t_{1/2}$ of recovery was calculated as mentioned previously.

Statistics

Behavioral Statistics. For the time course and drug effect on mechanical allodynia after nerve injury three experiments were done separately: (1) rufinamide 25 mg/kg, rufinamide 50 mg/kg, and DMSO 30%; (2) rufinamide 5 mg/kg, rufinamide 10 mg/kg, and DMSO 30%; and (3) amitriptyline 10 mg/kg, amitriptyline 20 mg/kg, and saline. The log values of withdrawal thresholds were assessed for each experiment using an Anova two-ways with Bonferroni correction for repeated measures from preinjection to 24 h after injection. For the development of allodynia, baseline and preinjection were compared by using the Wilcoxon matched-pairs signed rank test (Bonferroni's correction for multiple testing) because baseline values are skewed. For clarity purposes on figure 1, a mean value of both DMSO groups is used and values are presented as mean ± SD also for baseline. For the drug effect on naïve animals, data were analyzed with Kruskal-Wallis test and Dunn's correction for multiple testing. The numerical data are presented as median with 95% CI.

Electrophysiological Statistics. Data are presented as mean ± SD and were analyzed using paired student *t* tests for drug effect.

All hypotheses were challenged using two-tailed testing and P value less than 0.05 was used as the level of significance. Statistical analysis was performed using Prism 5 for windows, version 5.03, GraphPad Software, San Diego, CA.

Results

1. Behavior

1.1 Rufinamide Reduces Mechanical Allodynia after SNI. All animals developed allodynia 1 week after surgery (P < 0.05, preinjection vs. baseline for all groups). Rufinamide significantly and dose-dependently alleviated SNI-induced allodynia (fig. 1A), with maximal effect from 0.10 ± 0.03 (mean ± SD) to 1.99 ± 0.26 g. The effect was seen already 20 min following injection, peaked at 60 min, lasted for at least 4 h, but had faded 24 h after drug administration. At the highest dose of rufinamide, allodynia-like behavior was completely reversed. The vehicle DMSO showed a tendency for anti-allodynic effect but the values did not reach statistical significance in multiple testing.

1.2 Amitriptyline Reduces Mechanical Allodynia after SNI. All animals showed allodynia before injection of amitriptyline (P < 0.05 preinjection vs. baseline for all groups). Amitriptyline alleviated the allodynic behavior from 60 to 240 min after injection and the effect had disappeared at 24 h (fig. 1B) with maximal effect from 0.25 ± 0.22 to 1.92 ± 0.85 g. There was no difference between 10 and 20 mg/kg.

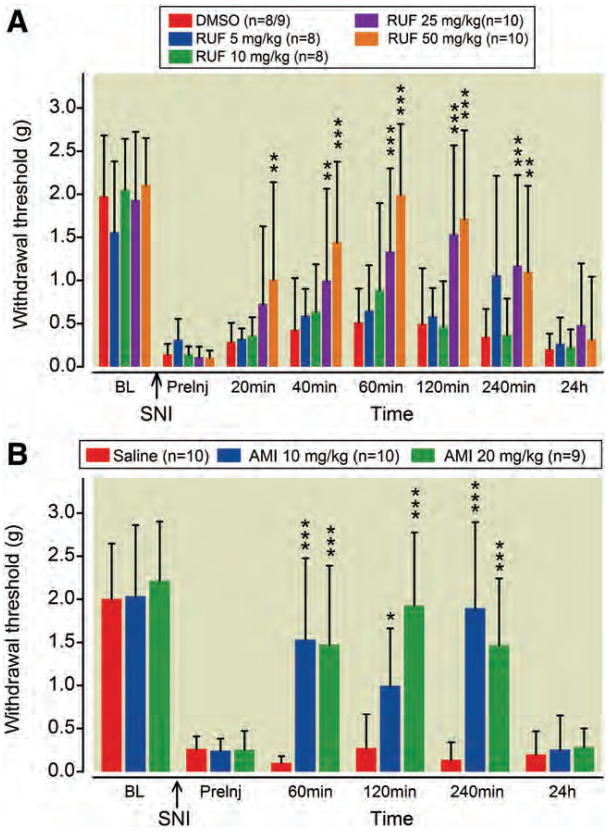

Fig.1. RUF and (AMI) alleviate mechanical allodynia after SNI. *A*, RUF dose-dependently alleviates neuropathic behavior following SNI from 20 to 240 min after injection with a peak at 60 min and a loss of effect at 24 h. *B*, AMI alleviates neuropathic behavior following SNI from 60 to 240 min after injection and lost its effect at 24 h, (*$P < 0.05$, **$P < 0.01$, ***$P < 0.001$ vs. PreInj). AMI = amitriptyline; BL = baseline; DMSO = dimethylsulfoxide; Preinj = pre-injection (1 week after SNI for RUF, 2 weeks for AMI); RUF = Rufinamide; SNI = spared nerve injury. Values are presented as mean ± SD.

1.3 Amitriptyline But Not Rufinamide Affects Basal Sensitivity. Rufinamide (50 mg/kg) did not modify basal mechanical sensitivity of naive animals or heat withdrawal latency. We therefore did not test lower doses (fig. 2, A and B). On the other hand, amitriptyline at 20 mg/kg increased withdrawal threshold for innocuous mechanical stimulation with von Frey hairs from 1.3 (0.6–1.9) (median and 95% CI) to 2.3 g (2.2–2.5) and increased withdrawal latency on heat stimulation compared with saline from 13.1 (10.4–15.5) (median, 95% CI) to 30.0 s (21.8–31.9). We therefore tested amitriptyline at 10 mg/kg and also observed antinociceptive effect on heat stimulation (withdrawal threshold from 10.5 [7.2–11.7] to 25.3 [16.4–27.7]), but no statistically significant difference on non-noxious mechanical stimulation (fig. 2, A and B).

Animals injected with rufinamide 50 mg/kg did not lower their total activity measured over 4 h after injection with the Activ-meter as compared with saline-injected controls.

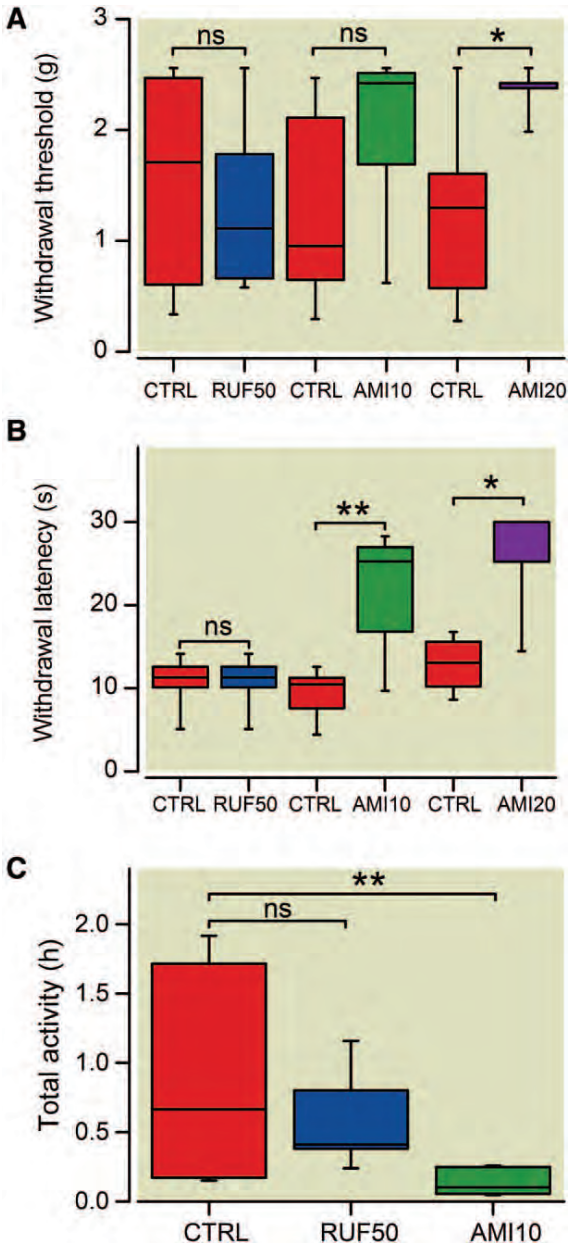

Fig. 2. RUF and AMI differentially affect basal sensitivity and activity of naïve animals. *A*, RUF at 50 mg/kg does not affect withdrawal threshold to mechanical stimulation with von Frey filaments as compared to AMI which significantly increased the threshold at the dose of 20 mg/kg (not statistically significant for 10mg/kg), n = 8. *B*, RUF at 50 mg/kg does not affect withdrawal latency to heat stimulation as compared to AMI which significantly increased the latency at the dose of 10 and 20 mg/kg, n = 8. *C*, The total activity (in hours) of the animals was measured using the Activ-meter system over a 4 h period following drug injection and compared with activity following saline. AMI (10 mg/kg) but not RUF (50 mg/kg) significantly reduces the activity compared with control, n = 6. Data are expressed as median (*horizontal line*) and *box* and *whiskers* with first and third quartiles (*box*), and minimum and maximum (*whiskers*), ns=non-significant, *$P < 0.05$, **$P < 0.01$ versus CTRL. AMI = amitriptyline; CTRL = control; RUF = Rufinamide.

Amitriptyline decreased total activity statistically significantly compared with saline-injected controls (fig. 2C).

Amitriptyline increased the score of sedation from 0 (saline group) to 2(0–3) (median, [range], n = 8). Rufinamide did not change the score (0).

1.4 Rufinamide Plasma Level Corresponds to Therapeutic Level for Epileptic Patients. At peak effect for mechanical allodynia, the range of plasma level for rufinamide was 68–86 mM.

2. Effect of Rufinamide on Nav1.7 Channel Compared with Amitriptyline and Mexiletine

2.1 Rufinamide Reduces Nav1.7 Peak Current. Rufinamide reduced I_{Na} induced by a single pulse depolarization using human embryonic kidney 293 cells stably expressing Nav1.7 (fig. 3). The most substantial reduction obtained with rufinamide was 28.3%, at a concentration of 500 µM. The drug could not be dissolved at higher concentration. A concentration of 100 µM was used for the rest of the testing to avoid the high DMSO concentration used for 500 µM. With high concentration of amitriptyline and mexiletine a complete inhibition of I_{Na} could be obtained and EC50 was used for the following experiments (fig. 3).

2.2 Rufinamide Shifts Steady-State Inactivation of Nav1.7. The voltage dependence of activation was examined using a series of 10 ms depolarizing test pulses from −80 to +85 mV from a holding potential of −100 mV. Rufinamide had no effect on voltage dependency of activation for Nav1.7 sodium channel, nor did amitriptyline and mexiletine. No statistically significant changes were seen in $V_{1/2}$ of activation. Slopes were slightly altered by rufinamide and mexiletine (fig. 4). For the steady-state inactivation experiments, cells were given a 500 ms conditioning pulse at voltages between −130 and −10 mV from a holding potential of −100 mV followed by a 20 ms test pulse. Normalized sodium currents (I_{Na}/Imax) measured during test pulses were plotted against conditioning voltage. Rufinamide shifted the steady-state inactivation relationship to more hyperpolarized value with a $V_{1/2}$ of inactivation shifting from −81.8±4.4 to −87.6±4.9 mV. The control drugs had a similar effect with shift of $V_{1/2}$ of inactivation, from −78.9±2.8 to −88.4±1.1 mV for amitriptyline and from −79.8±3.0 to −91.4±2.6 mV for mexiletine. The slopes of steady-state inactivation curves were not influenced by any of the tested drugs (fig. 4).

2.3 Rufinamide Prolongs the Recovery from Fast Inactivation of Nav1.7. Effects on the recovery from fast inactivation was examined with a standard double-pulse protocol consisting of a depolarizing pulse to −10 mV to inactivate the channels followed by a variable duration (0.25–2000 ms) step to the holding potential of −100 mV to promote recovery. The availability of the channels at the end of the recovery interval was assessed with a standard test pulse. The ratios of response of second/first pulse were plotted versus the recovery interval. The $t_{1/2}$ of recovery was interpolated. It was statistically significantly prolonged for the three tested drugs (fig. 5).

2.4 Rufinamide Shows Use-dependent Inhibition of Nav1.7. Frequency-dependent or use-dependent blocking refers to the accumulation of channels in inactivated state when subjected to a train of depolarizing pulses at high frequency. We applied a series of 50 pulses at varying frequencies (2, 5, 10, 25, 50 Hz) and plotted the normalized current against the pulse number. Rufinamide at 100 µM increased the use-dependent block at all frequencies tested, except 2 Hz. Amitriptyline and mexiletine also increased the use-dependent block, even at 2 Hz (fig. 6).

A

RUF (µM)	Inhibition (%)
50	12.5
100	21.2
500	28.3

AMI (µM)	Inhibition (%)
10	43.9
30	64.7
100	89.7

MEX (µM)	Inhibition (%)
30	21.7
100	43.4
160	67.7
300	77.1

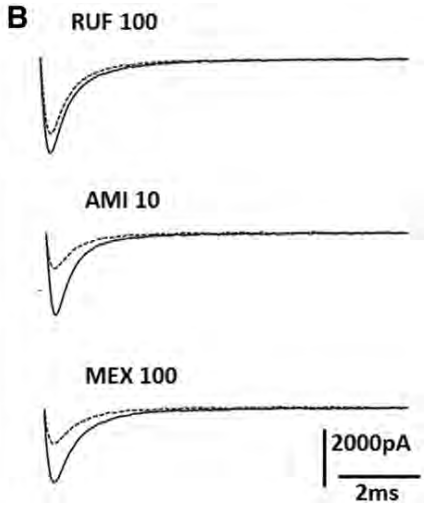

Fig. 3. Drugs inhibit voltage-gated sodium channel Nav 1.7 peak current. *A*, Percentage reduction of peak current after single pulse stimulation. *B*, Example of traces with the drug concentrations used afterwards in the biophysical properties testing, respectively, 100, 10, and 100 µM for RUF, AMI, and MEX. Transients were blanked. AMI = amitriptyline; MEX = mexiletine; RUF = Rufinamide.

Activation	$V_{1/2}$ ± SD (mV)		Slope ± SD	
CTRL	-25.8 ± 3.3	p=0.28	5.5 ± 0.8	p=0.02
RUF	-26.6 ± 2.8		6.1 ± 1.0	n=5
Inactivation	$V_{1/2}$ ± SD (mV)		Slope ± SD	
CTRL	-81.8 ± 4.4	P=0.0038	7.3 ± 2.4	p=0.45
RUF	-87.6 ± 4.9		7.6 ± 2.0	n=4

Activation	$V_{1/2}$ ± SD (mV)		Slope ± SD	
CTRL	-24.8 ± 1.2	p=0.21	5.2 ± 0.5	p=0.11
AMI	-27.1 ± 2.8		6.1 ± 1.0	n=5
Inactivation	$V_{1/2}$ ± SD (mV)		Slope ± SD	
CTRL	-78.9 ± 2.8	P=0.0019	7.8 ± 1.0	p=0.52
AMI	-88.4 ± 1.1		7.7 ± 0.9	n=5

Activation	$V_{1/2}$ ± SD (mV)		Slope ± SD	
CTRL	-25.3 ± 2.9	p=0.61	5.7 ± 0.8	p=0.03
MEX	-25.1 ± 3.6		6.5 ± 1.2	n=5
Inactivation	$V_{1/2}$ ± SD (mV)		Slope ± SD	
CTRL	-79.8 ± 3.0	p=0.0003	7.4 ± 0.7	p=0.2
MEX	-91.4 ± 2.6		9.0 ± 1.2	n=4

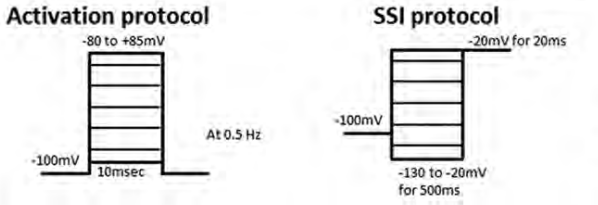

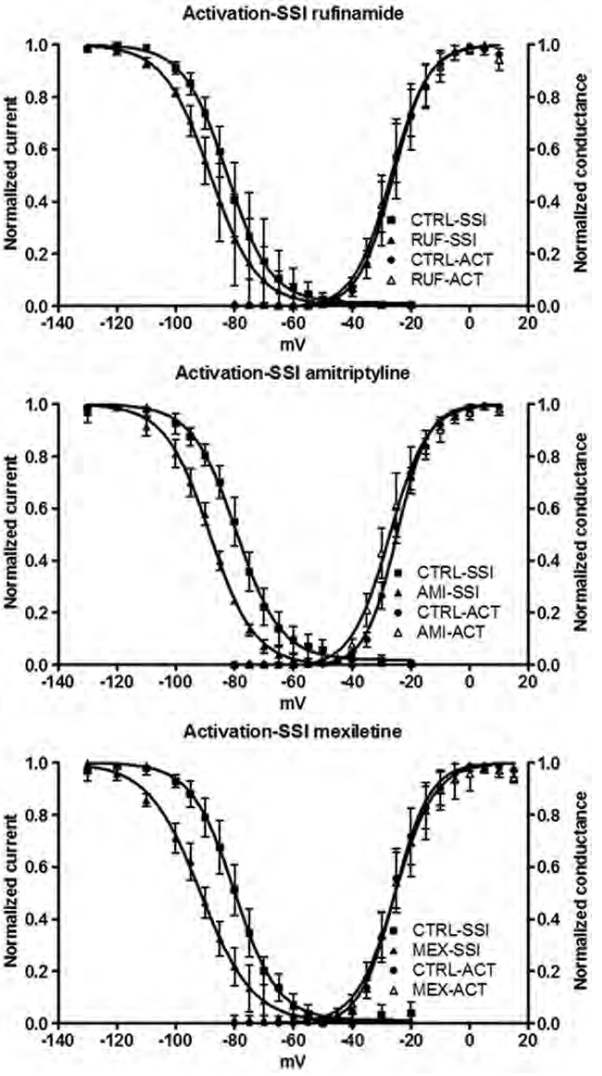

Fig. 4. Drugs induce a shift of inactivation properties of voltage-gated sodium channel Nav1.7. RUF, AMI, and MEX (at, respectively, 100, 10, and 100 μM) induce a hyperpolarizing shift in SSI without changing ACT properties of the voltage-gated sodium channel Nav1.7. $V_{1/2}$ of activation/inactivation, slopes, P values and n values are summarized in the tables. Insert: stimulation protocols. Values are mean ± SD. ACT = activation; AMI = amitriptyline; CTRL = control; MEX = mexiletine; RUF = Rufinamide; SSI = steady-state inactivation.

3. Rufinamide Influences INa in Dorsal Root Ganglion Neurons

We then wanted to validate the effect of rufinamide using dissociated mouse dorsal root ganglion neurons which contain also other Nav channels and the β-subunits. We first observed that rufinamide at 100 μM consistently induced a statistically significant 10.1% mean reduction in peak sodium current densities from 956 ± 396 to 850 ± 339 pA/pF ($P < 0.05$) despite a great variability in absolute values of current density (fig. 7A). We then assessed voltage dependence of activation and inactivation of the sodium current on the dorsal root ganglion with step protocols. The global effect of rufinamide on dorsal root ganglion was similar to the one observed using human embryonic kidney 293 cells expressing only Nav1.7. The voltage dependence of activation was unchanged and the inactivation curve was shifted with statistical significance toward more hyperpolarized potentials, from a $V_{1/2}$ of inactivation of −64.4 ± 16.8 mV to −69.4 ± 17.1 mV ($P < 0.0001$) (fig. 7B). Finally we observed that rufinamide also delayed $t_{1/2}$ of recovery from inactivation from 2.58 ± 2.12 to 6.24 ± 5.04 ms ($P < 0.05$) (fig. 7C).

Discussion

We here demonstrate that rufinamide alleviates mechanical allodynia-like behavior in the SNI model of neuropathic pain in mice. Its effect is comparable to amitriptyline, but with no interference on basal sensitivity and activity tests.

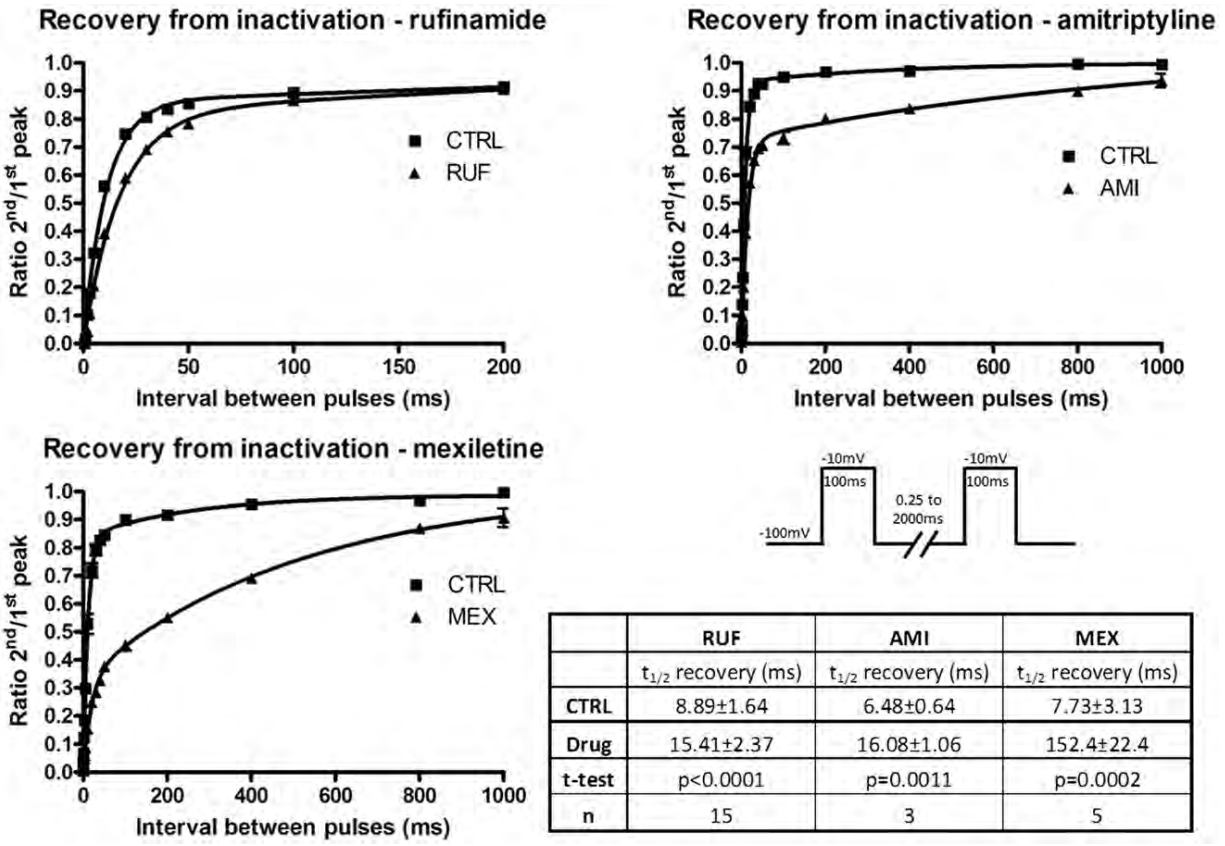

	RUF	AMI	MEX
	$t_{1/2}$ recovery (ms)	$t_{1/2}$ recovery (ms)	$t_{1/2}$ recovery (ms)
CTRL	8.89±1.64	6.48±0.64	7.73±3.13
Drug	15.41±2.37	16.08±1.06	152.4±22.4
t-test	p<0.0001	p=0.0011	p=0.0002
n	15	3	5

Fig. 5. Drugs induce a prolongation of recovery from inactivation of voltage-gated sodium channel Nav1.7. RUF, AMI, and MEX, at, respectively, 100, 10, and 100 μM, prolonged in a statistically significant way the half time ($t_{1/2}$) of recovery from inactivation of Nav1.7 channel. Values of interest are summarized in the table. Insert: stimulation protocol. Values are mean ± SD. AMI = amitriptyline; CTRL = control; MEX = mexiletine; RUF = Rufinamide.

We also show that rufinamide modulates Nav1.7. It stabilizes the channel in its inactivated state similarly to amitriptyline and mexiletine, and delays its recovery from inactivation. By the observation of rufinamide effect on total sodium currents recorded in dorsal root ganglion neurons, we finally validated a potential peripheral mechanism of action of rufinamide for the treatment of neuropathic pain.

Effect of Rufinamide on Mechanical Allodynia after SNI in Mice

To our knowledge, this is the first trial testing rufinamide in a model of neuropathic pain.

Amitriptyline is a first-line treatment for clinical neuropathic pain.[8] Amitriptyline alleviates neuropathic pain-like behavior in the chronic constriction injury[31,32] and spinal nerve ligation models[33] but failed to affect mechanical allodynia in these models[34,35] or on paw pressure hypersensitivity in a rat diabetes-related pain model.[36] In rats, amitriptyline decreased mechanical allodynia 3–5 days after SNI[37] but not after 2–4 weeks.[38] When administered perisurgically for 1 week, amitriptyline failed to prevent the development of mechanical allodynia in rodents.[39]

Despite diverging results explained by the different sensory modalities tested, timing, dose, and administration route or species/genetic background,[40,41] the SNI model remains a robust neuropathic pain model in rodents. In rats, mechanical allodynia following SNI does not respond to moderate doses of morphine, gabapentin, carbamazepine, MK-801[38], lidocaine, lamotrigine,[42] or rofecoxib.[43] Other groups showed a transient effect of high dose of morphine (6 mg/kg, effect < 3 h), mexiletine (37 mg/kg, < 1 h) or gabapentin (100 mg/kg, < 5 h)[44] and tocainide.[42] Side-effects and sedation are rarely mentioned but with high doses, many of the tested drugs in SNI could impair basal sensitivity.[38]

Rufinamide alleviates dose-dependently mechanical allodynia in this model, without inducing any changes in sedation or affecting basal sensitivity. Amitriptyline reduced allodynia, but also modified basal pain sensitivity and sedation score, which could participate in its anti-allodynic effect. Amitriptyline has been shown previously to change locomotor activity in rodents attributable to sedation, ataxia, changes in nociception, depression, or anxiety.[45–49] In one study, amitriptyline did not change locomotor activity in the chronic constriction injury model despite reducing allodynia.

Normalized current after 50 pulses				
	CTRL	RUF		p value
2Hz	1.04	0.93	n=5	0.11
5Hz	0.92	0.80	n=4	0.0032
10Hz	0.89	0.71	n=3	0.033
25Hz	0.69	0.48	n=4	0.017
50Hz	0.23	0.10	n=3	0.033

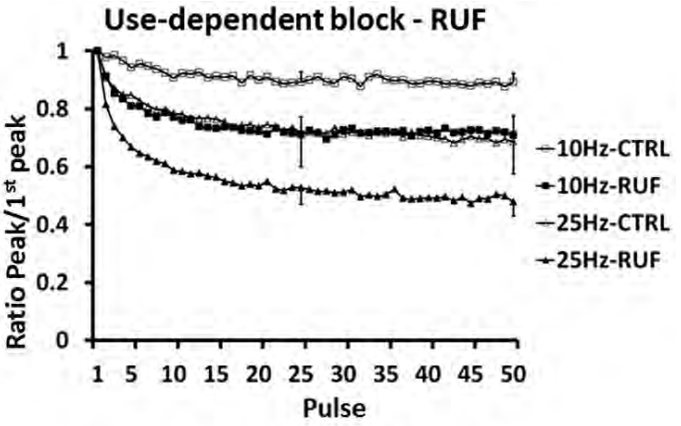

Normalized current after 50 pulses				
	CTRL	MEX		p value
2Hz	1.01	0.74	n=5	0.0085
5Hz	0.96	0.44	n=4	0.0002
10Hz	0.92	0.25	n=5	0.0006
25Hz	0.81	-0.06	n=4	0.0017
50Hz	0.30	-0.16	n=3	0.038

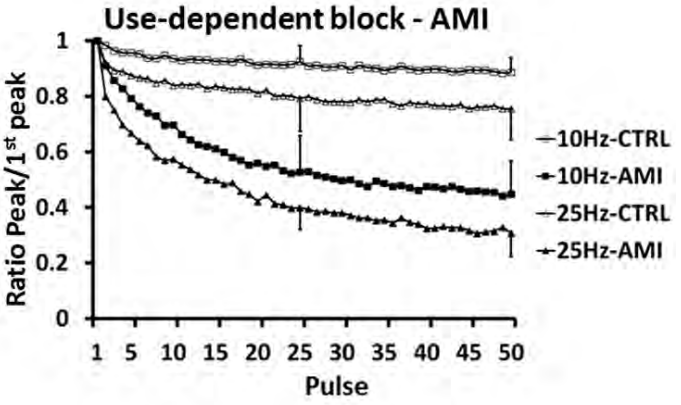

Normalized current after 50 pulses				
	CTRL	AMI		p value
2Hz	0.99	0.76	n=5	0.028
5Hz	0.93	0.59	n=5	0.0005
10Hz	0.89	0.45	n=5	0.0011
25Hz	0.76	0.31	n=5	0.0009
50Hz	0.26	0.09	n=5	0.0007

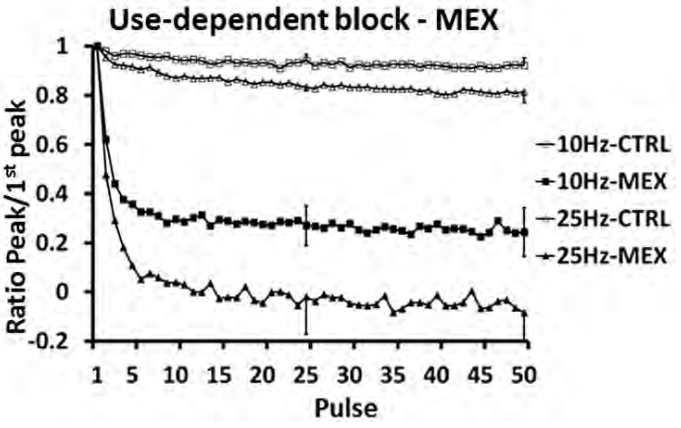

Fig. 6. Drugs induce a use-dependent block of voltage-gated sodium channel Nav1.7. RUF, AMI, and MEX, at, respectively, 100, 10, and 100 μM, all induced a statistically significant use-dependent block with stimulation frequencies from 2 to 50 Hz (except RUF at 2 Hz). All frequencies are shown in tables but for clarity purposes only 10 and 25 Hz are shown graphically. Values are mean ± SD. AMI = amitriptyline; CTRL = control; MEX = mexiletine; RUF = Rufinamide.

We are in agreement with others who showed an increase in thermal latency after acute amitriptyline treatment.[45,50]

Rufinamide Has the Potential of a New Treatment for Neuropathic Pain

As first-line therapy for the treatment of neuropathic pain, clinical guidelines propose tricyclic antidepressants (amitriptyline), serotonin and norepinephrine reuptake inhibitors (duloxetine and venlafaxine) or anticonvulsants targeting α2-δ subunit of calcium channels (gabapentin and pregabalin).[8,51] The most effective antidepressants in the treatment of neuropathic pain have sodium channel blocking properties,[52] which may contribute to their analgesic activity.[10,53] Sodium channel blockers as first-line evidence-based treatment recommendation have not yet been suggested except for two specific conditions: carbamazepine

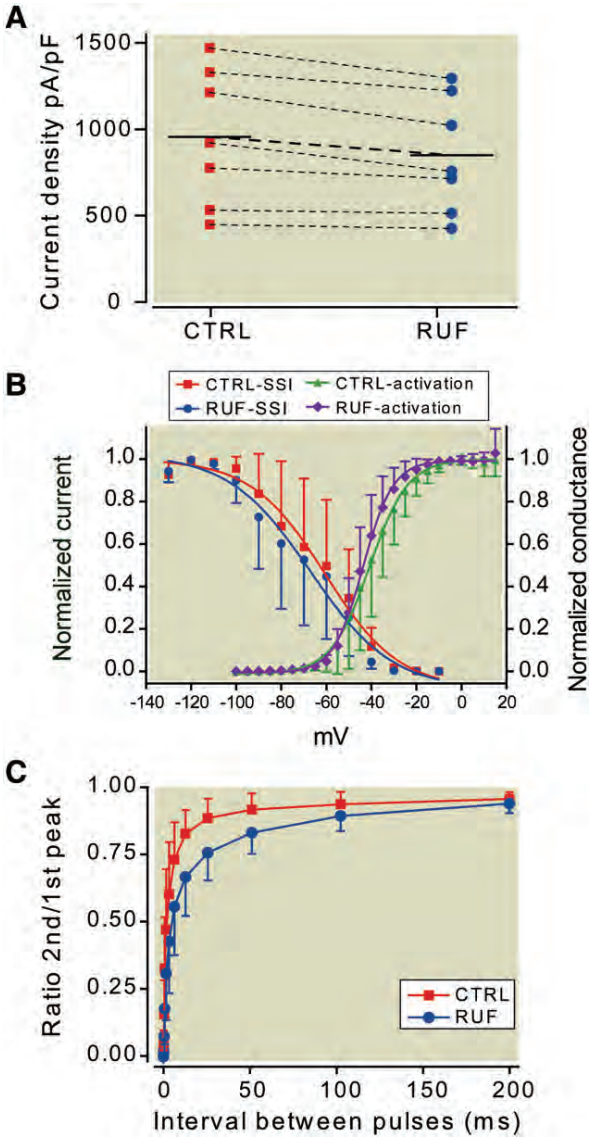

Fig. 7. Effects of rufinamide on freshly dissociated dorsal root ganglion neurons. *A,* RUF at 100 μM induced a 10% reduction in sodium peak current density ($P = 0.0084$, n = 7, horizontal bars represent mean values). *B,* It significantly shifted the SSI curve to a hyperpolarizing direction ($V_{1/2}$ of inactivation from –64.4±16.8 to –69.4±17.1 mV, $P < 0.0001$, n = 6) without changing activation properties ($V_{1/2}$ of activation from –40.6±8.4 to –43.4±5.1 mV, P = 0.17, n = 7). *C,* RUF also prolonged recovery from inactivation with half-time ($t_{1/2}$) for CTRL and RUF of, respectively, 2.58±2.12 and 6.24±5.04 ms, $P = 0.0028$, n = 6. Values are mean ± SD. CTRL = control; RUF = Rufinamide; SSI = steady-state inactivation.

in trigeminal neuralgia[51] and topical lidocaine in postherpetic neuralgia with irritable nociceptor.[11] The systemic delivery of a sodium channel blocker is limited by poor tolerability (and restricted availability in many countries) of mexiletine or high risk of drug interaction with carbamazepine.[54]

In clinical practice, the efficacy of amitriptyline on neuropathic pain is variable.[55,56] Amitriptyline is well known for its side-effects, predominantly sedation, hypotension, and anti-cholinergic effects, considerably reducing patient's compliance.[57] In particular, sedation has been known for a long time even at "light" dosage (50 mg).[58,59] For rufinamide, in a study on Lennox-Gastaut syndrome, the incidence of adverse events for somnolence or vomiting was more common in the rufinamide-treated group,[13] but causing only 2 or 3 patients out of 74 to withdraw from the study, respectively.

Drug interaction is also a major issue for pain therapy. Rufinamide presents favorable pharmacokinetic parameters; it is well absorbed orally and is not a substrate of cytochrome p450 system, thereby reducing its potential interactions. It is however a mild inducer of CYP3A4.[60] Rufinamide may be a mood-stabilizing molecule with anxiolytic properties[61] that could be an added value considering the large proportion of psychiatric mood-disorders encountered in chronic pain patients.[62] The toxicity studies in rodents show a greater safety ratio than other anticonvulsants.[24] Na channels are still a major target in the development of new analgesic drugs,[22,63] but rufinamide already being on the market, might offer a new treatment opportunity in the pain field, whereas other drugs trying their way through clinical trials have failed.[64,65] Rufinamide offers a valuable alternative to the current first-line treatments for the management of neuropathic pain.

Site of Action of Rufinamide

The site of action of rufinamide is unknown. Its effects on biophysical properties of sodium currents are similar to amitriptyline and mexiletine. Amitriptyline and mexiletine apparently interact with residues on the DIVS6 segment.[66,67] DIS6 (domain I segment 6), DIIIS6 (domain III segment 6), and DIVS6 (domain IV segment 6) segments may jointly form parts of the amitriptyline/local anesthetic receptor.[68]

Following the recent report of the crystal structure of the voltage-gated sodium channel, we hope new mechanistic knowledge will be gained in drug-channel interactions.[69]

We demonstrated the action of rufinamide on the peripherally expressed Nav1.7 isoform of sodium channel but we do not intend to show any specific Nav1.7 blocking properties. Indeed the drug is used in the treatment of epilepsy and therefore should also act on centrally expressed sodium channels. Rufinamide showed no relevant interaction with monoaminergic binding sites in radioligand binding studies and no interactions with benzodiazepine or γ-aminobutyric acid receptors, 5-HT1 and 5HT2 receptors, α- or β-adrenoceptors, or human recombinant metabotropic glutamate receptor subtypes 1b, 2, or 4 (mGluR1b, mGluR2, mGluR4). However, an inhibitory effect of rufinamide at the mGluR5 subtype was observed at 100 μM[60]. mGluR5 is upregulated in the dorsal root ganglia and spinal cord after spinal nerve ligation (but not after partial sciatic nerve ligation)[70] and peripheral mGluR5

agonists can produce thermal hyperalgesia.[71] In neuropathic pain, mGluR5 antagonists mostly show an effect on thermal sensitivity but not on mechanical allodynia.[70,72] The magnitude of effect mGluR5 antagonist on mechanical allodynia is below 40% of recovery toward baseline values for systemic administration on spinal nerve ligation model or chronic constriction injury in rats[73] and 66% reduction for intrathecal delivery with a shallow dose–response curve following spinal nerve ligation.[74] Antagonizing mGluR5 could prevent the development of mechanical allodynia after sciatic nerve constriction injury but not reverse it.[75,76] Altogether, the effects of mGluR5 antagonists are indeed not as potent as the complete reversal of established mechanical allodynia through rufinamide. Therefore, we suggest mGluR5 is not the major target for rufinamide.

Therapeutic plasmatic concentration for epilepsy (20–200 μM)[13] and plasmatic concentration in our study at the time of anti-allodynic effect (range 68–86 μM) are in the range of concentration used for *in vitro* testing (100 μM). Rufinamide at the concentration we used does not completely block the current but globally the channel is less excitable. After nerve injury, hyperexcitability and ectopic discharges at the neuroma or in the dorsal root ganglion[4] might be affected by the modulation of Na channel properties by rufinamide whereas there is no effect on nociception on a naïve nerve. We therefore suggest the anti-allodynic effect of rufinamide is related to its Na channel blocking properties.

Limitations of the Study

Differential Effect of Rufinamide, Amitriptyline, and Mexiletine on Nav1.7 Sodium Channel. We used the ED50 (half maximal effective concentration) of amitriptyline and mexiletine, 10 μM and 100 μM, respectively. The plasma concentrations of these two drugs are typically around 0.3 μM[77] and 2.3–9.3 μM[57]. Rufinamide was used at 100 μM, attributable to its low solubility in patch clamp solution. Our study is not intended to compare the effect size of the drugs on the different biophysical properties. The low solubility of rufinamide impeded a comparison of the three drugs at their ED50 values. The effect on peak current on Nav1.7 as well as on dorsal root ganglion neurons is low but nonetheless statistically significant and reproducible.

Effect of DMSO as Control

DMSO was used to dissolve rufinamide despite the potential neurotoxicity with prolonged administration at high dose.[78] It was also used as a treatment option in osteoarthritis[79] but only with relative efficacy on pain scores. We did not see any effect of DMSO on naïve animal sensitivity behavior regarding toxicity and compared the anti-allodynic of rufinamide with DMSO.

Conclusion and Future Directions

We here show that rufinamide dose-dependently alleviates neuropathic pain behavior in the SNI model in mice. We show *in vitro* electrophysiological data that rufinamide induces a hyperpolarizing shift in the steady-state inactivation curve, a use-dependent block and a delay in recovery from inactivation from Nav1.7-mediated current and *ex-vivo* data that the same stabilizing effect on inactivation is also present in dorsal root ganglion neurons. Sodium channels blockers still belong to the potential targets to treat neuropathic pain but often do not come on the market for toxicity or side-effects issues. Rufinamide is currently on the market and could therefore be used in clinical studies in the pain field rapidly. With the low rate of success from current chronic pain therapy, a new drug would be highly valued.

References

1. Breivik H, Collett B, Ventafridda V, Cohen R, Gallacher D: Survey of chronic pain in Europe: Prevalence, impact on daily life, and treatment. Eur J Pain 2006; 10:287–333
2. Dib-Hajj SD, Cummins TR, Black JA, Waxman SG: Sodium channels in normal and pathological pain. Annu Rev Neurosci 2010; 33:325–47
3. Berta T, Poirot O, Pertin M, Ji RR, Kellenberger S, Decosterd I: Transcriptional and functional profiles of voltage-gated Na(+) channels in injured and non-injured DRG neurons in the SNI model of neuropathic pain. Mol Cell Neurosci 2008; 37:196–208
4. Suter MR, Siegenthaler A, Decosterd I, Ji RR: Perioperative nerve blockade: Clues from the bench. Anesthesiol Res Pract 2011; 2011:124898
5. Devor M: Responses of nerves to injury in relation to neuropathic pain, Textbook of Pain, 5th edition. Edited by McMahon SB, Koltzenburg M. Elsevier, 2006, pp 905–28
6. Catterall WA, Goldin AL, Waxman SG: International Union of Pharmacology. XLVII. Nomenclature and structure-function relationships of voltage-gated sodium channels. Pharmacol Rev 2005; 57:397–409
7. Besson M, Piguet V, Dayer P, Desmeules J: New approaches to the pharmacotherapy of neuropathic pain. Expert Rev Clin Pharmacol 2008; 1: 683–93
8. Freynhagen R, Bennett MI: Diagnosis and management of neuropathic pain. BMJ 2009; 339:b3002
9. Saarto T, Wiffen PJ: Antidepressants for neuropathic pain. Cochrane Database Syst Rev 2007; Oct 17;(4):CD005454
10. Dick IE, Brochu RM, Purohit Y, Kaczorowski GJ, Martin WJ, Priest BT: Sodium channel blockade may contribute to the analgesic efficacy of antidepressants. J Pain 2007; 8:315–24
11. Challapalli V, Tremont-Lukats IW, McNicol ED, Lau J, Carr DB: Systemic administration of local anesthetic agents to relieve neuropathic pain. Cochrane Database Syst Rev 2005; Oct 19;(4):CD003345
12. Carroll IR, Kaplan KM, Mackey SC: Mexiletine therapy for chronic pain: Survival analysis identifies factors predicting clinical success. J Pain Symptom Manage 2008; 35:321–6
13. Glauser T, Kluger G, Sachdeo R, Krauss G, Perdomo C, Arroyo S: Rufinamide for generalized seizures associated with Lennox-Gastaut syndrome. Neurology 2008; 70: 1950–8
14. Cox JJ, Reimann F, Nicholas AK, Thornton G, Roberts E, Springell K, Karbani G, Jafri H, Mannan J, Raashid Y, Al-Gazali L, Hamamy H, Valente EM, Gorman S, Williams R, McHale DP, Wood JN, Gribble FM, Woods CG: An SCN9A channelopathy causes congenital inability to experience pain. Nature 2006; 444:894–8
15. Lampert A, O'Reilly AO, Reeh P, Leffler A: Sodium channelopathies and pain. Pflugers Arch 2010; 460:249–63

16. Faber CG, Hoeijmakers JG, Ahn HS, Cheng X, Han C, Choi JS, Estacion M, Lauria G, Vanhoutte EK, Gerrits MM, Dib-Hajj S, Drenth JP, Waxman SG, Merkies IS: Gain of function Nav1.7 mutations in idiopathic small fiber neuropathy. Ann Neurol 2012; 71:26–39
17. Dabby R, Sadeh M, Gilad R, Lampl Y, Cohen S, Inbar S, Leshinsky-Silver E: Chronic non-paroxysmal neuropathic pain — Novel phenotype of mutation in the sodium channel SCN9A gene. J Neurol Sci 2011; 301:90–2
18. Black JA, Dib-Hajj S, McNabola K, Jeste S, Rizzo MA, Kocsis JD, Waxman SG: Spinal sensory neurons express multiple sodium channel alpha-subunit mRNAs. Brain Res Mol Brain Res 1996; 43:117–31
19. Sangameswaran L, Fish LM, Koch BD, Rabert DK, Delgado SG, Ilnicka M, Jakeman LB, Novakovic S, Wong K, Sze P, Tzoumaka E, Stewart GR, Herman RC, Chan H, Eglen RM, Hunter JC: A novel tetrodotoxin-sensitive, voltage-gated sodium channel expressed in rat and human dorsal root ganglia. J Biol Chem 1997; 272:14805–9
20. Toledo-Aral JJ, Moss BL, He ZJ, Koszowski AG, Whisenand T, Levinson SR, Wolf JJ, Silos-Santiago I, Halegoua S, Mandel G: Identification of PN1, a predominant voltage-dependent sodium channel expressed principally in peripheral neurons. Proc Natl Acad Sci USA 1997; 94:1527–32
21. Herzog RI, Cummins TR, Ghassemi F, Dib-Hajj SD, Waxman SG: Distinct repriming and closed-state inactivation kinetics of Nav1.6 and Nav1.7 sodium channels in mouse spinal sensory neurons. J Physiol (Lond) 2003; 551(Pt 3):741–50
22. Cummins TR, Sheets PL, Waxman SG: The roles of sodium channels in nociception: Implications for mechanisms of pain. Pain 2007; 131:243–57
23. Cummins TR, Howe JR, Waxman SG: Slow closed-state inactivation: A novel mechanism underlying ramp currents in cells expressing the hNE/PN1 sodium channel. J Neurosci 1998; 18:9607–19
24. White HS, Franklin MR, Kupferberg HJ, Schmutz M, Stables JP, Wolf HH: The anticonvulsant profile of rufinamide (CGP 33101) in rodent seizure models. Epilepsia 2008; 49: 1213–20
25. Zimmermann M: Ethical guidelines for investigations of experimental pain in conscious animals. Pain 1983; 16:109–10
26. Decosterd I, Woolf CJ: Spared nerve injury: An animal model of persistent peripheral neuropathic pain. Pain 2000; 87:149–58
27. Suter MR, Papaloïzos M, Berde CB, Woolf CJ, Gilliard N, Spahn DR, Decosterd I: Development of neuropathic pain in the rat spared nerve injury model is not prevented by a peripheral nerve block. ANESTHESIOLOGY 2003; 99:1402–8
28. Bourquin AF, Süveges M, Pertin M, Gilliard N, Sardy S, Davison AC, Spahn DR, Decosterd I: Assessment and analysis of mechanical allodynia-like behavior induced by spared nerve injury (SNI) in the mouse. Pain 2006; 122:14.e1–14
29. Chaplan SR, Bach FW, Pogrel JW, Chung JM, Yaksh TL: Quantitative assessment of tactile allodynia in the rat paw. J Neurosci Methods 1994; 53:55–63
30. Boast CA, Pastor G, Gerhardt SC, Hall NR, Liebman JM: Behavioral tolerance and sensitization to CGS 19755, a competitive N-methyl-D-aspartate receptor antagonist. J Pharmacol Exp Ther 1988; 247:556–61
31. Ardid D, Guilbaud G: Antinociceptive effects of acute and 'chronic' injections of tricyclic antidepressant drugs in a new model of mononeuropathy in rats. Pain 1992; 49:279–87
32. Yasuda T, Iwamoto T, Ohara M, Sato S, Kohri H, Noguchi K, Senba E: The novel analgesic compound OT-7100 (5-n-butyl-7-(3,4,5-trimethoxybenzoylamino)pyrazolo[1,5-a]pyrimidine) attenuates mechanical nociceptive responses in animal models of acute and peripheral neuropathic hyperalgesia. Jpn J Pharmacol 1999; 79:65–73
33. Abdi S, Lee DH, Chung JM: The anti-allodynic effects of amitriptyline, gabapentin, and lidocaine in a rat model of neuropathic pain. Anesth Analg 1998; 87:1360–6
34. Esser MJ, Chase T, Allen GV, Sawynok J: Chronic administration of amitriptyline and caffeine in a rat model of neuropathic pain: Multiple interactions. Eur J Pharmacol 2001; 430:211–8
35. Pradhan AA, Yu XH, Laird JM: Modality of hyperalgesia tested, not type of nerve damage, predicts pharmacological sensitivity in rat models of neuropathic pain. Eur J Pain 2010; 14:503–9
36. Courteix C, Bardin M, Chantelauze C, Lavarenne J, Eschalier A: Study of the sensitivity of the diabetes-induced pain model in rats to a range of analgesics. Pain 1994; 57:153–60
37. Mao QX, Yang TD: Amitriptyline upregulates EAAT1 and EAAT2 in neuropathic pain rats. Brain Res Bull 2010; 81:424–7
38. Decosterd I, Allchorne A, Woolf CJ: Differential analgesic sensitivity of two distinct neuropathic pain models. Anesth Analg 2004; 99:457–63
39. Arsenault A, Sawynok J: Perisurgical amitriptyline produces a preventive effect on afferent hypersensitivity following spared nerve injury. Pain 2009; 146:308–14
40. Rode F, Thomsen M, Broløs T, Jensen DG, Blackburn-Munro G, Bjerrum OJ: The importance of genetic background on pain behaviours and pharmacological sensitivity in the rat spared serve injury model of peripheral neuropathic pain. Eur J Pharmacol 2007; 564:103–11
41. Hama AT, Borsook D: The effect of antinociceptive drugs tested at different times after nerve injury in rats. Anesth Analg 2005; 101:175–9
42. Erichsen HK, Hao JX, Xu XJ, Blackburn-Munro G: A comparison of the antinociceptive effects of voltage-activated Na+ channel blockers in two rat models of neuropathic pain. Eur J Pharmacol 2003; 458:275–82
43. Broom DC, Samad TA, Kohno T, Tegeder I, Geisslinger G, Woolf CJ: Cyclooxygenase 2 expression in the spared nerve injury model of neuropathic pain. Neuroscience 2004; 124:891–900
44. Erichsen HK, Blackburn-Munro G: Pharmacological characterisation of the spared nerve injury model of neuropathic pain. Pain 2002; 98:151–61
45. Rojas-Corrales MO, Casas J, Moreno-Brea MR, Gibert-Rahola J, Micó JA: Antinociceptive effects of tricyclic antidepressants and their noradrenergic metabolites. Eur Neuropsychopharmacol 2003; 13:355–63
46. Matson DJ, Broom DC, Carson SR, Baldassari J, Kehne J, Cortright DN: Inflammation-induced reduction of spontaneous activity by adjuvant: A novel model to study the effect of analgesics in rats. J Pharmacol Exp Ther 2007; 320:194–201
47. Enginar N, Hatipoğlu I, Firtina M: Evaluation of the acute effects of amitriptyline and fluoxetine on anxiety using grooming analysis algorithm in rats. Pharmacol Biochem Behav 2008; 89:450–5
48. Ogren SO, Cott JM, Hall H: Sedative/anxiolytic effects of antidepressants in animals. Acta Psychiatr Scand Suppl 1981; 290:277–88
49. Brocco M, Dekeyne A, Veiga S, Girardon S, Millan MJ: Induction of hyperlocomotion in mice exposed to a novel environment by inhibition of serotonin reuptake. A pharmacological characterization of diverse classes of antidepressant agents. Pharmacol Biochem Behav 2002; 71:667–80
50. Paudel KR, Das BP, Rauniar GP, Sangraula H, Deo S, Bhattacharya SK: Antinociceptive effect of amitriptyline in mice of acute pain models. Indian J Exp Biol 2007; 45:529–31
51. Dworkin RH, O'Connor AB, Backonja M, Farrar JT, Finnerup NB, Jensen TS, Kalso EA, Loeser JD, Miaskowski C, Nurmikko

TJ, Portenoy RK, Rice AS, Stacey BR, Treede RD, Turk DC, Wallace MS: Pharmacologic management of neuropathic pain: Evidence-based recommendations. Pain 2007; 132:237–51

52. Sudoh Y, Cahoon EE, Gerner P, Wang GK: Tricyclic antidepressants as long-acting local anesthetics. Pain 2003; 103:49–55
53. Wang SY, Calderon J, Kuo Wang G: Block of neuronal Na+ channels by antidepressant duloxetine in a state-dependent manner. ANESTHESIOLOGY 2010; 113:655–65
54. Attal N, Cruccu G, Haanpää M, Hansson P, Jensen TS, Nurmikko T, Sampaio C, Sindrup S, Wiffen P; EFNS Task Force: EFNS guidelines on pharmacological treatment of neuropathic pain. Eur J Neurol 2006; 13:1153–69
55. Robinson LR, Czerniecki JM, Ehde DM, Edwards WT, Judish DA, Goldberg ML, Campbell KM, Smith DG, Jensen MP: Trial of amitriptyline for relief of pain in amputees: Results of a randomized controlled study. Arch Phys Med Rehabil 2004; 85:1–6
56. Max MB, Lynch SA, Muir J, Shoaf SE, Smoller B, Dubner R: Effects of desipramine, amitriptyline, and fluoxetine on pain in diabetic neuropathy. N Engl J Med 1992; 326:1250–6
57. Baldessarini RJ: Drug therapy of depression and anxiety disorders, Goodman & Gilman's the Pharmacological Basis of Therapeutics, 11th edition. Edited by Shanahan F, Foltin J, Edmonson K, Brown RY. New York, The McGraw-Hill Companies, 2006, pp 429–60
58. Holmberg G: Sedative effects of maprotiline and amitriptyline. Acta Psychiatr Scand 1988; 77:584–6
59. Swift CG, Haythorne JM, Clarke P, Stevenson IH: Cardiovascular, sedative and anticholinergic effects of amitriptyline and zimelidine in young and elderly volunteers. Acta Psychiatr Scand Suppl 1981; 290:425–32
60. Perucca E, Cloyd J, Critchley D, Fuseau E: Rufinamide: Clinical pharmacokinetics and concentration-response relationships in patients with epilepsy. Epilepsia 2008; 49:1123–41
61. Fava M: The possible antianxiety and mood-stabilizing effects of rufinamide. Psychother Psychosom 2010; 79:194–5
62. McWilliams LA, Goodwin RD, Cox BJ: Depression and anxiety associated with three pain conditions: Results from a nationally representative sample. Pain 2004; 111:77–83
63. Bhattacharya A, Wickenden AD, Chaplan SR: Sodium channel blockers for the treatment of neuropathic pain. Neurotherapeutics 2009; 6:663–78
64. Gavva NR, Treanor JJ, Garami A, Fang L, Surapaneni S, Akrami A, Alvarez F, Bak A, Darling M, Gore A, Jang GR, Kesslak JP, Ni L, Norman MH, Palluconi G, Rose MJ, Salfi M, Tan E, Romanovsky AA, Banfield C, Davar G: Pharmacological blockade of the vanilloid receptor TRPV1 elicits marked hyperthermia in humans. Pain 2008; 136:202–10
65. Wallace MS, Rowbotham M, Bennett GJ, Jensen TS, Pladna R, Quessy S: A multicenter, double-blind, randomized, placebo-controlled crossover evaluation of a short course of 4030W92 in patients with chronic neuropathic pain. J Pain 2002; 3:227–33
66. Nau C, Seaver M, Wang SY, Wang GK: Block of human heart hH1 sodium channels by amitriptyline. J Pharmacol Exp Ther 2000; 292:1015–23
67. Weiser T, Qu Y, Catterall WA, Scheuer T: Differential interaction of R-mexiletine with the local anesthetic receptor site on brain and heart sodium channel alpha-subunits. Mol Pharmacol 1999; 56:1238–44
68. Wang GK, Russell C, Wang SY: State-dependent block of voltage-gated Na+ channels by amitriptyline via the local anesthetic receptor and its implication for neuropathic pain. Pain 2004; 110:166–74
69. Payandeh J, Scheuer T, Zheng N, Catterall WA: The crystal structure of a voltage-gated sodium channel. Nature 2011; 475:353–8
70. Hudson LJ, Bevan S, McNair K, Gentry C, Fox A, Kuhn R, Winter J: Metabotropic glutamate receptor 5 upregulation in A-fibers after spinal nerve injury: 2-methyl-6-(phenylethynyl)-pyridine (MPEP) reverses the induced thermal hyperalgesia. J Neurosci 2002; 22:2660–8
71. Gasparini F, Lingenhöhl K, Stoehr N, Flor PJ, Heinrich M, Vranesic I, Biollaz M, Allgeier H, Heckendorn R, Urwyler S, Varney MA, Johnson EC, Hess SD, Rao SP, Sacaan AI, Santori EM, Veliçelebi G, Kuhn R: 2-Methyl-6-(phenylethynyl)-pyridine (MPEP), a potent, selective and systemically active mGlu5 receptor antagonist. Neuropharmacology 1999; 38:1493–503
72. Walker K, Bowes M, Panesar M, Davis A, Gentry C, Kesingland A, Gasparini F, Spooren W, Stoehr N, Pagano A, Flor PJ, Vranesic I, Lingenhoehl K, Johnson EC, Varney M, Urban L, Kuhn R: Metabotropic glutamate receptor subtype 5 (mGlu5) and nociceptive function. I. Selective blockade of mGlu5 receptors in models of acute, persistent and chronic pain. Neuropharmacology 2001; 40:1–9
73. Zhu CZ, Wilson SG, Mikusa JP, Wismer CT, Gauvin DM, Lynch JJ III, Wade CL, Decker MW, Honore P: Assessing the role of metabotropic glutamate receptor 5 in multiple nociceptive modalities. Eur J Pharmacol 2004; 506:107–18
74. Dogrul A, Ossipov MH, Lai J, Malan TP Jr, Porreca F: Peripheral and spinal antihyperalgesic activity of SIB-1757, a metabotropic glutamate receptor (mGLUR(5)) antagonist, in experimental neuropathic pain in rats. Neurosci Lett 2000; 292:115–8
75. Fisher K, Fundytus ME, Cahill CM, Coderre TJ: Intrathecal administration of the mGluR compound, (S)-4CPG, attenuates hyperalgesia and allodynia associated with sciatic nerve constriction injury in rats. Pain 1998; 77:59–66
76. Fisher K, Lefebvre C, Coderre TJ: Antinociceptive effects following intrathecal pretreatment with selective metabotropic glutamate receptor compounds in a rat model of neuropathic pain. Pharmacol Biochem Behav 2002; 73:411–8
77. Coppen A, Ghose K, Montgomery S, Rama Rao VA, Bailey J, Christiansen J, Mikkleson PL, van Praag HM, van de Poel F, Minsker EJ, Kozulja VG, Matussek N, Kungkunz G, JÞrgensen A: Amitriptyline plasma-concentration and clinical effect. A World Health Organisation Collaborative Study. Lancet 1978; 1:63–6
78. Cavaletti G, Oggioni N, Sala F, Pezzoni G, Cavalletti E, Marmiroli P, Petruccioli MG, Frattola L, Tredici G: Effect on the peripheral nervous system of systemically administered dimethylsulfoxide in the rat: A neurophysiological and pathological study. Toxicol Lett 2000; 118:103–7
79. Brien S, Prescott P, Bashir N, Lewith H, Lewith G: Systematic review of the nutritional supplements dimethyl sulfoxide (DMSO) and methylsulfonylmethane (MSM) in the treatment of osteoarthritis. Osteoarthr Cartil 2008; 16: 1277–88

Year : 2013

Regulation of $Na_v1.7$ and $Na_v1.8$ voltage-gated sodium channels by Nedd4-2 and β-subunits and its implication in neuropathic pain

Cédric Laedermann